BNL-NCS-67469
Informal Report
ENDF-362
KAERI/TR-1511/2000

Neutron Cross Section Evaluations of Fission Products Below the Fast Energy Region

April 2000

Soo-Youl Oh and Jonghwa Chang
Nuclear Data Evaluation Laboratory
Korea Atomic Energy Research Institute

Said Mughabghab
National Nuclear Data Center
Brookhaven National Laboratory

BROOKHAVEN
NATIONAL LABORATORY

BNL-NCS-67469
Informal Report
ENDF-362
KAERI/TR-1511/2000

NEUTRON CROSS SECTION EVALUATIONS OF FISSION PRODUCTS BELOW THE FAST ENERGY REGION*

April 2000

Soo-Youl Oh and Jonghwa Chang
Nuclear Data Evaluation Laboratory
Korea Atomic Energy Research Institute

Said F. Mughabghab
National Nuclear Data Center
Brookhaven National Laboratory

*This work is supported by the U.S. Department of Energy under Contract DE-AC02-98CH10886.

DISCLAIMER

ABSTRACT

Neutron cross section evaluations of the fission-product isotopes, ^{95}Mo, ^{99}Tc, ^{101}Ru, ^{103}Rh, ^{105}Pd, ^{109}Ag, ^{131}Xe, ^{133}Cs, ^{141}Pr, ^{141}Nd, ^{147}Sm, ^{149}Sm, ^{150}Sm, ^{151}Sm, ^{152}Sm, ^{153}Eu, ^{155}Gd, and ^{157}Gd were carried out below the fast neutron energy region within the framework of the BNL-KAERI international collaboration. In the thermal energy region, the energy dependence of the various cross-sections was calculated by applying the multi-level Breit-Wigner formalism. In particular, the strong energy dependence of the coherent scattering lengths of ^{155}Gd and ^{157}Gd were determined and were compared with recent calculations of Lynn and Seeger. In the resonance region, the recommended resonance parameters, reported in the BNL compilation, were updated by considering resonance parameter information published in the literature since 1981. The s-wave and, if available, p-wave reduced neutron widths were analyzed in terms of the Porter-Thomas distribution to determine the average level spacings and the neutron strength functions. Average radiative widths were also calculated from measured values of resolved energy resonances. The average resonance parameters determined in this study were compared with those in the BNL and other compilations, as well as the ENDF/B-VI, JEF-2.2, and JENDL-3.2 data libraries. The unresolved capture cross sections of these isotopes, computed with the determined average resonance parameters, were compared with measurements, as well as the ENDF/B-VI evaluations. To achieve agreement with the measurements, in a few cases minor adjustments in the average resonance parameters were made.

Because of astrophysical interest, the Maxwellian capture cross sections of these nuclides at a neutron temperature of 30 keV were computed and were compared with other compilations and evaluations.

ACKNOWLEDGEMENTS

The authors gratefully acknowledge the financial support of the Ministry of Science and Technology, Korea. The cooperation of the U.S. Department of Energy in the preparation of this publication is acknowledged. We also wish to thank Alexsandra Lopez for her secretarial help in the preparation of this manuscript.

TABLE OF CONTENTS

TABLE OF CONTENTS (cont.)

List of Figures

List of Figures (cont.)

List of Figures (cont.)

List of Figures (cont.)

List of Tables

List of Tables (cont.)

List of Tables (cont.)

List of Tables (cont.)

I. INTRODUCTION

Evaluated neutron data play a major role in the design of nuclear reactors, as well as reactor safety analysis. The evaluated ENDF/B VI data libraries currently being used for applications, such as burn-up credit for spent fuel transportation, disposal criticality analysis and design of future advanced fuel do not take advantage of the recent measured cross section information. The consequence of not using the latest experimental data is likely to result in large uncertainties that have to be addressed by overly conservative assumptions or design margins.

Although the current ENDF/B-VI libraries contain data for fission product nuclides that are of importance to long term criticality or dose calculations of spent fuel, the data for many of the other fission products and higher actinides that are not major contributors to in-reactor performance may be of significant importance for criticality and dose calculations involving long-term discharge fuel. Many of such evaluations were based on rather perfunctory evaluations conducted in the 1973 to 1984 time period. Even though new measured data has become available since then, because of priority and resource considerations, these data were not re-evaluated to take advantage of the new information, but were simply copied over from earlier versions of the ENDF/B library into the current one without modification. To a certain extent, the same situation applies to the JEF-2 and JENDL-3 libraries. **Table 1**, which lists nineteen fission products of importance for criticality safety and transportation, gives in columns 1, 2, 3, and 4 the ranking of the fission product isotope according to DeHart [De95], the fission product nuclide, the ENDF/B-VI release date, and the data source of the neutron resonance parameters, respectively.

To address the deficiency in and increase the accuracy of fission product nuclear data, a BNL-KAERI collaboration was initiated in 1998. Under this project of international collaboration, the fission product nuclides listed in Table 1 were re-evaluated in the thermal, resolved resonance region, and the unresolved resonance region.

We present in Section II the evaluation methods for the thermal, resolved and unresolved energy regions; in Section III, we report the results and discussion for each fission product nuclide; in Section IV we give comparisons with other evaluations; and in Section V, we summarize the conclusions of the present evaluation project.

Table 1. Ranking of Fission Products for a 4.5% U-235 Fuel and 50 GWD/MTU[a]

RANK	FISSION PRODUCT	ENDF-VI EVALUATION DATE	DATA SOURCE OF RESONANCE PARAMETERS
1	^{149}Sm	1978	Mughabghab (1973)
2	^{143}Nd	1974	Mughabghab (1984)
3	^{103}Rh	1978	Mughabghab (1973)
4	^{151}Sm	1989	Mughabghab(1984)
5	^{155}Gd	1977	Mughabghab (1973)
6	^{131}Xe	1978	Ribon (1969)
7	^{133}Cs	1978	Garg (1965)
8	^{99}Tc	1978	Mughabghab (1973)
9	^{152}Sm	1980	Mughabghab (1984)
10	^{153}Eu	1986	Mughabghab (1973)
11	^{145}Nd	1980	Mughabghab (1984)
12	^{150}Sm	1980	Mughabghab (1984)
13	^{147}Sm	1988	Mughabghab (1984)
14	^{109}Ag	1983	Mughabghab (1973)
15	^{95}Mo	1990	Mughabghab (1973)
16	^{101}Ru	1980	Mughabghab (1981)
17	^{105}Pd	1989	Mughabghab (1981)
18	^{157}Gd	1977	Mughabghab (1973)
19	^{141}Pr	1980	Mughabghab (1973)

For Cooling Times Over 5 Years, Gd-155 Ranks 1.

[a] [De95]

II. EVALUATION METHODS

II.A. Thermal Cross Sections

In the present work, we followed closely the same evaluation procedure of the various thermal cross sections as that described in [Mu81].

The capture cross section, σ_γ, for a single resonance at energy E_o, represented by the Breit-Wigner formalism, is given by:

$$\sigma_\gamma(E) = \sigma_0 \frac{\Gamma_\gamma}{\Gamma}\sqrt{\frac{E_0}{E}}\frac{1}{1+y^2},$$

$$y = \frac{2}{\Gamma}(E - E_0), \qquad (1)$$

$$\sigma_0 = \frac{2.608\times10^6}{E_0}\left(\frac{A+1}{A}\right)^2 \frac{g\Gamma_n}{\Gamma}.$$

In this relation, Γ_n, Γ_γ, and Γ are the scattering width, the radiative width, and total width of the resonance, respectively; σ_o is the peak total cross section; A is the atomic mass number; g is the statistical spin weight factor defined below.

If N s-wave resonances of a nucleus are located away from the thermal energy, then their contribution to the thermal capture cross section can be approximated by the following expression:

$$\sigma_\gamma(0.0253\text{eV}) = 4.099\times10^6\left(\frac{A+1}{A}\right)^2 \sum_{j=1}^{N}\frac{g\Gamma_{nj}^0\Gamma_{\gamma j}}{E_{oj}^2}. \qquad (2)$$

The spin-dependent scattering lengths, a_+ and a_-, associated with spin states I+1/2 and I−1/2, where I is the spin of the target nucleus, can be written as:

$$a_\pm = R' + \sum_{j=1}^{N}\frac{\lambda_j\Gamma_{nj}}{2(E-E_j)+i\Gamma_j} \qquad (3)$$

where R' is the potential scattering length and λ is De Broglie's wave length divided by 2π. The summation is carried out over N s-wave resonances with the same spin. For those cases where resonances are located farther away from thermal energy region, the above relation can be simplified to the following:

$$a_\pm(\text{fm}) = R' - 2.277\times10^3\left(\frac{A}{A+1}\right)^2 \sum_{j=1}^{N}\frac{\Gamma_{nj}^0}{E_{0j}}. \qquad (4)$$

The total coherent scattering length for non-zero spin target nuclei, is then the sum of the spin-dependent coherent scattering widths, a_+ and a_-, weighted by the spin statistical factors, g_+ and g_-:

$$\begin{aligned} a &= g_+ a_+ + g_- a_- \\ g_+ &= (I+1)/(2I+1) \\ g_- &= I/(2I+1) \end{aligned} \tag{5}$$

The coherent, incoherent, and total scattering cross sections can then be expressed in terms of the scattering lengths by the following relations:

$$\sigma_{coh} = 4\pi(g_+ a_+ + g_- a_-)^2 \tag{6}$$

$$\sigma_{inc}(spin) = 4\pi g_+ g_- (a_+ - a_-)^2 \tag{7}$$

$$\sigma_s = 4\pi(g_+ a_+^2 + g_- a_-^2) \tag{8}$$

To calculate capture cross sections, coherent scattering amplitudes, and various spin-dependent scattering cross sections in terms of neutron-resonance parameters, the above relations, Eq. 1 to Eq. 8, were applied. These relations were previously implemented in the BNL computer code PSY325, which was used extensively in previous studies [Mu81, Mu84], as well as in the present evaluation.

If the results of the cross-section calculations do not agree with measurements within the uncertainty limits, then one or two negative energy (bound) levels are invoked. As a first step in the determination of the parameters of a bound level, we called upon Eq. 2 and Eq. 4. In addition, we assumed the radiative width of the bound level to be equal to the average s-wave radiative width of the nucleus under study. This quantity, as well as the potential scattering radius, is obtained from either measurements or the systematic investigations of average neutron resonance parameters, as well as optical model computations [Mu81, Mu84].

For target nuclei with non-zero spin, we relied in some favorable cases on gamma-ray spectra measurements of thermal neutrons to deduce the spins of the bound levels. In other cases, where two bound levels were stipulated, we made assumptions on their individual contributions. To carry out the final adjustments of the parameters of the bound level, the INTER computer code was used. In the final step of the analysis, the point wise energy-dependent cross sections were generated by the ENDF programs and then were compared graphically with measurements. Furthermore, the Westcott g factors, the capture resonance integrals, and the Maxwellian capture cross sections at a temperature of 30 keV were calculated by the INTER computer code.

II.B. Resolved Resonance Region

1. Assignment of Orbital Angular Momentum Quantum Numbers

The Bayesian approach [Mu81, Sm91] is adopted in this evaluation to distinguish p-wave from s-wave resonances for cases where the orbital angular momentum, l, have not been determined from measurements. Even though there is a potential danger of incorrect assignments of l [Mu81, Ga81], the Bayesian approach was used in several cases in the past [for instance, Bo68, Mi79].

For a resonance with a neutron width weighted by the spin statistical factor, $g\Gamma_n$, the probability that this resonance is a p-wave resonance is given according to Bayes' theorem of conditional probability by:

$$P(p|g\Gamma_n) = \frac{P(g\Gamma_n|p)P_p}{P(g\Gamma_n|s)P_s + P(g\Gamma_n|p)P_p + P(g\Gamma_n|d)P_d + \cdots}, \tag{9}$$

where $P(g\Gamma_n|s)$ is the probability that the neutron width is $g\Gamma_n$ if the resonance is an s-wave resonance, and P_s, P_p, and P_d are *a priori* probabilities that the resonance is an s-, p-, or d-wave resonance, respectively. Restricting the analysis to s- and p-wave resonances, the above equation reduces to:

$$P(p|g\Gamma_n) = \left(1 + \frac{P(g\Gamma_n|s)\langle D_1\rangle}{P(g\Gamma_n|p)\langle D_0\rangle}\right)^{-1} \tag{10}$$

where the level-spacing ratio $\langle D_1\rangle/\langle D_0\rangle$ is substituted for the ratio P_s/P_p. The probability density functions (pdf) for s- and p-wave resonances were derived [Oh99] from the χ^2 distribution proposed by Porter and Thomas[Po56]. The results are:

for s-wave,

$$p(x_0)dx_0 = \left(w_{01}\sqrt{\frac{w_{01}}{g_{01}}\frac{S_0}{S_{01}}}\frac{exp\left(-\frac{w_{01}x_0}{2g_{01}}\frac{S_0}{S_{01}}\right)}{\sqrt{2\pi x_0}} + w_{02}\sqrt{\frac{w_{02}}{g_{02}}\frac{S_0}{S_{02}}}\frac{exp\left(-\frac{w_{02}x_0}{2g_{02}}\frac{S_0}{S_{02}}\right)}{\sqrt{2\pi x_0}} \right) dx_0, \tag{11A}$$

for p-wave,

$$p(x_1)dx_1 = \left(w_{11}\sqrt{\frac{3w_{11}}{g_{11}}\frac{S_1}{S_{11}}}\frac{exp\left(-\frac{3w_{11}x_1}{2g_{11}}\frac{S_1}{S_{11}}\right)}{\sqrt{2\pi x_1}} + \frac{3w_{12}^2}{g_{12}}\frac{S_1}{S_{12}}exp\left(-\frac{3w_{12}x_1}{g_{12}}\frac{S_1}{S_{12}}\right) \right.$$

$$+\frac{3w_{13}^2}{g_{13}}\frac{S_1}{S_{13}}exp\left(-\frac{3w_{13}x_1}{g_{13}}\frac{S_1}{S_{13}}\right)+w_{14}\sqrt{\frac{3w_{14}}{g_{14}}\frac{S_1}{S_{14}}}\frac{exp\left(-\frac{3w_{14}x_1}{2g_{14}}\frac{S_1}{S_{14}}\right)}{\sqrt{2\pi x_1}}\Bigg]dx_1, \quad (12A)$$

In these relations, $x_0 = g\Gamma_n^0/\langle g\Gamma_n^0\rangle$ and $x_1 = g\Gamma_n^1/\langle g\Gamma_n^1\rangle$. w_{lj} and g_{lj} are the weights and the statistical factors, respectively, corresponding to the j-th resonance spin, J_j, arranged in ascending order, which can be formed from a given l value and target spin, I. The weight is defined by the ratio of the number of J_j l-wave resonances to the total number of l-wave resonances such that $w_{lj} = \langle D_l\rangle/\langle D_{lj}\rangle$. Note that for spin zero target nuclides, weights w_{01} and w_{02} are 1 and 0, respectively. Concerning the pdf for a p-wave resonance, the second and third terms in Eq. 12 take into account the degree of freedom of 2 for the same J formation. Thus, in Eq. 12A, weights are set as $w_{12} = w_{13} = 0$ for I = 0, $w_{13} = 0$ for I = 1/2, and $w_{11} = 0$ for I = 1. Finally, in the derivation of Eq. 11 and Eq. 12, the neutron strength function is defined by:

$$S_l = \langle g\Gamma_n^l\rangle/(2l+1)\langle D_l\rangle \text{ and } S_{lj} = \langle \Gamma_{nj}^l\rangle/\langle D_{lj}\rangle. \quad (13)$$

The J-dependent average level spacing is calculated by the Bethe formula:

$$\frac{1}{\langle D_{lj}\rangle} = C\,(2J_j+1)\,exp\left(-\frac{(J_j+1/2)^2}{2\sigma^2}\right), \quad (14)$$

where σ is the spin dispersion parameter. The constant C is obtained from $\langle D_0\rangle$ and the relation $1/\langle D_0\rangle = \sum_j 1/\langle D_{0j}\rangle$.

By applying Eq. 11A and Eq. 12A to Eq. 10, along with additional relations, such that:

$$dx_0 = \frac{d(g\Gamma_n)}{S_0\langle D_0\rangle\sqrt{E}V_0} \text{ and } dx_1 = \frac{d(g\Gamma_n)}{3S_1\langle D_1\rangle\sqrt{E}V_1} \quad (15)$$

where the penetrabilities, $V_0 = 1$ and $V_1 = k^2R^2/(1+k^2R^2)$, we can calculate the probability that a resonance at energy E eV and a width = $g\Gamma_n$ is a p-wave resonance. However, such a calculation requires detailed information, such as S_{lj}, which may not be available. Therefore, some simplification is necessary.

When we assume the (2J+1) law of level density, the weight becomes $w_{lj} = g_{lj}/G_l$, where $G_l \equiv \sum_j g_{lj}$. Note that $G_0 = 1$ whereas $G_1 = 3$ for I = 0, $G_1 = 9/4$ for I = 1/2, and $G_1 = 2$ for I ≥ 1. In addition, with the relation $S_{lj} = \mu_{lj} S_l$, where μ_{lj} is the multiplicity of J_j, Eq. 11A and Eq. 12A become:

$$p(x_0)dx_0 = \frac{exp\left(-\frac{x_0}{2}\right)}{\sqrt{2\pi x_0}}dx_0 = \frac{exp\left(-\frac{g\Gamma_n}{2\langle D_0\rangle S_0 V_0\sqrt{E}}\right)}{\sqrt{2\pi g\Gamma_n\sqrt{E}\langle D_0\rangle S_0 V_0}}d\left(g\Gamma_n\right), \text{ and} \tag{11B}$$

$$p(x_1)dx_1 = \left\{\alpha\sqrt{\frac{3}{G_1}}\frac{1}{\sqrt{2\pi x_1}} + (1-\alpha)\frac{3}{2G_1}\right\}exp\left(-\frac{3x_1}{2G_1}\right)dx_1$$

$$= \left(\frac{\alpha}{\sqrt{2\pi g\Gamma_n\sqrt{E}V_1\langle D_0\rangle S_1}} + \frac{1-\alpha}{2\sqrt{E}V_1\langle D_0\rangle S_1}\right)exp\left(-\frac{g\Gamma_n}{2\sqrt{E}V_1\langle D_0\rangle S_1}\right)d\left(g\Gamma_n\right), \tag{12B}$$

where $\alpha = 1$ for $I = 0$, $\alpha = 2/3$ for $I = 1/2$, and $\alpha = 1/2$ for $I \geq 1$. Applying Eq. 11B and Eq. 12B to Eq. (10) results in:

$$P(p|g\Gamma_n) = \left[1 + \frac{\langle D_1\rangle}{\langle D_0\rangle}\sqrt{\frac{S_1V_1}{S_0V_0}}\frac{exp\left\{\frac{g\Gamma_n}{2\langle D_0\rangle\sqrt{E}}\left(\frac{1}{S_1V_1} - \frac{1}{S_0V_0}\right)\right\}}{\alpha + (1-\alpha)\sqrt{\frac{\pi g\Gamma_n}{2\sqrt{E}\langle D_0\rangle S_1V_1}}}\right]^{-1}. \tag{16}$$

This formula is applied in the computer code, PTANAL (see Appendix B). Note that $\langle D_1\rangle/\langle D_0\rangle$, as well as α, depends on the target spin. In general, since the known values of S_1 are less certain than those of S_0, a set of probabilities was calculated for three different values of S_1 to access the sensitivity of the calculated probabilities on the p-wave strength function. We note that, regardless of the magnitude of the calculated probability, the l value of a resonance, as determined from measurements, was not altered.

2. Assignment of Resonance Spins

Several methods to assign the spin J of a resonance from measurements are available. For details, refer to {Mu81]. However, for weak and high-energy resonances, spins are difficult to measure. For those resonances, a method of random assignment is applied in the present study. The probability that the spin is J_j is calculated by:

$$P(J_j) = \frac{N_{lj}}{\sum_i N_{li}} = \frac{1/\langle D_{lj}\rangle}{\sum_i 1/\langle D_{li}\rangle}. \tag{17}$$

When we assume (2J+1) law, Eq. 17 becomes:

$$P(J_j) = \frac{(2J_j + 1)}{2(2I + 1)} \frac{1}{G_t}. \tag{18}$$

With the above equation as the pdf, and on the basis of a random number, uniform in the [0,1] interval, the J value of a resonance is assigned.

II.C. Unresolved Resonance Region

1. Determination of Average Level Spacings and Strength Functions

After the determination of l values for all resonances, the reduced neutron widths are analyzed in terms of the Porter-Thomas distribution [Po 57] to obtain the average reduced neutron width, the average level spacing and the neutron strength function for the unresolved resonance region. If the number of measured resonances is large enough for a statistical sample, the distribution of reduced neutron widths is analyzed in terms of the Porter-Thomas (PT) distribution.

$$p(x)dx = \frac{e^{-x/2}}{\sqrt{2\pi x}}dx, \quad x = \frac{g\Gamma_n^l}{\langle g\Gamma_n^l \rangle}. \tag{19}$$

Its corresponding cumulative distribution function (cdf) is given by:

$$P(x) \equiv \int_0^x p(x)dx = erf\left(\sqrt{x/2}\right). \tag{20}$$

This pdf is exactly the same as Eq. 11B for s-wave resonances but slightly differs from Eq. 12B for p-wave resonances. **Figure 1** shows the complement distribution function, cdf, *i.e.* $1 - P(x)$, corresponding to Eq. 12B for the p-wave case. Note that Eq. 12B is reduced to Eq. 19 for I = 0 nuclide. Maximum relative difference of about 10% between I = 0 and I ≥ 1 cases is observed. Note that the cdf for p-wave case corresponding to Eq. 12B is:

$$P(x) = \alpha\, erf\left(\sqrt{\frac{3x}{2G_1}}\right) + (1-\alpha)\left\{1 - exp\left(-\frac{3x}{2G_1}\right)\right\}. \tag{21}$$

For computational brevity, Eq. 20 was adopted in the analysis for both s- and p-wave resonances. As will be described later, because of the small number of assigned p-wave resonances, the average parameters obtained from such analysis have to be adjusted to reproduce the capture cross sections in the unresolved resonance region in most cases. Thus an approximate model is satisfactory for the fitting of p-wave reduced widths. However, derived rigorous cdf's (Eq. 21) will be implemented in a later version of the PTANAL program.

After sorting M measured l-wave reduced neutron widths in descending order, their distribution is fitted to the complement distribution function, cdf, using the following model:

$$1 + \varepsilon_1 = N_r\left\{1 - erf\left(\sqrt{g\Gamma_{n1}^l / 2\langle g\Gamma_n^l \rangle}\right)\right\},$$
$$2 + \varepsilon_2 = N_r\left\{1 - erf\left(\sqrt{g\Gamma_{n2}^l / 2\langle g\Gamma_n^l \rangle}\right)\right\},$$
$$\cdots$$

$$m+\varepsilon_m = N_r\left\{1-erf\left(\sqrt{g\Gamma_{nm}^l/2\langle g\Gamma_n^l\rangle}\right)\right\}, \tag{22}$$

where N_r is the number of 'expected' total number of l-wave resonances and $\langle g\Gamma_n^l\rangle$ is the average reduced neutron width. Since resonances with small neutron widths are usually missed in measurements, it is necessary to exclude resonances whose reduced widths are smaller than a certain magnitude. Then the number of resonances is reduced to m from a total M measured resonances. By setting a cutoff value, *i.e.* minimum magnitude of reduced width, the effect of missed small resonances on the resulting average parameters is reduced significantly. The error term ε_i is the propagated error from $g\Gamma_{ni}^l \pm \delta\, g\Gamma_{ni}^l$, which is approximately calculated by:

$$\varepsilon_i = M\frac{exp\left(-\dfrac{g\Gamma_{ni}^l}{2\overline{g\Gamma_n^l}}\right)}{\sqrt{2\pi\, g\Gamma_{ni}^l\, \overline{g\Gamma_n^l}}}\delta\, g\Gamma_{ni}^l,\ \overline{g\Gamma_n^l} = \sum g\Gamma_{ni}^l/M\ . \tag{23}$$

Now two parameters, N_r and $\langle g\Gamma_n^l\rangle$, are determined through the fitting procedure. The Levenberg-Marquardt method [Pr86] is used in this analysis. For $\langle D_l\rangle$ and $\langle g\Gamma_n^l\rangle$, the uncertainty of each quantity consists of two parts:

$$\frac{\delta\langle D_l\rangle}{\langle D_l\rangle} = \sqrt{\frac{Var(N_r)}{N_r^2}+\frac{0.52^2}{N_r}} \text{ and } \frac{\delta\langle g\Gamma_n^l\rangle}{\langle g\Gamma_n^l\rangle} = \sqrt{\frac{Var(\langle g\Gamma_n^l\rangle)}{\langle g\Gamma_n^l\rangle^2}+\frac{2}{N_r}}\ . \tag{24}$$

The first term originates from the fitting, and the second term is the inherent uncertainty. The variances of N_r and $\langle g\Gamma_n^l\rangle$, as well as the covariance of these two parameters, are obtained from the fitting analysis. The inherent uncertainty of $\langle D_l\rangle$ is adopted from Wigner's surmise [Wi57] and that of $\langle g\Gamma_n^l\rangle$ from the Porter and Thomas distribution [Po56]. Note that the uncertainty of the level spacing, obtained by Dyson and Mehta [Dy63], $\delta D_l/D_l = 0.45/N\cdot\sqrt{\ln N+2.18}$, is much smaller than that obtained from Wigner's surmise. The resulting neutron strength function with a known energy interval ΔE becomes:

$$S_l = \frac{\langle g\Gamma_n^l\rangle N_r}{(2l+1)\Delta E} \tag{25}$$

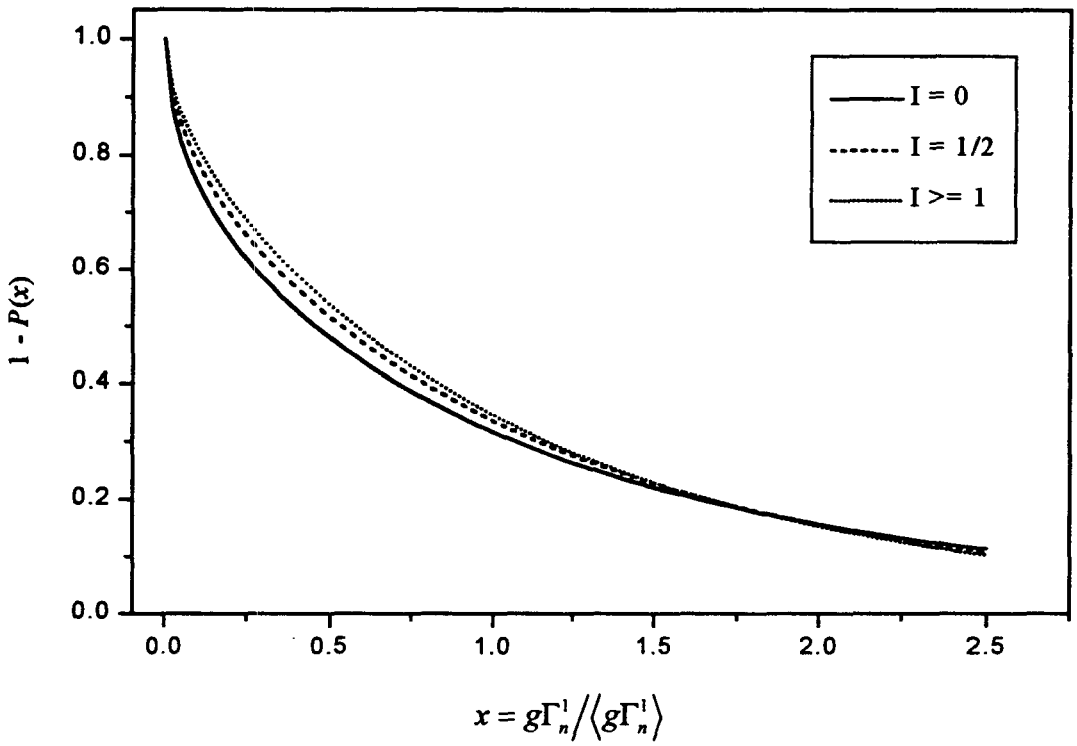

Fig. 1. Complement cdf for p-wave Neutron Reduced Widths

The corresponding relative uncertainty of S_l is:

$$\frac{\delta S_l}{S_l} = \sqrt{\left(\frac{Var(N_r)}{N_r^2} + \frac{2\,Cov(N_r, \langle g\Gamma_n^l \rangle)}{N_r \langle g\Gamma_n^l \rangle} + \frac{Var(\langle g\Gamma_n^l \rangle)}{\langle g\Gamma_n^l \rangle^2} \right) + \frac{0.52^2 + 2}{N_r}} \tag{26}$$

In most cases, analyzed in this work, the uncertainty due to the fitting is much smaller than the inherent uncertainty.

2. Determination of Average Radiative Widths

Average radiative widths of neutron resonances are determined from measurements in the resolved energy region by calculating the weighted, as well as unweighted, values. For nuclei with unmeasured radiative widths, we called upon the systematic study of s-, p- and d-wave radiative widths as a function of atomic mass number, as described in [Mu84]. In some cases, final adjustments of the radiative widths were made in order to fit measured capture cross sections in the unresolved energy region. In other cases, we were guided by the recent theoretical calculations of radiative widths on the basis of giant dipole resonance [Mu99].

III. RESULTS AND DISCUSSION

III.A. ^{95}Mo

1. Thermal Region

Positive-energy resolved resonance parameters and an effective scattering radius, R' = 7.0 fm, were adopted from Mughabghab's BNL compilation [Mu81]. However, in the resent evaluation, the parameters of a bound level were determined to reproduce a thermal capture cross section of 13.6 b and a bound coherent scattering length of 6.93±0.06 fm [Ko87a, Ko91]. A capture cross section of 13.6 b was obtained by weighting 14.0±0.5 b in the BNL compilation and 13.4±0.3 b of Koester *et al.* [Ko87a]. The derived bound level parameters are: E_0= −26.8 eV, Γ_n= 126 meV, Γ_γ= 150 meV and J = 2. As shown in **Table 2**, the capture cross sections from the various indicated sources are in good agreement with each other, within the associated uncertainty limits. However, the present thermal scattering cross section is larger than those reported in other evaluated libraries.

2. Resolved Resonance Parameters

Resonance parameters, extending to an energy of 2.14 keV, were adopted from the BNL compilation [Mu81] with minor revisions. For resonances at energies of 1.3407, 1.4955, 1.5895, 1.7661 and 2.1301 keV for which neutron scattering widths are not quoted in the BNL compilation, the $2g\Gamma_n$ values were deduced from the total cross section measurement of natural Mo [Wy68]. Because of the lack of data in the energy region 2.14–3.23 keV, resonances above 2.14 keV were not included in the present evaluation. Of a total of 55 resonances, 20 (including 12 identified in the BNL compilation) were assigned as s-wave resonances, whereas 35 (7 identified in the BNL compilation) were assigned as p-wave on the basis of Bayesian analysis. Spins of resonances for which the spins were not determined were assigned randomly by assuming that the level density is proportional to (2J+1). It is worth noting that Bayesian analysis for the resonance at 630.0 eV with a relatively large neutron width (24 meV) suggests s-wave assignment. On the other hand, this resonance is determined as a p-wave resonance by measurements. Weighted averaging of the known twelve radiative widths, two of which are p-wave resonances, resulted in an average value of 158±14 meV. However, because of the importance of valence capture of p-wave resonances in this mass region [Mu71], we adopted a radiative width of 180 meV for p-wave resonances [Mu76]. For s-wave resonances for which radiative widths are unknown, a value of 150 meV was assumed.

The distribution of reduced neutron widths was analyzed by fitting the widths to a Porter-Thomas distribution. **Figure 2** shows the fit for the cumulative number of s-wave resonances having a $\sqrt{g\Gamma_n^0}$ larger than the value indicated on the x-axis. None of the weak resonances was excluded in the fitting procedure. The fit resulted in $\langle D_0 \rangle$ = 80.7±13.1 eV and $\langle g\Gamma_n^0 \rangle$ = 3.64±1.25 meV. These values yield s-wave strength function of S_0 = 0.45±0.16. The present $\langle D_0 \rangle$ is consistent with the value of (80±25 eV) [Mu76], but not with 55±8 eV [Mu81], 58±5 eV Zh92], and 105±10 eV [Re98]. The S_0 value is consistent with Musgrove's value (0.48±0.10), slightly larger than that recommended in the BNL compilation (0.35±0.07) [Mu81], and smaller than

(0.60±0.10) [Re98]. For p-wave resonances, those with a $g\Gamma_n^1$ value smaller than 25 meV were excluded from the fitting procedure. The final fit, shown in **Fig. 3**, resulted in $\langle D_1 \rangle$ = 34.7±4.3 eV and S_1 = 6.54±1.68. The latter value is consistent with those reported in the BNL compilation [Mu81] (7±2), Koester *et al.* [Ko87b] (6.2±0.7), and Musgrove *et al.* [Mu76] (7.5±2.5).

3. Unresolved Resonance Parameters

The present unresolved resonance region covers the energy range up to 206.27 keV, which corresponds to inelastic neutron scattering to the first excited level of ^{95}Mo at 204.12 keV. The average resonance parameters for s- p-, and d-wave resonances are provided. Since the upper energy range of the unresolved region is relatively high, d-wave contribution is not negligible. The level spacing varies with energy according to Gilbert-Cameron's level density formula with associated parameters adopted from Mughabghab and Dunford [Mu98a]. From the (2J+1) dependence of the level density, level spacings of p- and d-waves were assumed to be 1/2 and 1/3 of that for the s-wave resonances, respectively.

In the unresolved resonance region, average capture cross section measurements of Musgrove *et al.* [Mu76], which were corrected later by Allen *et al.* [Al82], and Kapchigashev and Popov [Ka64] were considered in this evaluation. These two sets show good agreement with each other. In the first attempt, we adopted values of $\langle D_0 \rangle$, S_0 and S_1 deduced from the resolved resonances, S_2 read from a spherical optical model calculation in the BNL compilation [Mu84], and $\langle \Gamma_\gamma \rangle$ of 150 meV for s- and d-wave whereas 180 meV for p-wave resonances. The resulting calculated capture cross section is larger by 10% to 15% than the measurements throughout the whole energy region. Subsequently, $\langle D_0 \rangle$ was adjusted to 69.4 eV to obtain good agreement with the measurements as shown in **Fig. 4**. Note that the present $\langle D_0 \rangle$ is twice that of $\langle D_1 \rangle$ obtained from the analysis of resolved p-wave resonances. The finalized parameters of the present study are listed in the last column of **Table 3**. We note that unresolved resonance parameters were not provided in the ENDF/B-VI and JEF-2.2 evaluations.

Maxwellian-averaged capture cross section for a temperature of 30 keV was computed as 336 mb. The integration was performed up to an energy of 206 keV. The present cross section is compared with 292±12 mb [Wi87] (see Beer's compilation [Be92]) and 380±50 mb [Mu81].

Table 2. Thermal Characteristics (^{95}Mo)

Quantity	Unit	BNL [Mu81]	98CRC [Ho98]	ENDF/ B-VI	JEF-2.2	JENDL-3.2	Present
R'	fm	7.0±0.2		5.50	7.0	7.0	7.0
σ_γ^0	barn	14.0±0.5	13.4±0.3	14.6	14.0	14.0	13.6
σ_s^0	barn			2.48	5.21	5.57	6.41
gw*				0.9990	0.9987	0.9994	1.0000
RI-capt.**	barn	109±5	109±5	113	110	119	111
RI-total**	barn			291	306	334	315

*Westcott factor for capture cross section.
** Integrated from 0.5 eV to 100 keV with 1/E spectrum.

Table 3. Average Resonance Parameters for the Unresolved Resonance Region (^{95}Mo)

Quantity	Unit	BNL [Mu81]	ENDF/ B-VI	JEF-2.2	JENDL-3.2*	Present	
						PT Analysis	Adopted
R'	Fm	7.0±0.2			6.68		7.0
$\langle D_0 \rangle$	eV	55±8			78.86	80.7±13.1	69.4**
S_0	$\times 10^{-4}$	0.35±0.07			0.37	0.45±0.16	0.45
$\langle \Gamma_{\gamma 0} \rangle$	meV	160±20			232		150
$\langle D_1 \rangle$	eV				39.43	34.7±4.3	34.7**
S_1	$\times 10^{-4}$	7±2			5.48	6.54±1.68	6.54
$\langle \Gamma_{\gamma 1} \rangle$	meV				232		180
$\langle D_2 \rangle$	eV				26.29		23.1**
S_2	$\times 10^{-4}$				0.365		1.70
$\langle \Gamma_{\gamma 2} \rangle$	meV				232		150

* Average parameters at the low energy range of the unresolved region (2.04 keV).
** Value at the neutron separation energy of ^{96}Mo.

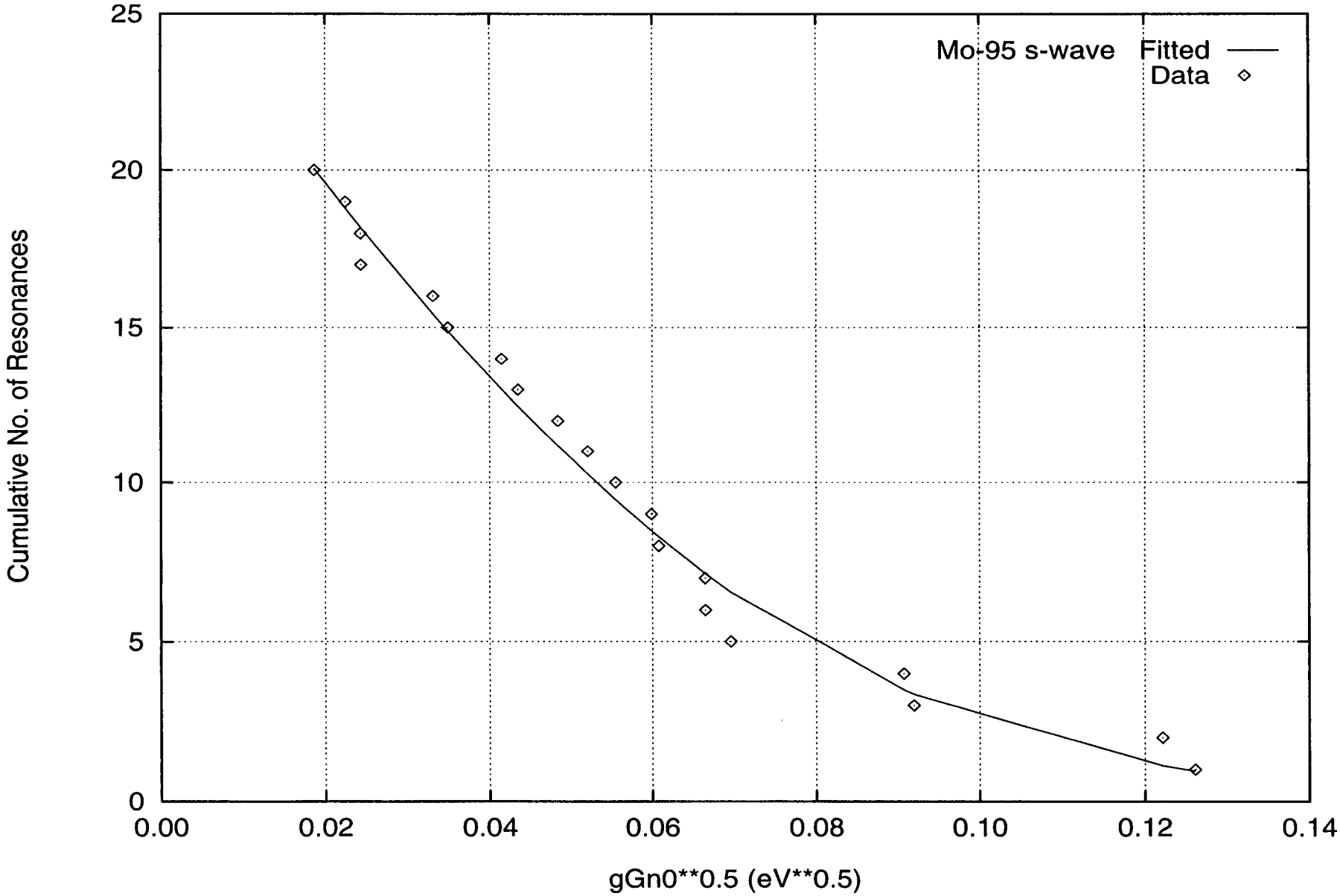

Fig. 2. Complement of the Cumulative Distribution of Neutron Reduced Widths (^{95}Mo, s-wave)

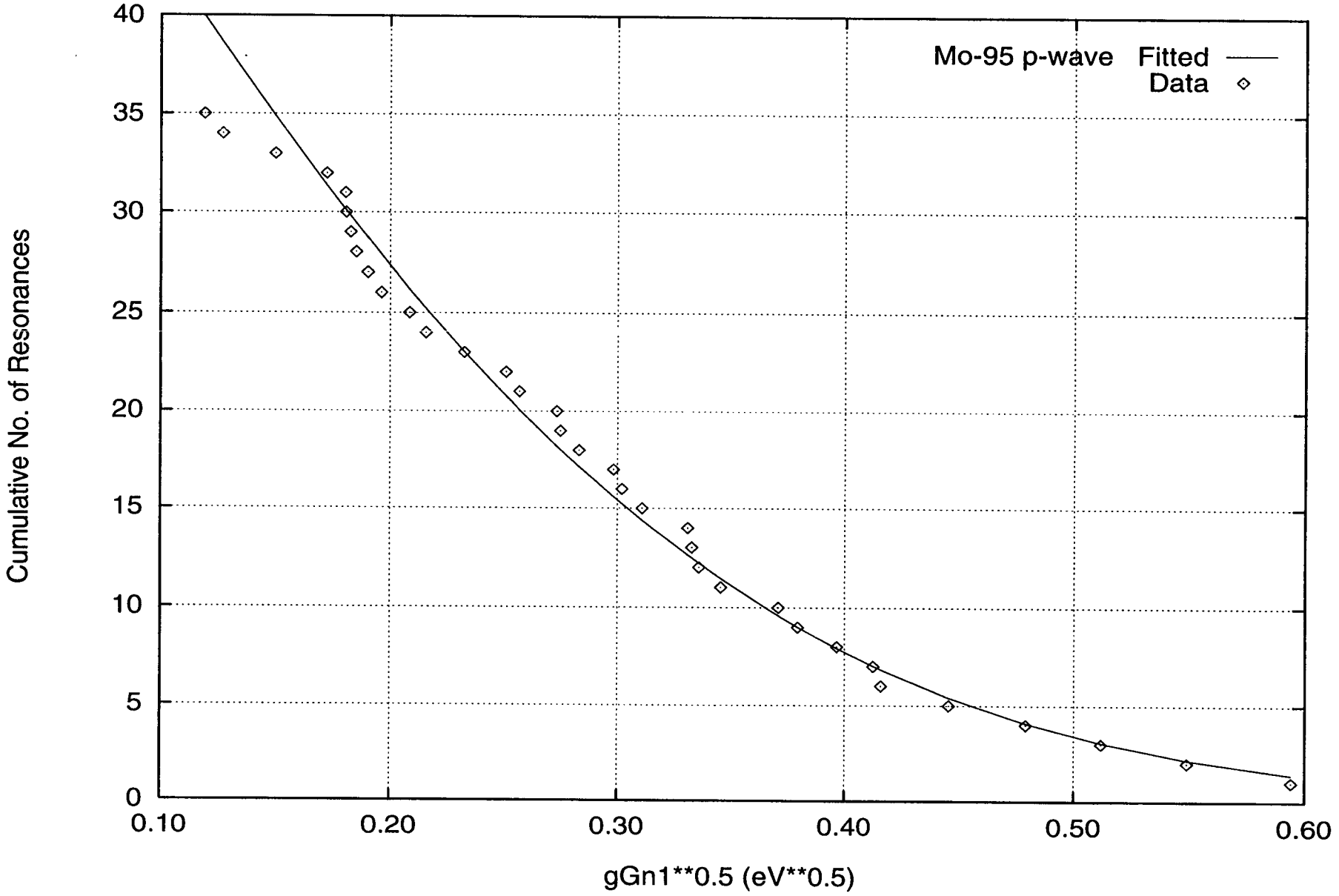

Fig. 3. Complement of the Cumulative Distribution of Neutron Reduced Widths (^{95}Mo, p-wave)

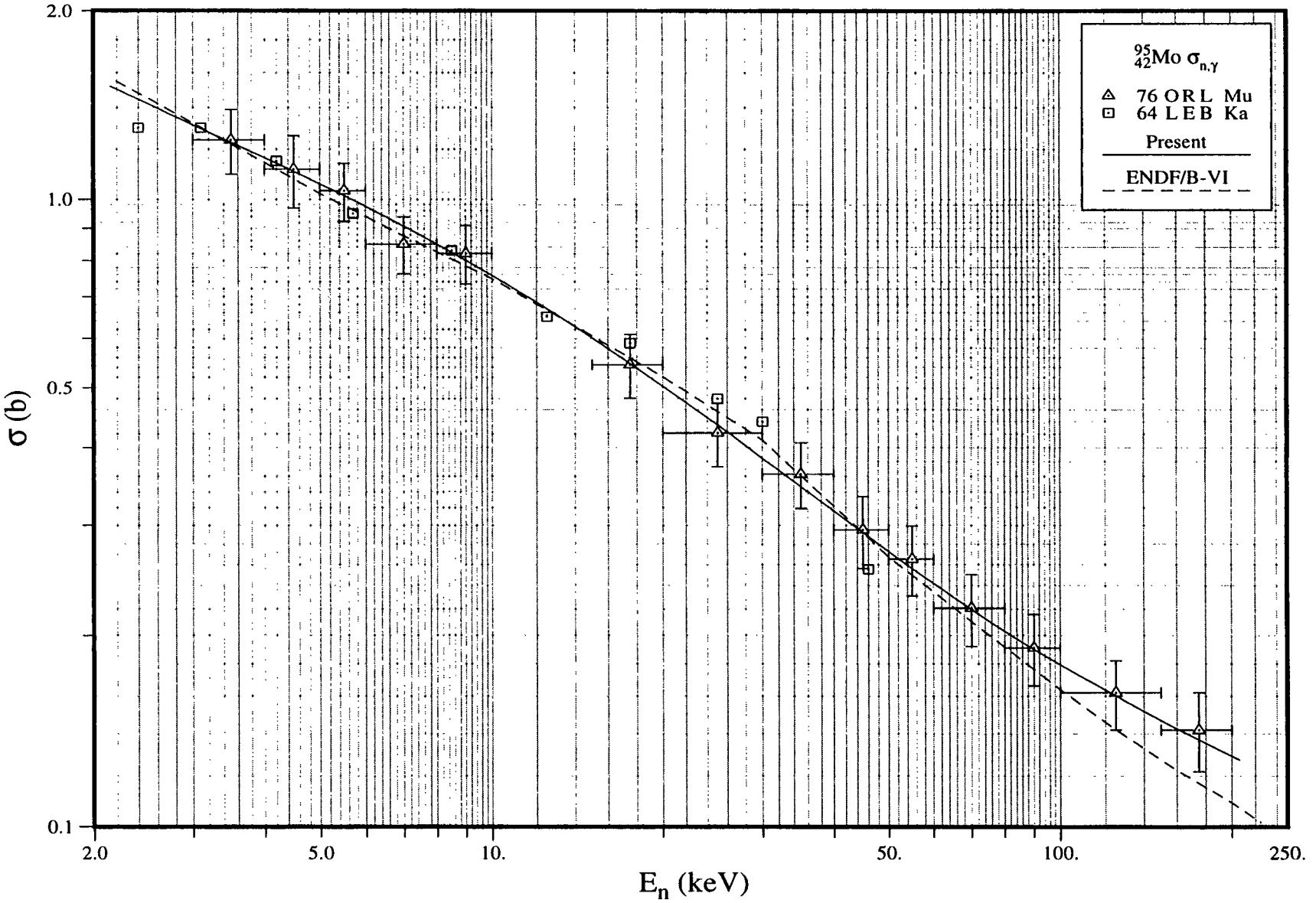

Fig. 4. Capture Cross Section in the Unresolved Resonance Region (^{95}Mo)

III.B. ^{99}Tc

1. Thermal Region

The thermal capture cross section at 0.0253 eV (2200 m/sec) and the bound coherent scattering amplitude were adopted from the BNL compilation [Mu81]. The capture cross section recently measured by Harada *et al.* [Ha95] was not considered since it was based on an incorrect half-life of ^{100}Tc. Harada *et al.* used 15.5 sec, while the recent recommended value is 15.8 sec [Au95]. A bound level was invoked to fit a coherent scattering amplitude of $b' = 6.8 \pm 0.3$ fm [Mu81] and the thermal capture cross section [Mu81]. To determine the parameters of the bound level, a potential scattering radius of $R' = 7.0$ fm, based on systematics study and optical model calculations [Mu84], was applied in the analysis. The resulting parameters are: $E_0 = -20.318$ eV, $J = 4$, $\Gamma_n = 35.5$ meV, and $\Gamma_\gamma = 109.5$ meV. **Table 4** summarizes the present calculated thermal values which are compared with previous evaluations. The calculated Westcott factor for capture is $g_W = 1.0036$.

2. Resolved Resonance Parameters

The BNL resonance parameter compilation of ^{99}Tc [Mu81] is based on available measurements prior to 1981. Recent measurements carried out at Geel by the Saclay group [Gu97, Ra97] reported resonance parameters up to 600 eV. This information was incorporated in the present evaluation. Because resonances above an energy of 1000 eV are not resolved, the upper energy of the resolved resonance region was set at this energy. The favored spin of the first resonance at 5.61 eV is 5. Since spins of other resonances were not determined experimentally, these were assigned randomly on the basis of the 2J+1 law for the density of resonances. **Figure 5** displays the result of the Porter-Thomas distribution analysis of reduced neutron widths, on the assumption that all resonances are treated as s-wave levels. Note that below 0.01 $(eV)^{1/2}$, there is an excess of weak resonances, indicating the presence of p-wave resonances. With this cutoff value, the analysis was carried out (**Fig. 6**), leading to an average s-wave level spacing, $D_0 = 15.4 \pm 2.0$ eV, and an s-wave strength function, $S_0 = 0.43 \pm 0.10$. Angular momentum assignments ($l = 0, 1$) were carried out with the help of Bayesian methodology. **Figure 7** displays the Porter-Thomas distribution for p-wave resonances. For a cutoff value of $(g\Gamma_n^l)^{1/2} > 0.13$ $(eV)^{1/2}$, we obtain the following values: $D_1 = 6.0 \pm 0.9$ eV and $S_1 = 7.3 \pm 1.6$. The latter value is consistent with optical model calculation [Mu84]. A comparison between the present average resonance parameters and previous evaluations is shown in **Table 5**.

Special attention was paid to the evaluation of the radiative width of the first positive-energy resonance at 5.58 eV. On the basis of recent [Gu97] and previous [Fi78, Wa70] measurements, we obtain $\Gamma_\gamma = 140$ meV for this resonance.

3. Unresolved Resonance Parameters

We set the boundary between the resolved and unresolved energy regions at 991 eV. Since the first excited level of ^{99}Tc is 140.5108 keV, the upper limit of the unresolved resonance region was set to 141.94 keV.

Three capture cross section measurements [Ch73, Li77, Ma82] are relevant to the unresolved energy region. When compared with the ORNL data [Ma82a], the RPI data [Li77] is high while the KFK data [Ch73] is low. As a starting point, the parameters obtained from the Porter-Thomas analysis in the resolved energy region were applied in the unresolved energy region. In addition, the average p-wave radiative width and the d-wave strength function are obtained from the systematics investigations [Mu84]. An energy-dependent level spacing with the relevant parameters of Mughabghab and Dunford [Mu98a], as well as a spin dispersion parameter of 2.8 [Mu98b], were applied in the calculation of the capture cross section. To fit the ORNL data [Ma82a], the average s-wave radiative width was adjusted from 173 meV to 130 meV. This value is consistent, within the error limits, with 115 ± 17 meV determined by Macklin [Ma82a]. In addition, an adjustment of the p-wave strength function was made from a value of 7.3 to 6.0.

The final unresolved resonance parameters are listed in **Table 6** and are compared with existing evaluated data files. The present parameters are also compared with those recommended in RIPL [Re98]: $\langle D_0 \rangle = 12.8 \pm 1.8$ eV, $S_0 = 0.48 \pm 0.07$, and $\langle \Gamma_{\gamma 0} \rangle = 160 \pm 50$ meV. The capture cross section constructed with the present average parameters is shown in **Fig. 8**.

Maxwellian average capture cross section for a temperature of 30 keV was calculated by the INTER computer code as 795 mb, which is consistent with a value of 782 ± 40 mb reported in Beer's compilation [Be92]. The calculation is performed up to 1 MeV with the aid of supplementary capture cross section in the energy region from 141.94 keV to 1 MeV, imported from ENDF/B-VI.

Table 4. Thermal Characteristics (^{99}Tc)

Quantity	Unit	BNL [Mu81]	98CRC [Ho98]	ENDF/B-VI	JEF-2.2	JENDL-3.2	Present
R'	fm	6.0 ± 0.5	-	7.91	6.0	6.0	7.0
b'	fm	6.8 ± 0.3	6.8 ± 0.3	7.38		5.22	6.75
σ_γ	barn	20 ± 1	23 ± 2	19.6	19.1	19.6	20.0
σ_s	barn	-	-	6.88	3.54	3.43	5.81
RI-capt.	barn	340 ± 20	400 ± 40	350	304	312	312

Table 5. Parameters of the 5.58 eV Resonance of ^{99}Tc

Parameter	Unit	BNL [Mu81]	ENDF/B-VI*	JENDL-3.2	Gunsing [Gu97]	Present
$g\Gamma_n$	meV	1.755	2.25	1.885	1.864	1.806
Γ_γ	meV	177 ± 18	134	168.1	149.2	140

* ENDF/B-VI uses a bound resonance at –6.4 eV.

Table 6. Average Resonance Parameters for Unresolved Resonance Region (^{99}Tc)

Quantity	Unit	ENDF/B-VI	JEF-2.2	JENDL-3.2	BNL [Mu81]	Present	
						PT Analysis	Adopted
R'	fm	7.91	6.80	6.216	6.0±0.5		7.00
$<D_0>$	eV	12.1	18.34	20.6	10.7±1.8	15.4±2.0	15.4**
S_0	$\times 10^{-4}$	0.43	0.55	0.54*	0.45±0.05	0.43±0.10	0.43
$<\Gamma_{\gamma 0}>$	meV	122	131	187	160		130
$<D_1>$	eV	6.10	9.49	10.29		6.0±0.9	7.68**
S_1	$\times 10^{-4}$	3.88	8.94	5.52*		7.3±1.6	6.0
$<\Gamma_{\gamma 1}>$	meV	122	131	187			140
$<D_2>$	eV	-	6.70	6.86			5.25**
S_2	$\times 10^{-4}$	-	0.55	0.64*			1.0
$<\Gamma_{\gamma 2}>$	meV	-	131	187			130

* Value at the low energy (4.219 keV) range of the unresolved resonance region.
** Value at the neutron separation energy of ^{100}Tc.

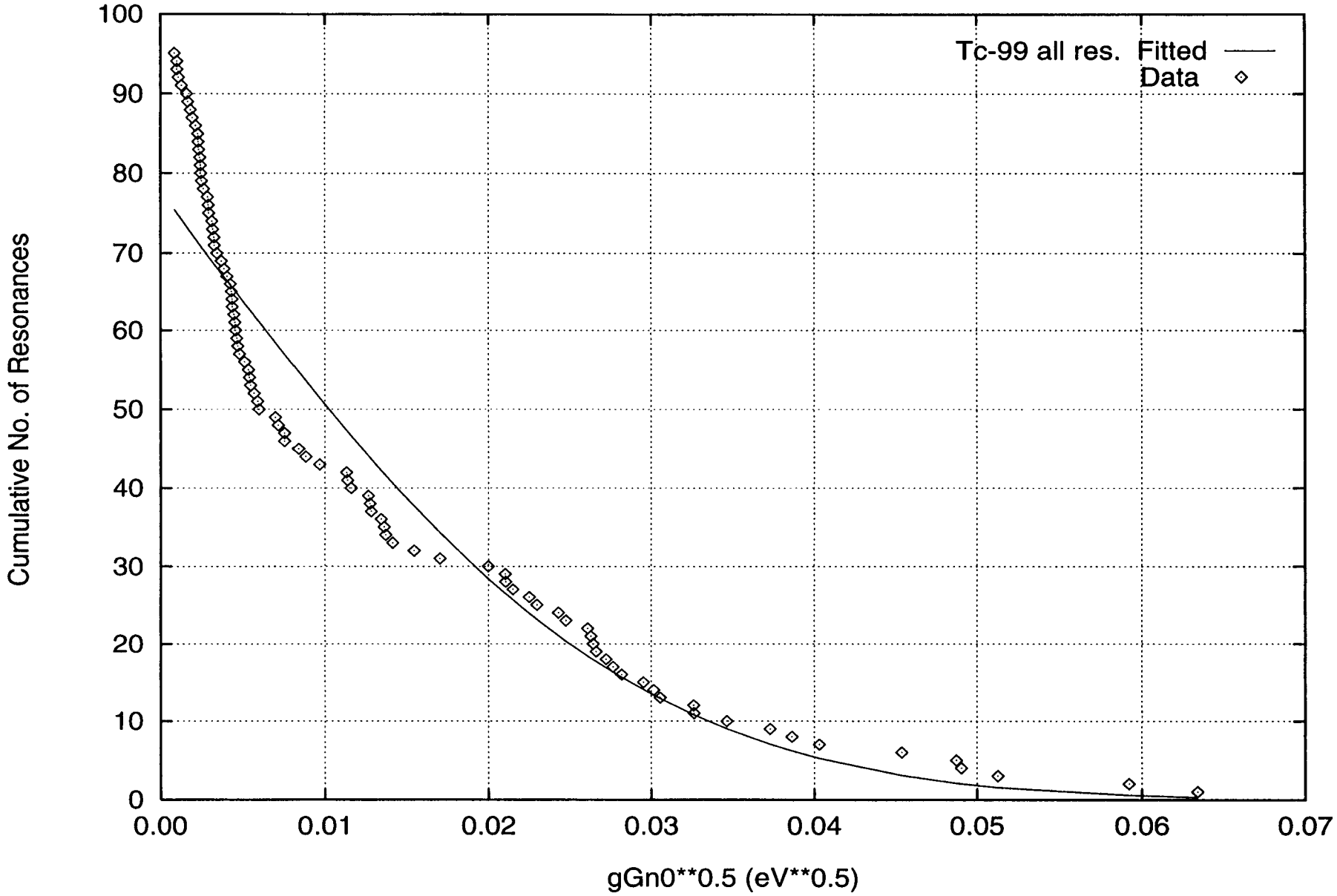

Fig. 5. Complement of the Cumulative Distribution of Neutron Reduced Widths (^{99}Tc). All resonances were assumed as s-wave.

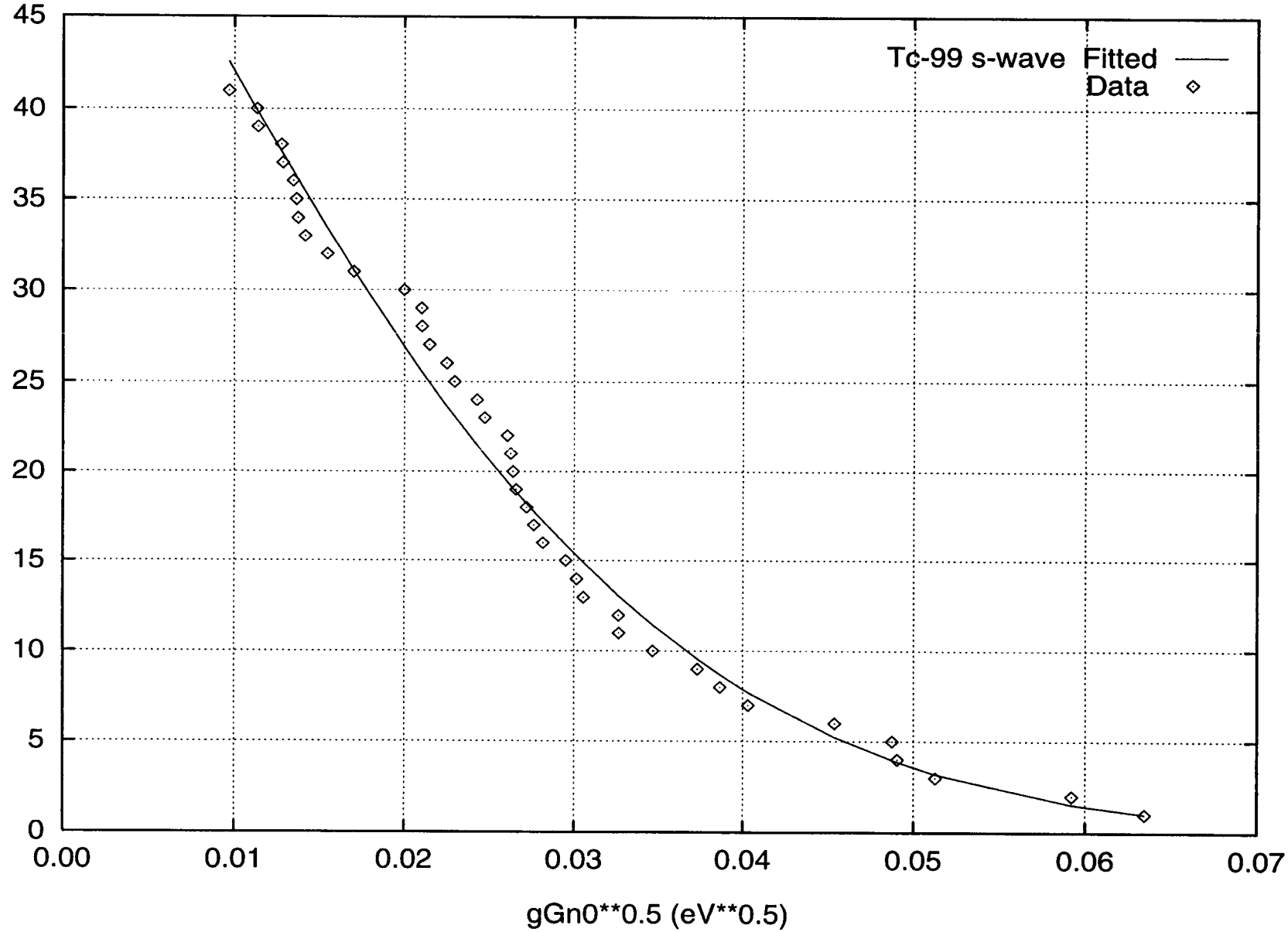

Fig. 6. Complement of the Cumulative Distribution of Neutron Reduced Widths (^{99}Tc, s-wave)

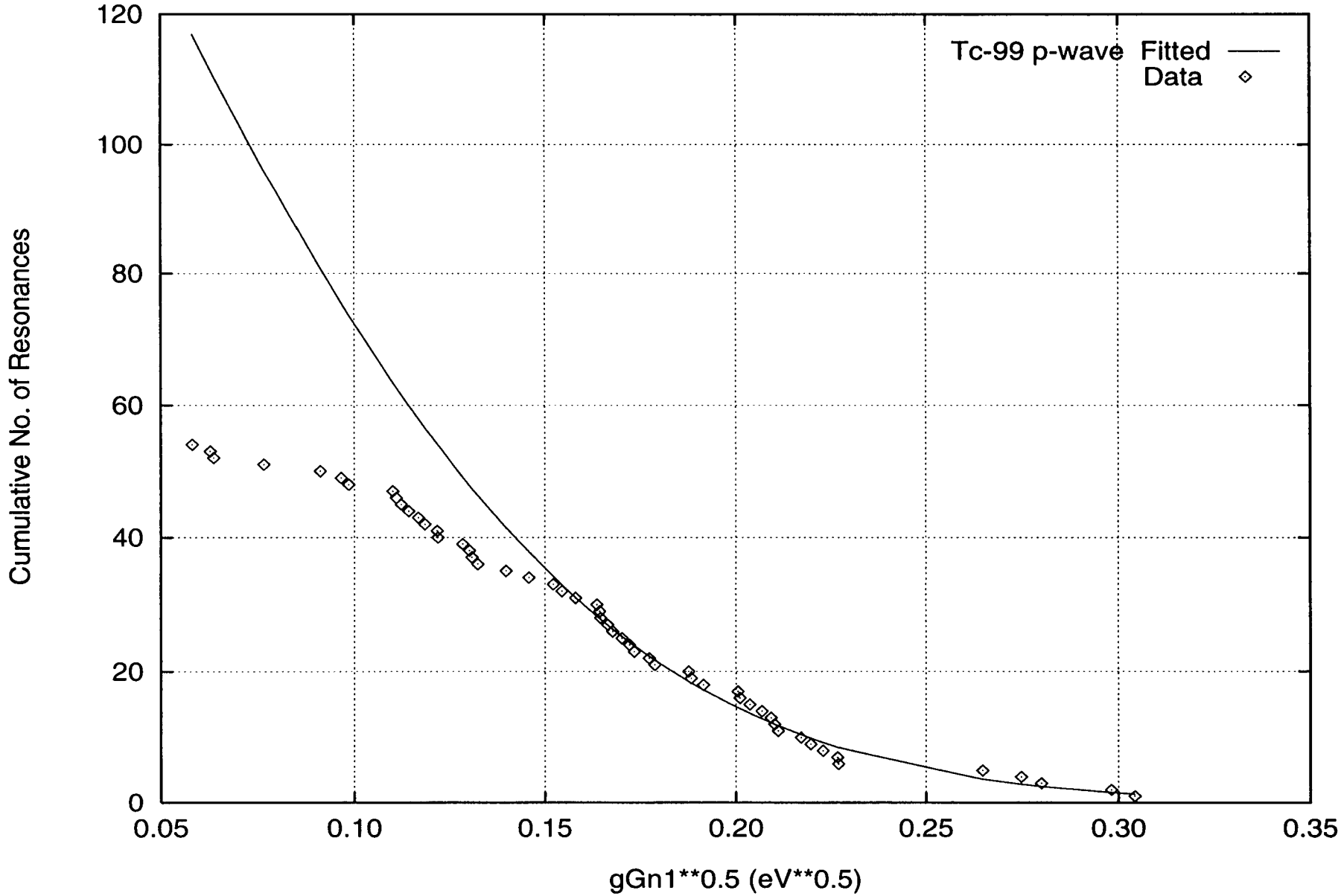

Fig. 7. Complement of the Cumulative Distribution of Neutron Reduced Widths (^{99}Tc, p-wave)

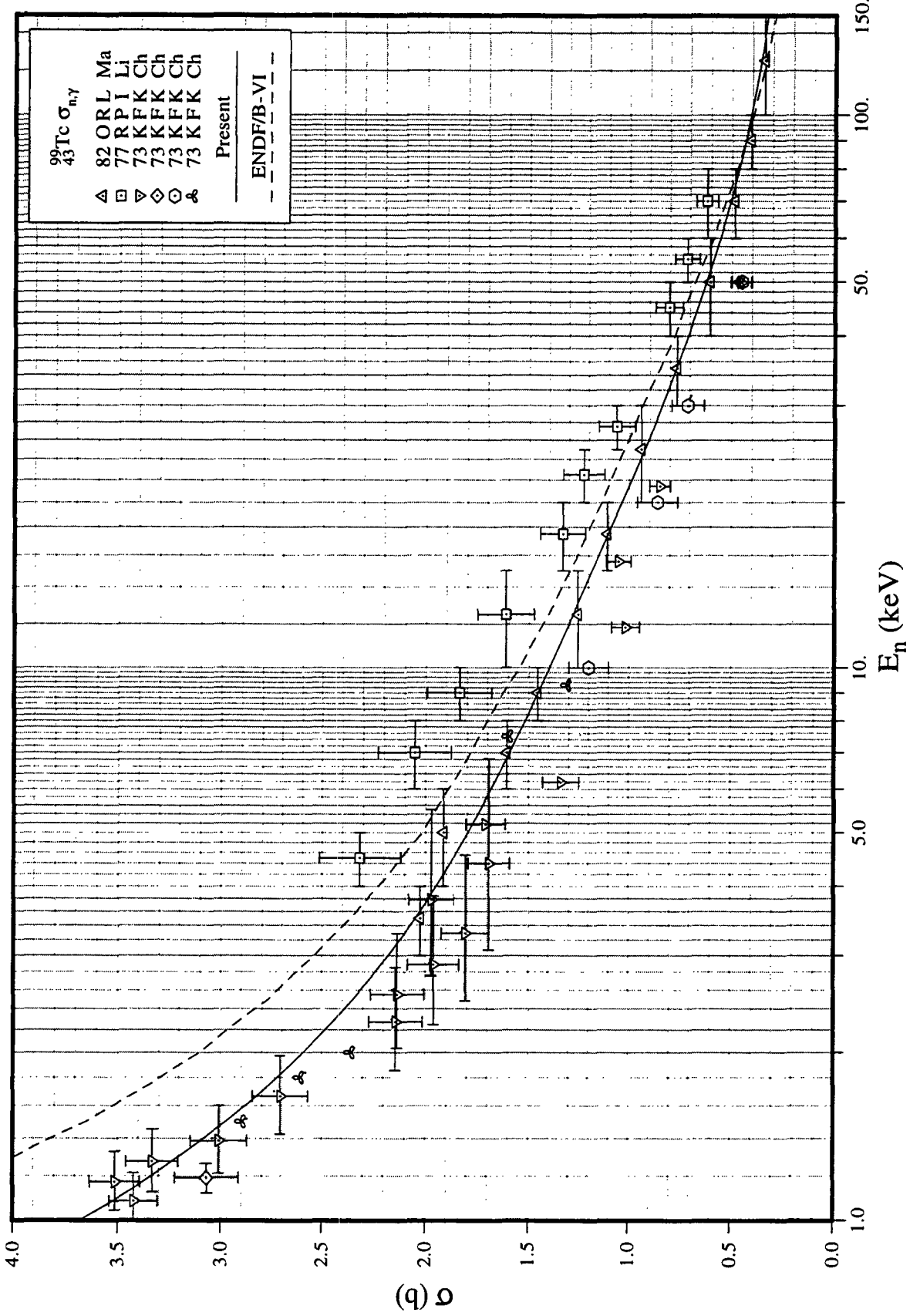

Fig. 8. Capture Cross Section in the Unresolved Resonance Region (^{99}Tc)

III.C. ^{101}Ru

1. Thermal Region

A capture cross section of 3.45 b is computed at 0.0253 eV from the present evaluation of the resonance parameters. This value is consistent with Halperin's measurement [Ha65], which yields $\sigma_\gamma = 3.0$ b, and with Mughabghab's BNL compilation [Mu81], $\sigma_\gamma = 3.4 \pm 0.9$ b. The former value is obtained by correcting for reactor neutrons by using a resonance integral of 100 b as calculated from the resonance parameters. Bound levels are not required to describe the capture cross section at thermal energies. A comparison of our thermal cross sections, as well as resonance integrals, with other evaluations is made in **Table 7**.

2. Resolved Resonance Parameters

Measurement by Anufriev *et al.* [An85] in the energy region from thermal energy to 1720 eV, which was not cited in the BNL compilation [Mu81], was included in the present evaluation. In addition, weak observed resonances, identified as belonging to ^{101}Ru, were included in the present evaluation. Because of poor energy resolution [An85], the resonance parameters above 62 eV were not considered. Above this energy, the resonance parameters of the BNL compilation were adopted. Because of lack of measurements in the energy region from 1.035 to 2.661 keV, Macklin and Halperin's [Ma80] resolved resonance parameters above 2.6 keV were not included in this evaluation.

The average radiative width, calculated from the known 11 radiative widths below 1.035 keV, is 184±10 meV; this value was assumed for resonances with unreported radiative widths. This average is consistent with the values, 180±15 meV reported in the BNL compilation, 187±16 meV, determined by Macklin and Halperin [Ma80] for 10 resonances in the energy region 2.874-4.433 keV, and 175 meV of Popov *et al.* [Po79]. However, it is smaller than 219±19 meV determined by Anufriev *et al.* [An85]. Of a total of 48 resonances, 41 were assigned as s-wave and 7 as p-wave from the Bayesian analysis. Resonance spins were assigned randomly on the basis of the (2J+1) dependence of the level density to resonances for which the spin was not determined.

The distribution of reduced neutron widths was analyzed by fitting the widths to the Porter-Thomas distribution. As shown in **Fig. 9** none of the weak resonances was excluded from the fitting. The fit resulted in $\langle D_0 \rangle = 19.3 \pm 1.8$ eV and $\langle g\Gamma_n^0 \rangle = 1.21 \pm 0.28$ meV. These values yield s-wave strength function of $S_0 = 0.62 \pm 0.15$. The present $\langle D_0 \rangle$ is consistent with values reported in the BNL compilation (D = 16±2 eV), RIPL [Re98] (18±3 eV), and Popov *et al.* [Po79] (18±2 eV). The S_0 value is consistent with those of Macklin and Halperin [Ma80] (0.59±0.04) and Popov *et al.* [Po79] (0.61±0.13). However, it is somewhat larger than the values quoted in the BNL compilation (0.54±0.04), RIPL [Re98] (0.56±0.05), and Anufriev *et al.* [An85] (0.547±0.015). For p-wave resonances, a fit to the Porter-Thomas distribution yielded unreliable results due to the limited number of assigned p-wave resonances.

3. Unresolved Resonance Parameters

The present unresolved resonance region covers the energy range from 1.035 keV to 128.49 keV. The latter energy corresponds to the threshold energy of inelastic neutron scattering to the first excited level of ^{101}Ru. In this region, the average resonance parameters for s-, p- and d-wave were provided. Since the upper energy of the unresolved resonance region is relatively high, d-wave contribution is not negligible. An energy-dependent level spacing according to Gilbert-Cameron level density formula with associated parameters adopted from Mughabghab and Dunford [Mu98a] was applied in the calculations. On the basis of the (2J+1) dependence of the level density, level spacings for p- and d-waves were assumed to be 1/2 and 1/3 of the s-wave spacing, respectively.

The average capture cross section measurement by Macklin and Halperin [Ma80], corrected later by Macklin and Winters [Ma81], was considered in this evaluation. As a first attempt in the evaluation of the capture cross section, the following parameters were implemented: 1) $\langle D_0 \rangle$ and S_0 values which were derived from resolved resonances; 2) S_1 and S_2 values of Macklin and Halperin; and 3) $\langle \Gamma_\gamma \rangle$ = 184 meV for s-, p- and d-wave resonances. These parameters resulted in a calculated capture cross section which is in good agreement with the measurement [Ma80, Ma81] below 100 keV, but above 100 keV 5% it is larger than the measurement. Subsequently, to achieve an improved fit at the high energy, S_2 was reduced to 1.2. This S_2 value is consistent with reported measured values in the mass region around A=100 [Mu84, Fig. 5]. The finalized parameters of the present evaluation are listed in **Table 8**. The capture cross section data and the final calculated fit are shown in **Fig. 10**.

Maxwellian-averaged capture cross section for a temperature of 30 keV was computed as 970 mb. In the INTER calculation up to 1 MeV, the capture cross sections for the energy region from 127 keV to 1 MeV were adopted from the ENDF/B-VI evaluation. The present cross section is compared with 996±40 mb reported in Beer's compilation [Be92] and 1011 mb in the BNL compilation [Mu81].

Table 7. Thermal Characteristics (^{101}Ru)

Quantity	Unit	BNL Compilation	98CRC [Ho98]	ENDF/ B-VI	JEF-2.2	JENDL-3.2	Present
R'	fm			5.617	6.9	6.1	6.53
σ_γ^0	barn	3.4±0.9	5±1	3.43	3.41	3.36	3.45
σ_s^0	barn			3.23	5.05	3.74	4.50
gw*				1.003	1.001	1.001	1.0016
RI-capt.**	barn	100±20	110±30	111	111	100	111
RI-total**	barn			184	200	173	200

* Westcott factor for capture cross section.

** Integrated from 0.5 eV to 100 keV with 1/E spectrum.

Table 8. Average Resonance Parameters for the Unresolved Resonance Region (^{101}Ru)

Quantity	Unit	BNL [Mu81]	ENDF/VI	JEF-2.2	JENDL-3.2*	Present	
						PT Analysis	Adopted
R'	fm		5.617	6.90	5.062		6.53
$\langle D_0 \rangle$	eV	**	20.42	18.29	25.58	19.3±1.8	19.3$^+$
S_0	$\times 10^{-4}$	0.54±0.04	0.59	0.59	0.59	0.62±0.15	0.62
$\langle \Gamma_{\gamma 0} \rangle$	meV	180±15	180	180.3	173		183.7
$\langle D_1 \rangle$	eV		8.75	9.53	12.79		9.65$^+$
S_1	$\times 10^{-4}$	6.1±0.4	6.00	6.10	6.10		6.10
$\langle \Gamma_{\gamma 1} \rangle$	meV		180	190.4	173		183.7
$\langle D_2 \rangle$	eV		6.30	6.76	8.53		6.43$^+$
S_2	$\times 10^{-4}$		2.00	1.12	0.53		1.20
$\langle \Gamma_{\gamma 2} \rangle$	meV		180	180.3	173		183.7

* Average parameters at the low energy (1.06 keV) of the unresolved region.

** mean observed level spacing = 16±2 eV.

+value at the neutron separation energy of ^{102}Ru.

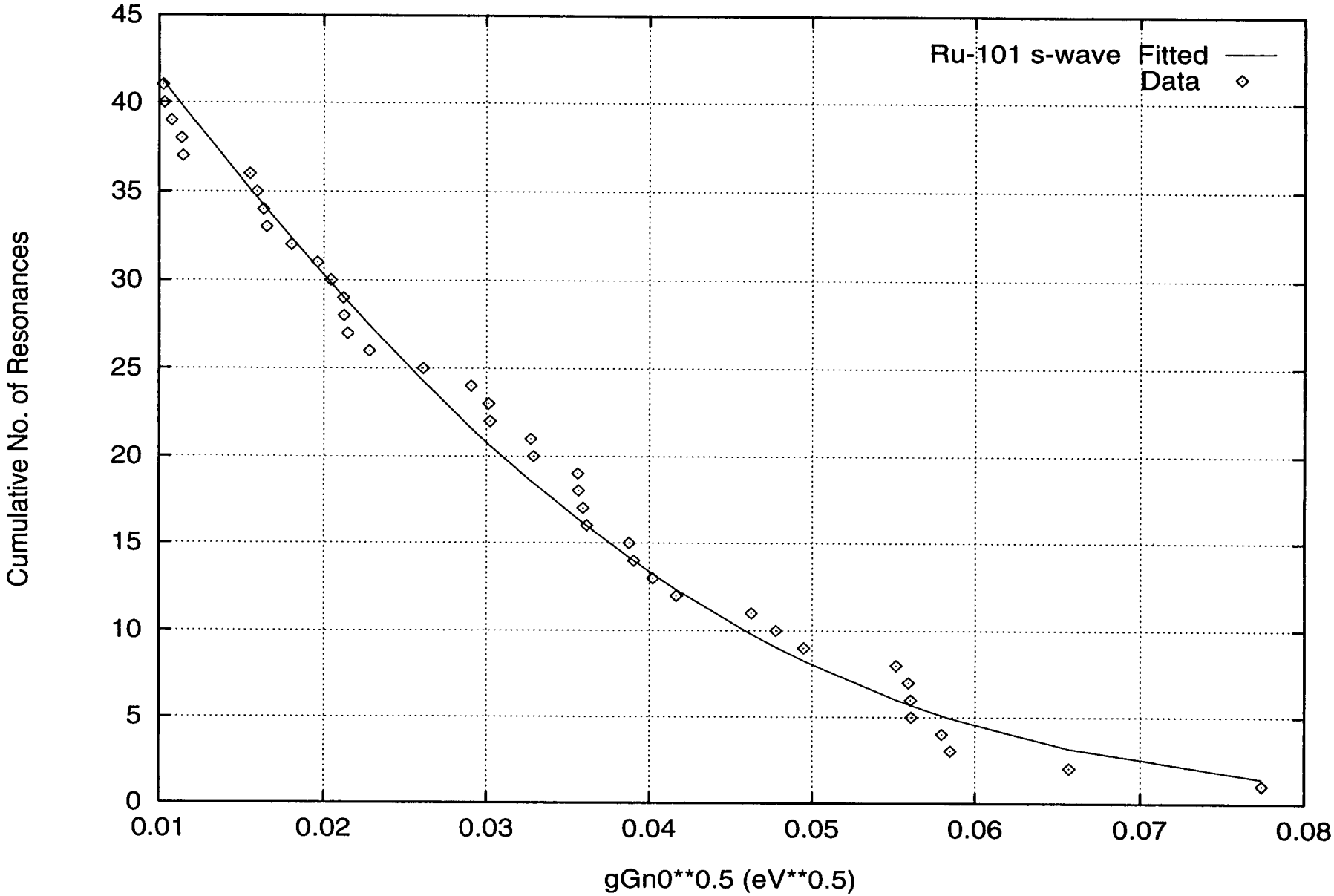

Fig. 9. Complement of the Cumulative Distribution of Neutron Reduced Widths (^{101}Ru, s-wave)

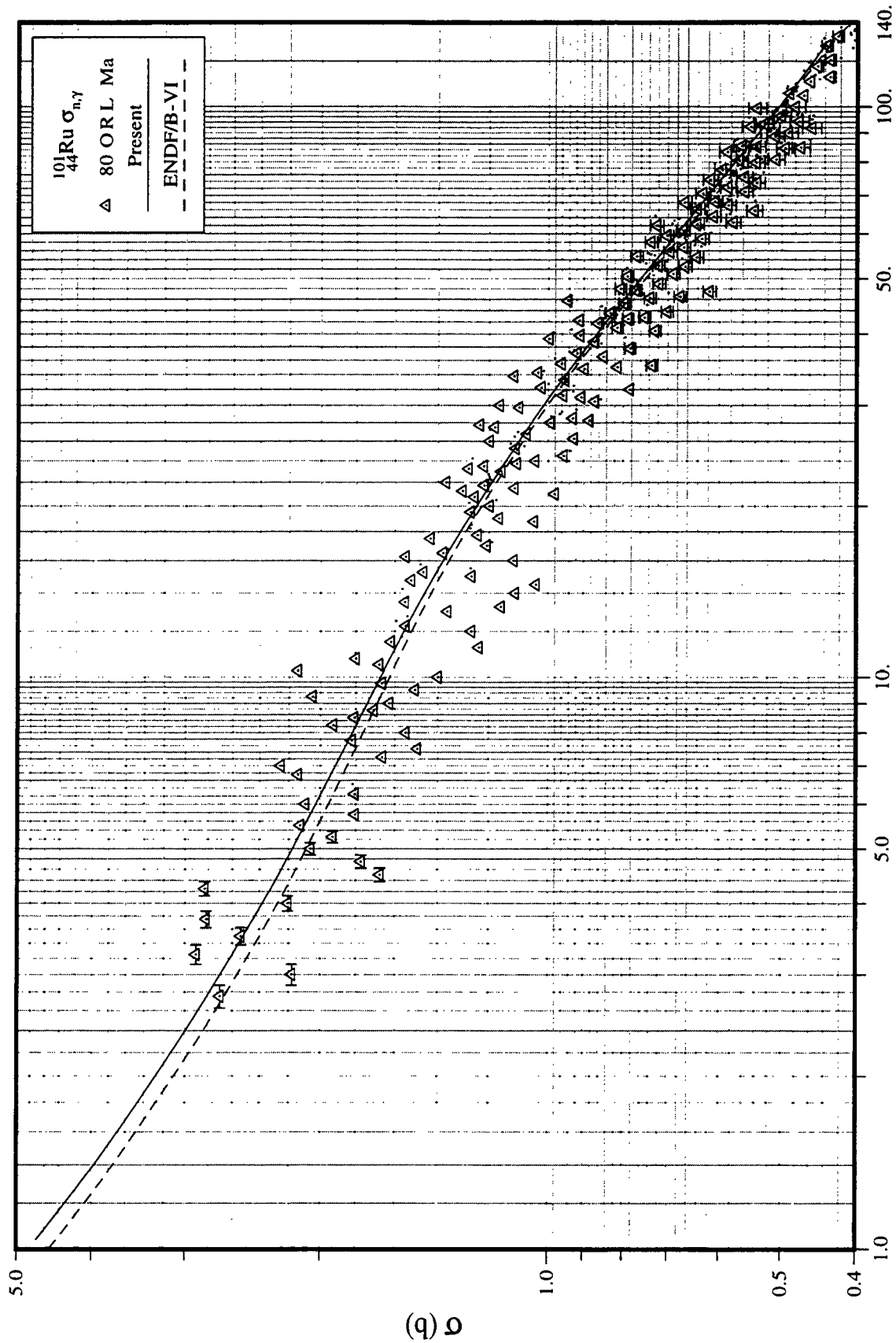

Fig. 10. Capture Cross Section in the Unresolved Resonance Region (^{101}Ru)

III.D. ^{103}Rh

1. Thermal Region

Known positive-energy neutron resonances account for the thermal capture cross section [Mu81], but not the bound coherent scattering length, $b' = 5.88 \pm 0.04$ fm, reported by Koester [Ko91]. On this basis, a bound level is postulated to account for the discrepancy in the coherent scattering length. This is achieved by decreasing the radiative width of the first resonance at 1.259 eV from 154 meV to 151 meV. This provides about 2.25 barns of capture contribution for the bound level. With this condition, the parameters of a bound level are determined as: $E_0 = -55$ eV, $\Gamma_n = 101$ meV, and $\Gamma_\gamma = 160$ meV. In this calculation, an effective scattering radius of 6.56 fm was adopted from the work of Ribon [Ri70]. The Westcott factor for capture is calculated as 1.0229. The thermal characteristics are summarized in **Table 9** and are compared with other evaluations.

2. Resolved resonance parameters

Transmission data of Ribon [Ri70] at Saclay covered the energy region up to 4140 eV. In addition, the capture data of Carlson [Ca71b] covered the energy region up to 989 eV. Macklin [Ma80] reported parameters from capture measurements in the energy region from 2644 to 4163 eV. The upper limit of the present resolved resonance region is set to 4.116 keV.

According to Macklin [Ma80], there is a problem with Ribon's energy scale [Ri70]. In this evaluation, correlation analysis between Macklin's energies and those of Ribon show that the time of flights are related by:

$$t = 0.99906891 + 6.0584518 \times 10^{-5} t_{Ribon} \ .$$

We note that Macklin's $g\Gamma_n$ values are about 1.5 times larger than those of Ribon in the overlapping energy regions. On the other hand, there is good agreement between Ribon's and Carlson's $g\Gamma_n$ values. Because of these considerations, Macklin's scattering widths are not included in the present evaluation. This is additionally supported by the observation that the derived average parameters, S_0, S_1, and S_2 [Ma80] are about a factor 1.5 larger than the corresponding values obtained from the systematics studies [Mu81]. However, we adopted Macklin's energy scale.

The *l* assignments were performed by the Bayesian method. For all observed resonances, the resulting cumulative Porter-Thomas distributions are displayed in **Fig. 11**. For s- and p-wave resonances, the fits are shown in **Fig. 12** and **Fig. 13,** respectively. The average resonance parameters for s- and p-wave resonances, derived from this analysis, are summarized in **Table 10** and are compared with [Mu81], as well as other evaluations.

3. Unresolved Resonance Parameters

Since the first excited level of ^{103}Rh is 39.756 keV, the upper limit of the unresolved resonance region is set to 40.15 keV.

With the exception of minor adjustments in the s-wave radiative width and the p-wave strength function, the average resonance properties, obtained from the analysis of the resolved energy region, were adopted. The level spacing is assumed to vary with energy and spin according to the Gilbert-Cameron's level density formula; the associated parameters [Mu98a] and spin dispersion parameter of 3.1 were adopted from [Mu98b]. The average p-wave radiative width and the d-wave average parameters, assumed in this evaluation, are based on the systematics investigation [Mu84]. The capture cross section in the unresolved energy region, generated on the basis of the present average parameters, listed in the last column of **Table 10**, is shown in **Fig. 14**. In the present evaluation, the capture data by Wisshak *et al.* at Karlsruhe [Wi90] and Bokhovko at Obninsk [Bo85] were considered. Earlier measurements were reported in the curve book of McLane *et al.* [Mc88]. The calculated capture cross section of the present study shows good agreement with the recent data of [Wi90] up to 100 keV.

Maxwellian average capture cross section for a temperature of 30 keV for the energy region 10^{-5} eV to 225 keV was computed as 809 mb. This is in excellent agreement with a value of 810 ± 15 mb [Be92].

Table 9. Thermal Characteristics (^{103}Rh)

Quantity	Unit	BNL [Mu81]	ENDF/B-VI	JEF-2.2	JENDL-3.2	Present
R'	fm	6.2 ± 0.3	7.09	6.20	6.20	6.56
b'	fm	5.0 ± 0.1	6.13			5.88
σ_γ	barns	145 ± 2	147	146	147	145
σ_s	barns		4.69	3.43	3.28	4.37
RI-capt.	barns	1100 ± 50	1035	1035	1040	1036

Table 10. Average Resonance Parameters in Unresolved Resonance Region (^{103}Rh)

Value	Unit	ENDF/B-VI	JEF-2.2	JENDL-3.2[a]	BNL [Mu81]	Present	
						PT Analysis	Adopted
R'	fm	7.09	6.20[b] (6.56)[c]	6.20[b] (6.521)[c]	6.2±0.3		6.56
$<D_0>$	eV	10.12	25.77	32.13$^+$	16±1	28.6±1.6	28.6[d]
S_0	$\times 10^{-4}$	0.43	0.485	0.445	0.53±0.05	0.57±0.09	0.57
$<\Gamma_{\gamma 0}>$	meV	153	161.25	230	160±15		170
$<D_1>$	eV	13.5	11.86	14.28$^+$		14.5±0.6	14.3[d]
S_1	$\times 10^{-4}$	5.6	6.332	4.15	5.5±0.9	5.0±0.6	4.81
$<\Gamma_{\gamma 1}>$	meV	153	161.25	230			150
$<D_2>$	eV		7.52	8.57$^+$			9.48[d]
S_2	$\times 10^{-4}$		0.595	0.53			1.0
$<\Gamma_{\gamma 2}>$	meV		161.25	230			140

a) Value at the low energy (3.58 keV) of the unresolved resonance region.
b) For the resolved energy region.
c) For the unresolved energy region.
d) Value at the neutron separation energy of ^{104}Rh.

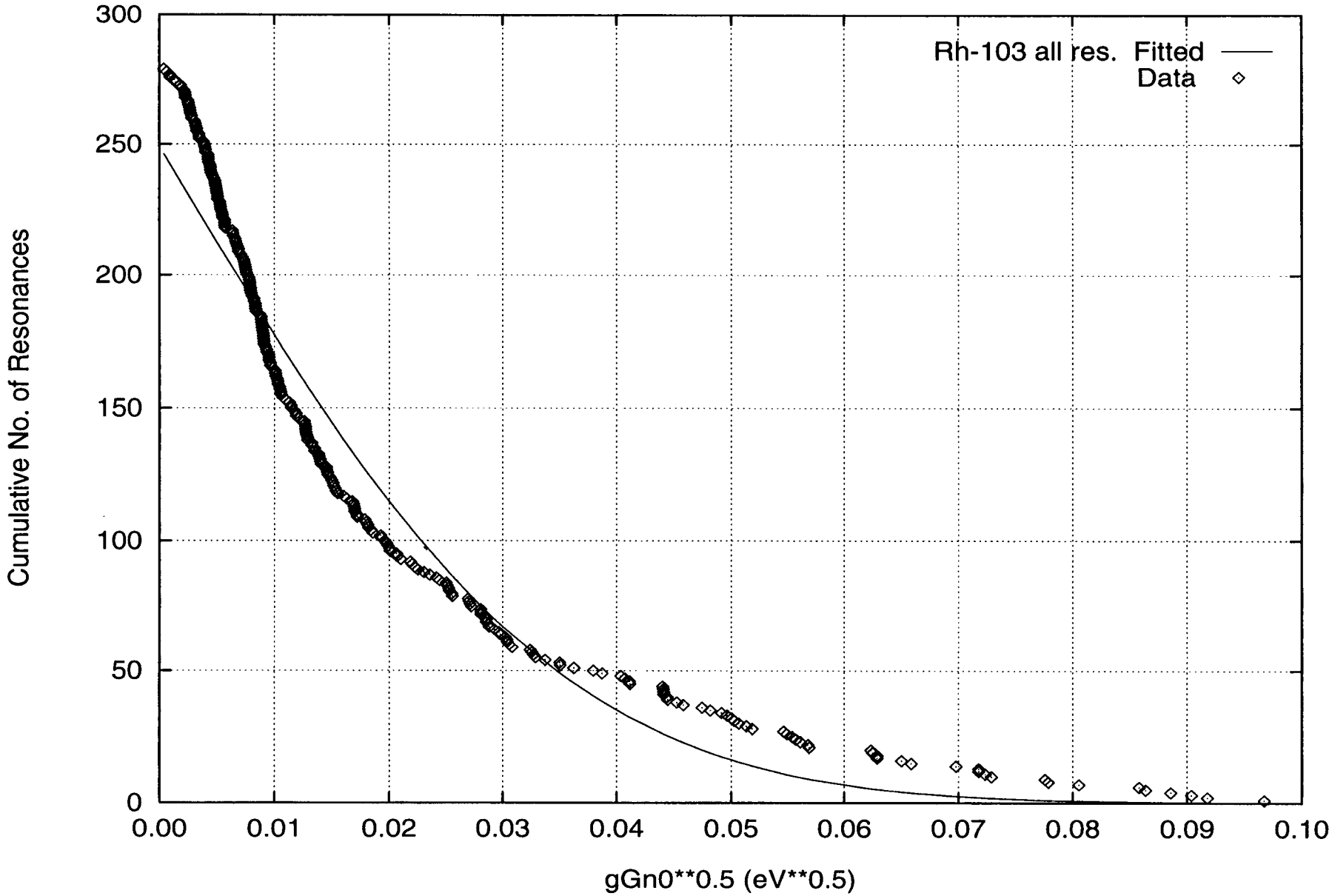

Fig. 11. Complement of the Cumulative Distribution of Neutron Reduced Widths (^{103}Rh). All resonances were assumed as s-wave.

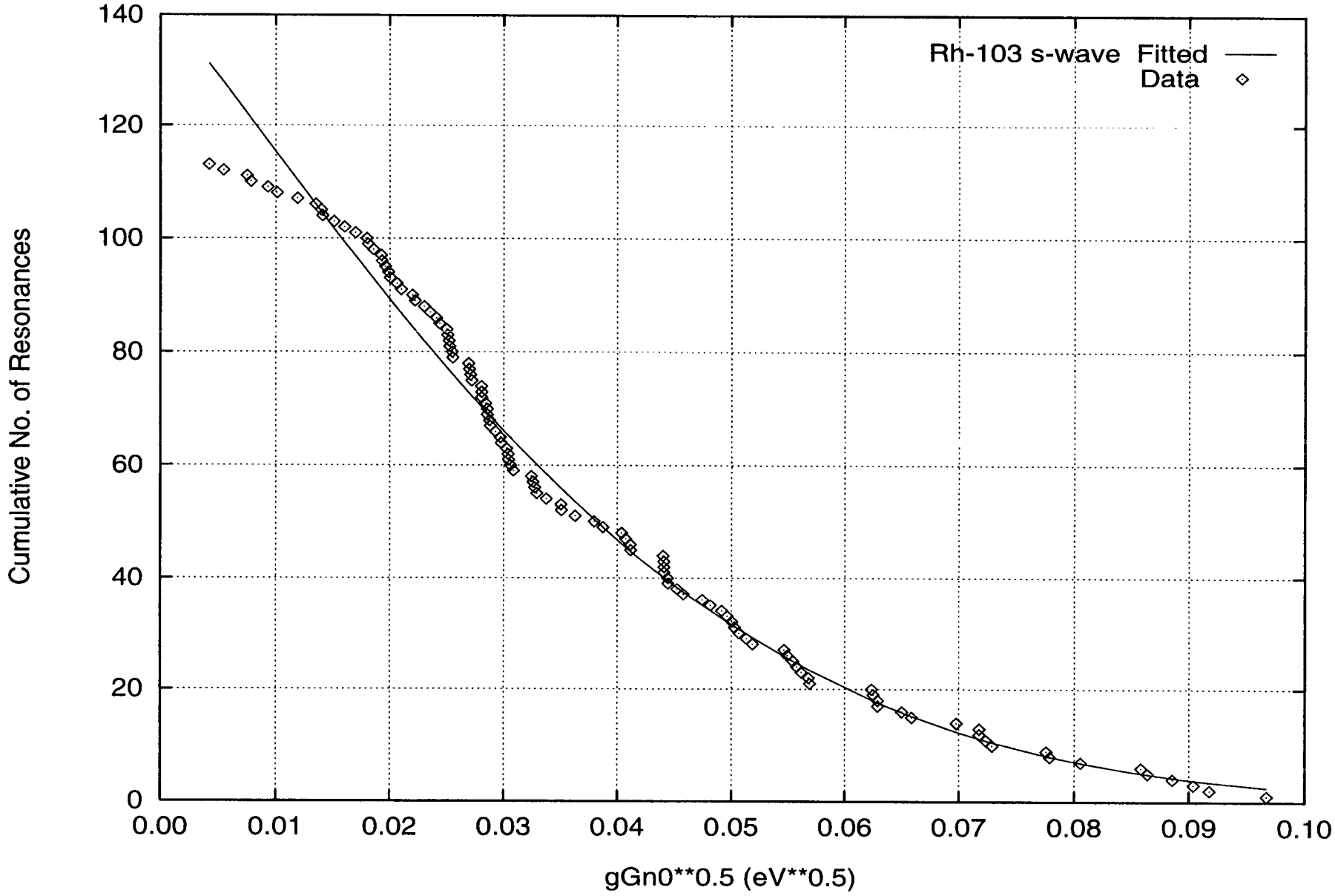

Fig. 12. Complement of the Cumulative Distribution of Neutron Reduced Widths (^{103}Rh, s-wave)

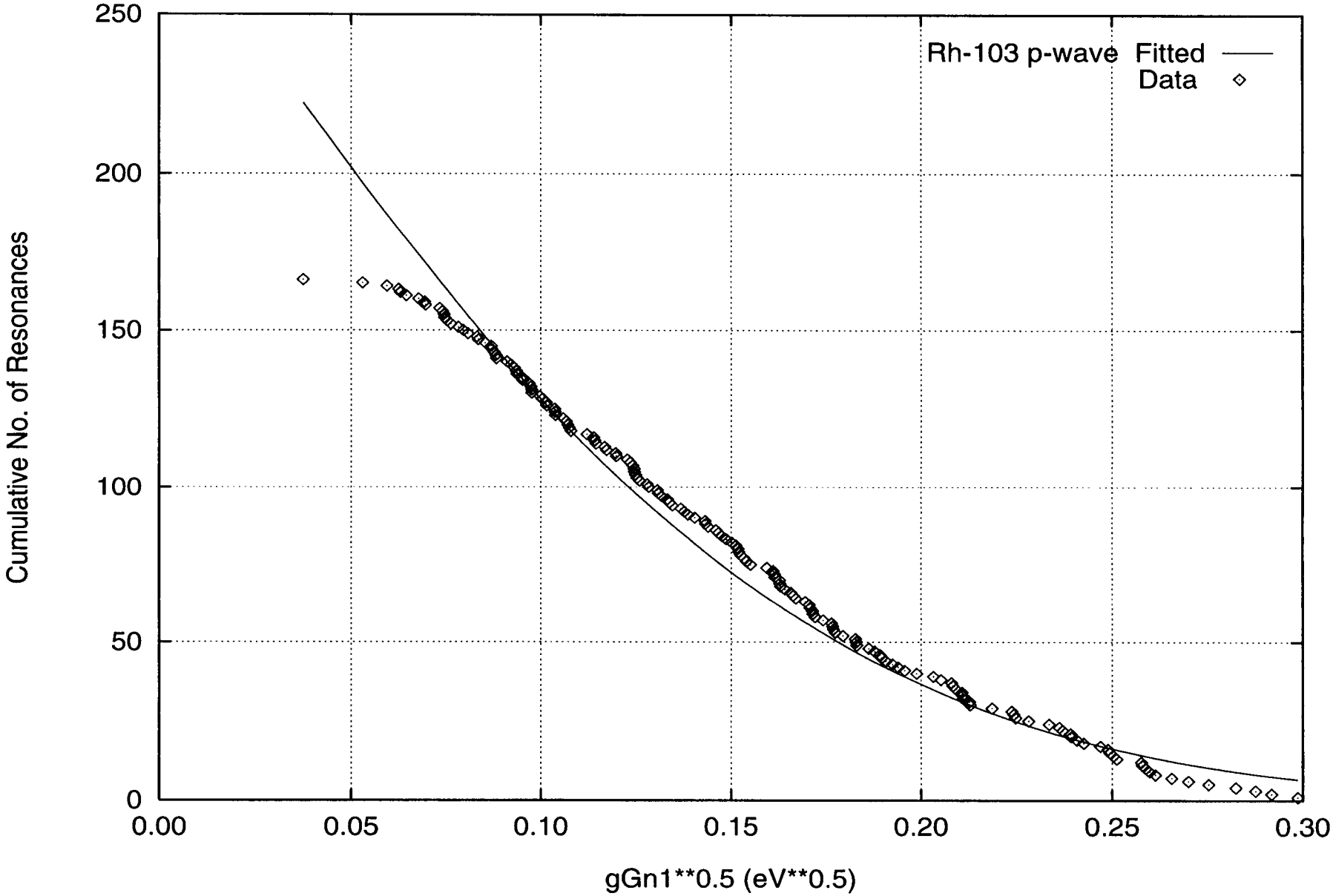

Fig. 13. Complement of the Cumulative Distribution of Neutron Reduced Widths (^{103}Rh, p-wave)

Fig. 14. Capture Cross Section in the Unresolved Resonance Region (^{103}Rh)

III.E. ^{105}Pd

1. Thermal Region

An evaluated thermal capture cross section of ^{105}Pd, $\sigma_\gamma^0 = 20.8$ b, was obtained by taking a weighted average of 22.0±1.5 b [Bu82] and 20.4±0.9 b. The latter was derived by subtracting the isotopic contributions from a value of 6.6±0.1 b for the natural element [An80]. Since the contribution of positive energy resonances to the thermal capture cross section at 0.0253 eV is only 2.3 b, one or more s-wave bound levels are required to fit the thermal capture cross section. An examination of the gamma-ray spectra of thermal neutrons [Or70] indicates that two bound levels with spins 2 and 3 and about equal contribution to the thermal capture cross section are required. As a starting point in the fitting procedure, we adopted Glaettli *et al.*'s [Gl87] incoherent scattering length, $b_+ - b_- = -5.2\pm3.8$ fm, and a coherent scattering length, b = 7.3 fm, by the subtraction method. However, with these values it was not possible to obtain consistent results. Final adjustments, principally in the incoherent scattering length, had to be made. The bound level parameters are presented in **Table 11**. With these parameters, $\sigma_{coh} = 7.263$ b (b = 7.61 fm), $\sigma_{inc} = 0.052$ b ($b_+ - b_- = -1.3$ fm), and $\sigma_\gamma^0 = 20.9$ b. Comparisons of the thermal cross sections and resonance integrals of the present evaluation with those of ENDF/B-VI, JEF-2 and JENDL-3 are summarized in **Table 12**. Note the large difference between the present evaluation of the scattering cross section and those in the other evaluations.

2. Resolved Resonance Parameters

Resonance parameters measured by Staveloz *et al.* [St79] were adopted in this evaluation. These preliminary results were the main source in Mughabghab's BNL compilation in 1981 [Mu81]. Of a total of 198 positive-energy resonances, 141 resonances were assigned as s-wave and 57 as p-wave on the basis of the Bayesian analysis. Uncertainty-weighted averaging of 70 radiative widths, which were reported by Staveloz *et al.* [St79], resulted in an average value of 148±4 meV; this value was assumed for the remaining resonances. Resonance spins were assigned randomly to those resonances for which the spin had not been determined. This random assignment assumes that the level density is proportional to (2J+1).

The distributions of s- and p-wave reduced neutron widths were analyzed by fitting to a Porter-Thomas distribution. For the s-wave case, resonances with reduced widths smaller than 0.08 meV were excluded in the fitting procedure to minimize the χ^2 value. In **Fig. 15**, the fit to the data resulted in $\langle D_0 \rangle = 10.32\pm0.47$ eV and $\langle g\Gamma_n^0 \rangle = 0.68\pm0.08$ meV. These values yield s-wave strength function of $S_0 = 0.66\pm0.08$. The present $\langle D_0 \rangle$ is consistent with values reported by Staveloz *et al.* [St79], BNL compilation (10.0±0.5) [Mu81], and RIPL [Re98] (10.3±0.5). The present S_0 is consistent with those reported in the BNL compilation (0.6±0.1), RIPL (0.60±0.05), and by Staveloz *et al.* (0.63±0.07). In addition, the possible deviation from a Porter-Thomas distribution with one degree of freedom was investigated. Pandita and Agrawal [Pa92] calculated ν as 1.69 for this nuclide and suggested that intermediate structure is a possible reason for a deviation from a Porter-Thomas distribution (ν=1). However, as depicted in **Fig. 16,** concentration of strength in the considered energy region was not observed. Even though the fitting with ν=2 (**Fig. 17**) seems slightly better than that for ν=1, the latter was adopted in the

present evaluation. For the p-wave population, resonances for which the reduced widths are smaller than 15 meV were excluded in the fitting (**Fig. 18**). This procedure resulted in $\langle D_1 \rangle = 5.07 \pm 0.76$ eV and $S_1 = 4.56 \pm 1.00$. This p-wave level spacing is consistent with other evaluations. The derived p-wave strength function is also consistent, within the associated uncertainty range, with values of 5.8±0.3 in the BNL compilation [Mu81] and 4.1±0.4 of Koester [Ko87].

3. Unresolved Resonance Parameters

The present unresolved energy region extends to 283.2 keV, which corresponds to the threshold energy of inelastic neutron scattering to the first excited level of ^{105}Pd at 280.51 keV. In this region, average capture cross sections measured by Macklin *et al.* [Ma81, Ma79], and Cornelis *et al.* [Co82] were taken into consideration. These two data sets show good agreement with each other.

For this isotope, s-, p- and d-wave average resonance parameters were provided. Since the upper energy is relatively high, d-wave contribution is not negligible. The level spacing is assumed to vary with energy according to Gilbert-Cameron level density formula in which the associated parameters were adopted from Mughabghab and Dunford [Mu98a]. From the (2J+1) dependence of level density, spacings of p- and d-wave resonances were assumed to be 1/2 and 1/3 of the s-wave spacing, respectively. In the calculation of the capture cross-section, the following parameters were initially applied: 1) $\langle D_0 \rangle$ and S_0 values which were deduced from the resolved resonances; 2) S_1 which was adopted from the BNL compilation; 3) S_2 which was assumed to be the same as S_0; and 4) a $\langle \Gamma_\gamma \rangle$ of 148 meV for s-, p- and d-waves. These parameters resulted in a calculated cross section, which is larger by about 15% at the low energy region and lower by a few % at the high region than the measurements. Subsequently, to obtain good agreement with the measurements, S_0 and S_2 were adjusted to the values listed in **Table 13**. The resulting calculated capture cross section is shown in **Fig. 19**.

Maxwellian-averaged capture cross section for a temperature of 30 keV was computed as 1.19 b. This value is in excellent agreement with 1.20±0.06 b [Be92] and 1.19 b in the BNL compilation [Mu81].

Table 11. Bound Level Resonance Parameters (^{105}Pd)

Energy (eV)	l and Resonance Spin	Scattering Width (meV)	Capture Width (meV)
−29.64	l=0, J=2.0	173.0	148.0
−15.84	l=0, J=3.0	25.68	148.0

Table 12. Thermal Characteristics (^{105}Pd)

Quantity	Unit	BNL [Mu81]	98CRC [Ho98]	ENDF/ B-VI	JEF-2.2	JENDL-3.2	Present
R'	fm	6.6±0.3		6.60	6.695	7.05	6.60
σ_γ^0	barn	20.0±3.0	22±2	20.1	21.8	20.3	20.9
σ_s^0	barn	5.0±0.6		5.01	5.22	5.13	7.36
gw*				0.9973	0.9951	0.9986	0.9995
RI-capt.**	barn	62.2	60±20	111	93.1	96.8	95.2
RI-total**	barn			200	175	168	186

* Westcott factor for capture cross section.
** Integrated from 0.5 eV to 100 keV with 1/E spectrum.

Table 13. Average Resonance Parameters for the Unresolved Resonance Region (^{105}Pd)

Quantity	Unit	BNL [Mu81]	ENDF/ B-VI	JEF-2.2	JENDL-3.2*	Present	
						PT Analysis	Adopted
R'	fm	6.6±0.2		6.695	4.60		6.6
$\langle D_0 \rangle$	eV	10.0±0.5		10.3	5.30	10.32±0.47	10.3**
S_0	$\times 10^{-4}$	0.6±0.1		0.58	0.60		0.50
$\langle \Gamma_{\gamma 0} \rangle$	meV	145±8		155	145	0.66±0.08	148
$\langle D_1 \rangle$	eV			5.16	2.65	5.07±0.76	5.16**
S_1	$\times 10^{-4}$	5.8±0.3		4.80	5.80	4.56±1.00	5.80
$\langle \Gamma_{\gamma 1} \rangle$	meV			155	145		148
$\langle D_2 \rangle$	eV			3.44	1.77		3.43**
S_2	$\times 10^{-4}$			0.60	0.98		0.80
$\langle \Gamma_{\gamma 2} \rangle$	meV			155	145		148

* Average parameters at the low energy end (2.049 keV) of the unresolved region.
** Value at the neutron separation energy of ^{106}Pd.

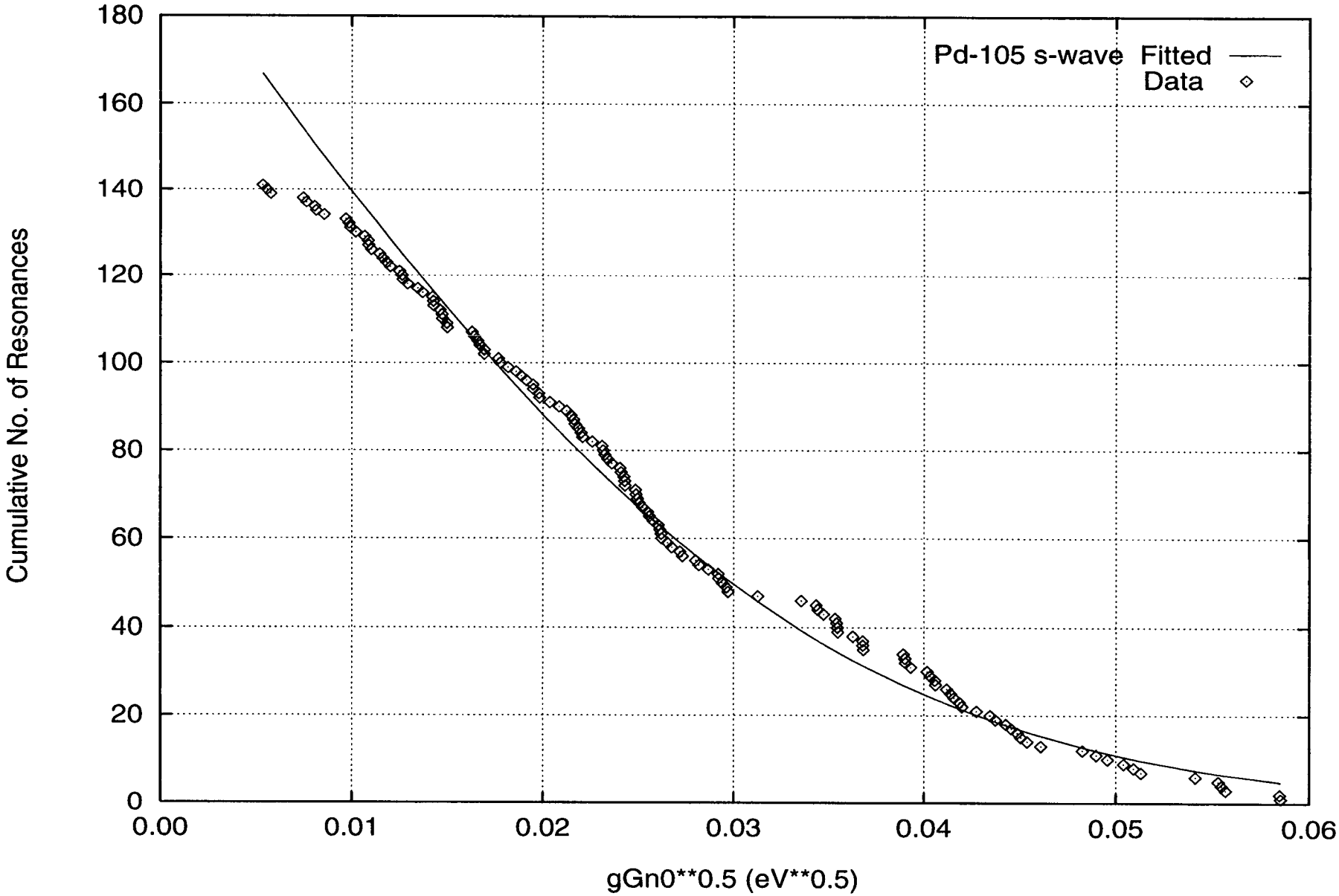

Fig. 15. Complement of the Cumulative Distribution of Neutron Reduced Widths (^{105}Pd, s-wave)

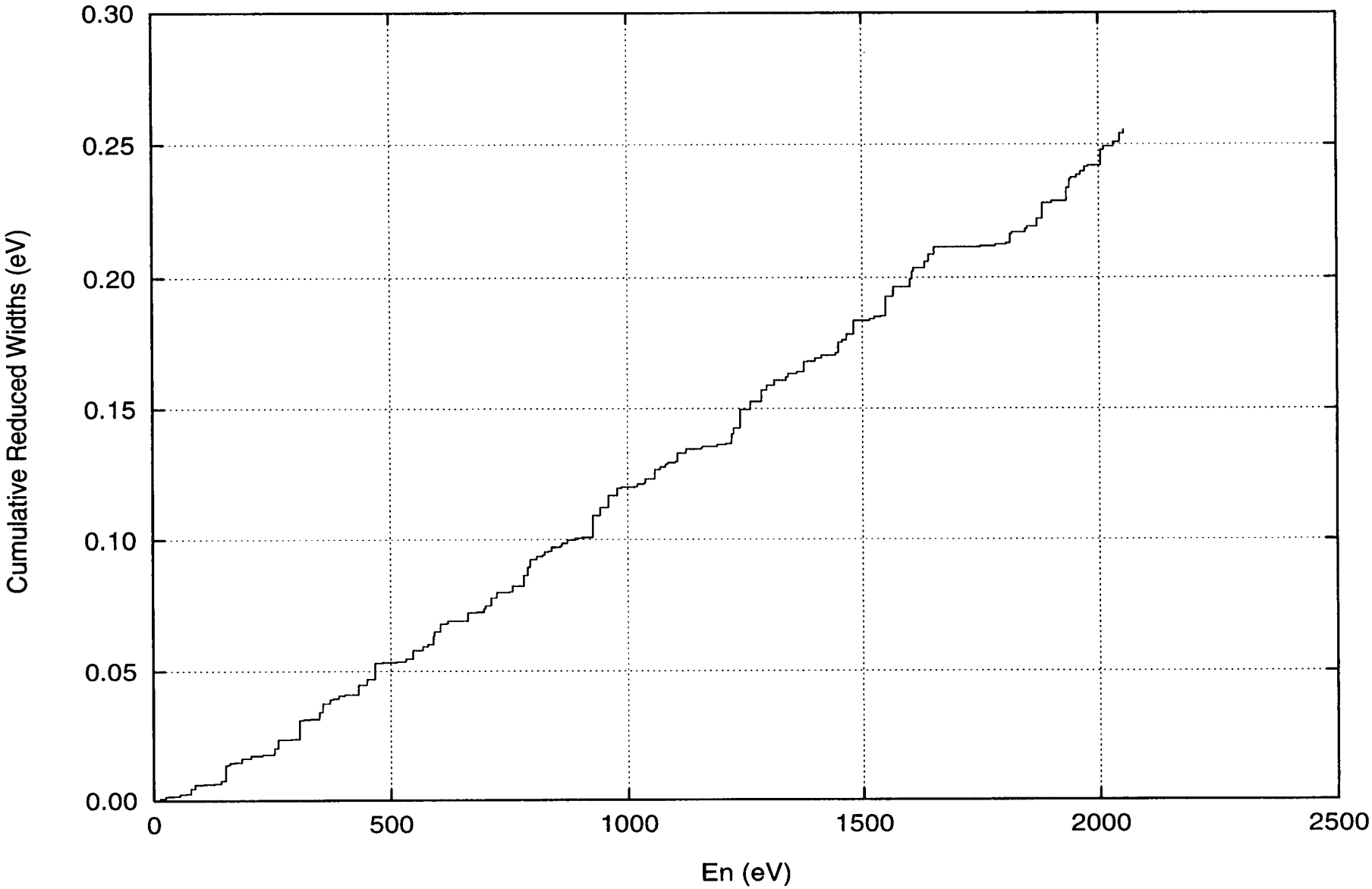

Fig. 16. Staircase Plot of the Neutron Reduced Widths (^{105}Pd, s-wave)

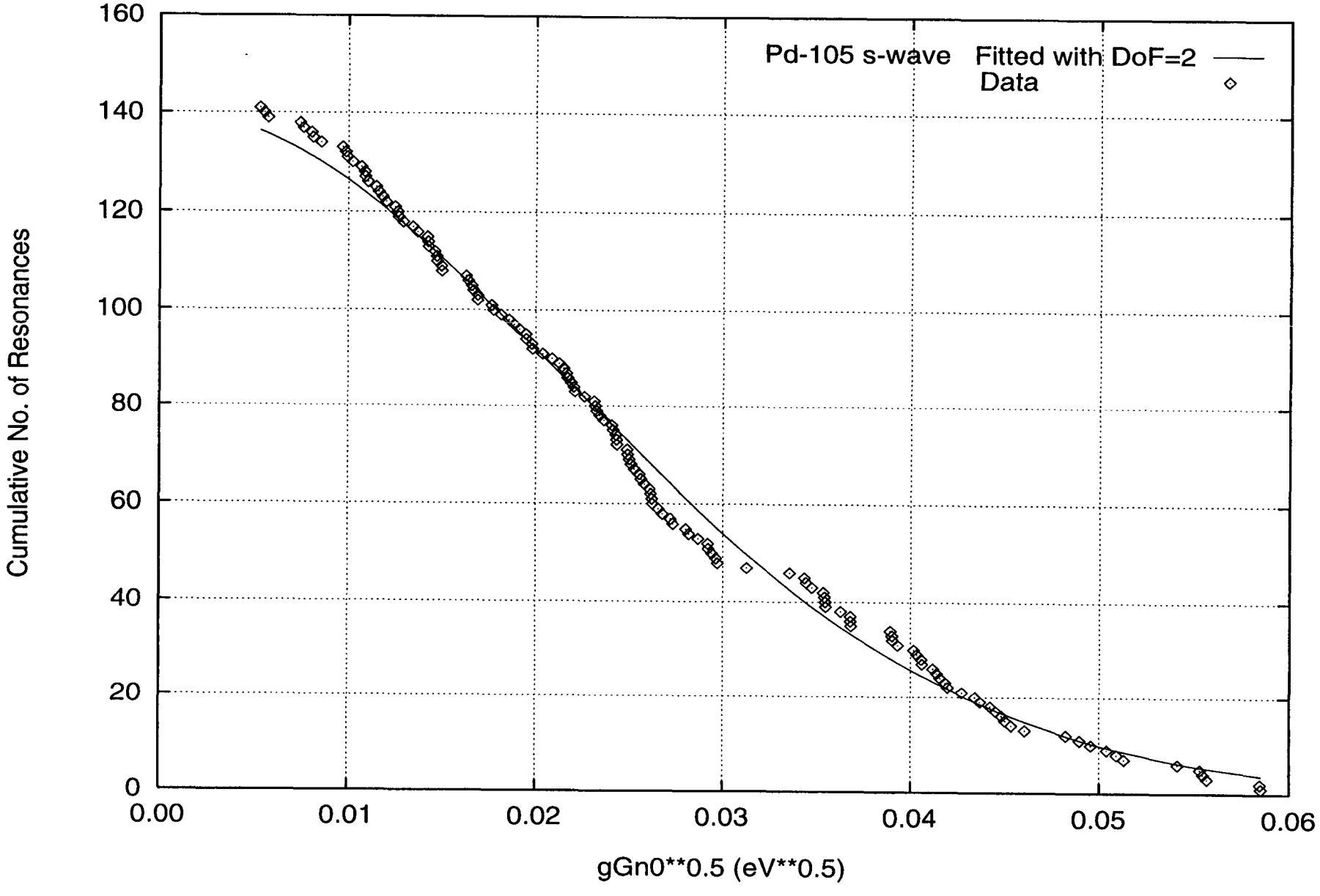

Fig. 17. Complement of the Cumulative Distribution of Neutron Reduced Widths (^{105}Pd, s-wave: fitted with the degree of freedom of 2)

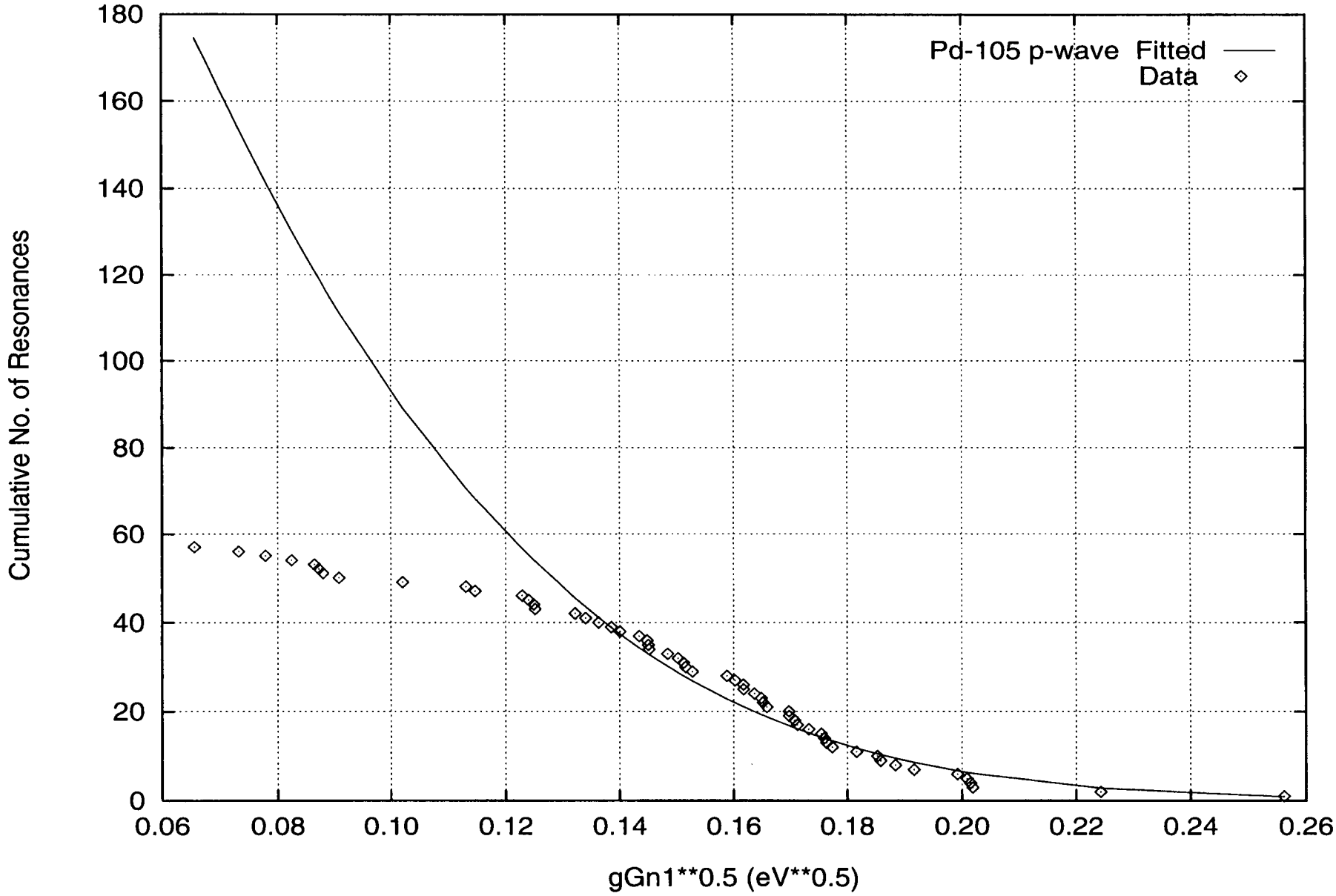

Fig. 18. Complement of the Cumulative Distribution of Neutron Reduced Widths (^{105}Pd, p-wave)

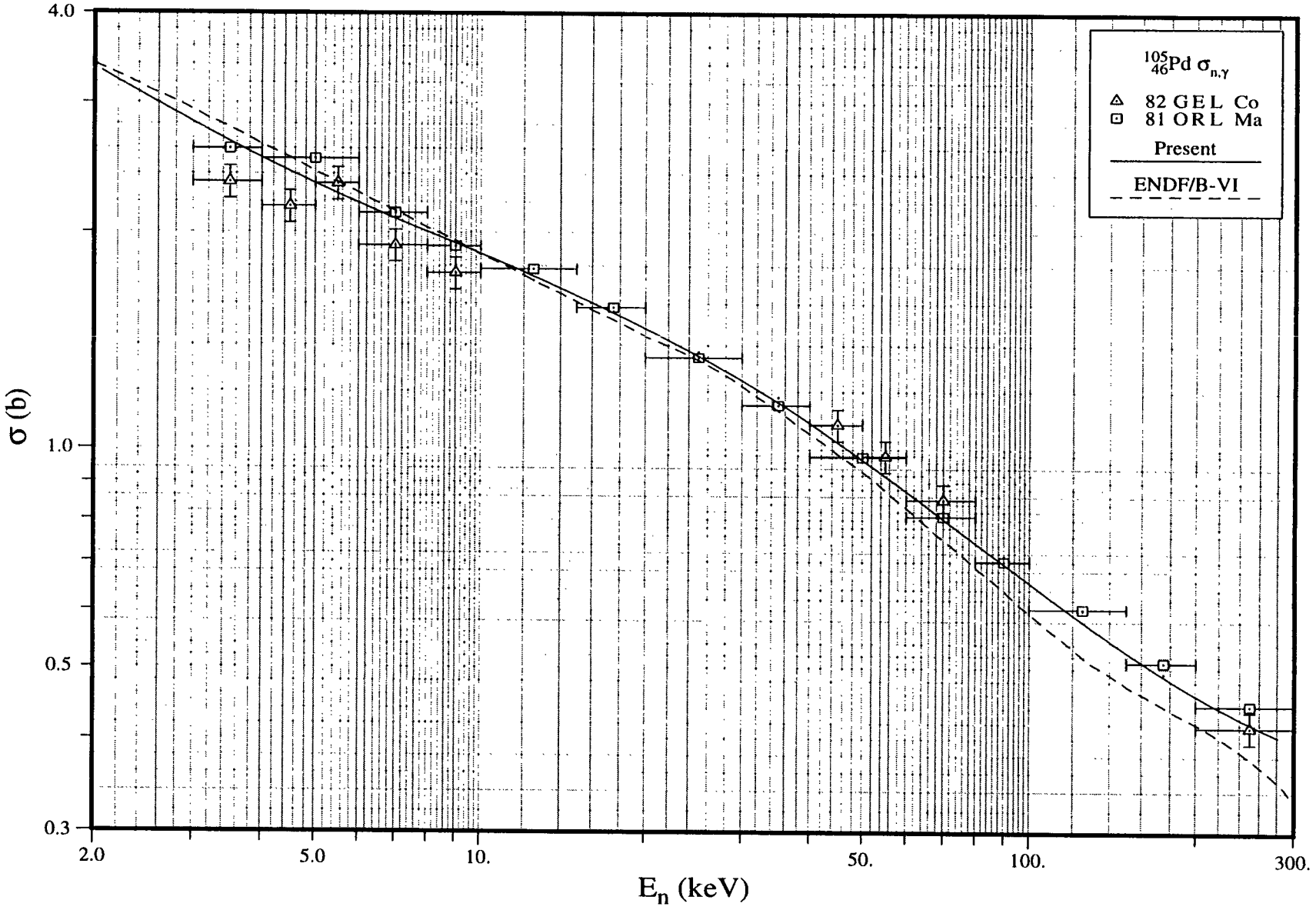

Fig. 19. Capture Cross Section in the Unresolved Resonance Region (^{105}Pd)

III.F. ^{109}Ag

1. Thermal Region

The resolved resonance parameters in the energy region from 5.9 eV to 2.5 keV, as well as the effective scattering radius, R' = 6.6 fm, were adopted from the BNL compilation [Mu81]. Since positive energy resonances account for the thermal capture cross section and the spin-dependent coherent scattering amplitudes, no bound levels are required. As shown in **Table 14**, only minor differences exist between the present thermal cross sections, those reported in the BNL compilation [Mu81], and existing evaluated libraries.

2. Resolved Resonance Region

To resolve a discrepancy in the existing cross section measurements of ^{109}Ag, several new measurements, which reported resonance parameter information since the BNL compilation [Mu81], were carried out [Ma82], [Mi83], [Co97], and [Lo97]. These data were incorporated partially in the ENDF/B-VI revision and JENDL-3. In the present evaluation, the parameters of neutron resonances up to 2.506 keV were basically adopted from the BNL compilation [Mu81]. Below this energy region, the spin assignments of Corvi *et al.* [Co97] and the neutron widths of Lowie *et al.* [Lo97] were adopted. The resonance parameters from 2.6 keV to 5.0 keV are based on the data of Macklin [Ma82b] and Mizumoto *et al.* [Mi83]. Even though individual resonance parameters were reported [Ma82b, Mi83] up to 7 keV, the upper energy region of the resolved energy region was set to 4.996 keV in this evaluation. Above 5 keV, the cross sections are represented by average resonance parameters.

For weak resonances in the energy region from 2.5 keV to 5.0 keV, the $g\Gamma_n$ values were calculated from the reported capture areas [Ma82b] for an assumed spin statistical factor, g, and an assumed constant radiative width of 143 meV. In this procedure, consistency, within the quoted uncertainties, was achieved with the parameters of Mizumoto *et al.* [Mi83]. For strong resonances, the scattering widths of Mizomoto *et al.* were adopted. In some favorable cases, the capture areas [Ma82b] were combined with the transmission data [Mi83] to deduce spins of resonances. Of a total number of 307 resonances, 236 were assigned as l=0 and the remaining as l=1 by Bayesian analysis. Resonance spins were assigned randomly to those resonances for which the spin is not reported in the BNL compilation [Mu81], Lowie *et al.* [Lo97], or determined in the present analysis. The weighted-average value of the radiative widths of 21 s-wave resonances was calculated as 129.9±2.6 meV, which is in very good agreement with that in the BNL compilation (130 meV) [Mu81] and RIPL (130±20 meV) [Re98].

The distributions of reduced neutron widths for s- and p-wave resonances were analyzed in terms of the Porter-Thomas distribution. For the s-wave case, those resonances with reduced neutron widths less than 0.4 meV were excluded in order to obtain a good fit. The result of the analysis, depicted in **Fig. 20**, shows that there is a surplus of s-wave resonances with reduced widths in the range of 0.1 meV – 0.4 meV, possibly belonging to the l=1 population. However, as shown in **Fig. 21**, the staircase plot suggests that there is a minor, if any, spurious p-wave resonances. The Porter-Thomas fitting resulted in $\langle D_0 \rangle$ = 20.0±0.8 eV and $\langle g\Gamma_n^0 \rangle$ = 1.04±0.10 meV. These values yield s-wave strength function of S_0 = 0.52±0.05. The present $\langle D_0 \rangle$ value is

consistent with 20±2 eV [Mi83] but is much larger than the values, 14±2 eV [Mu81] and 15.1±1.4 eV [Re98]. The present S_0 is in good agreement, within the uncertainty limits, with reported values: 0.46±0.15 [Mu81], 0.45±0.05 [Mi83], but not with 0.75±0.08 [Re98]. For p-wave resonances, the fitting analysis, with a cutoff of 11.5 meV for the p-wave reduced width, resulted in $\langle D_1 \rangle$ = 10.5±2.1 eV and S_1 = 1.31±0.29 (**Fig. 22**). Even though the level spacing seems to be reasonable, the p-wave strength function is quite low in this mass region (S_1 = 3.8±0.6) [Mu81]. It may stem from the fact that some strong to medium-strong resonances, assigned as s-wave by the Bayesian analysis, may in fact be p-wave resonances.

3. Unresolved Resonance Region

In the unresolved energy region, 5 keV–88.8 keV, the average capture cross section measured by Macklin [Ma82b] was adopted as the reference cross section. The cross section measurements of Bokhovko *et al.* [Bo87] and Mizumoto *et al.* [Mi83] show relatively good agreement with Macklin's measurements. Earlier measurements reported in the Neutron Cross Section Curves [Mc88] are discrepant with these three measurements. Since the d-wave strength function has a minimum value in this mass region [Mu81], the small d-wave contribution to the capture cross section below 88 keV, was not included in the analysis of ^{109} Ag. The average resonance parameters which were applied in the present calculation are listed in the last column of **Table 15**. We adopted S_0 value which was increased by its uncertainty to improve the fit. From the $(2J+1)\cdot \exp\{-(J+1/2)^2/2\sigma^2\}$ dependence of the level spacing, the average level spacing of p-wave is calculated as 1/2.005 of the s-wave spacing for a spin dispersion parameter σ =3.2 [Mu98b]. The adopted average gamma width is obtained by weighting Macklin's value of 146±6 meV [Ma82b] and a value of 129.9±2.6 meV derived from resolved resonances. **Figure 23** compares our calculated capture cross section with measurements [Bo87, Mi83, Ma82b], as well as the ENDF/B-VI evaluation.

Maxwellian-averaged capture cross section for a temperature of 30 keV was computed as 787 mb. In extending the energy region up to 1 MeV, the capture cross-section in the region 88.8 keV to 1 MeV was adopted from the ENDF/B-VI evaluation. The present computed cross section is to be compared with a value of 779±23 mb [Be92].

Table 14. Thermal Characteristics (^{109}Ag)

Quantity	Unit	BNL [Mu81]	98CRC [Ho98]	ENDF/B-VI	JEF-2.2	JENDL-3.2	LIPAR-5 [Ab97]	Present
R'	fm	6.6±0.2		6.60	6.60	7.05		6.60
σ_γ^0	barn	91.0±1.0	91.2	91.0	90.8	90.5	90.7	90.8
σ_s^0	barn	2.55±0.06		2.25	2.30	2.48	2.42	2.12
gw*				1.006	1.005	1.005	1.0050	1.0053
RI-capt.**	barn	1400±400	1480	1471	1473	1470	1467	1476
RI-total**	barn			1691	1690	1689		1691

* Westcott factor for capture cross section.
** Integrated from 0.5 eV to 100 keV with 1/E spectrum.

Table 15. Average Resonance Parameters for the Unresolved Resonance Region (^{109}Ag)

Quantity	Unit	ENDF/B-VI	JEF-2.2	JENDL-3.2*	BNL [Mu81]	Present	
						PT Analysis	Adopted
R' (URR)	fm		6.30	6.618	6.6±0.2		6.60
$\langle D_0 \rangle$	eV		16.07	19.40	14±2	20.0±0.8	20.0**
S_0	$\times 10^{-4}$		0.64	0.54	0.46±0.15	0.52±0.05	0.57
$\langle \Gamma_{\gamma 0} \rangle$	meV		132.3	130	130		133
$\langle D_1 \rangle$	eV		7.379	8.621		10.5±2.1	9.97**
S_1	$\times 10^{-4}$		3.95	4.263	3.8±0.6	1.31±0.29	3.0
$\langle \Gamma_{\gamma 1} \rangle$	meV		132.2	130			133
$\langle D_2 \rangle$	eV		4.664	5.173			
S_2	$\times 10^{-4}$		2.5	0.53			
$\langle \Gamma_{\gamma 2} \rangle$	meV		132.2	130			

* Average parameters at the low energy (7.01 keV) of the unresolved region.
** Value at the neutron separation energy of ^{110}Ag.

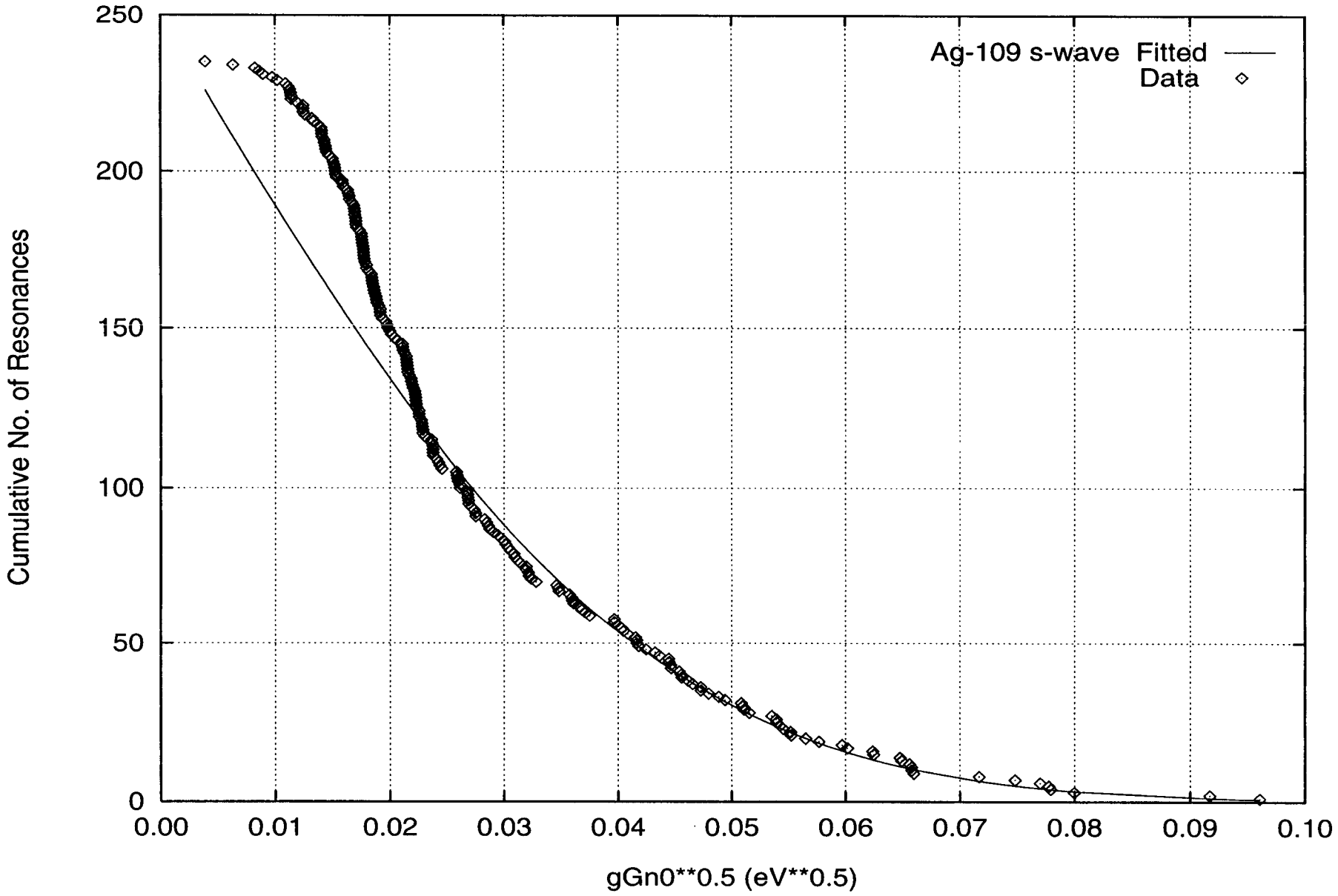

Fig. 20. Complement of the Cumulative Distribution of Neutron Reduced Widths (^{109}Ag, s-wave)

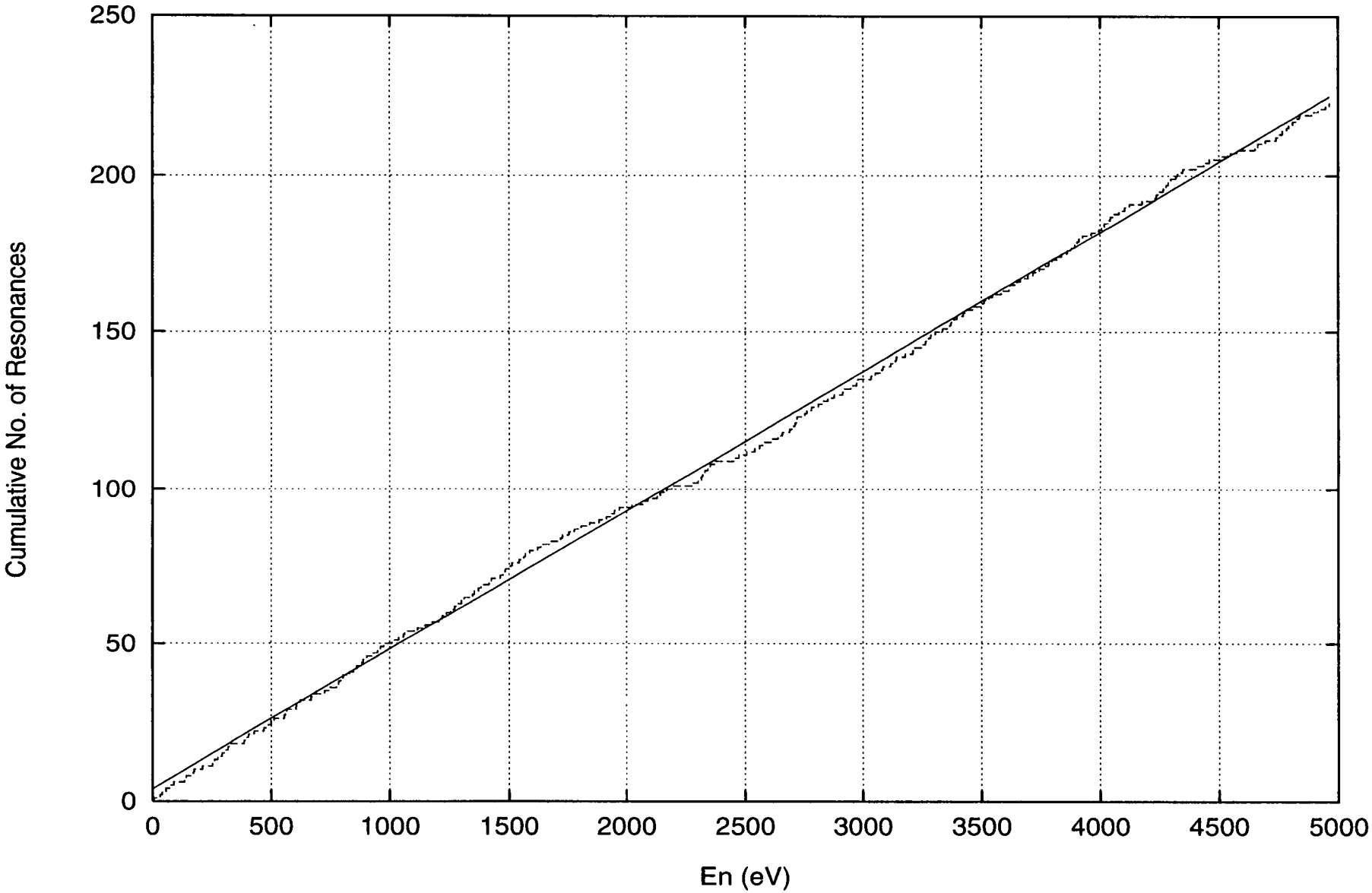

Fig. 21. Staircase Plot of the Number of Resonances (^{109}Ag, s-wave).
The dashed line shows the data and the solid line fits linearly to the data.

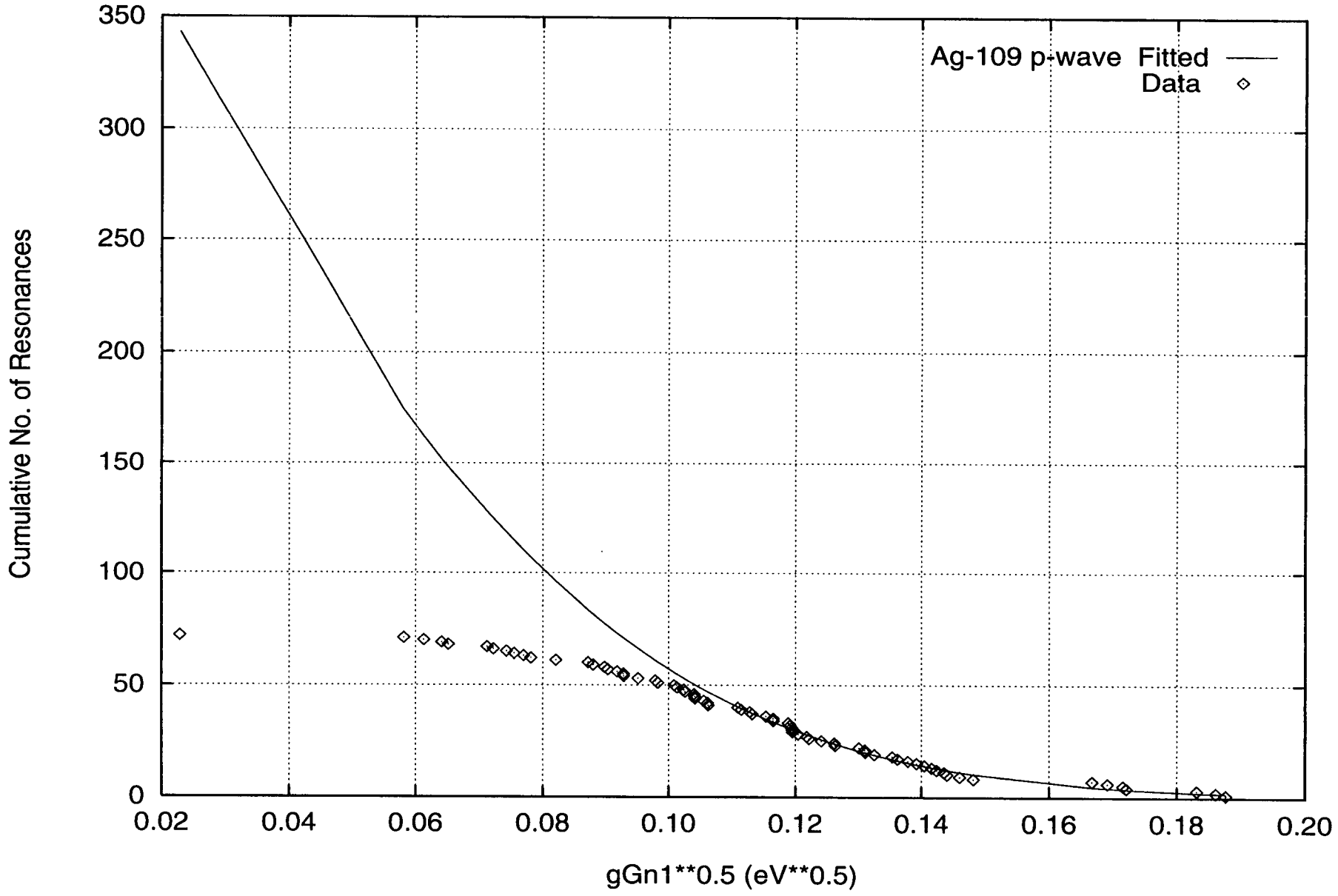

Fig. 22. Complement of the Cumulative Distribution of Neutron Reduced Widths (^{109}Ag, p-wave)

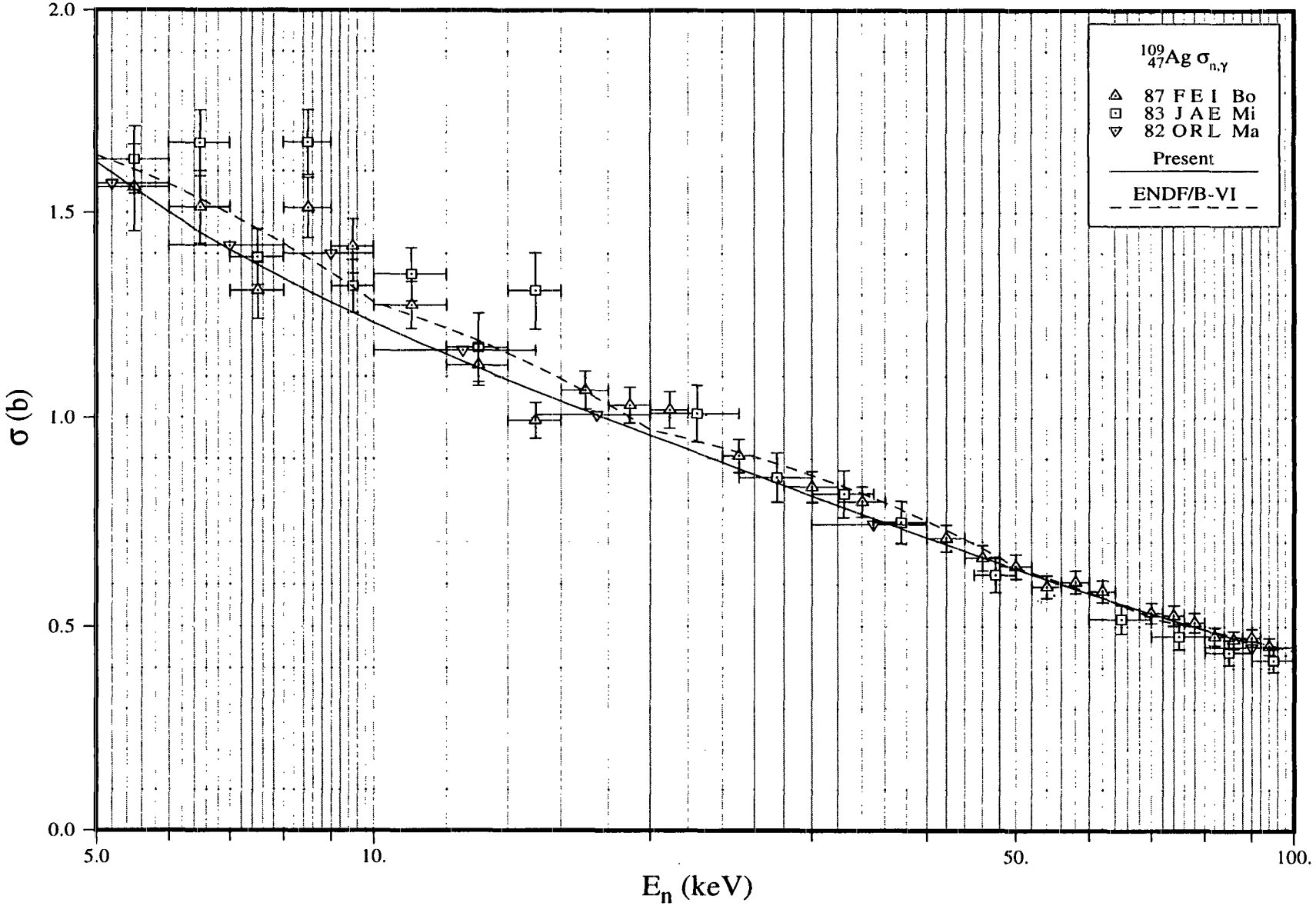

Fig. 23. Capture Cross Section in the Unresolved Resonance Region (^{109}Ag)

III.G. ^{131}Xe

1. Thermal Region

To reproduce a thermal capture cross section of 90 b, a bound level was stipulated. This capture cross-section was obtained by subtracting the isotopic contributions (mainly ^{129}Xe and ^{131}Xe) from the natural element thermal capture cross section of 23.9±1.2 b [Mu81]. An effective potential scattering radius, R'= 5.4 fm, was adopted from a deformed optical model calculation reported in the BNL compilation [Mu81, Fig. 1]. The resonance parameters of the bound level were determined as: E_0 = -26.65 eV, J = 2, Γ_n = 303.5 meV, and Γ_γ = 112 meV. The contribution of a bound level to the thermal capture cross section was calculated as 22.1 b. A comparison between the present thermal cross sections, as well as resonance capture and total integrals, with those of ENDF/B-VI, JEF-2 and JENDL-3 is presented in **Table 16**. While there is general agreement among the various evaluated thermal capture cross sections, discrepancies in the evaluated scattering cross sections exist. The capture resonance integral of the ENDF/B-VI evaluation deviates from those of the present evaluation, JEF-2.2, JENDL-3.2, and the BNL compilation [Mu81].

2. Resolved Resonance Parameters

The resolved resonance parameters were adopted from the measurement of Ribon [Ri69]. On the basis of reported Γ and $2ag\Gamma_n$, where a is the abundance of Xe isotopes, five resonances at energies of 339.0, 703.5, 1380.3, 1891.0, and 2234.3 eV were assigned to ^{131}Xe in the present study, in addition to the 41 resonances identified by Ribon for ^{131}Xe. A p-wave resonance at 3.2 eV [Sk96] was included in the present evaluation. The present resolved energy region extends to 3.95 keV. Of a total of 47 positive-energy resonances, 45 were assigned as s-wave and 2 as p-wave resonances by Bayasian analysis. Spins were assigned randomly to resonances for which the spin is unknown. This random assignment assumes that the level density is proportional to (2J+1). The uncertainty-weighted averaging of 10 determined radiative widths resulted in an average value of 112±11 meV. This average value was assumed for those resonances for which radiative widths are unknown. The present average value is consistent with that reported in RIPL [Re98] (114±37 meV), as well as that which is obtained from the s-wave systematics of radiative widths in the BNL compilation [Mu84, Fig. 6] around this mass region.

The distribution of reduced neutron widths for s-wave resonances was analyzed by fitting 36 resonances below 2 keV to the Porter-Thomas distribution. As shown in **Fig. 24,** for a cutoff value of 0.4 meV for the reduced width, the fit resulted in $\langle g\Gamma_n^0 \rangle$ = 3.37±0.85 meV and $\langle D_0 \rangle$ = 42.8±5.0 eV. These values yield s-wave strength function of S_0 = 0.79±0.20. The present $\langle D_0 \rangle$ is smaller than that presented in the BNL compilation, but is consistent with (45±15 eV) [Re98]. While the present S_0 value deviates from the values (1.2±0.4) [Mu81] and (1.2±0.3) [Re98], it is consistent with Ribon's value of $0.85^{+0.19}_{-0.17}$ [Ri69].

3. Unresolved Resonance Parameters

The present unresolved resonance region covers the energy range from 3.95 keV to 80.8 keV. The latter energy corresponds to the threshold energy for neutron inelastic scattering to the first excited level of ^{131}Xe. For this nucleus, s-, p- and d-wave average resonance parameters were provided. The level spacing varies with energy according to Gilbert-Cameron level density formula with associated parameters adopted from Mughabghab and Dunford [Mu98a] (neutron separation energy = 8.936 MeV, pairing energy = 2.16 MeV, and level density parameter = 10.58 MeV^{-1}). The dependence of the level spacing on $\exp\{-(J+1/2)^2/2\sigma^2\}$, as well as (2J+1), was taken into account. With a value of $\sigma = 3.0$ [Mu98b] for the spin dispersion parameter, the level spacings for p- and d-wave resonances are calculated as 1/1.73 and 1/2.21 of the s-wave spacing, respectively.

Unfortunately, capture cross section measurements were unavailable in the unresolved resonance region. The present unresolved resonance parameters are listed in the last column of **Table 17**. The s-wave average parameters are based on the analysis carried out in the resolved energy region. The value of S_1 is obtained from a deformed optical model calculation [Mu84, Fig. 4], and the value of S_2 was assumed to be same as that of S_0. An average radiative width of 112 meV was assumed for p- and d-wave resonances. The capture cross section, constructed from the present average resonance parameters, is shown in **Fig. 25** and is compared with other evaluations. The present cross section is consistent with the ENDF/B-VI evaluation.

The average capture cross section over a Maxwellian spectrum at 30 keV was calculated as 306 mb. This value is apparently lower than that recommended in Beer's compilation, 453 ± 81 mb [Be92]. However, since Beer's value, as well as those reported in Bao's compilation [Ba87], is not based on measurements, the validity of the present evaluation is to be resolved by future measurements.

Table 16. Thermal Characteristics (^{131}Xe)

Quantity	Unit	BNL [Mu81]	98CRC [Ho98]	ENDF/ B-VI	JEF-2.2	JENDL-3.2	Present
R'	fm			5.85	5.40	5.31	5.40
σ_γ^0	barn	85±10	90±10	90.6	85.1	85.0	90.0
σ_s^0	barn			4.32	24.3	24.0	1.19
gw*				0.9996	1.001	1.001	1.0014
RI-capt.	barn	900±100	900±100	1016	890	900	882
RI-total	barn			2877	2958	2938	2765

* Westcott factor for capture cross section.

Table 17. Average Resonance Parameters for the Unresolved Resonance Region (^{131}Xe)

Quantity	Unit	BNL [Mu81]	ENDF/ B-VI	JEF-2.2	JENDL-3.2*	Present	
						PT Analysis	Adopted
R'	fm				5.63		5.40
$\langle D_0 \rangle$	eV	70±20			35.5	42.8±5.0	42.8**
S_0	$\times 10^{-4}$	1.2±0.4			0.70	0.79±0.20	0.79
$\langle \Gamma_{\gamma 0} \rangle$	meV				114		112.3
$\langle D_1 \rangle$	eV				17.7		24.7**
S_1	$\times 10^{-4}$				1.58		1.40
$\langle \Gamma_{\gamma 1} \rangle$	meV				114		112.3
$\langle D_2 \rangle$	eV				11.3		19.4**
S_2	$\times 10^{-4}$				0.99		0.79
$\langle \Gamma_{\gamma 2} \rangle$	meV				114		112.3

* Average parameters at the low energy bound of the unresolved resonance region (2.25 keV).

** Value at the neutron separation energy of ^{132}Xe.

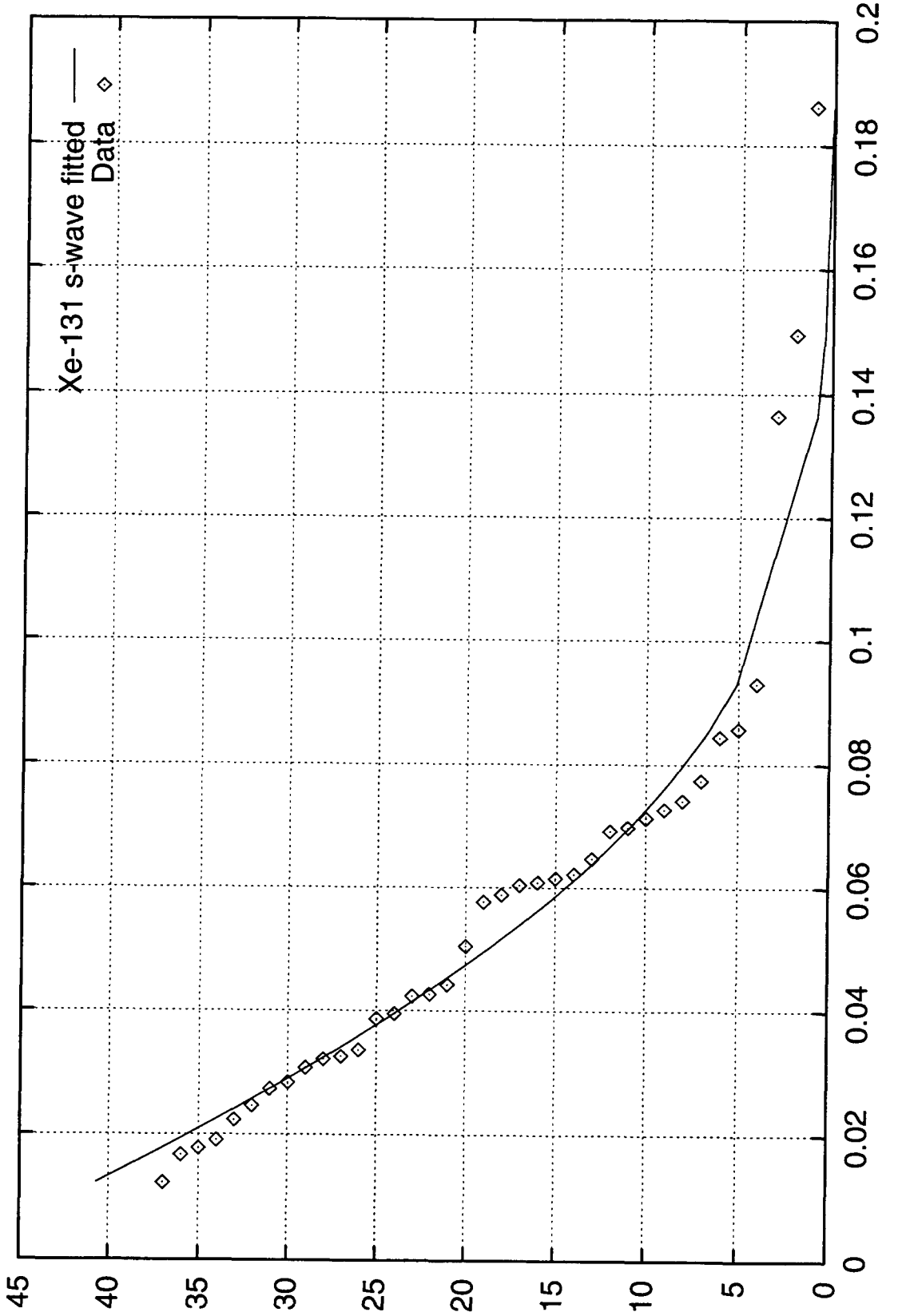

Fig. 24. Complement of the Cumulative Distribution of Neutron Reduced Widths (^{131}Xe, s-wave)

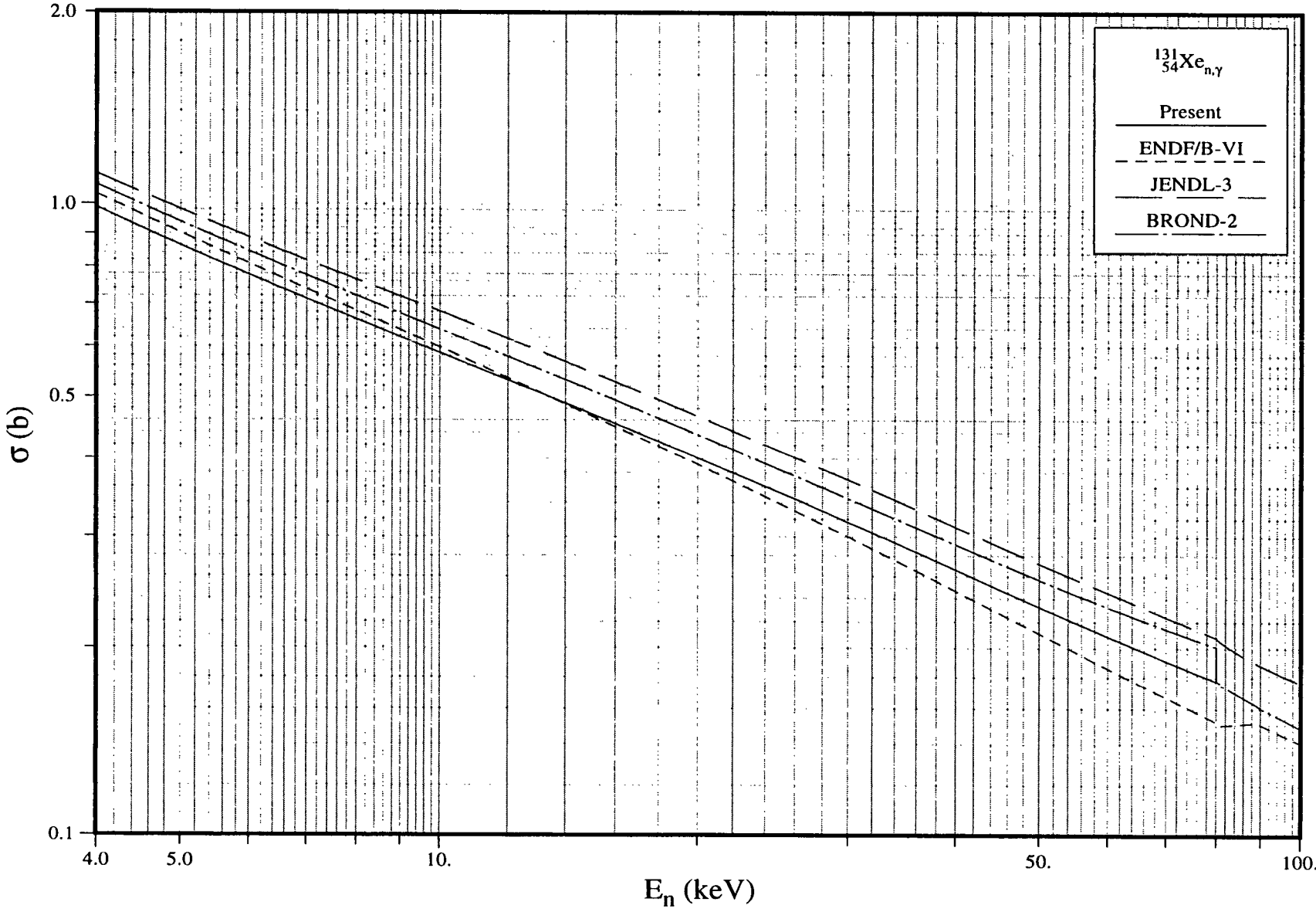

Fig. 25. Capture Cross Section in the Unresolved Resonance Region (^{131}Xe)

III.H. ^{133}Cs

1. Thermal Region

In the present evaluation, two bound levels were invoked to reproduce a thermal capture cross section, σ_γ^0 =29.0±1.5 b, recommended in Mughabghab's BNL compilation [Mu81], an incoherent scattering length, $b_+ - b_-$ = 2.61±0.3 fm, measured by Glaettli *et al.* [Gl79], and a bound coherent scattering length, b = 5.42±0.02 fm, adopted from Koester's compilation [Ko91]. An effective scattering radius, R' = 5.3 fm was obtained from the BNL compilation [Mu81]. In addition, the thermal capture contribution of the bound level with spin 4 was assumed as 3 times that of the bound level with spin 3. The contribution of positive energy resonances to the thermal capture cross section was calculated as 19.5 b. The bound level resonance parameters are listed in **Table 18**. A comparison of the present thermal cross sections and resonance integrals with those of ENDF/B-VI.5, JEF-2.2 and JENDL-3.2 evaluations is presented in **Table 19**. The thermal capture cross sections are in very good agreement with each other. The capture resonance integral of the present evaluation is in good agreement with those recommended in the BNL compilation [Mu81] and Holden compilation [Ho98].

2. Resolved Resonance Parameters

The primary source of resolved resonance parameters for this nuclide is the BNL compilation [Mu81]. In addition to this source, measurements by Nakajima *et al.* [Na90], Macklin [Ma82c], and Popov and Tzeciak [Po81] were incorporated into the present set of parameters. By combining the capture data with the transmission data, radiative widths of some resonances were derived in favorable cases. The resolved energy region extends up to 3.99 keV. Resonances above 3.99 keV [Na90, Ma82] were represented with average resonance parameters in the unresolved resonance region. On the basis of Bayesian analysis, 148 and 39 resonances were assigned as s-wave and p-wave resonances, respectively. Resonance spins were assigned randomly to those resonances with unknown spins. The random assignment assumes the level density is proportional to (2J+1). The uncertainty-weighted averaging of 31 measured radiative widths resulted in an average value of 123±4 meV. This value was assumed for those resonances for which the radiative widths are unknown. The present average value is consistent with values presented in the BNL compilation (120 meV) [Mu81], RIPL [Re98] (120±10 meV), Nakajima *et al.* [Na90] (119±3 meV), and Macklin [Ma82c] (134±8 meV), within the associated uncertainty range.

The distributions of s- and p-wave reduced neutron widths were analyzed in terms of the Porter-Thomas distribution. For s-wave resonances, those with reduced widths smaller than 0.2 meV were excluded in the analysis. The fit for the s-wave resonances, **Fig. 26**, resulted in $\langle g\Gamma_n^0 \rangle$ = 1.44±0.17 meV and $\langle D_0 \rangle$ = 19.8±0.9 eV. These values yield an s-wave strength function of S_0 = 0.73±0.09. The present $\langle D_0 \rangle$ is consistent with values recommended in the BNL compilation (20.65±2.3 eV) [Mu81] and RIPL [Re98] (21±2 eV). However, it deviates from the values reported by Nakajima *et al.* [Na90], 22.4±1.5 eV, and Anufriev *et al.* [An78], 16.3±2.3 eV. The present S_0 is consistent again with values in the BNL compilation, 0.70±0.07, and RIPL, 0.76±0.10, as well as with that reported by Nakajima *et al.* [Na90] 0.77±0.09. For p-wave resonances, the χ^2 value of the fit for all the observed resonances was very large. It is clear from

Fig. 27 that many weak p-wave resonances were missed. Subsequently, resonances with reduced widths, $\langle g\Gamma_n^1 \rangle$, smaller than 12.5 meV were excluded from the analysis. As shown in **Fig. 27,** we obtained a good fit, with a 95% confidence limit, which resulted in $\langle g\Gamma_n^1 \rangle$ = 5.27±1.25 meV, $\langle D_1 \rangle$ = 14.0±3.5 eV and S_1 = 1.25±0.37. Because of the small sample size for the p-wave population, the uncertainties of the derived average quantities are large.

3. Unresolved Resonance Parameters

The present unresolved resonance region covers the energy range from 3.99 keV to 81.6 keV. The latter energy corresponds to the threshold energy of neutron inelastic scattering to the first excited level of ^{133}Cs. For this nucleus, s-, p- and d-wave average resonance parameters were provided. The level spacing varies with energy according to Gilbert-Cameron level density formula with associated parameters adopted from Mughabghab and Dunford [Mu98a] (neutron separation energy = 6.891 MeV, pairing energy = 0.0 MeV, and level density parameter = 14.2 MeV^{-1}). Because of the large target spin of this nuclide, 7/2, the dependence of level spacing on $(2J+1)\ \exp\{-(J+1/2)^2/2\sigma^2\}$ was taken into account. With a value of σ = 2.8 for the spin dispersion parameter [Mu98b], the level spacing for p- and d-wave resonances were calculated as 1/1.87 and 1/2.49 of the s-wave spacing, respectively. These values deviate from 1/2 and 1/3, obtained by assuming only a (2J+1) dependence of the level spacing.

In the unresolved resonance region, the average capture cross sections measured by Bokhovko *et al.* [Bo91], Yamamuro *et al.* [Ya83], and Macklin [Ma82c] were taken into consideration. These measurements agree with each other, while earlier data, included in McLane's compilation [Mc88], deviate from the above measurements. As shown in **Fig. 28**, the present unresolved resonance parameters resulted in a good fit to the experimental data. The present parameters are listed in the last column of **Table 20**. The values of $\langle \Gamma_\gamma \rangle$, $\langle D_0 \rangle$ and S_0 are those which were obtained from the analysis of resolved energy region. The present value of S_1 was adopted from a deformed optical model calculation [Mu84, Fig. 4]; the value of S_2 was assumed to be the same as that of S_0. It is noted that the p- and d-wave strength functions are consistent with those derived by Bokhovko *et al.* [Bo91] (S_1 = 1.3±0.4 and S_2 = 0.7±0.2). The average capture cross section for a Maxwellian spectrum at 30 keV is calculated as 513 mb. For comparisons with other calculations, see **Table 56.**

Table 18. Bound Level Resonance Parameters (^{133}Cs)

Energy (eV)	*l* and Resonance Spin	Neutron Width (meV)	Capture Width (meV)
–41.32	*L*=0, J=4.0	273.6	123.0
–25.21	*l*=0, J=3.0	34.1	123.0

Table 19. Thermal Characteristics (^{133}Cs)

Quantity	Unit	BNL [Mu81]	98CRC [Ho98]	ENDF/ B-VI	JEF-2.2	JENDL-3.2	Present
R'	fm	5.3±0.5		7.517	5.30	5.35	5.30
σ_γ^0	barn	29.0±1.5	30.4	29.7	29.1	29.0	29.0
σ_s^0	barn			4.98	3.88	4.29	3.97
gw*				1.004	1.002	1.002	1.0029
RI-capt.	barn	437±26	422	383	439	396	421
RI-total	barn			518	556	508	535

*Westcott factor for capture cross section.

Table 20. Average Resonance Parameters for Unresolved Resonance Region (^{133}Cs)

Quantity	Unit	BNL [Mu81]	ENDF/ B-VI	JEF-2.2	JENDL-3.2*	Present	
						PT Analysis	Adopted
R'	fm	5.3±0.5		5.50	5.84		5.30
$\langle D_0 \rangle$	eV	20.65±2.3		21.8	16.53	19.8±0.9	19.8**
S_0	$\times 10^{-4}$	0.7±0.07		0.8	0.70	0.73±0.09	0.73
$\langle \Gamma_{\gamma 0} \rangle$	meV	120		125.3	120.0		123.0
$\langle D_1 \rangle$	eV			11.25	8.27	14.0±3.5	10.6**
S_1	$\times 10^{-4}$			4.0	1.40	1.25±0.37	1.40
$\langle \Gamma_{\gamma 1} \rangle$	meV			125.3	120.0		123.0
$\langle D_2 \rangle$	eV			7.91	5.51		7.95**
S_2	$\times 10^{-4}$			1.64	1.30		0.73
$\langle \Gamma_{\gamma 2} \rangle$	meV			125.3	120.0		123.0

* Average parameters at the low energy of the unresolved resonance region (5.98 keV).

** Value at the neutron separation energy of ^{134}Cs.

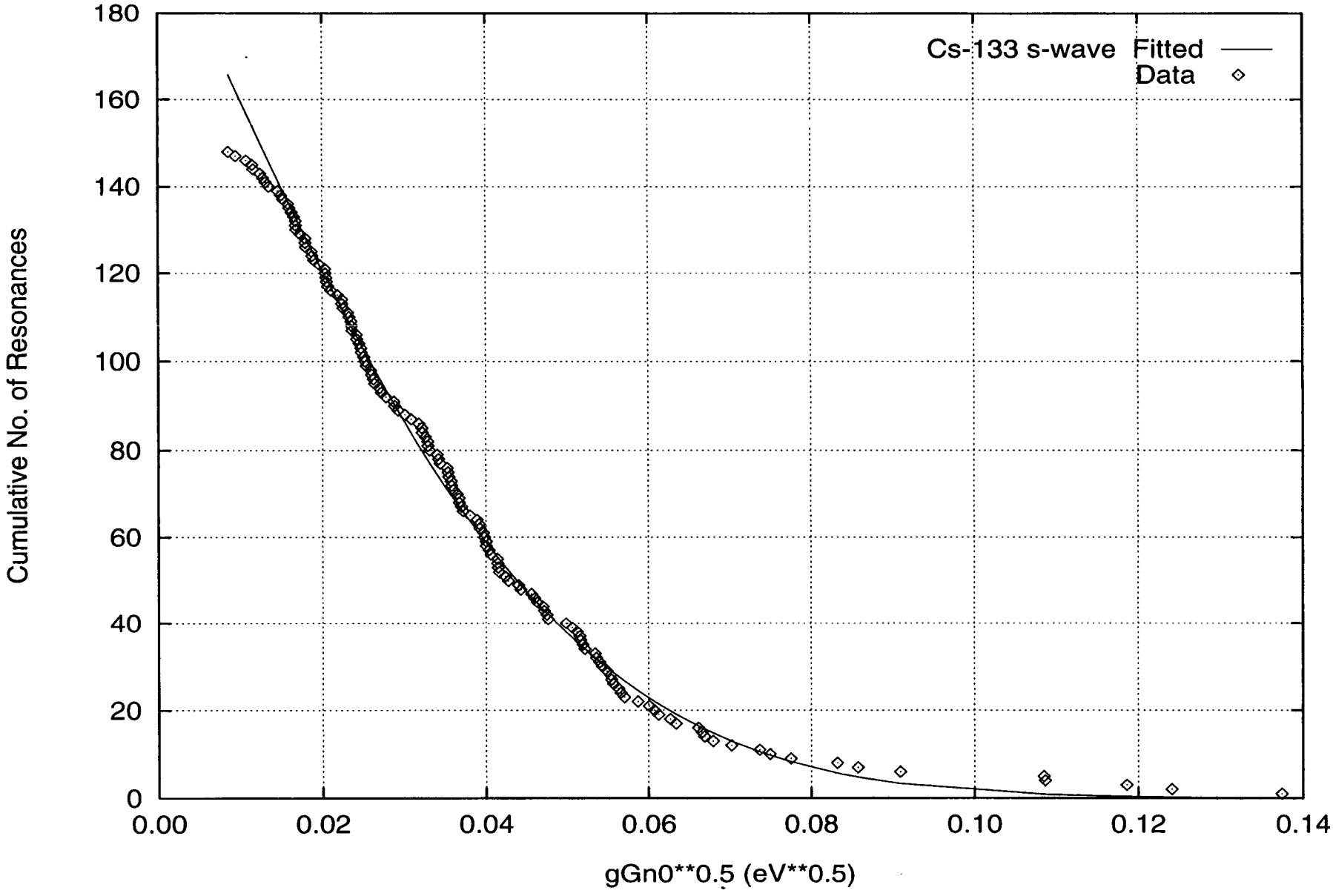

Fig. 26. Complement of the Cumulative Distribution of Neutron Reduced Widths (^{133}Cs, s-wave)

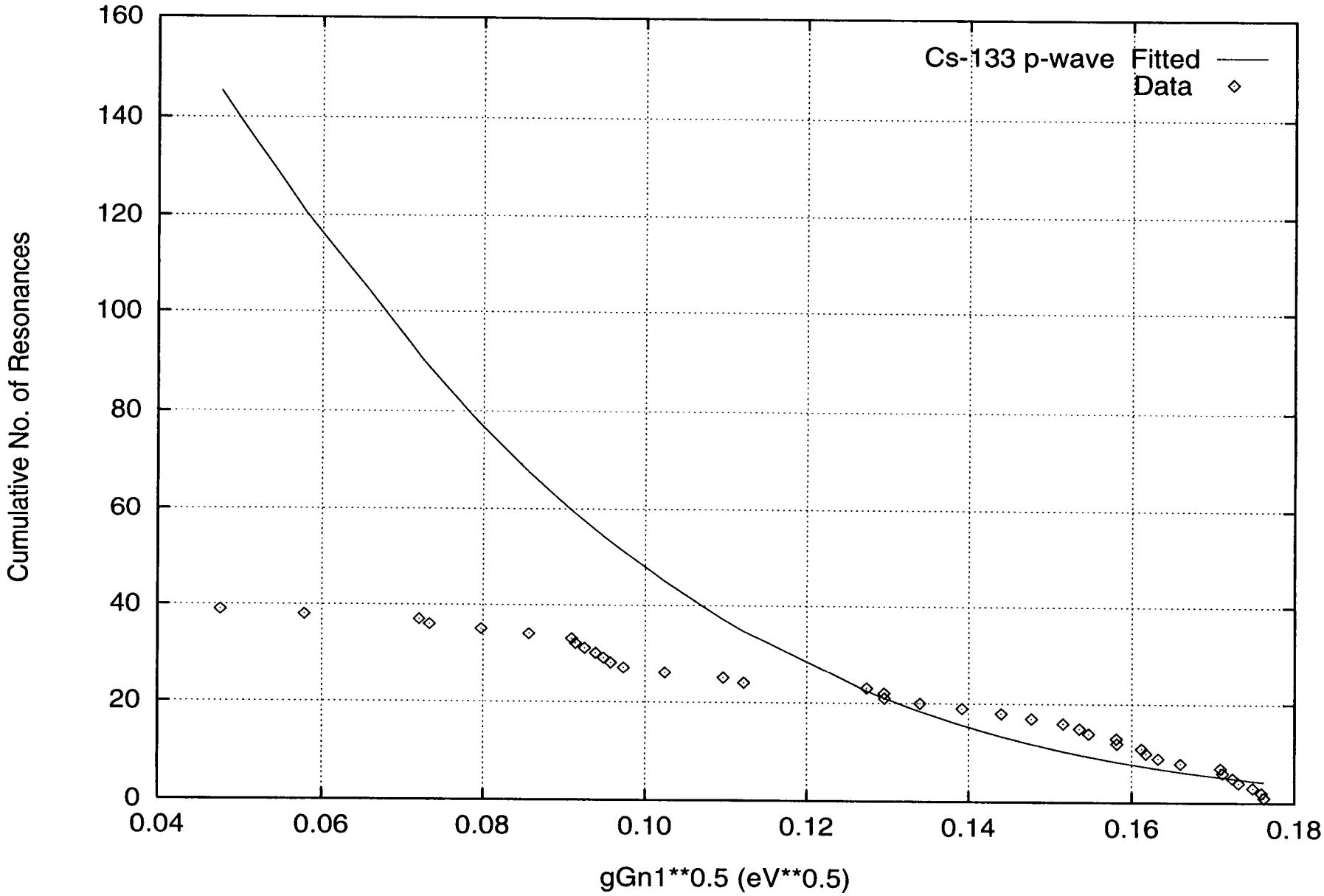

Fig. 27. Complement of the Cumulative Distribution of Neutron Reduced Widths (^{133}Cs, p-wave)

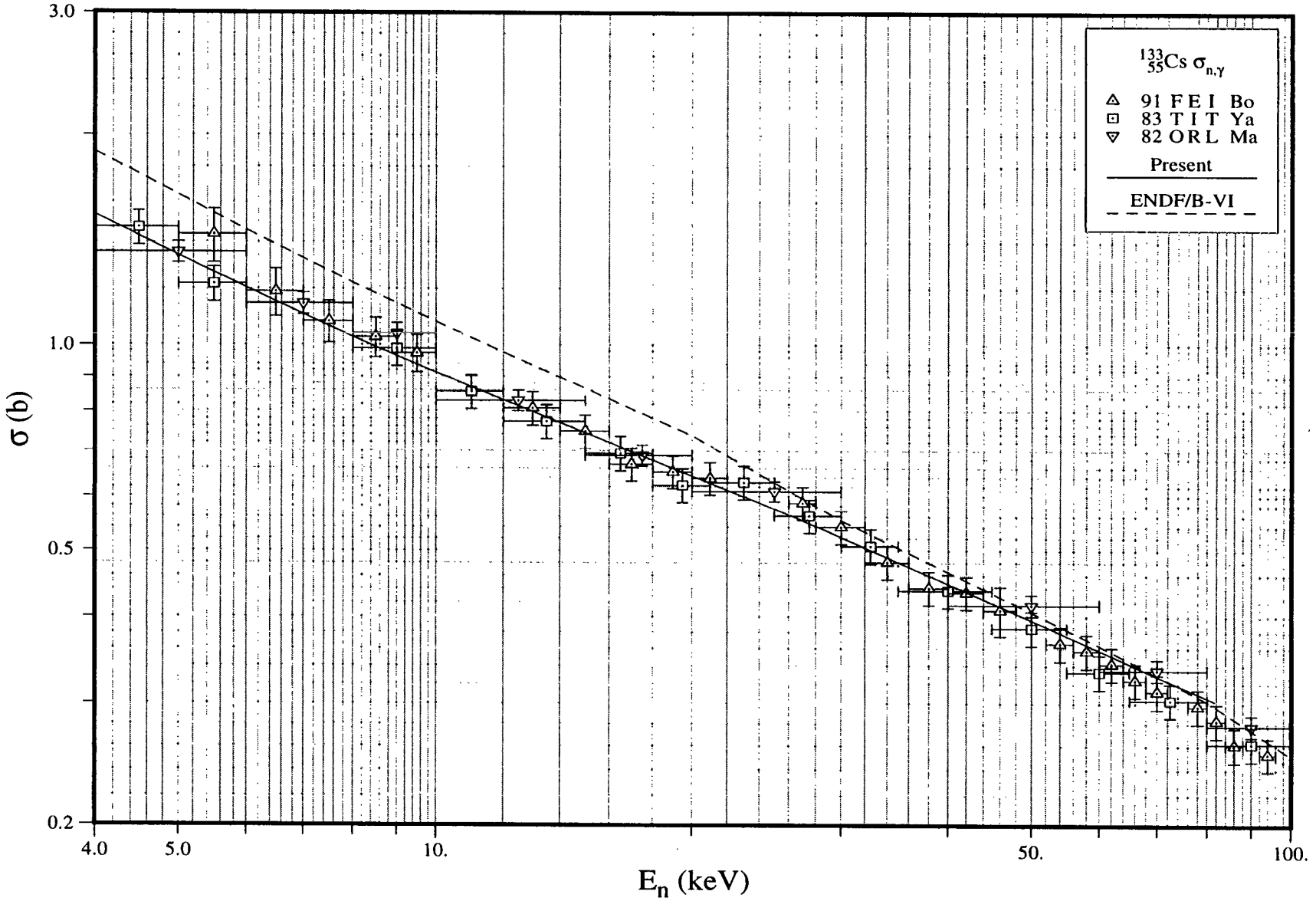

Fig. 28. Capture Cross Section in the Unresolved Resonance Region (^{133}Cs)

III.I. ^{141}Pr

1. Thermal Region

Positive-energy resolved resonance parameters and an effective scattering radius R' of 4.93 fm were adopted basically from Mughabghab's BNL compilation [Mu81]. However, two new bound levels were invoked to reproduce a thermal capture cross section of 11.5 b [Mu81], a bound coherent scattering length of 4.58±0.05 fm [Ko91], and an incoherent scattering length (b_+–b_-) of –7.2±0.07 fm [Ak76, Ko91]. An attempt to fit the thermal capture and scattering cross sections with a single bound level resulted in an unreasonable value for the scattering radius (R'=7.2 fm), which is at variance with a value of 4.9±0.5 fm [Mu81]. On this basis, two bound levels were invoked. To determine the parameters of the two bound levels, we assumed that the capture cross section for the bound level with spin 3 is equal to the other bound with spin 4. The resulting parameters for the two bound levels are listed in **Table 21**.

As shown in **Table 22**, the various quantities computed in the present study are generally in good agreement with those in the JEF-2 and JENDL-3 evaluations. However, a disagreement between the present evaluation and that of ENDF/B-VI for the capture and total resonance integrals exists.

2. Resolved Resonance Parameters

Resonance parameters up to 10.049 keV were adopted basically from the BNL compilation [Mu81]. In addition to these data, new measurements were taken into consideration. These are the capture and scattering widths of Taylor *et al.* [Ta79], the spin determinations of Alfimenkov *et al.* [Al82a], and the *l* assignments of Morgenstern *et al.* [Mo69]. Uncertainty-weighted averaging of known 69 radiative widths resulted in a value of 86±2 meV, which was assumed for resonances with unknown radiative widths. Of a total of 126 resonances, 79 (61 previously assigned by measurements) were assigned as s-wave and 47 (6 previously assigned) as p-wave by Bayesian analysis. We remark that resonances, with relatively large neutron widths, which were determined as p-wave resonances by the transmission measurements, were assigned as s-wave resonances by the Bayesian analysis. As an example, the p-wave resonance at 3395 eV with $g\Gamma_n$ =80 meV was determined by Bayesian analysis as s-wave with a probability of 0.98. Spins of resonances with undetermined values were assigned randomly on the basis of (2J+1) law.

The distribution of reduced neutron widths was analyzed on the basis of the Porter-Thomas distribution. For s-wave resonances, **Fig. 29** shows the calculated cumulative numbers of s-wave resonances with widths larger than a given $\sqrt{g\Gamma_n^0}$ value. The fit resulted in $\langle D_0 \rangle$ = 118.0±7.2 eV and $\langle g\Gamma_n^0 \rangle$ = 20.9±3.4 meV. These values yield s-wave strength function of S_0 = 1.77±0.3. The present $\langle D_0 \rangle$ is consistent with values reported by Taylor *et al.* [Ta79], 116±10 eV, and RIPL [Re98], 110±20, but is larger than that in the BNL compilation, 88±9 eV [Mu81]. The S_0 value is consistent with those reported in [Ta79], 1.8, RIPL, 1.7±0.3, and the BNL compilation [Mu81], 1.5±0.2. As shown in **Fig. 30**, the p-wave Porter-Thomas distribution without excluding weak resonances resulted in $\langle D_1 \rangle$ = 101.6±10.9 eV and S_1 = 0.65±0.14. The p-wave level spacing is unreasonably large when compared with an expected value of about 60 eV.

This indicated that several p-wave resonances were not detected experimentally. On the other hand, the p-wave strength function is consistent with the systematics study of p-wave strength functions in this mass region [Mu81].

3. Unresolved Resonance Parameters

The upper energy of the unresolved energy region was set to 146.47 keV, which corresponds to the threshold energy for neutron inelastic scattering to the first excited level of ^{141}Pr at 145.44 keV.

The capture cross section measurements of Taylor *et al.* [Ta79], subsequently corrected by Allen *et al.* [Al82b], Zaikin *et al.* [Za71], Konks *et al.* [Ko64], and Gibbons *et al.* [Gi61] were taken into consideration in this evaluation. Other measurements in the EXFOR database [EX], which deviated considerably from these measurements, were not considered.

In this energy region, average resonance parameters for s-, p- and d-waves were provided. Since the upper energy of the unresolved energy region is relatively high, d-wave contribution is not negligible. An energy-dependent level spacing according to Gilbert-Cameron level density formula, with parameters adopted from Mughabghab and Dunford [Mu98a], was adopted. From the (2J+1) dependence of the level density, level spacings for p- and d-wave resonances were calculated as 1/2 and 1/3 of the value for s-wave spacing, respectively. In the first attempt, the following average parameters were implemented in the computation of the capture cross section: 1) the average resonance parameters, $\langle D_0 \rangle$, S_0 and S_1, derived from the resolved resonance region; 2) S_2 = 3.0, obtained from a spherical optical model calculation [Mu84]; and 3) $\langle \Gamma_\gamma \rangle$ = 86 meV for s-, p-, and d-wave resonances. The resulting calculation is in very good agreement with the measurements in the 10 - 40 keV region [Ta79]. However, in the high energy region, there is a discrepancy of up to 30%. To achieve an improved fit in the high-energy region, S_2 was decreased to 0.6 and S_1 was slightly increased to 0.75. This small d-wave strength function is in reasonable agreement with measured strength function data in this mass region [Mu84]. Our finalized parameters for the unresolved region are listed in the last column of **Table 23** and are compared with other evaluations. The calculated capture cross section with the adjusted parameters is shown in **Fig. 31** and is compared with measurements [Ta79, Za71, Ko64, Gi63].

Maxwellian-averaged capture cross section for a temperature of 30 keV was computed as 117 mb. This cross section is in excellent agreement with 119±15 mb reported in Beer's compilation [Be92] and 111±15 mb in the BNL compilation [Mu81].

Table 21. Bound Level Resonance Parameters (^{141}Pr)

Energy (eV)	*l* and Resonance Spin	Scattering Width (meV)	Capture Width (meV)
–48.12	*l*=0, J=3.0	411.2	86.0
–17.81	*l*=0, J=2.0	47.6	87.3

Table 22. Thermal Characteristics (^{141}Pr)

Quantity	Unit	BNL [Mu81]	98CRC [Ho98]	ENDF/ B-VI	JEF-2.2	JENDL-3.2	Present
R'	fm	4.9±0.5		6.278	4.40	4.90	4.93
B	fm	4.45±0.05	4.58±0.05				4.58
σ_γ^0	barn	11.5±0.3	11.5	11.5	11.5	11.5	11.5
σ_s^0	barn	2.54±0.06		2.18	2.59	2.54	2.71
gw*				1.002	0.9997	0.9990	0.9995
RI-capt.**	barn	17.4±2.0	14±3	19.0	17.9	18.4	17.6
RI-total**	barn			303	234	239	237

* Westcott factor for capture cross section.

** Integrated from 0.5 eV to 100 keV with 1/E spectrum.

Table 23. Average Resonance Parameters for Unresolved Resonance Region (^{141}Pr)

Quantity	Unit	BNL compilation	ENDF/ B-VI	JEF-2	JENDL-3*	Present	
						PT Analysis	Adopted
R'	fm	4.9±0.5		4.40	5.181		4.93
$\langle D_0 \rangle$	eV	88±9		120.0	134.2	118.0±7.2	118.0**
S_0	$\times 10^{-4}$	1.5±0.2		1.00	1.50	1.77±0.30	1.77
$\langle \Gamma_{\gamma 0} \rangle$	meV			85	86		86
$\langle D_1 \rangle$	eV			62.2	67.1	101.6±10.9	59.0**
S_1	$\times 10^{-4}$			1.00	1.20	0.65±0.14	0.75
$\langle \Gamma_{\gamma 1} \rangle$	meV			85	86		86
$\langle D_2 \rangle$	eV			44.1	44.7		39.3**
S_2	$\times 10^{-4}$			3.574	1.50		0.60
$\langle \Gamma_{\gamma 2} \rangle$	meV			85	86		86

* Average parameters at the low energy (13.23 keV) of the unresolved region.

** Value at the neutron separation energy of ^{142}Pr.

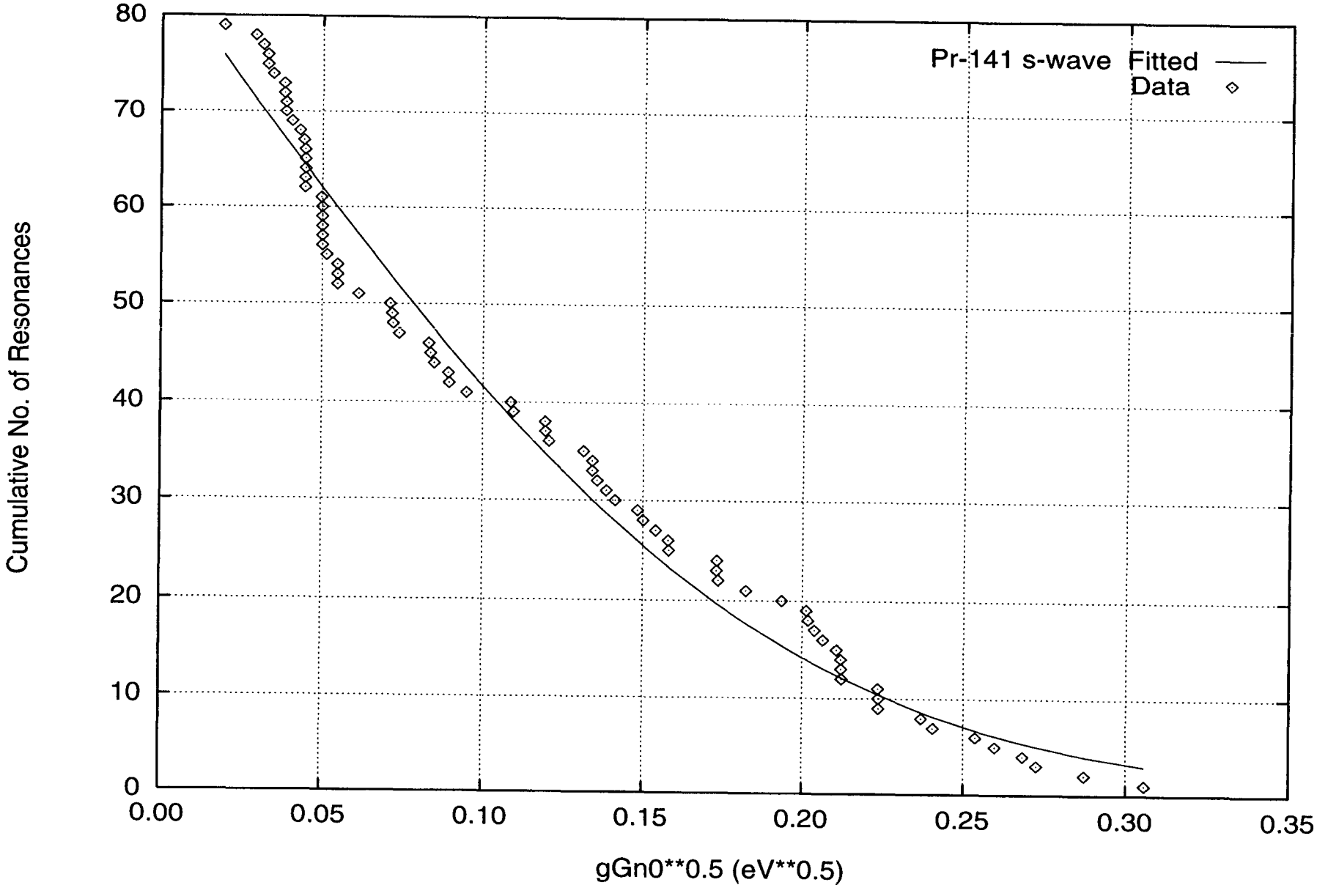

Fig. 29. Complement of the Cumulative Distribution of Neutron Reduced Widths (^{141}Pr, s-wave)

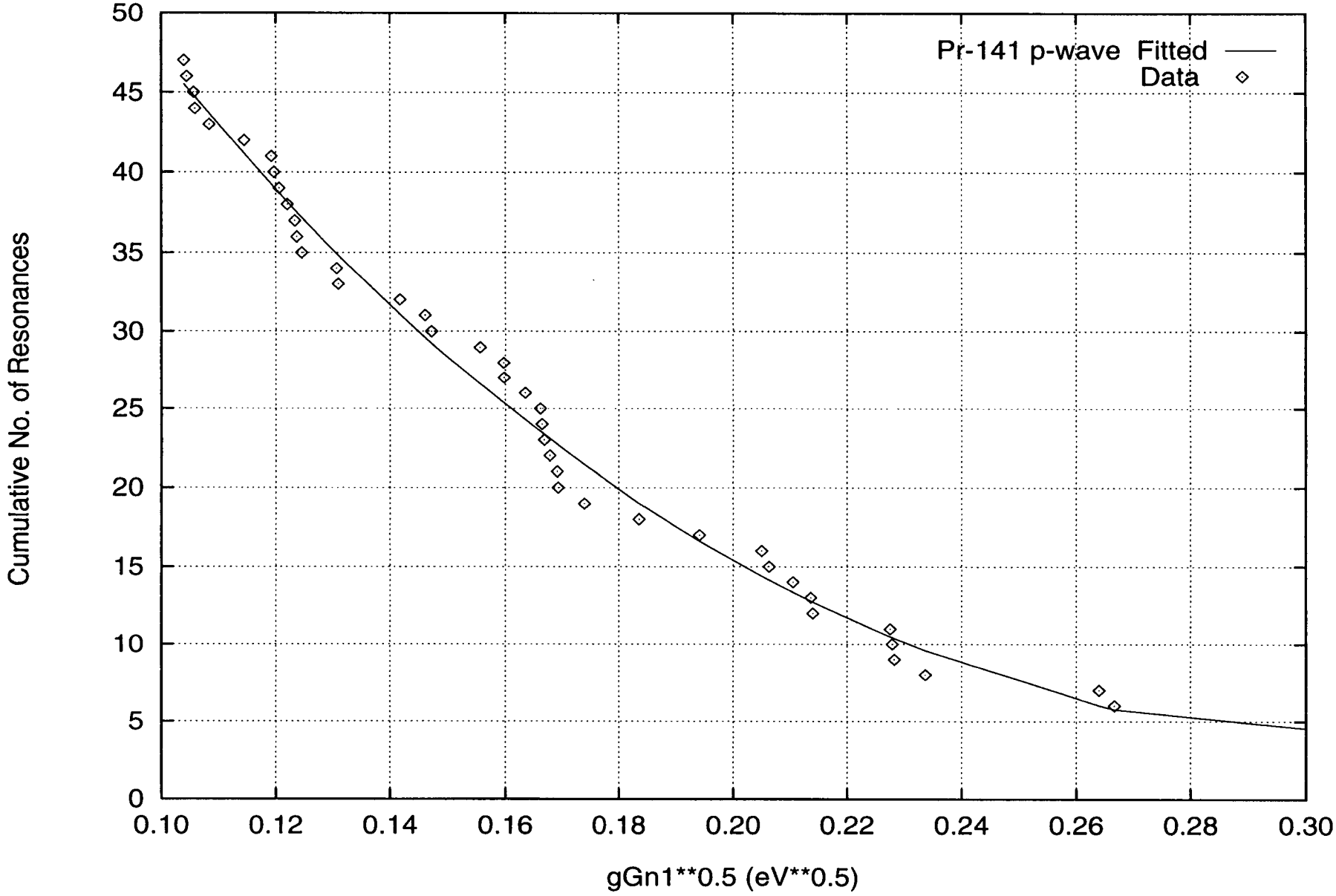

Fig. 30. Complement of the Cumulative Distribution of Neutron Reduced Widths (^{141}Pr, p-wave)

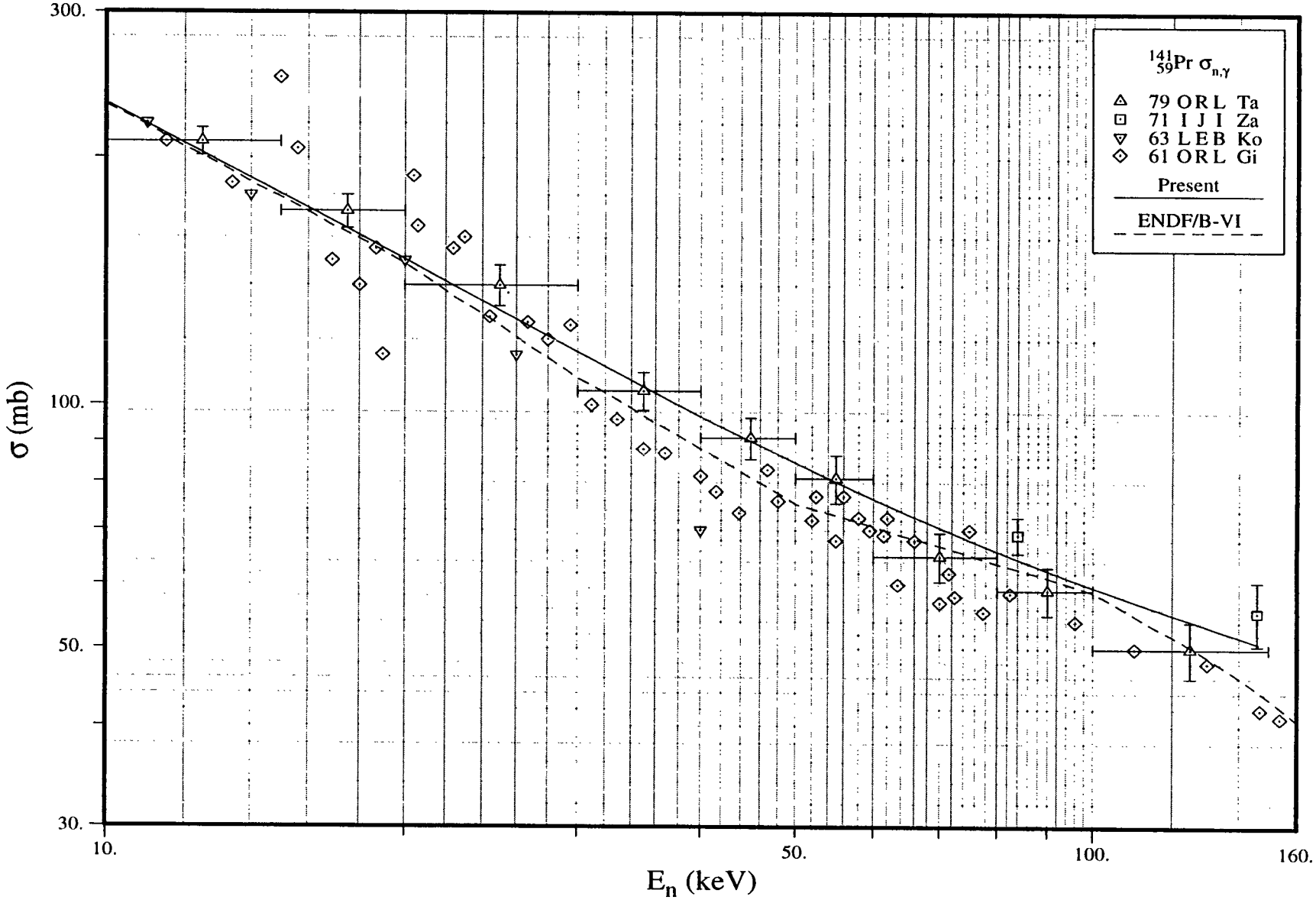

Fig. 31. Capture Cross Section in the Unresolved Resonance Region (^{141}Pr)

III.J. ^{143}Nd

1. Thermal Region

Since the contributions of positive energy resonances to the thermal capture cross section of ^{143}Nd is only 2.7 barns, a bound level is invoked to explain its thermal capture cross section, 325 ± 10 b [Mu81]. The spin of the bound level is assumed as 3 on the basis of gamma-ray spectra measurements at thermal energy. The energy for a bound level is determined as -6.5 eV with a reduced neutron width of 104.7 meV for an assumed radiative width of 72.3 meV. The Westcott factor for capture was calculated as 0.9966. **Table 24** summarizes thermal parameters and compares our results with other sources.

2. Resolved Resonance Parameters

The resonance parameters in the BNL compilation [Mu81] are mainly based on the data of Tellier at Saclay [Te71] and Musgrove *et al.* at ORNL [Mu77]. However, Allen *et al.* [Al82a] reported that a correction factor is required for the ORNL data. A re-evaluation of the resonance parameters was carried out by reducing the reported capture areas by 0.9507 [Mu77] and re-computing Γ_γ with the known $g\Gamma_n$ values. The spin assignments by Cauvin *et al.* [Ca71a] and Rohr *et al.* [Ro71] were adopted. Spins for other resonances were assigned randomly on the basis of the (2J+1) dependence of the level density.

On the basis of the Porter-Thomas distribution for all observed resonances (**Fig. 32**), an excess of weak resonances, interpreted as p-wave, was observed. The orbital angular momenta of resonances were determined by applying Bayesian analysis. **Figures 33** and **34** display the Porter-Thomas distributions for s- and p-wave resonances, respectively. The average resonance parameters obtained from this analysis are displayed in **Table 25**.

The upper limit of the resolved resonance region is set at 5503 eV.

3. Unresolved Resonance Parameters

Several capture measurements were carried out in the keV energy region. Musgrove *et al.* [Mu77] covered the energy region from 3 keV to 100 keV. More recent measurement by Wisshak *et al.* [Wi98] covered the energy region from 3 to 225 keV. Other measurements, made by Yamamuro *et al.* at JAERI [Ya79] and Bokhovko *et al.* at Obninsk [Bo85], are significantly high at a few keV when compared with the data of Musgrove *et al.* [Mu77] and Wisshak *et al.* [Wi98].

As a starting point, the average resonance parameters obtained from the resolved resonance region were used. The level spacing was assumed to vary with energy and spin according to the Gilbert-Cameron's level density relation with associated parameters of [Mu98a] and a spin dispersion parameter of 3.5 [Mu98b]. In addition, p-wave strength function of 0.8 [Mu81] was assumed. P-wave average radiative width of 40 meV and d-wave strength function of 1.5 were adopted from the systematics [Mu81]. These parameters resulted in a calculated capture cross section smaller than that of Wisshak *et al.* [Wi98] in the energy region up to

several keV. To achieve agreement with the data [Wi98], the s-wave average level spacing was adjusted to 36 eV from a value of 38 ± 2eV. This adjusted value is within the uncertainty limits of that obtained from the Porter-Thomas distribution analysis. **Figure 35** shows the resulting capture cross section, constructed from the average parameters that are listed in the last column of **Table 25**.

In addition to the (n,α) reaction, the neutron inelastic scattering to the first excited level is open at an energy of 747 keV. The upper energy limit of the unresolved resonance region was set at 225 keV.

Maxwellian average capture cross section for a 30 keV temperature was computed as 239 mb for an upper energy limit of 1 MeV. From 225 keV to 1 MeV, the point-wise capture cross section of the ENDF/B-VI evaluation was adopted. Our result is compared with a value of 244.6±3.1 mb of Wisshak *et al.* [Wi98] and 242±10 mb reported in Beer's compilation [Be92].

Table 24. Thermal Parameters (^{143}Nd)

Quantity	Unit	BNL Compilation	98CRC [Ho98]	ENDF/B-VI	JEF-2.2	JENDL-3.2	Present
R'	fm			5.54	5.60	5.60	5.60
b'	fm			16.7		17.3	16.7
σ_γ	barns	325 ± 10	330 ± 10	325	323	330	325
σ_s	barns	80 ± 2		80.6	80.8	80.3	80.4
RI-capt.	barns	128 ± 30	128 ± 30	130	130	130	130

Table 25. Average Resonance Parameters in the Unresolved Resonance Region (^{143}Nd)

Quantity	Unit	ENDF/B-VI	JEF-2.2	JENDL-3.2[a]	BNL Compilation	Present	
						PT Analysis	Adopted
R'(URR)	fm	5.54	7.34	4.14			5.60
$<D_0>$	eV	32.5	36.0	36.4	45 ± 4	38.0 ± 2.0	36.0[b]
S_0	$\times 10^{-4}$	3.5	3.4	2.62	3.2 ± 0.3	3.62 ± 0.51	3.62
$<\Gamma_{\gamma 0}>$	meV	80	76~68	79.1	80 ± 9		79.9
$<D_1>$	eV	18.4	18.0	18.2			19.3[b]
S_1	$\times 10^{-4}$	0.8	0.6	1.04	0.8 ± 0.3		0.8
$<\Gamma_{\gamma 1}>$	meV	80	74~65	79.1			40.0
$<D_2>$	eV	12.3	12.0	12.1			14.5[b]
S_2	$\times 10^{-4}$	1.0	3.0	1.78			1.50
$<\Gamma_{\gamma 2}>$	meV	80	96~64	79.1			79.9

a: value at the low energy (5 keV) of the unresolved energy region.
b: value at the neutron separation energy of ^{144}Nd.

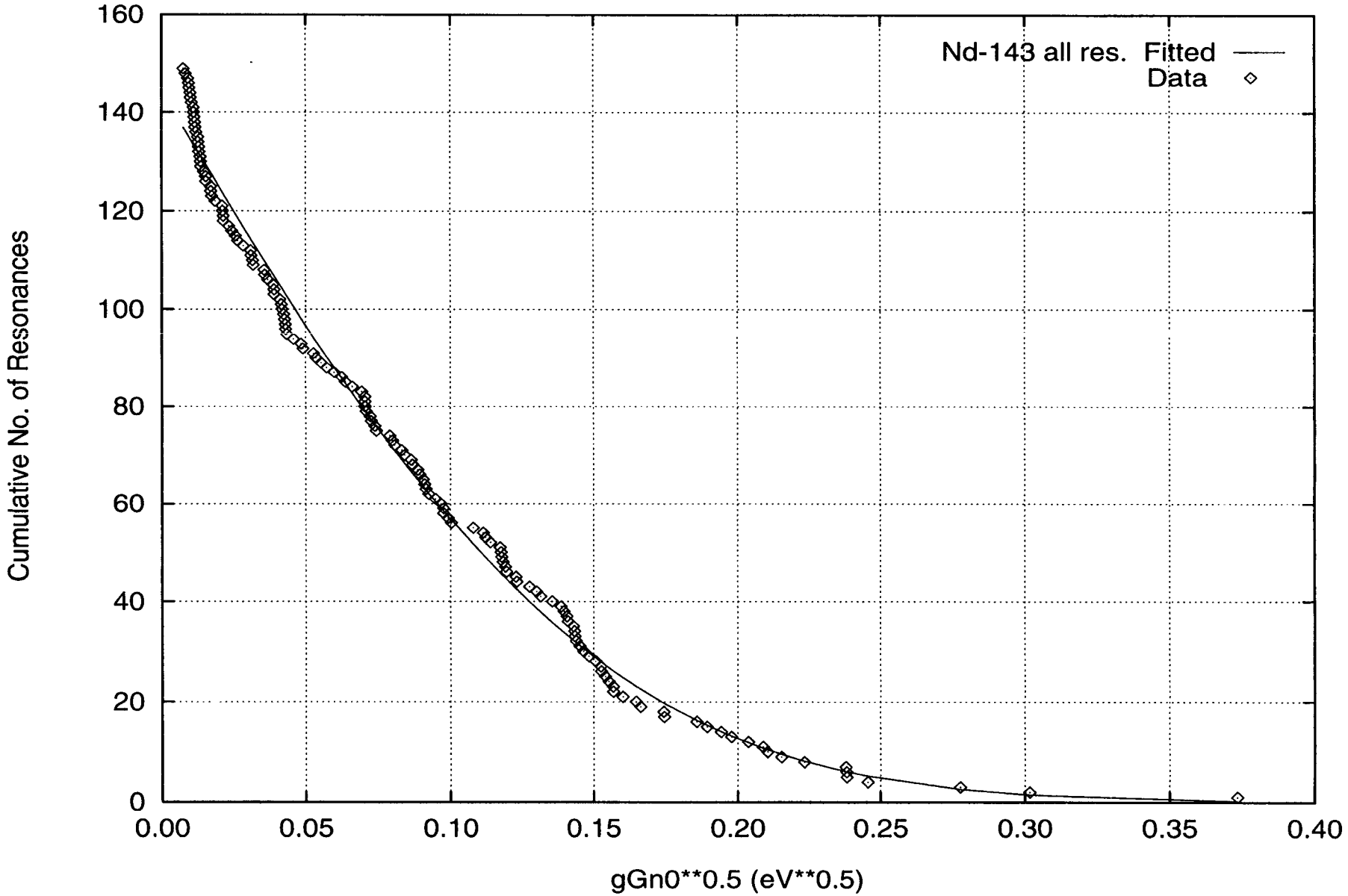

Fig. 32. Complement of the Cumulative Distribution of Neutron Reduced Widths (^{143}Nd).
All resonances were assumed as s-wave.

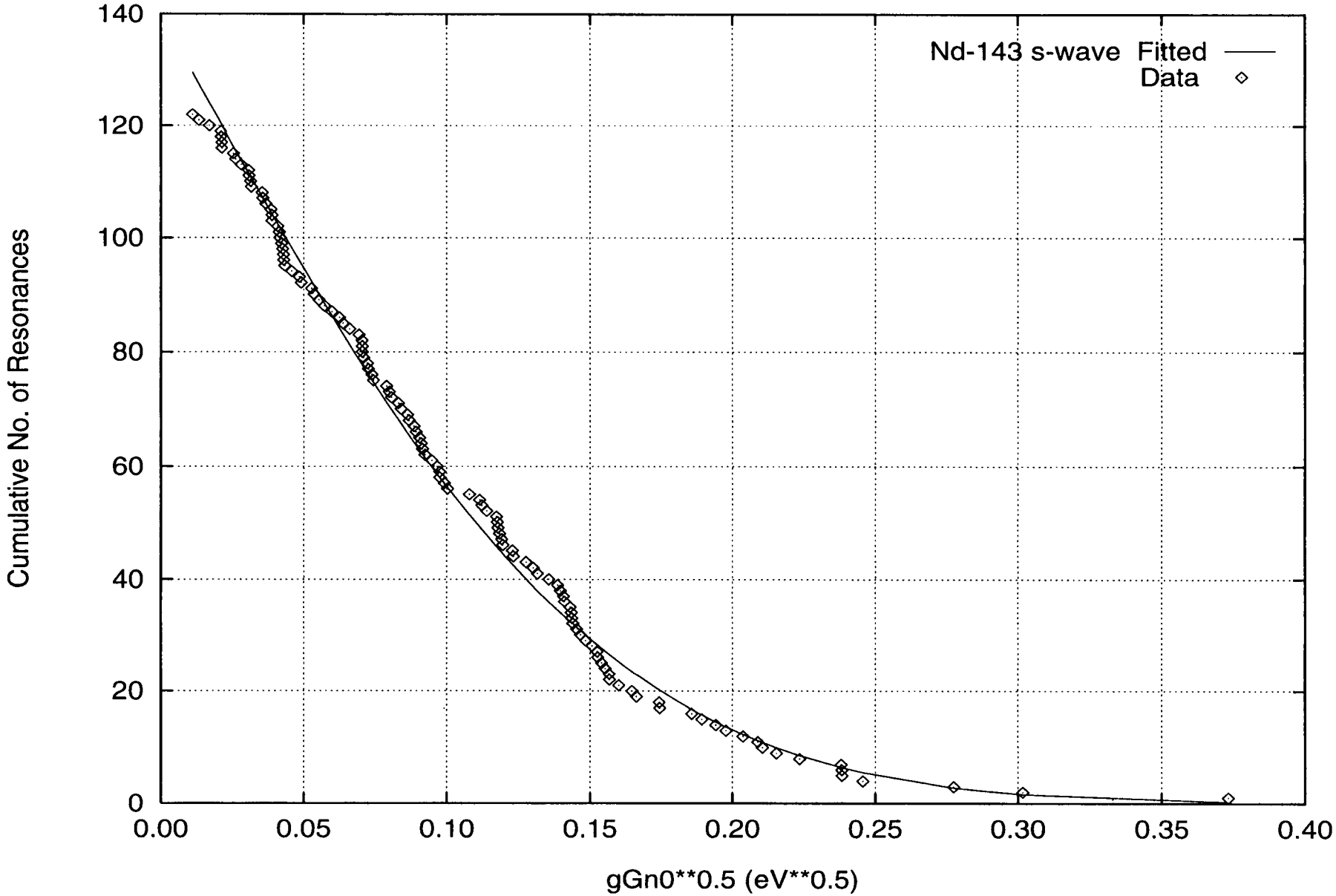

Fig. 33. Complement of the Cumulative Distribution of Neutron Reduced Widths (^{143}Nd, s-wave)

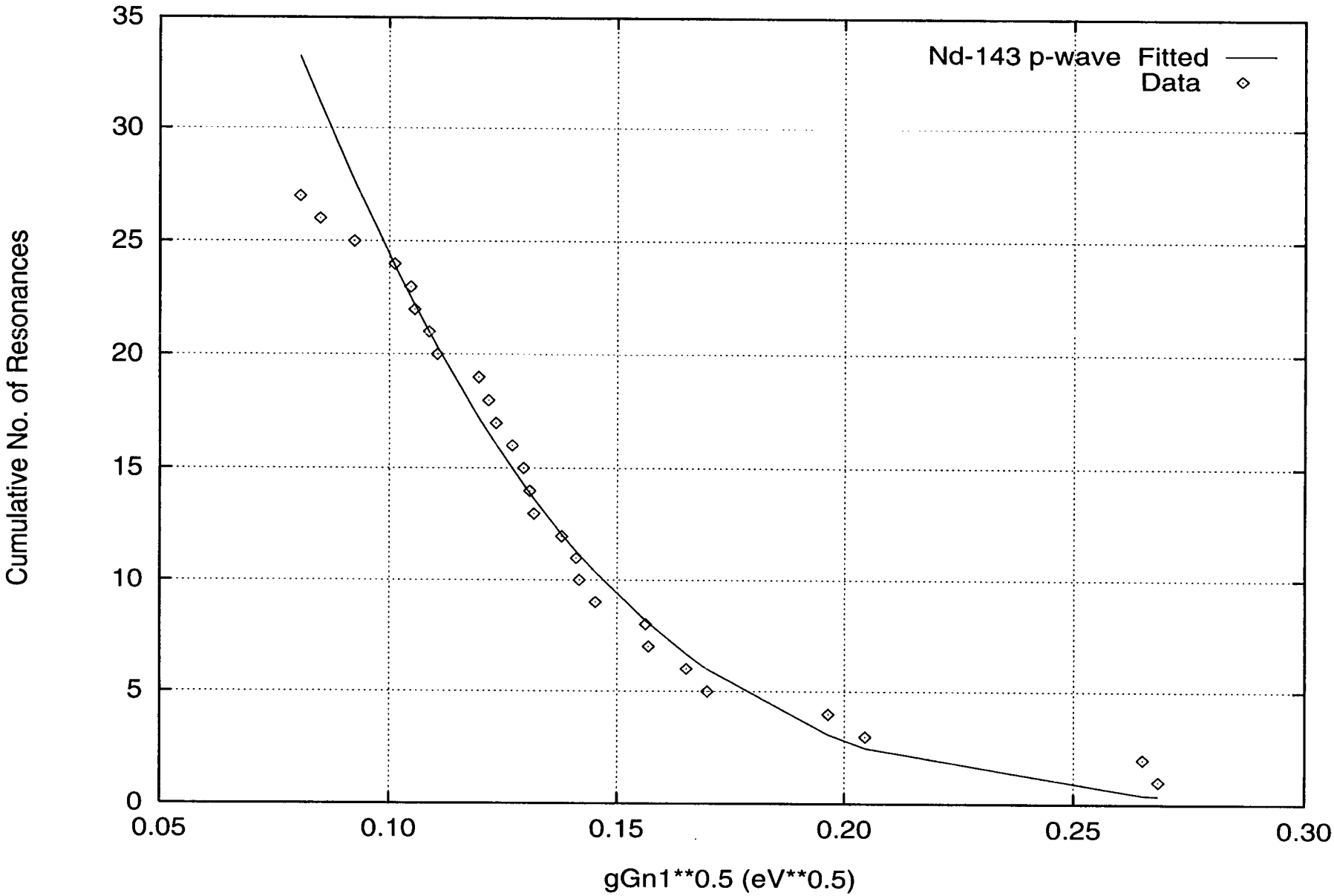

Fig. 34. Complement of the Cumulative Distribution of Neutron Reduced Widths (^{143}Nd, p-wave)

Fig. 35. Capture Cross Section in the Unresolved Resonance Region (^{143}Nd)

III.K. ^{145}Nd

1. Thermal Characteristics

The thermal scattering and capture cross sections are evaluated by taking a weighted average of the results of Pattenden *et al.* [Pa58], Tattersall *et al.* [Ta60], Lucas *et al.* [Lu77], Vertebnyi *et al.* [Ve74], and Anufriev *et al.* [An79]. The present evaluated cross sections are included in **Table 26** and are compared with other evaluations. A bound level is required to fit the capture and scattering cross sections in the thermal energy region. Its derived parameters are: $E_0 = -25.334$ eV, J=3, $\Gamma_n = 976.7$ meV for an assumed $\Gamma_\gamma = 76.5$ meV. The bound coherent scattering amplitude is computed as 8.73 fm for an assumed potential scattering radius of 6.00 fm, adopted from a deformed optical model calculation [Mu81]. The calculated Westcott factor for capture is 1.0000.

2. Resolved Resonance Parameters

The evaluated resonance parameters [Mu81] are mainly based on the transmission data of Tellier at Saclay [Te71], the capture data of Rohr *et al.* at Geel [Ro71], and Musgrove *et al.* at ORNL [Mu77]. In evaluating the resonance parameters, the ORNL capture areas [Mu77] were decreased by a factor of 0.9507 as reported by Allen *et al.* [Al82]. A comparison of the scattering widths of the weak resonances of Rohr *et al.* [Ro71] with those of Tellier *et al.* [Te71], Karzhavina *et al.* [Ka69], and Anufriev *et al.* [An79] indicated that the capture areas of Rohr *et al.* are low by about 20%. This conclusion is also supported by the fact that the derived radiative widths of Rohr are low when compared with the results of Musgrove *et al.* [Mu77]. On this basis, the capture areas [Ro71] were increased by 20%. The capture widths of the strong resonances were then recalculated with the aid of the known scattering widths [Te71]. For weak resonances, an average $\Gamma_\gamma = 76.5$ meV was assumed. A weak resonance reported at 18.9 eV [An79] is also included in the file.

Spin assignments, made by Cauvin *et al.* [Ca71a] and Stolovy *et al.* [St72], were considered. In addition, other spin assignments for strong resonances were made by us on the basis of the following criterion: resonances with a large capture area are assigned as J=4 and those with a low value as J=3. The scattering widths of weak resonances were calculated from the renormalized capture areas of Musgrove *et al.* [Mu77] for an assumed average radiative width of 76.5 meV for the two possible spin values, 3 and 4. Subsequently, an average value was computed from the two results. The spins of the remaining resonances were assigned randomly on the basis of the (2J+1) law.

The analysis of reduced neutron widths for resonances below 4.0 keV in terms of the Porter-Thomas distribution shows that few weak s-wave resonances are missed. A least squares fit, carried out for resonances having $(g\Gamma_n^0)^{1/2} > 0.05$ eV, is shown in **Fig. 36**. The average resonance parameters derived from this analysis are listed in Table 2. The Bayesian analysis shows that, with the exception of the 18.9 eV resonance, all observed resonances are s-wave resonances. However, in the resonance parameter file, the weak resonance at 18.9 eV was treated as an s-wave resonance.

3. Unresolved resonance parameters

The low- and high-energy limits of the unresolved resonance region were set at 3979 eV and 67.69 keV respectively; the latter corresponds to the threshold energy for inelastic neutron scattering to the first excites state of ^{145}Nd.

The capture data by Nakajima *et al.* at JAERI [Na78], Bokovko *et al.* at Obninsk [Bo85], and Wisshak *et al.* at Karlsruhe [Wi98] were considered in this evaluation. Wisshak *et al.*'s measurement covers the energy range from 3 to 225 keV.

The average s-wave resonance properties obtained from the resolved resonance analysis were used without adjustment. In addition, the p-wave average radiative width and the d-wave strength function were obtained from the systematics [Mu84]. The average parameters are summarized in **Table 27**. The energy-dependent level spacing of Gilbert-Cameron with the parameters of [Mu98a] and a spin dispersion parameter of 3.5 [Mu98b] was adopted. Our calculated capture cross section in the unresolved energy region is shown in **Fig. 37** and is compared with the ENDF/B-VI evaluation and measured data. The present calculations strongly support Wisshak *et al.*'s measurement [Wi98]. Note that the JENDL-3.2 evaluation adopted Nakajima *et al.*'s measurement [Na78], which is high when compared with other measurements [Wi98, Bo85]. In addition, the average radiative widths for s-, p- and d-wave resonances in JENDL-3.2 are quite high when compared with our values (**Table 27**). The large s-wave radiative width of JENDEL-3.2 is not consistent with that obtained from the resolved energy region.

Maxwellian average capture cross section for a temperature of 30 keV was computed as 423 mb. The calculation was carried out up to 1 MeV; the capture cross section was constructed with the present parameters up to 67.69 keV and those of ENDF/B-VI from 67.69 keV to 1 MeV. An excellent agreement was obtained with a value of 424.8 ± 4.5 mb [Wi98]; the reported value in the Beer's compilation is 485 ± 100 mb [Be92].

Table 26. Thermal Characteristics (^{145}Nd)

Quantity	Unit	BNL Compilation	98CRC [Ho98]	ENDF/B-VI	JEF-2.2	JENDL-3.2	Present
R'	fm			6.8	6.0	6.0	6.0
b'	fm			9.9			8.73
σ_γ	barns	42 ± 2	47 ± 6	42.1	41.9	43.8	49.8
σ_s	barns			17.4	18.3	20.3	18.7
RI-capt.	barns	240 ± 35	260 ± 40	231	231	204	245

Table 27. Average Resonance Parameters in the Unresolved Resonance Region (^{145}Nd)

Quantity	Unit	ENDF/B -VI	JEF-2.2	JENDL-3.2 [a]	BNL Compilation	Present	
						P-T	Present
R'(URR)	fm	6.80	5.00	7.683			6.00
$<D_0>$	eV	17.3	18.2	17.2	22±2	18.0±0.8	18.0 [b]
S_0	$\times 10^{-4}$	4.00	5.20	2.93	4.4±0.4	4.75±0.52	4.75
$<\Gamma_{\gamma 0}>$	meV	75.0	89.1	97.5	75±9		76.5
$<D_1>$	eV	8.66	9.40	8.61			9.64 [b]
S_1	$\times 10^{-4}$	0.80	0.98	0.69	0.8±0.4	-	1.20
$<\Gamma_{\gamma 1}>$	meV	75.0	88.1	97.5			40.0
$<D_2>$	eV	5.78	6.60	5.74			7.25 [b]
S_2	$\times 10^{-4}$	1.00	3.90	3.51			0.80
$<\Gamma_{\gamma 2}>$	meV	75.0	89.1	97.5			76.5

a: value at energy 5.1 keV of the unresolved energy region.
b: value at the neutron separation energy of ^{146}Nd.

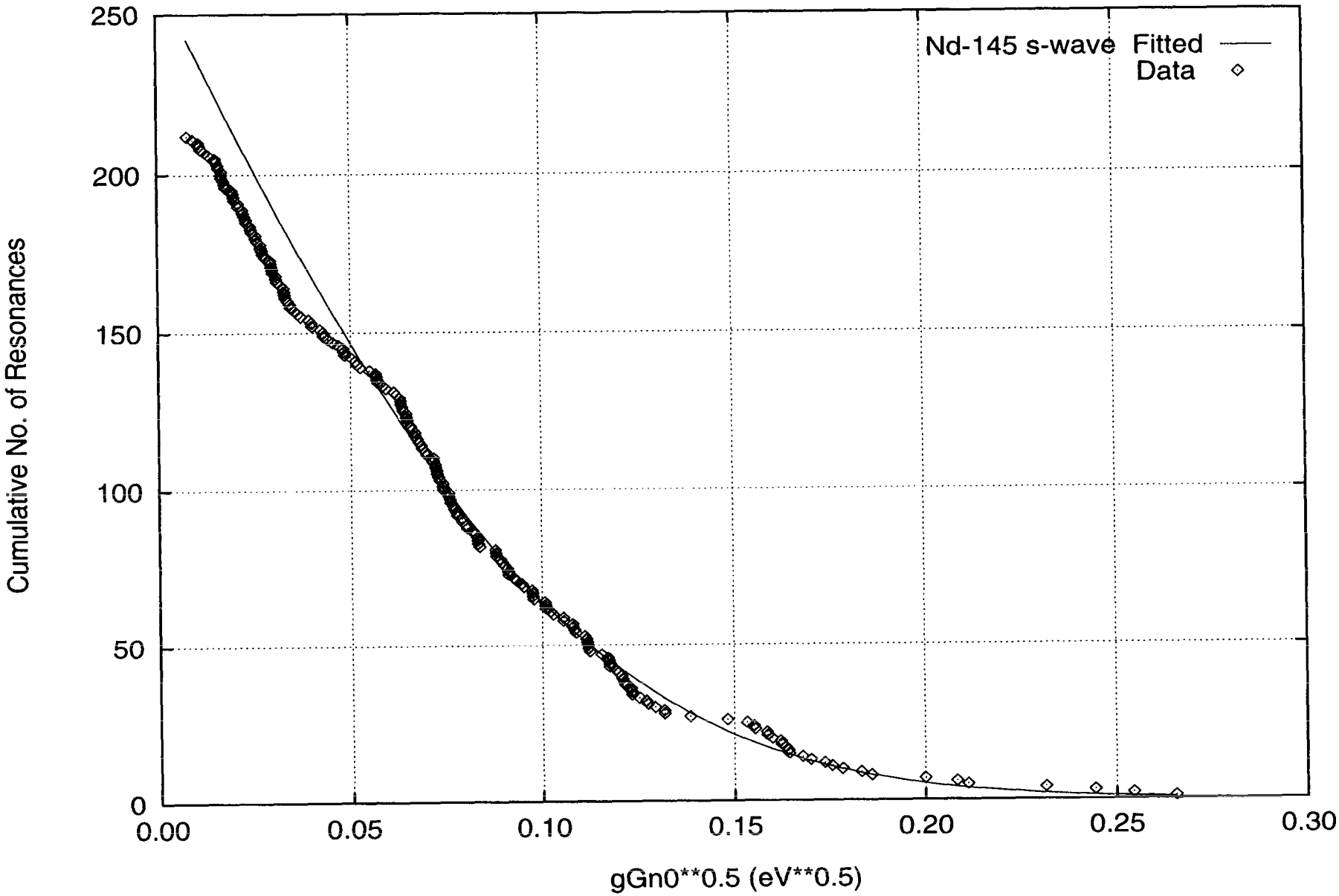

Fig. 36. Complement of the Cumulative Distribution of Neutron Reduced Widths (^{145}Nd, s-wave)

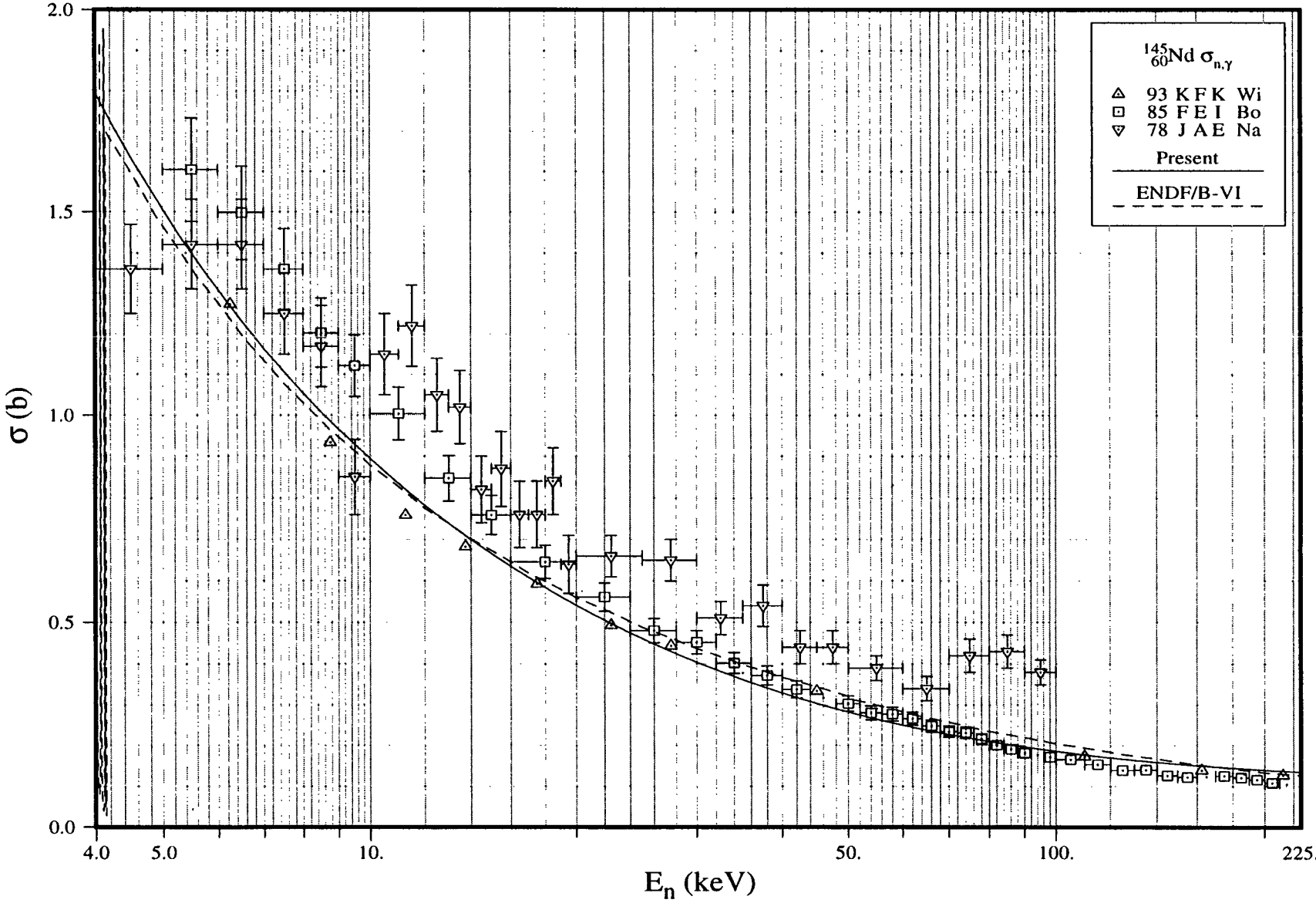

Fig. 37. Capture Cross Section in the Unresolved Resonance Region (^{145}Nd)

III.L. ^{147}Sm

1. Thermal Region

Since the contribution of positive energy resonances to the thermal capture cross section is 21.4 b, a bound level was invoked to reproduce a thermal capture cross section of σ_γ^0 = 50.0 b. The latter value was obtained by re-normalizing the measurement of Fenner and Large [Fe67] (σ_γ^0 = 51±3 b, I_γ = 640±200 b) to a capture resonance integral of I_γ = 700 b. The bound coherent scattering length, b_{coh} =14±3 fm, recommended in the BNL compilation, was not considered in the determination of the bound level parameters for two reasons: a) a value of 14 fm was previously deduced from the transmission measurement of Eiland *et al.* [Ei74] which suffered from a large uncertainty due to neutron absorption in the moisture and b) this large value of b_{coh} resulted in unrealistic resonance parameters for the bound level. On the other hand, an effective scattering radius R'= 8.3 fm, adopted from the BNL compilation [Mu84], resulted in the following parameters for the bound level: E_0 = –2.50 eV, J = 4, Γ_n = 1.67 meV, Γ_γ = 73.8 meV. A comparison of the thermal cross sections and resonance integrals of the present evaluation with those of ENDF/B-VI, JEF-2.2, JENDL-3.2, and LIPAR-5 [Ab97] evaluations is presented in **Table 28**. With the exception of the capture cross section, the present quantities are in good agreement with those of JENDL-3.2 evaluation.

2. Resolved Resonance Parameters

The primary source of the resolved resonance parameters for this nuclide is the BNL compilation [Mu84]. In addition to this source, recent results of Georgiev *et al.* [Ge93] were incorporated into the present set of parameters. The present resolved energy region extends up to 1.998 keV. On the basis of Bayesian analysis, the observed 211 resonances were assigned as s-wave resonances. Resonance spins were assigned randomly to those resonances for which the spin is unknown. This random assignment assumed that the level density is proportional to (2J+1). The weighted averaging of 28 known radiative widths resulted in an average value of 73.8±1.5 meV, which was assumed for the remaining resonances with undetermined radiative widths. This average value is consistent with 69±2 meV recommended in the BNL compilation [Mu84] and RIPL [Re98].

The distribution of reduced neutron widths was analyzed in terms of the Porter-Thomas distribution. Those resonances with reduced widths smaller than 1.0 meV were excluded in the fitting procedure to obtain a best fit to the data. The fit, shown in **Fig. 38**, resulted in $\langle g\Gamma_n^0 \rangle$ = 2.94±0.29 meV and $\langle D_0 \rangle$ = 6.05±0.23 eV. These values yield an s-wave strength function, S_0 = 4.86±0.50. The present $\langle D_0 \rangle$ is consistent with a value recommended in the BNL compilation [Mu84], (5.7±0.5 eV), but is slightly higher than that recommended in the RIPL [Re98], (5.1±0.5 eV). In addition, the present S_0 is consistent with a 4.8±0.5 reported in the BNL compilation and RIPL.

3. Unresolved Resonance Parameters

The present unresolved resonance region covers the energy range from 1.998 keV to 122.05 keV. The latter energy corresponds to the threshold energy for inelastic neutron scattering to the first excited level of ^{147}Sm at 121.22 keV. For this nucleus, s-, p- and d-wave average resonance parameters were provided. The level spacing varies with energy according to Gilbert-Cameron level density formula with associated parameters adopted from Mughabghab and Dunford [Mu98a] (neutron separation energy = 8.14 MeV, pairing energy = 2.14 MeV, and level density parameter = 17.5 MeV^{-1}). The dependence of level spacing on $\exp\{-(J+1/2)^2/2\sigma^2\}$, as well as (2J+1), was taken into account for this nucleus. With a value of $\sigma = 3.4$ for the spin dispersion parameter [Mu98b], the level spacing for p- and d-wave resonances were calculated as 1/1.86 and 1/2.47 of the s-wave spacing, respectively. Note that these values deviate slightly from 1/2 and 1/3, obtained by assuming only (2J+1) dependence of the level spacing.

In the unresolved resonance region, the average cross sections measured by Wisshak *et al.* [Wi93], Macklin [Ma86], and Bokhovko *et al.* [Bo85] were taken into consideration. These measurements agree with each other, while the data sets of Kononov *et al.* [Ko77] and Mizumoto *et al.* [Mi81] deviate from the above measurements. As shown in **Fig. 39**, the present unresolved resonance parameters resulted in a good fit to the experimental data. The present parameters are listed in the last column of **Table 29**. The values of $\langle\Gamma_\gamma\rangle$, $\langle D_0\rangle$ and S_0 are those which resulted from the analysis in the resolved resonance region. The value of S_1 was adopted from a deformed optical model calculation [Mu84, Fig. 4], while S_2 was adjusted to 2.50 to reproduce the measured capture cross sections at the high energy limit. We note that S_1 is consistent with a value derived by Bokhovko *et al.* [Bo91] ($S_1 = 0.8\pm0.2$), while S_2 deviates from those reported by Bokhovko *et al.* (4.8±1.0), and Kononov *et al.* [Ko81] (1.29±0.28).

Maxwellian-averaged cross section for a temperature of 30 keV was computed as 890 mb. The present cross section is compared with 973.1±10 mb of Wisshak *et al.* [Wi93] and 1005±100 mb presented in Beer's compilation [Be92].

Table 28. Thermal Characteristics (^{147}Sm)

Quantity	Unit	BNL compilation	98CRC [Ho98]	ENDF/ B-VI	JEF-2.2	JENDL-3.2	LIPAR-5 [Ab97]	Present
R'	fm	8.3±0.2		8.30	8.30	8.30		8.30
σ_γ^0	barn	57±3	56±4	57.5	57.2	58.0	56.7	50.0
σ_s^0	barn			39.1	39.9	1.06	3.8	1.06
gw*				0.9990	1.001	0.9946	0.9942	0.9965
RI-capt.	barn		710±50	789	793	779	721	777
RI-total	barn			1660	1639	1524		1505

*Westcott factor for capture cross section.

Table 29. Average Resonance Parameters for the Unresolved Resonance Region (^{147}Sm)

Quantity	Unit	BNL compilation	ENDF/ B-VI	JEF-2.2	JENDL-3.2	Present	
						PT Analysis	Adopted
R'	fm	8.3±0.2	8.30	6.37	6.64		8.30
$\langle D_0 \rangle$	eV	5.7±0.5	5.70	6.32	5.70	6.05±0.23	6.05*
S_0	$\times 10^{-4}$	4.8±0.5	4.80	4.26	4.80	4.86±0.50	4.86
$\langle \Gamma_{\gamma 0} \rangle$	meV	69±2	69.0	87.6	69.0		73.8
$\langle D_1 \rangle$	eV		2.85	3.25	2.85		3.25*
S_1	$\times 10^{-4}$		0.65	1.75	1.00		0.80
$\langle \Gamma_{\gamma 1} \rangle$	meV		69.0	87.6	69.0		40.0
$\langle D_2 \rangle$	eV			2.28	1.90		2.45*
S_2	$\times 10^{-4}$			6.50	4.70		2.50
$\langle \Gamma_{\gamma 2} \rangle$	meV			87.6	69.0		73.8

*Value at the neutron separation energy of ^{148}Sm.

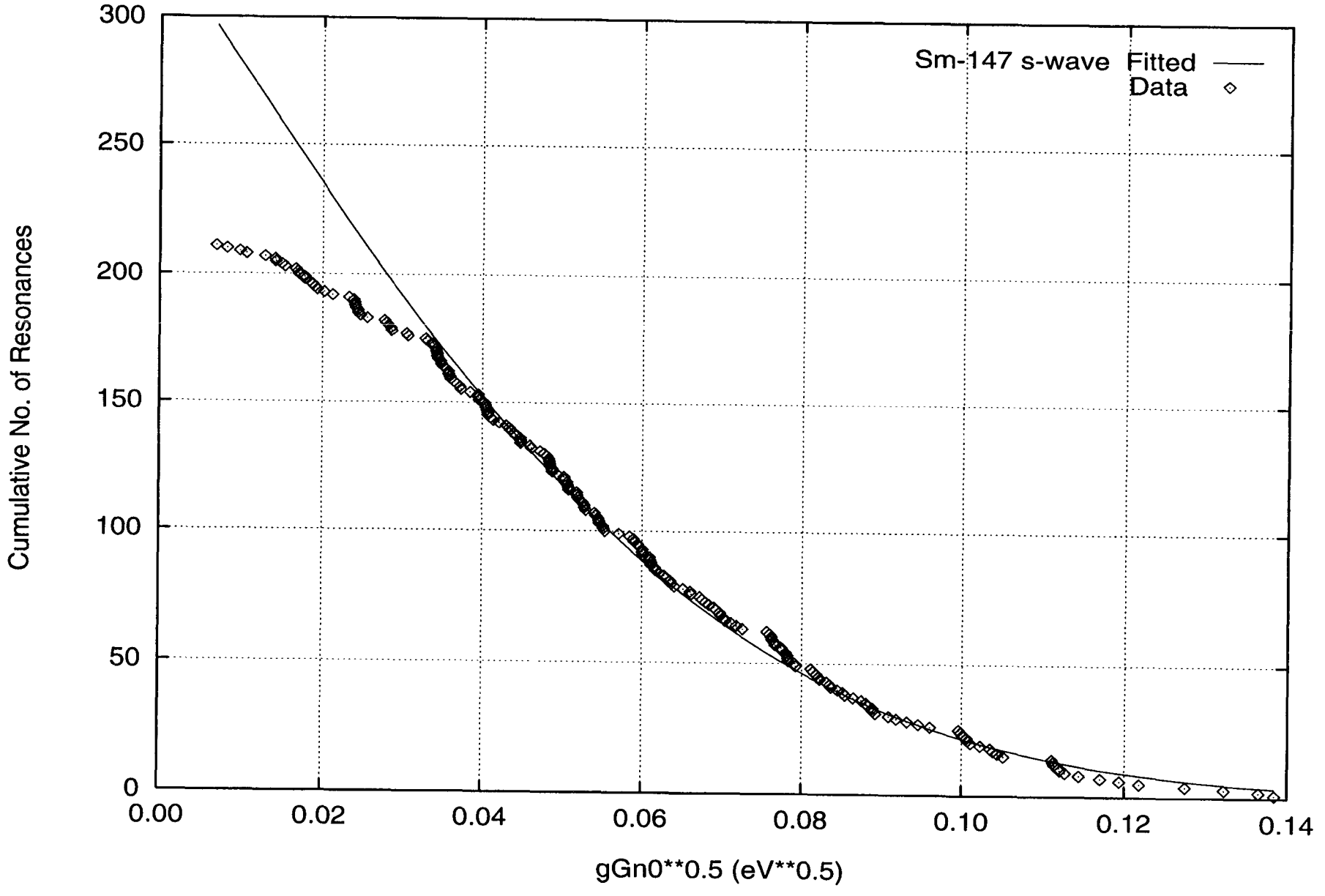

Fig. 38. Complement of the Cumulative Distribution of Neutron Reduced Widths (^{147}Sm, s-wave)

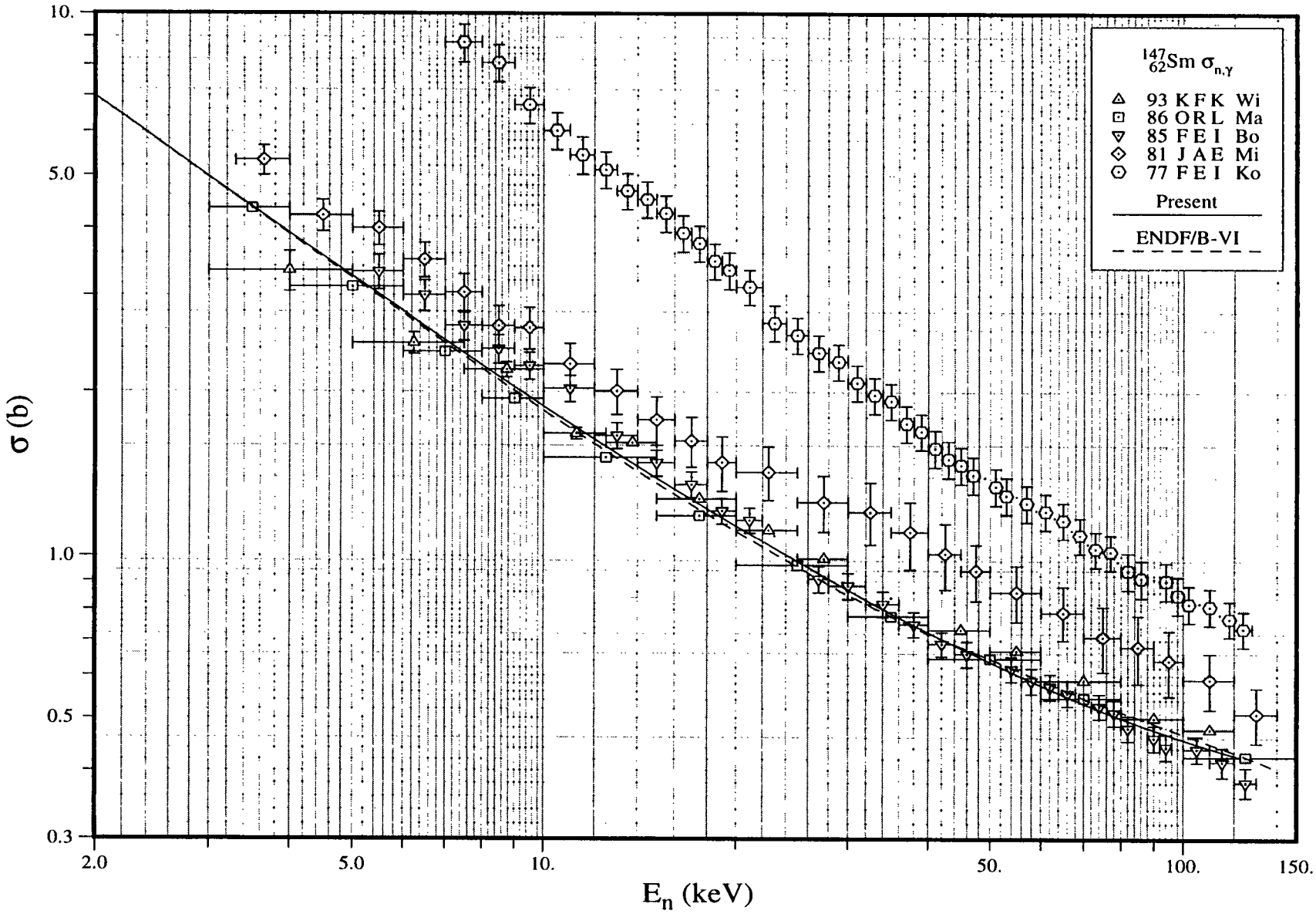

Fig. 39. Capture Cross Section in the Unresolved Resonance Region (^{147}Sm)

III.M. ^{149}Sm

1. Thermal Cross Sections

The thermal capture cross section is adopted from the Mughabghab's BNL compilation [Mu84]. The spin of the bound level is assigned as 3 according to the (n,α) measurements of Dakowski [Da67]. The energy and reduced neutron width of the bound level were determined as 1.5 eV and 7.243 meV, respectively. Since the first resonance at 0.0923 eV is close to the thermal energy, the coherent scattering length (b') varies strongly with energy. Word and Werner [Wo82] measured the energy dependence of the bound coherent scattering length in the energy range from 0.02945 to 0.09274 eV. Subsequently, Lynn and Seeger [Ly90] carried out R-matrix analysis in the low energy region by considering only the resonance at 0.09274 eV. The influence of other positive energy resonances was taken into account by energy dependent background terms. The R-matrix calculation [Ly90], represented by a dashed line in **Fig. 40**, is compared with measurement [Wo82]. By applying multi-level Breit-Wigner formalism [Mu81, Eq.3], we have also carried out computations of the energy-dependence of the $Re(b')$ for two cases. In one case, represented by a solid line, the effect of the bound level, as well as all positive energy resonances, was considered. In the second, denoted by a dotted line, the effect of the bound level was excluded. As shown in **Fig. 40**, our results support the important contribution of the bound level.

Our results, listed in **Table 30,** are in very good agreement with the reference values, reported in the BNL compilation [Mu84], but are discrepant with those of the ENDF/B-VI evaluation. The present Westcott factor for capture is calculated as 1.7171.

2. Resolved Resonance Parameters

Recent scattering, capture, and gamma-ray multiplicity measurements by Georgiev [Ge92] determined radiative widths and spins of resonances in the energy region 15.85 - 272.8 eV. These resonance parameters, along with the scattering widths of the BNL compilation of [Mu84], were incorporated into a new evaluation of the resolved resonance parameters.

The weighted-average capture width of 61 resonances is determined as 56.7±8.9 meV. This result seems quite low, because of the dominant weights of the first two resonances at 0.0973 eV and 0.872 eV. However, we opted to adopt an un-weighted average of 78.5 meV.

All the observed resonances were assigned as s-wave according to Bayesian analysis. The Porter-Thomas distribution shows that many weak s-wave resonances are missed. A least-squares fit for values of $\left(g\Gamma_n^0\right)^{1/2} > 0.024$, represented by a solid line, is shown in **Fig. 41**. The average resonance parameters, determined from this analysis, are displayed in **Table 31** and are compared with other evaluations. The derived s-wave parameters are to be compared also with those reported in RIPL [Re98]: $\langle D_0 \rangle = 2.10\pm0.30$ eV, $S_0 = 6.30\pm1.20$, and $\langle \Gamma_\gamma \rangle = 62\pm 2$ meV.

The upper energy limit of the resolved resonance region was set to 520 eV.

3. Unresolved resonance parameters

The average s-wave resonance parameters, obtained from the resolved resonance region, were applied without adjustments in the unresolved energy region. The p- and d-wave strength functions, as well as the p-wave average radiative width, were adopted from the systematics [Mu84]. The average parameters, implemented in the unresolved energy region, are summarized in **Table 31** and are compared with other evaluations. The level spacing was assumed to vary with energy according to Gilbert-Cameron level density relation [Mu98a].

Neutron inelastic scattering to the first excited level of ^{149}Sm is open at an energy of 22.507 keV. The upper energy limit of the unresolved resonance region was set to 100 keV. Competition widths in the energy region from 22.5 keV to 100 keV were not provided. The energy of the second excited level is 277.075 keV. The capture cross section, constructed from the present parameters, is compared in **Fig. 42** with measurements of Wisshak *et al.* [Wi93], Macklin [Ma86], Kononov *et al.* [Ko77] and Hockenberry *et al.*

Maxwellian average capture cross section for a temperature of 30 keV, computed as 1866 mb, is to be compared with 1819.9±17.2 mb [Wi93] and 1409±95 mb [Be92]. The calculation was extended up to 1 MeV. The capture cross section was constructed with the present parameters up to an energy of 100 keV; from 100 keV to 1 MeV, it was borrowed from the ENDF/B-VI evaluation.

Table 30. Thermal Characteristics (^{149}Sm)

Quantity	Unit	BNL Compilation	98CRC [Ho98]	ENDF/ B-VI	JEF-2.2	JENDL-3.2	Present
R'	fm	8.3 ± 0.2		5.093	8.30	7.52	8.30
Re(b')	fm	-24	-19.08*	-24.2		-24.1	-19.08
σ_γ	barns	40140 ± 600	40100 ± 600	39730	40480	40150	40530
σ_s	barns	197		139	176	173	194
RI-capt.	barns	3390	3310 ± 500	3258	3484	3490	3482

* Value of Lynn [Ly90].

Table 31. Average Resonance Parameters in the Unresolved Resonance Region (^{149}Sm)

Quantity	Unit	ENDF/B-VI	JEF-2.2	JENDL-3.2 [a]	BNL Compilation	Present	
						PT Analysis	Adopted
R' (URR)	fm	5.093	5.09	7.90	8.3 ± 0.2		8.30
$<D_0>$	eV	3.42	1.97	1.54	2.2 ± 0.2	2.45 ± 0.11	2.45 [b]
S_0	$\times 10^{-4}$	3.20	4.13	4.60	4.6 ± 0.6	4.53 ± 0.54	4.53
$<\Gamma_{\gamma 0}>$	meV	62.0	75.1	62.0	62 ± 2		78.5
$<D_1>$	eV	1.71	1.01	0.77^{+}			1.31 [b]
S_1	$\times 10^{-4}$	0.50	2.32	0.30	0.3 ± 0.1		1.00
$<\Gamma_{\gamma 1}>$	meV	62.0	75.1	62.0			40.0
$<D_2>$	eV		0.707	0.514^{+}			0.987 [b]
S_2	$\times 10^{-4}$		6.50	4.90			4.00
$<\Gamma_{\gamma 2}>$	meV		75.1	62.0			78.5

a: At the low energy of the unresolved resonance region, 0.52 keV.
b: At the neutron separation energy of ^{150}Sm.

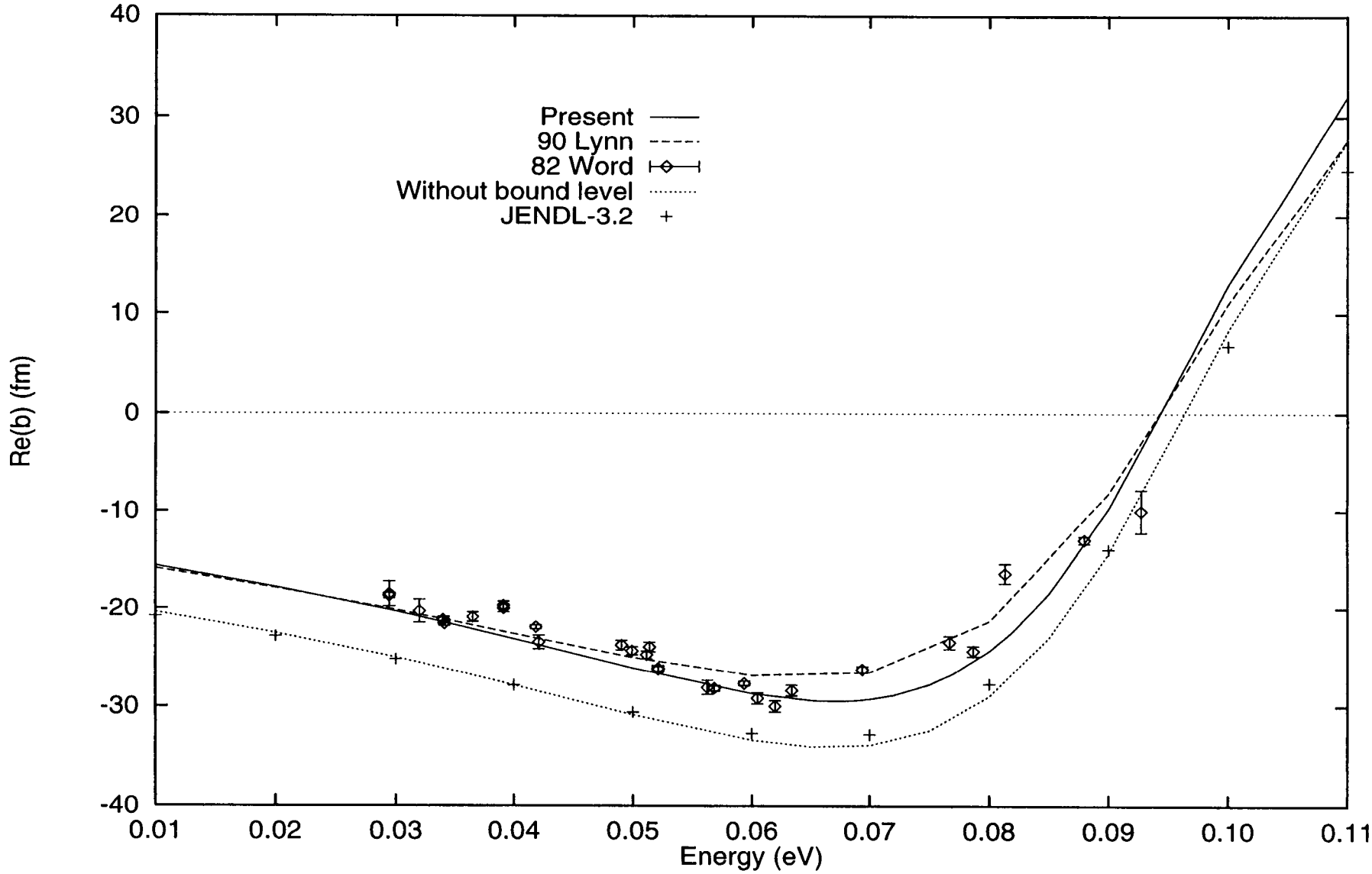

Fig. 40. Real Part of the Bound Coherent Scattering Length of ^{149}Sm

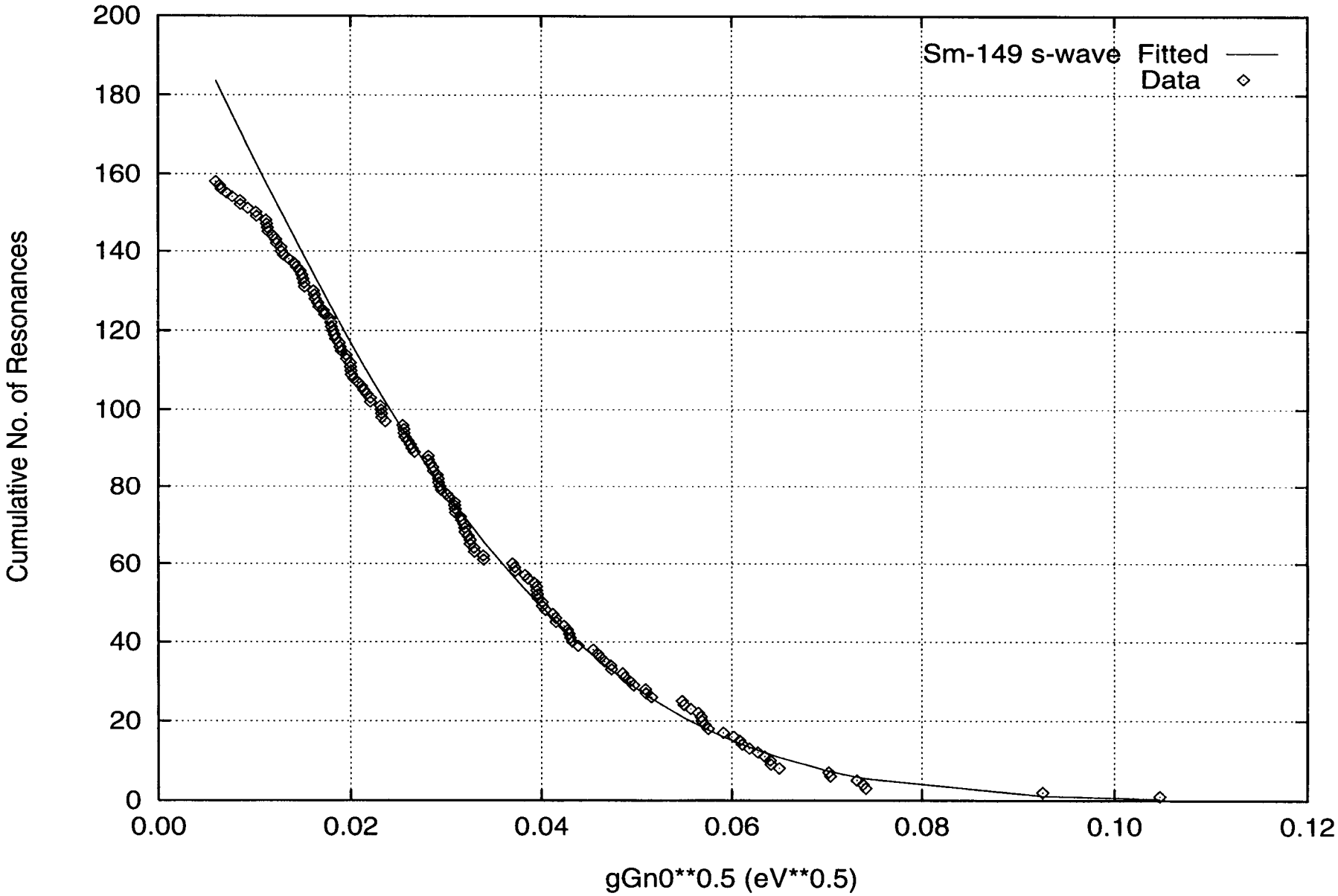

Fig. 41. Complement of the Cumulative Distribution of Neutron Reduced Widths (^{149}Sm, s-wave)

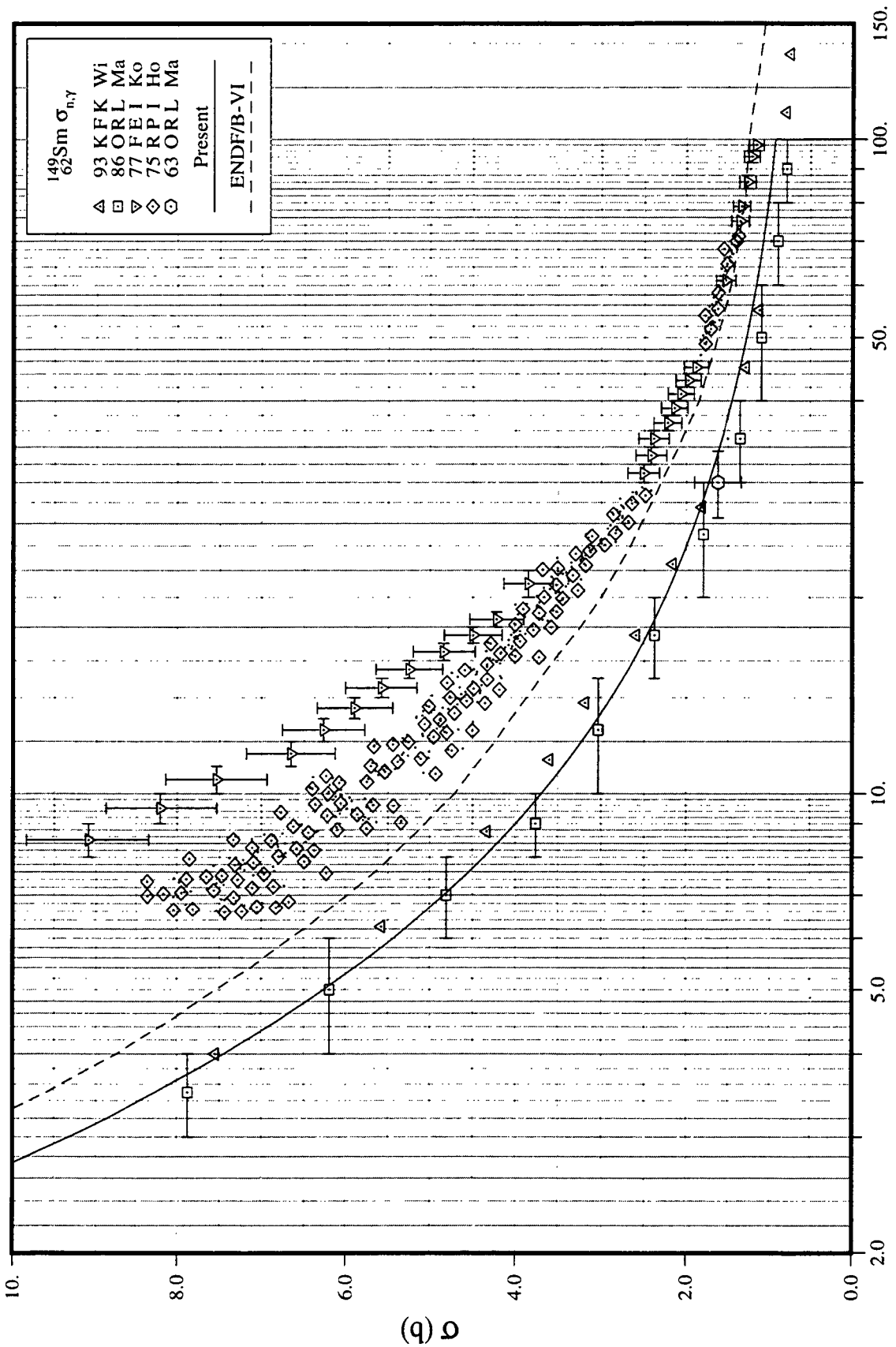

Fig. 42. Capture Cross Section in the Unresolved Resonance Region (^{149}Sm)

III.N. ^{150}Sm

1. Thermal Region

To reproduce a thermal capture cross section of 100 b, as well as a thermal elastic scattering cross section of 27.6 b, one bound level was invoked. The reference thermal capture cross section was obtained by weighting Maxwellian-averaged values 97±10 b of Halperin *et al.* [Ha62] and 101±5 b of Aitken and Cornish [Ai61]. The latter value is adjusted from the original value of 102±5 b on the basis of a revised value for the resonance integral. The reference scattering cross section was obtained by subtracting the capture cross section from the total cross section, 127.5 b [Ei74], in which a paramagnetic scattering cross section of 7.5 b [Ei74] was excluded. The bound resonance parameters are; E_0 = -11.72 eV, Γ_n = 176.6 meV, Γ_γ = 60.2 meV. In these calculations, an effective scattering radius (R') of 8.0 fm was adopted from a deformed optical model calculation [Mu81, Fig. 2]. The contribution of positive energy resonances to the thermal capture cross section was calculated as 69.5 b. The bound coherent scattering length was calculated as 14.8 fm (4.7 fm without a bound level), which is consistent with a value of 14±3 fm in the BNL compilation [Mu84].

A comparison of the various thermal cross sections and resonance integrals of the present evaluation and those of ENDF/B-VI, JEF-2 and JENDL-3 is presented in **Table 32**. While there is general agreement between the various evaluations of the thermal capture cross sections and capture resonance integrals, our evaluated scattering cross section deviates from those in the other cross section libraries.

2. Resolved Resonance Parameters

Because measurements were not carried out since the date of the BNL compilation, the resolved resonance parameters of the present evaluation were based on [Mu84].

On the basis of Bayesian analysis, the reported 22 resonances [Mu84] were assigned as s-wave. An average radiative width of 60±5 meV, based on [Mu84], was assumed for all resonances except for the first two positive-energy resonances for which radiative widths were determined experimentally [Mu84]. It is noted that this average value is much smaller than 87±16 meV reported in RIPL [Re98].

The distributions of reduced neutron widths were analyzed in terms of the Porter-Thomas distribution. Resonances with reduced widths smaller than 3 meV were excluded in the fitting procedure to obtain a minimum χ^2 value. **Figure 43** shows the fit to the data, which resulted in $\langle g\Gamma_n^0 \rangle$ = 20.1±6.6 meV and $\langle D_0 \rangle$ = 46.5±8.6 eV. These values yield s-wave strength function of S_0 = 4.31±1.42. The present $\langle D_0 \rangle$ is consistent with values recommended in the BNL compilation [Mu84] (55±9 eV) and RIPL [Re98] (46±8 eV) within the associated uncertainties. The present S_0 value is larger than those in the BNL compilation (3.6±1.1) and RIPL (3.4±0.6), but consistent with them within the uncertainties. Because of the limited number of resonances, the uncertainties of the derived average quantities are rather large.

3. Unresolved Resonance Parameters

The present unresolved resonance region covers the energy range from 1.563 keV to 336.1 keV. The latter energy corresponds to neutron inelastic scattering to the first excited level of ^{150}Sm at 333.86 keV. For this nuclide, s-, p- and d-wave average resonance parameters were provided. The level spacing varies with energy according to Gilbert-Cameron level density formula, in which the associated constants were adopted from Mughabghab and Dunford [Mu98a, Mu98b] (neutron separation energy = 5.596 MeV, pairing energy = 1.22 MeV, and level density parameter = 21.76 MeV^{-1}). The dependence of level spacing on $\exp\{-(J+1/2)^2/2\sigma^2\}$, as well as (2J+1), was taken into account for this nucleus. With a value of σ = 3.7 for the spin dispersion parameter [Mu98b], the level spacings for p- and d-wave resonances are calculated as 1/2.78 and 1/4.04 of the s-wave spacing, respectively. These values deviate from 1/3 and 1/5, obtained by assuming only a (2J+1) dependence of the level spacing.

In the unresolved resonance region, cross sections measurements carried out by Wisshak *et al.* [Wi93], Winters *et al.* [Wi86], and Macklin *et al.* [Ma63] were taken into consideration. The data of Kononov *et al.* [Ko78] deviate significantly from the others. As shown in **Fig. 44**, our computed capture cross section is in very good agreement with the experimental data [Wi93, Wi78]. The present average resonance parameters are listed in the last column of **Table 33**. Values of $\langle D_0 \rangle$ and S_0 are those which were derived from the analysis of the resolved region. The present value of S_1 was adopted from a deformed optical model calculation [Mu84, Fig. 4], while that of S_2 was adjusted to reproduce the capture cross section measured by Wisshak *et al.* [Wi93] above 50 keV. An average radiative width of 60 meV was assumed for s- and d-wave resonances. A p-wave radiative width of 40 meV was determined in the present analysis to reproduce the capture cross section in the low energy region. This value is consistent with the systematics of p-wave radiative widths around mass number of 150 [Mu84, Fig. 7].

Table 32. Thermal Characteristics (^{150}Sm)

Quantity	Unit	BNL compilation	98CRC [Ho98]	ENDF/ B-VI	JEF-2.2	JENDL-3.2	Present
R'	fm			6.41	6.40	8.08	8.00
σ_γ^0	barn	104±4	102±5	104	103	109	100
σ_s^0	barn			19.0	21.2	8.34	27.7
gw*				1.000	0.9979	0.9938	0.9985
RI-capt.**	barn	358±50	290±30	338	339	325	334
RI-total**	barn			830	840	799	890

* Westcott factor for capture cross section.

** Integrated from 0.5 eV to 100 keV with 1/E spectrum.

Table 33. Average Resonance Parameters for the Unresolved Resonance Region (^{150}Sm)

Quantity	Unit	BNL compilation	ENDF/ B-VI	JEF-2.2	JENDL-3.2*	Present	
						PT Analysis	Adopted
R'	fm		6.41		5.92		8.00
$\langle D_0 \rangle$	eV	55±9	48.0		59.8	46.5±8.6	46.5**
S_0	$\times 10^{-4}$	3.6±1.1	3.60		3.60	4.31±1.42	4.31
$\langle \Gamma_{\gamma 0} \rangle$	meV	60±5	60.0		60.0		60.0
$\langle D_1 \rangle$	eV		15.0		20.0		16.7**
S_1	$\times 10^{-4}$	0.08±0.02	0.60		1.40		1.00
$\langle \Gamma_{\gamma 1} \rangle$	meV		60.0		60.0		40.0
$\langle D_2 \rangle$	eV		6.00		12.0		11.5**
S_2	$\times 10^{-4}$		2.90		2.30		3.50
$\langle \Gamma_{\gamma 2} \rangle$	meV		60.0		60.0		60.0

* Average parameters at the low energy bound of the unresolved resonance region (1.54 keV).
** At the neutron separation energy of ^{151}Sm.

Maxwellian average capture cross section for a temperature of 30 keV, computed as 409 mb, is to be compared with 421.9±3.8 mb [Wi93] and 434±26 mb [Be92].

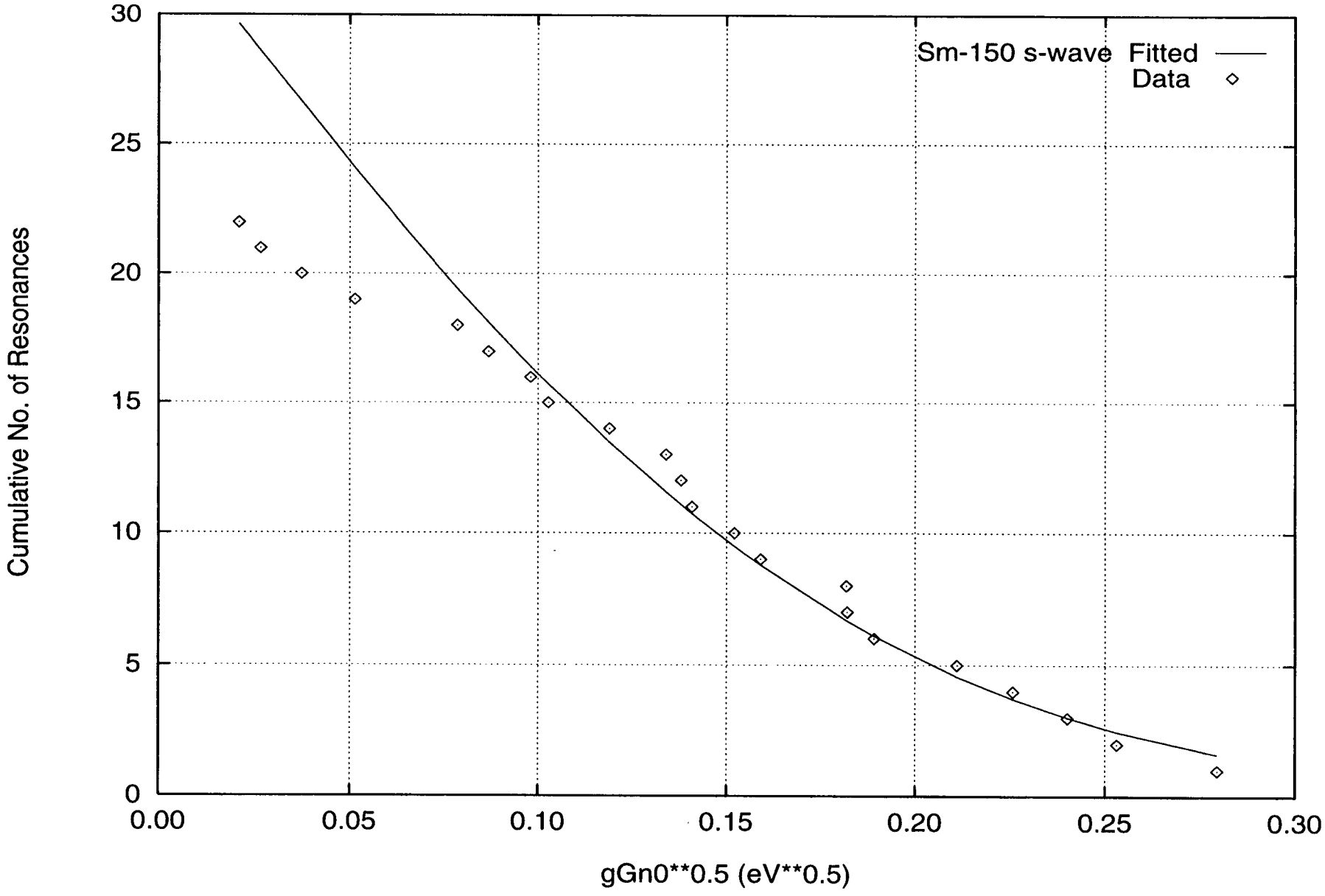

Fig. 43. Complement of the Cumulative Distribution of Neutron Reduced Widths (^{150}Sm, s-wave)

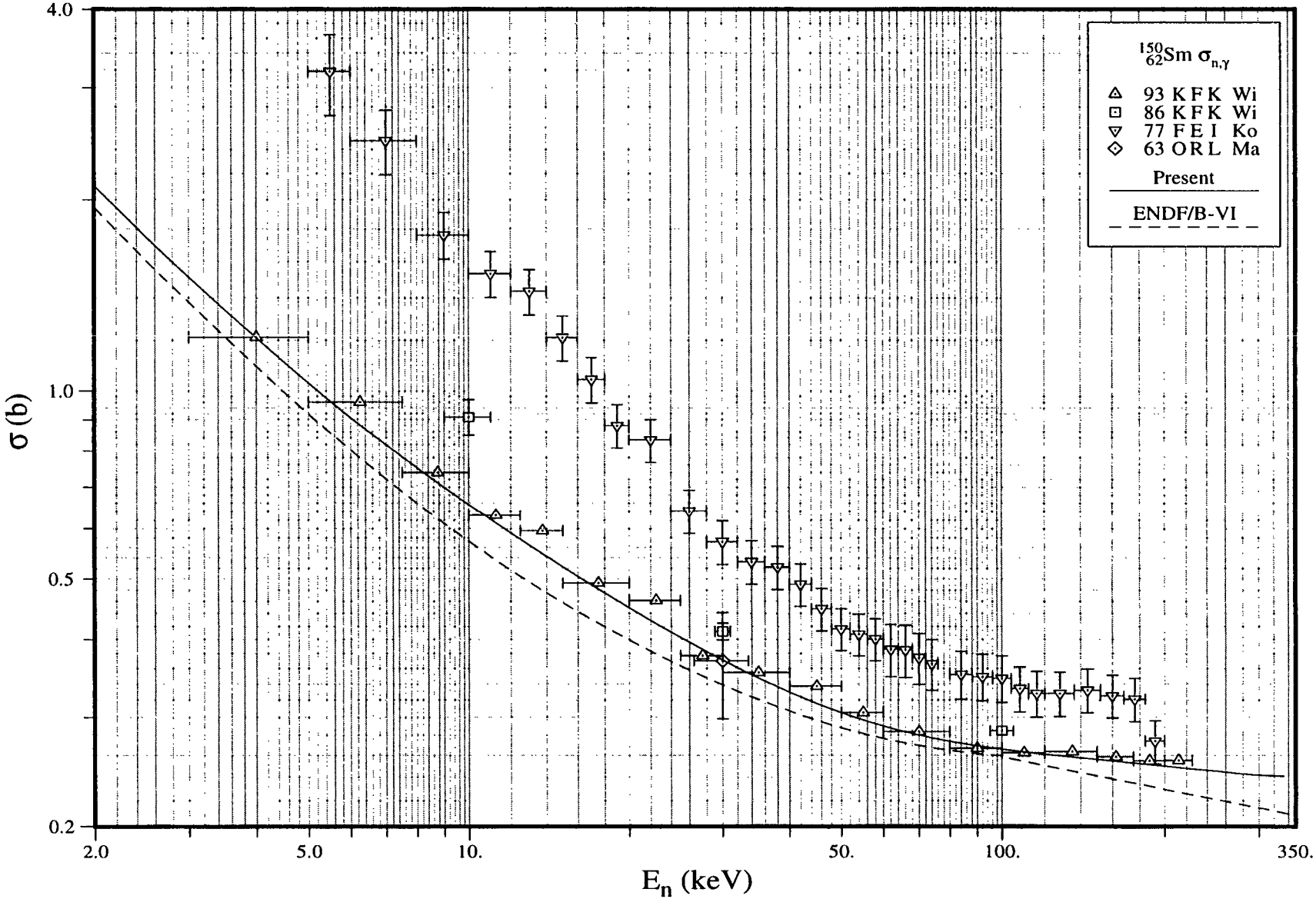

Fig. 44. Capture Cross Section in the Unresolved Resonance Region (^{150}Sm)

III.O. ^{151}Sm

1. Thermal Characteristics

Since the contribution of positive energy resonances [Mu84] to the thermal capture cross section is 235 b, a bound level was stipulated to reproduce a thermal capture cross section (σ_γ^0) of 15200±300 b [Mu84]. The resonance parameters of the bound level were determined as: $E_0 = -0.12$ eV, $J = 2$ ($l = 0$), $\Gamma_n = 0.752$ meV, and $\Gamma_\gamma = 92.9$ meV. The effective scattering radius of 8.3 fm was adopted from a deformed optical model calculation [Mu84]. A comparison of the thermal cross sections and resonance integrals of the present evaluation with those of ENDF/B-VI, JEF-2 and JENDL-3 evaluations is presented in **Table 34**. While there is general agreement in the various evaluations of the thermal capture cross sections, as well as the capture resonance integrals, large discrepancies exist in the value of the thermal scattering cross section. Because the scattering cross section is only 0.5% of the capture cross section, scattering measurements in the thermal region are not available. The calculated Westcott factor, 0.9274, shows that this nuclide is a non-1/v absorber.

2. Resolved Resonance Parameters

Because of the unavailability of measurements since 1984, the present evaluation adopted the resolved resonance parameters of the BNL compilation [Mu84]. The resolved energy region extends to 296 eV. On the basis of Bayesian analysis, all 120 resonances were assigned as s-wave resonances. All the resonance spins were assigned randomly on the assumption that the level density is proportional to (2J+1). The uncertainty-weighted average for 13 radiative widths resulted in a value of 92.9±3.7 meV. This value was assumed for the remaining resonances, as well as the bound level. The present average value is in very good agreement with the values (92±7 meV) [Mu84] and (95±4 meV) [Re98].

The distribution of s-wave reduced neutron widths was analyzed in terms of the Porter-Thomas-distribution. Resonances with reduced widths smaller than 0.3 meV were excluded in the fitting procedure (**Fig. 45**). The fit resulted in $\langle g\Gamma_n^0 \rangle = 0.60 \pm 0.08$ meV and $\langle D_0 \rangle = 1.48 \pm 0.09$ eV. These values yield s-wave strength function of $S_0 = 4.06 \pm 0.56$. The present $\langle D_0 \rangle$ is consistent, within the associated uncertainty, with (1.2±0.2 eV) [Mu84]. However, it deviates from a recommended value of 1.04±0.15 eV [Re98]. The present S_0 is consistent with values in the BNL compilation (4.2±0.4) [Mu84] and RIPL (3.4±0.5) [Re98] within the associated uncertainties.

3. Unresolved Resonance Parameters

The unresolved resonance region covers the energy range from 296 eV to 66.24 keV. The latter energy corresponds to neutron inelastic scattering to the second excited level of ^{151}Sm at 65.83 keV. The energy of the first excited level at 4.82 keV is very low when compared with other fission products. However, the inelastic neutron scattering cross section was not taken into account as a competition channel in MF=2 in the present evaluation. **Table 35** presents the various evaluations of the capture and inelastic scattering cross sections at 10 keV, where the inelastic scattering cross section to the first excited level shows a peak. As indicated,

disagreements exist in the various evaluations because of differences in the nuclear model calculations, as well as the model parameters.

For this nuclide, s-, p- and d-wave average resonance parameters were provided. The level spacing varies with energy according to Gilbert-Cameron level density formula with associated parameters adopted from Mughabghab and Dunford [Mu98] (neutron separation energy = 8.258 MeV, pairing energy = 2.32 MeV, and level density parameter = 21.43 MeV^{-1}). The dependence of the level spacing on spin by the relation $(2J+1)\ \exp\{-(J+1/2)^2/2\sigma^2\}$ was taken into account in this evaluation. With a value of $\sigma = 3.7$ for the spin dispersion parameter, level spacings for p- and d-wave resonances were calculated as 1/1.84 and 1/2.38 of the s-wave spacing, respectively.

In the unresolved resonance region, capture cross section measurements are not reported. The adopted average resonance parameters are listed in the last column of **Table 36**. The ENDF/B-VI evaluation does not include unresolved resonance parameter file. The values of $\langle\Gamma_{\gamma 0}\rangle$, $\langle D_0\rangle$ and S_0 are those which resulted from the analysis of the resolved energy region. The present values of S_1 and S_2 were adopted from the systematics of strength functions near this mass region [Mu84, Figs. 4 and 5], while the value of $\langle\Gamma_{\gamma 1}\rangle$ was assumed from systematics of p-wave radiative widths [Mu84, Fig. 7]. These parameters resulted in a computed capture cross section that is represented by a solid line in **Fig. 46**. The present calculation is compared with existing evaluations, as well as a recent calculation of Toukan *et al.* [To95], represented by diamonds. Our results are in reasonable agreement with those of the ENDF/B-VI evaluation, but not with the JEF-2 evaluation, and are larger than those of Toukan [To95]. We note that other calculations of Toukan resulted in capture cross sections which are lower by 20%, on the average, than those measured by Wisshak *et al.* [Wi93] for the four Sm isotopes, $^{147-150}$Sm.

Maxwellian average capture cross section for a temperature of 30 keV was calculated as 2569 mb. In these calculations, which were extended up to 1 MeV, the capture cross section was reconstructed from the present resonance parameters up to 66.2 keV and from the ENDF/B-VI evaluation for the energy region from 66.2 keV to 1 MeV. Our calculated Maxwellian average capture cross section is large when compared with 1932±206 mb [Be92] and 1825±450 mb [To95].

Table 34. Thermal Characteristics (^{151}Sm)

Quantity	Unit	BNL compilation	98CRC [Ho98]	ENDF/ B-VI	JEF-2	JENDL-3	LIPAR-5 [Ab97]	Present
R'	fm			8.30	7.20	7.95		8.30
σ_γ^0	barn	15200±300	15200±300	15250	15190	15160	15160	15170
σ_s^0	barn			43.5	39.3	50.4	34.4	62.0
gw*				0.9308	0.9271	0.9278	0.9256	0.9274
RI-capt.**	barn	3520±160	3520±60	3449	3465	3410	3397+	3430
RI-total**	barn			3726	3765	3752		3765

* Westcott factor for capture cross section.

** Integrated from 0.5 eV to 100 keV with 1/E spectrum; For present calculation, ENDF/B-VI cross sections were imported for an energy region 66.2 keV to 100 keV.

\+ Integrated from 0.5 eV to 100 eV.

Table 35. Capture and Inelastic Scattering Cross Sections at 10 keV of ^{151}Sm

	ENDF/B-VI	JEF-2.2	JENDL-3.2
Capture CS (barn)	5.28	6.40	3.80
Inel. Scatt. CS (barn)	4.96	1.53	0.56

Table 36. Average Resonance Parameters for the Unresolved Resonance Region (^{151}Sm)

Quantity	Unit	BNL compilation	ENDF/ B-VI	JEF-2.2	JENDL-3.2*	Present	
						PT Analysis	Adopted
R'	fm			7.46	5.72		8.3
$\langle D_0 \rangle$	eV	1.2±0.2		1.20	4.85	1.48±0.09	1.48**
S_0	$\times 10^{-4}$	4.2±0.4		4.5	4.20	4.06±0.56	4.06
$\langle \Gamma_{\gamma 0} \rangle$	meV	92±7		96.0	92.0		92.9
$\langle D_1 \rangle$	eV			0.60	2.43	14.0±3.5	0.80**
S_1	$\times 10^{-4}$			1.0	1.40	1.25±0.37	0.80
$\langle \Gamma_{\gamma 1} \rangle$	meV			94~95	92.0		40.0
$\langle D_2 \rangle$	eV			0.40	1.62		0.62**
S_2	$\times 10^{-4}$			4.0	2.30		2.5
$\langle \Gamma_{\gamma 2} \rangle$	meV			95~100	92.0		92.9

* Average parameters at the low energy bound of the unresolved resonance region (0.25 keV).

** At the neutron separation energy of ^{152}Sm.

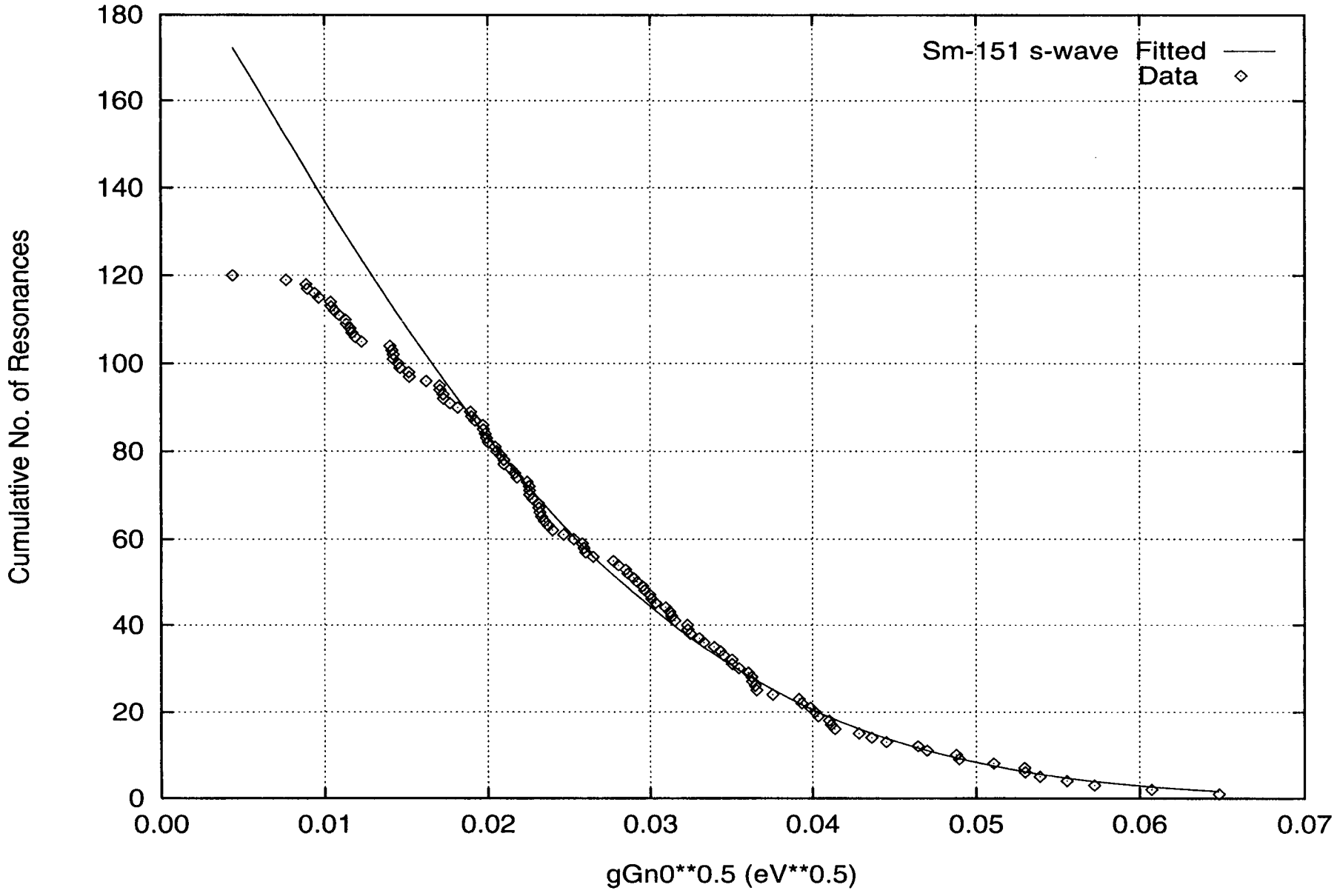

Fig. 45. Complement of the Cumulative Distribution of Neutron Reduced Widths (^{151}Sm, s-wave)

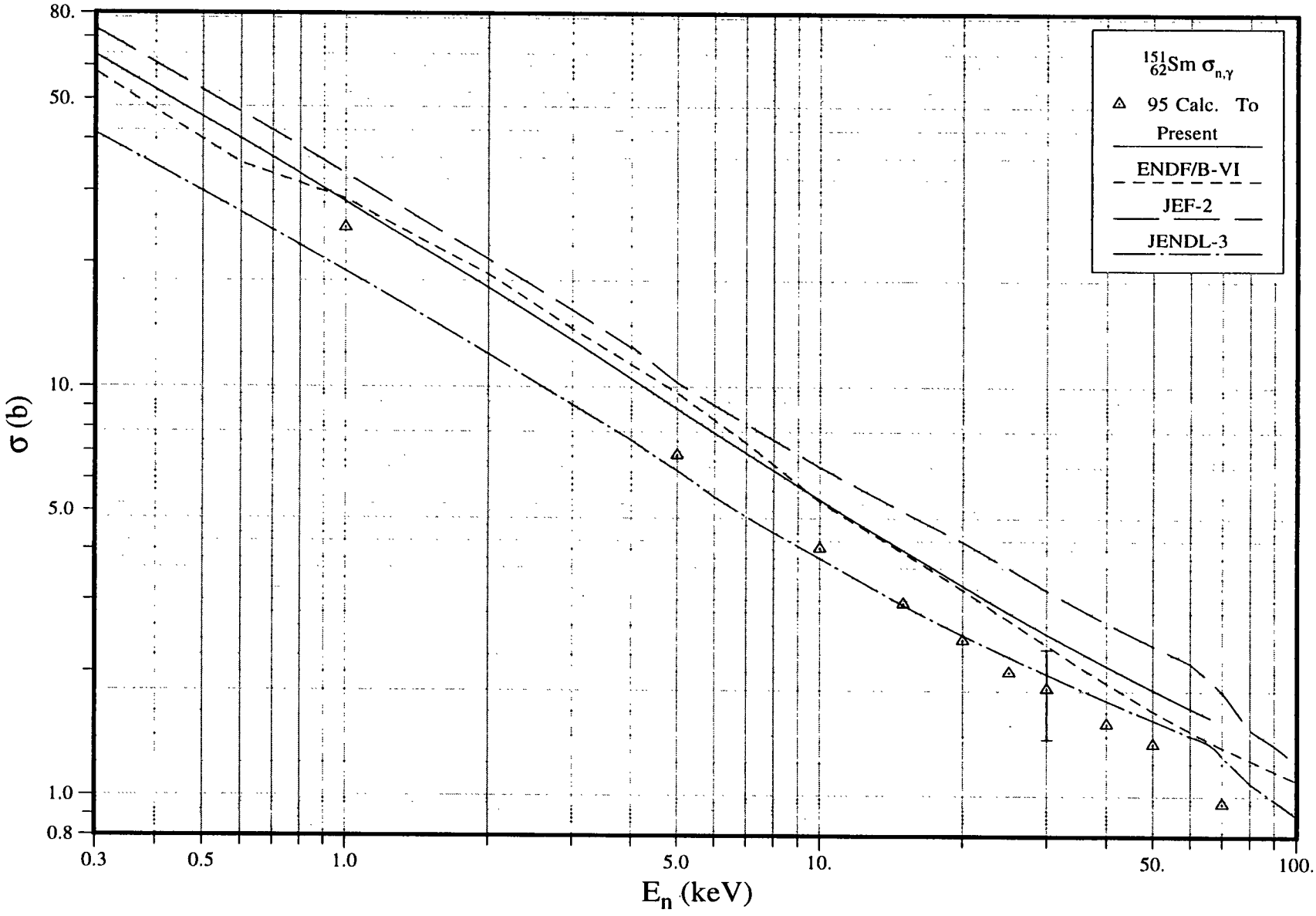

Fig. 46. Capture Cross Section in the Unresolved Resonance Region (^{151}Sm)

III.P. ^{152}Sm

1. Thermal Region

The resolved resonance parameters, including those of a bound level, and an effective scattering radius R' of 8.3 fm were adopted from the BNL compilation [Mu84]. The contribution of the bound level to the thermal capture cross section at 0.0253 eV is only 2.1 barns. The coherent scattering amplitude of –5.0 fm [Mu84] is also accounted for by the bound level. As shown in **Table 37**, the present values are essentially the same as those in the BNL compilation [Mu84] and are in good agreement with those in the ENDF/B-VI and JEF-2.2 valuations. There is disagreement between our calculated scattering cross section and resonance integrals and those of the JENDEL-3.2 evaluation.

2. Resolved Resonance Parameters

Because new measurements in the resolved energy region were not carried out since 1984, the resonance parameters reported in the BNL compilation [Mu84] were adopted without modification.

All 91 reported resonances [Mu84] were assigned as s-wave on the basis of the Bayesian analysis. The weighted-average value of nine determined radiative widths resulted in a $\langle\Gamma_{\gamma 0}\rangle = 60.0\pm5.4$ meV. This value is in very good agreement with that presented in the BNL compilation, 61±7 meV [Mu84]. This average was assumed for the remaining resonances.

The distribution of reduced neutron widths was analyzed by fitting the widths to the Porter-Thomas distribution. As shown in **Fig. 47**, none of the resonances was excluded from the fitting procedure. The analysis resulted in $\langle D_0\rangle$ = 47.5±2.7 eV and $\langle g\Gamma_n^0\rangle$ = 10.6 ±1.6 meV. These values yield a strength function for s-wave resonances of (2.23±0.35), which is in very good agreement with (2.2±0.3) reported in the BNL compilation [Mu84]. The present $\langle D_0\rangle$ is also consistent, within the associated uncertainty, with 51.8±3.3 eV [Mu84]. The resolved energy region consists of 92 s-wave resonances up to 5101.2 eV.

3. Unresolved Resonance Parameters

The unresolved energy region of the present evaluation extends from 5 keV to 122.58 keV, the latter energy corresponding to neutron inelastic scattering to the first excited state of ^{152}Sm.

In the energy range 5 to 200 keV, the capture cross sections of Luo *et al.* [Lu94], Wisshak *et al.* [Wi93] and Bohkovko *et al.* [Bo85] were taken into account. The measurement of Kononov *et al.* [Ko78] was disregarded because the capture cross section is consistently larger than recent data (**Fig. 48**). Earlier measurements, reported in the Neutron Cross Section Curve book [Mc88], were not taken into account, largely because of their inconsistencies with recent measurements. As depicted in **Fig. 48**, ENDF/B-VI, JEF-2 and JENDL-3 evaluations, are larger than recent data [Lu94, Wi93, Bo85] by about 10% to 30% in the energy region from 70 keV to 120 keV .

As a starting point, the s-wave average resonance parameters, $\langle D_0 \rangle$, S_0 and $\langle \Gamma_{\gamma 0} \rangle$, derived from the resolved energy region, as well as $S_1 = 0.55$ and $S_2 = 2.2$ [Mu84], were adopted in this energy region. These parameters resulted in a calculated capture cross section, which is low by ~30% and ~10% at about energies of 5 keV and 120 keV respectively, when compared with measurement [Wi93]. To achieve agreement with the measurements [Lu94, Wi93, Bo85], $\langle D_0 \rangle$ was set to 34.6 eV and $\langle \Gamma_{\gamma 0} \rangle$ was increased from 61 eV to 72.7 eV to satisfy s-wave gamma strength function of 0.0021 [Bo91]. In addition, $\langle \Gamma_{\gamma 2} \rangle$ was adjusted to reproduce the capture cross section at high energies. The resulting average resonance parameters are listed in **Table 38**. The calculated capture cross section is shown in **Fig. 49**.

In the present evaluation, the level spacing varies with energy according to Gilbert-Cameron level density relation. Parameters for the level density, neutron separation energy, pairing energy, and the single level nuclear density, are found in Mughabghab and Dunford [Mu98a, Mu98b]. The average level spacing and reduced widths, listed in the last column, are the values at the neutron separation energy.

Maxwellian-averaged capture cross section for a temperature of 30 keV, computed as 460 mb, is to be compared with, 473.2±4.4 mb [Wi93], 401±24 mb [Be92], and 445±25 mb [Bo91].

Table 37. Thermal Characteristics (^{152}Sm)

Quantity	Unit	BNL Comp.	98CRC [Ho98]	ENDF/ B-VI	JEF-2.2	JENDL-3.2	LIPAR-5 [Ab97]	Present
R'	Fm	8.3±0.2		8.3	8.3	8.2		8.3
σ_γ^0	barn	206±6	206±15	207	206	206	201.5	206
σ_s^0	barn	3.0±0.2		3.12	2.93	0.95	7.49	3.11
gw*				1.004	1.003	1.003	1.0032	1.0035
RI-capt.**	barn	2970±100	3000±300	2981	2977	2770	2958+	2976
RI-total**	barn			9055	9048	8740		9045

* Westcott factor for capture cross section.

** Integrated from 0.5 eV to 100 keV with 1/E spectrum.

\+ Integrated from 0.5 eV to 2.15 keV.

Table 38. Average Resonance Parameters for the Unresolved Resonance Region (^{152}Sm)

Quantity	Unit	ENDF/ B-VI	JEF-2.2	JENDL-3.2*	BNL Comp.	Present	
						PT Dist'n Analysis	Adopted
R' (URR)	fm	7.665	6.438	7.556	8.3±0.2		8.3
$\langle D_0 \rangle$	eV	28.00	52.52	33.46	51.8±3.3	47.5±2.7	34.6
S_0	$\times 10^{-4}$	2.50	2.30	2.20	2.2±0.3	2.23±0.35	2.23
$\langle \Gamma_{\gamma 0} \rangle$	meV	61.0	71.82	61.0	61±7		72.7
$\langle D_1 \rangle$	eV	9.33	17.89	11.15			11.5
S_1	$\times 10^{-4}$	0.60	1.60	0.55	0.55±0.08		0.60
$\langle \Gamma_{\gamma 1} \rangle$	meV	61.0	71.82	61.0			61.0
$\langle D_2 \rangle$	eV	5.54	11.22	6.69			6.91
S_2	$\times 10^{-4}$	3.00	6.80	2.30			1.50
$\langle \Gamma_{\gamma 2} \rangle$	meV	61.0	71.82	61.0			34.0

* Average parameters at the low energy (5.029 keV) of the unresolved region.

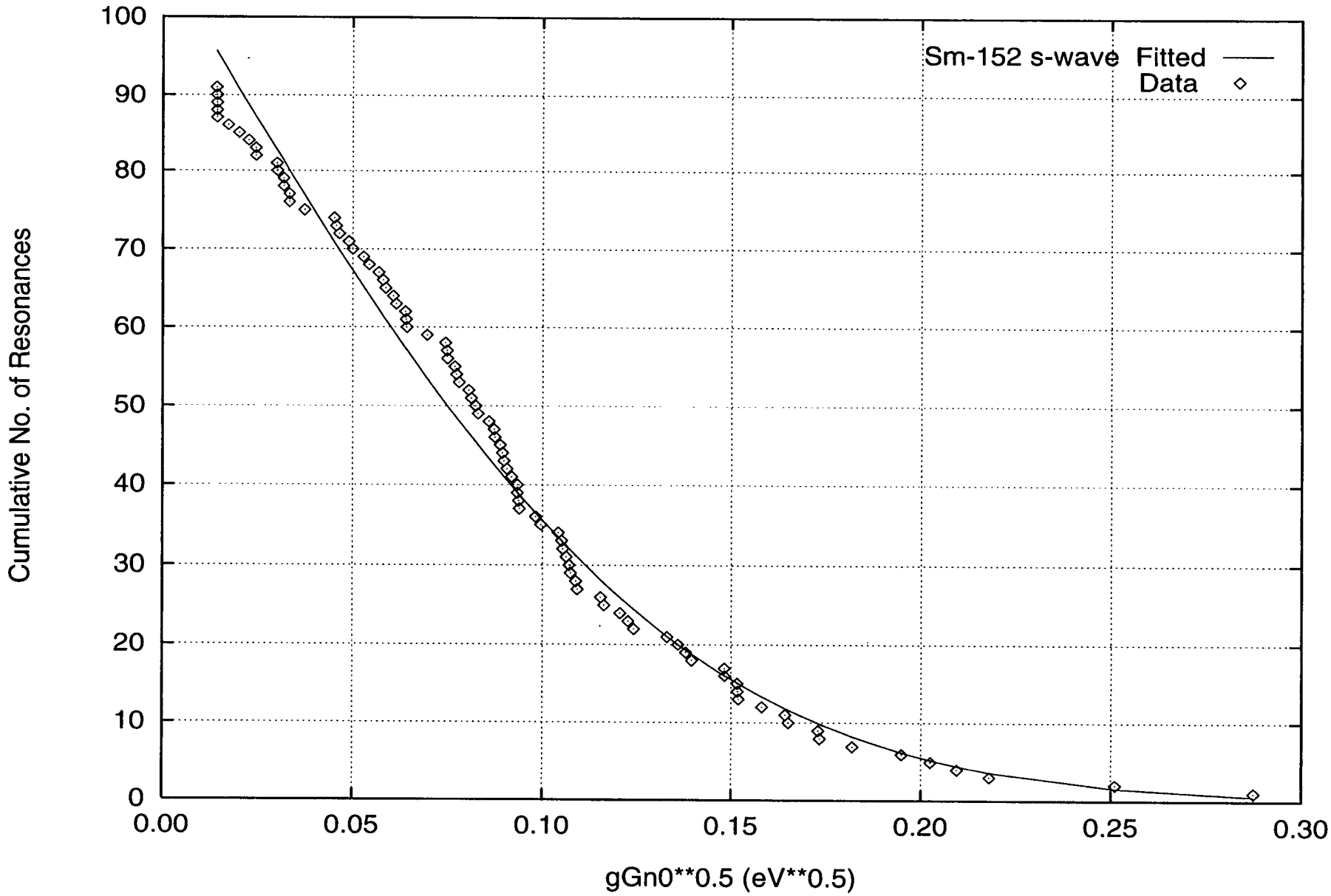

Fig. 47. Complement of the Cumulative Distribution of Neutron Reduced Widths (^{152}Sm, s-wave)

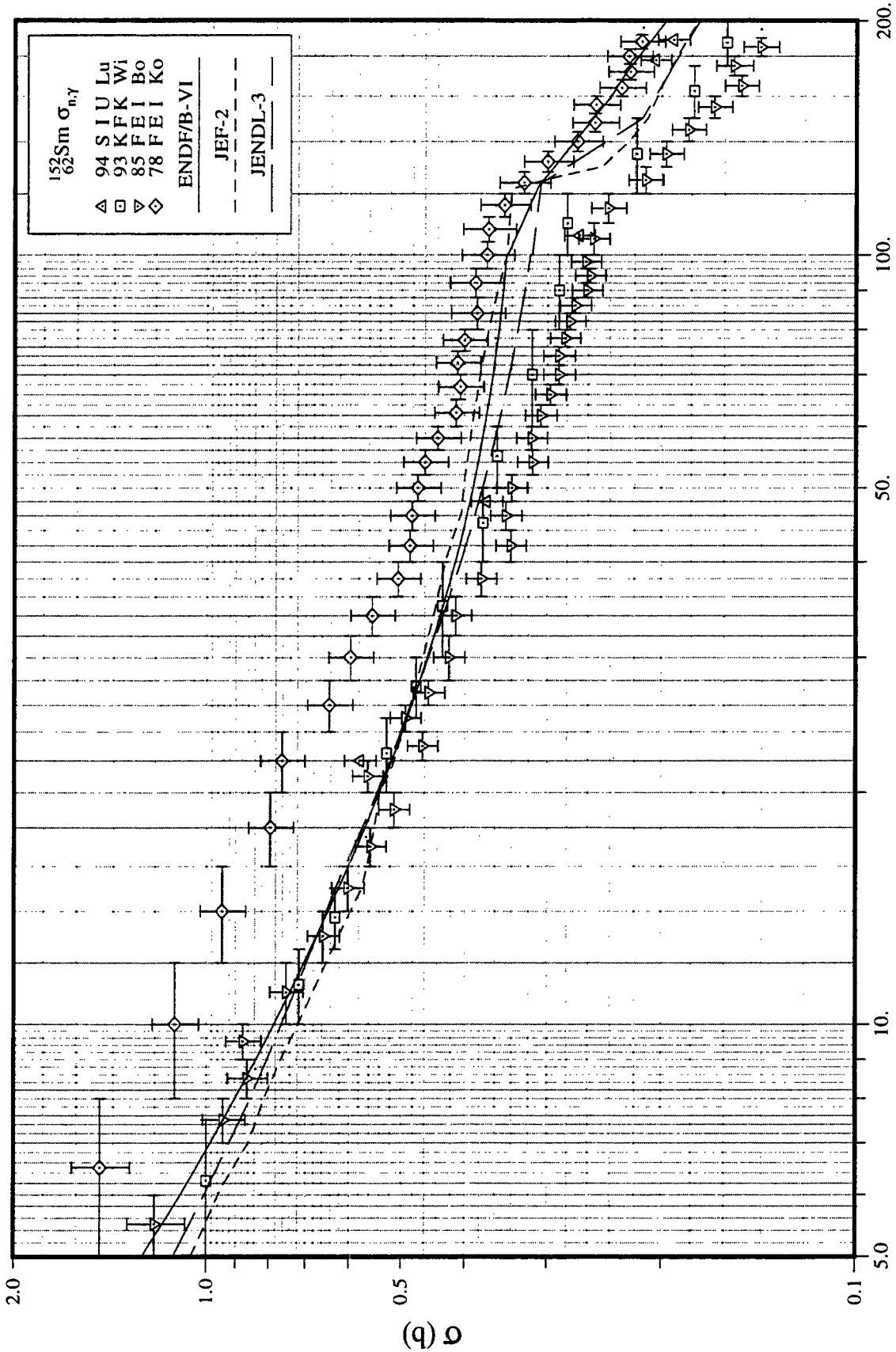

Fig. 48. Capture Cross Sections in the Evaluated Libraries in the Unresolved Resonance Region (^{152}Sm)

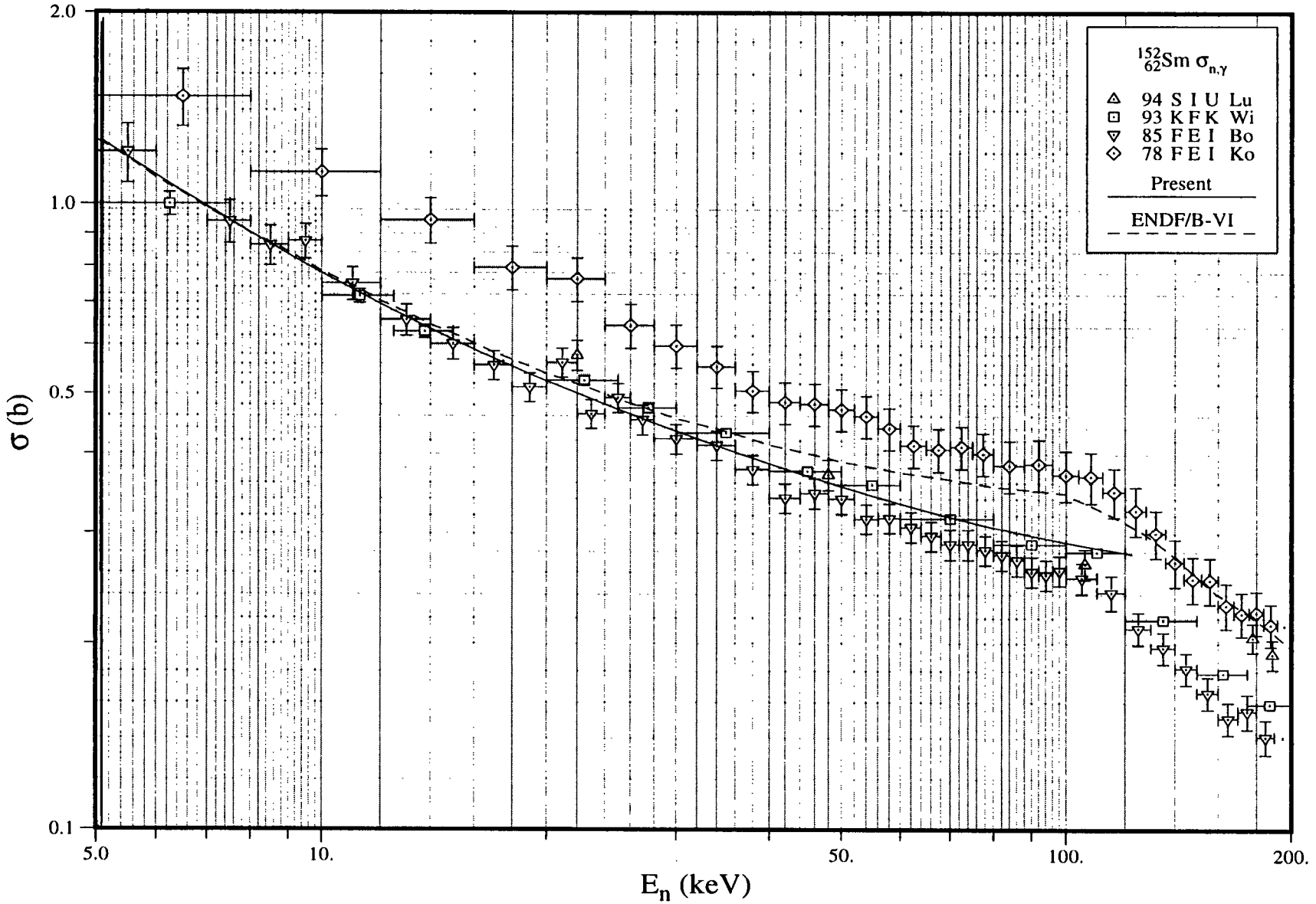

Fig. 49. Capture Cross Section in the Unresolved Resonance Region (^{152}Sm)

III.Q. ^{153}Eu

1. Thermal Characteristics

The resolved resonance parameters, including those of a bound level, and the effective scattering radius R' (8.2 fm) were adopted from Mughabghab's BNL compilation [Mu84]. The calculated capture cross section at 0.0253 eV due to the bound level is 256.8 barn. As shown in **Table 39**, the present values are in good agreement with those reported in the BNL compilation [Mu84], as well as JENDL-3.2 evaluation. The present resonance integrals are significantly lower than those in the ENDF/B-VI.5 and JEF-2.2[1] evaluations.

2. Resolved Resonance Parameters

The resonance parameters up to an energy of 97.8 eV were adopted from the BNL compilation [Mu84].

On the basis of Bayesian analysis, all of the 71 resonances are assigned as s-wave. Note that the s-wave strength function shows a peak while the p-wave strength function has a minimum around this mass region. Only the resonance at 2.456 eV has a spin. Resonance spins were assigned randomly to all the other resonances on the basis of the (2J+1) dependence of the level density. The weighted-average value for the known 55 radiative widths resulted in $\langle \Gamma_{\gamma 0} \rangle$ = 93±2 meV, which was assumed for the remaining resonances.

The distribution of reduced neutron widths was analyzed by fitting to the Porter-Thomas distribution. Three resonances for which $g\Gamma_n^0$ is smaller than 0.015 meV were excluded from the fitting procedure. **Figure 50** shows the cumulative number of resonances for which the widths are greater than the value given on the x-axis versus $\sqrt{g\Gamma_n^0}$. The fit resulted in $\langle D_0 \rangle$ = 1.14±0.08 eV and $\langle g\Gamma_n^0 \rangle$ = 0.27±0.05 meV. These numbers yield s-wave strength function of S_0 = 2.37±0.43. The present $\langle D_0 \rangle$ and S_0 are consistent, within the uncertainty ranges, with those reported in the BNL compilation [Mu84] ($\langle D_0 \rangle$ = 1.3±0.2 eV and S_0 = 2.5±0.2) and RIPL [Re98] ($\langle D_0 \rangle$ = 1.1±0.2 eV and S_0 = 2.2±0.3).

3. Unresolved Resonance Parameters

The unresolved resonance region covers the energy region from 97.8 eV to 83.91 keV. The upper energy range corresponds to the threshold energy of neutron inelastic scattering to the first excited level of ^{153}Eu at 83.37 keV. In the unresolved region, the average resonance parameters for s-, p- and d-wave resonances were provided. Since the upper energy of this region is relatively high, d-wave resonance contribution to the capture cross section is not negligible. We adopted a level spacing varying with the energy according to the Gilbert-Cameron's level density relation. Parameters for the formula, neutron separation energy, pairing energy and level density, are found in Mughabghab and Dunford [Mu98a Mu98b]. From the

---

[1] Both ENDF/ B-VI and JEF-2 contain the same resonance data, which had been imported from ENDF/B-V. However, since they have different background cross sections in File 3, the resulting thermal cross sections are different from each other.

(2J+1) dependence of the level density, level spacings for p- and d-waves were assumed to be 1/2 and 1/3 of the s-wave spacing, respectively.

Capture cross sections measured by Xia *et al.* [Xi94], Yu *et al.* [Yu93], Macklin and Young [Ma87], and Bokhovko *et al.* [Bo85], as well as earlier measurements were taken into account. The cross sections of Mizumoto *et al.* [Mi79], Kononov *et al.* [Ko77] and Hockenbury *et al.* [Ho75] are consistently higher than recent measurements in the energy range of 5~100 keV. The values of $\langle D_0 \rangle$, S_0 and $\langle \Gamma_{\gamma 0} \rangle$, deduced from the resolved resonances, and of S_1 and S_2 of the BNL compilation [Mu84] resulted in a calculated capture cross section, which is in good agreement with the data in the 1~30 keV range, but low by ~15% around 80 keV. Subsequently, the S_1 was increased to 0.6 to improve the fit at the high energy region. The calculated capture cross section is shown in **Fig. 51**. The finalized average resonance parameters are listed in the last column of **Table 40**.

Maxwellian-averaged capture cross section for a temperature of 30 keV was computed as 2.52 barn. The integration was performed up to an energy of only 83.9 keV; this upper energy cutoff may result in an error of about 12% [Be92]. The present cross section is to be compared with values of 3.17±0.3 b reported in Beer's compilation [Be92] and 2.45±0.07 b [Bo91].

Table 39. Thermal Characteristics (^{153}Eu)

Quantity	Unit	BNL Compil.	98CRC [Ho98]	ENDF/ B-VI	JEF-2.2	JENDL-3.2	LIPAR-5 [Ab97]	Present
R'	fm	8.2±0.2		8.8	8.8	8.63		8.20
σ_γ^0	barn	312±7	300±20	313	300	313	312	312
σ_s^0	barn	9.7±0.7		9.04	6.75	10.3	7.68	9.00
gw*		0.9663		0.9662	0.9662	0.9869	0.9801	0.9871
RI-capt.**	barn	1420±100	1800±400	1499	1448	1410	1305+	1408
RI-total**	barn			1699	1644	1605		1590

* Westcott factor for capture cross section.

** Integrated from 0.5 eV to 83 keV with 1/E spectrum.

\+ Integrated from 0.5 eV to 46.5 eV.

Table 40. Average Resonance Parameters for the Unresolved Resonance Region (^{153}Eu)

Quantity	Unit	BNL Compil.	ENDF/ B-VI	JEF-2.2	JENDL-3.2*	Present	
						PT Analysis	Adopted
R'	fm	8.2±0.2	8.80	8.80	6.421		8.20
$\langle D_0 \rangle$	eV	1.3±0.2	1.30	1.30	1.661	1.14±0.08	1.14**
S_0	$\times 10^{-4}$	2.5±0.2	2.50	2.50	2.79	2.37±0.43	2.37
$\langle \Gamma_{\gamma 0} \rangle$	meV	93±3	95.82	95.82	94.0		93.0
$\langle D_1 \rangle$	eV		0.65	0.65	0.831		0.57**
S_1	$\times 10^{-4}$	0.3±0.1	0.60	0.60	1.497		0.60
$\langle \Gamma_{\gamma 1} \rangle$	meV		95.82	95.82	94.0		93.0
$\langle D_2 \rangle$	eV				0.554		0.38**
S_2	$\times 10^{-4}$	5.4±1.2			3.116		5.40
$\langle \Gamma_{\gamma 2} \rangle$	meV				94.0		93.0

* Average parameters at the low energy (97.2 eV) of the unresolved region.
** At the neutron separation energy of ^{154}Eu .

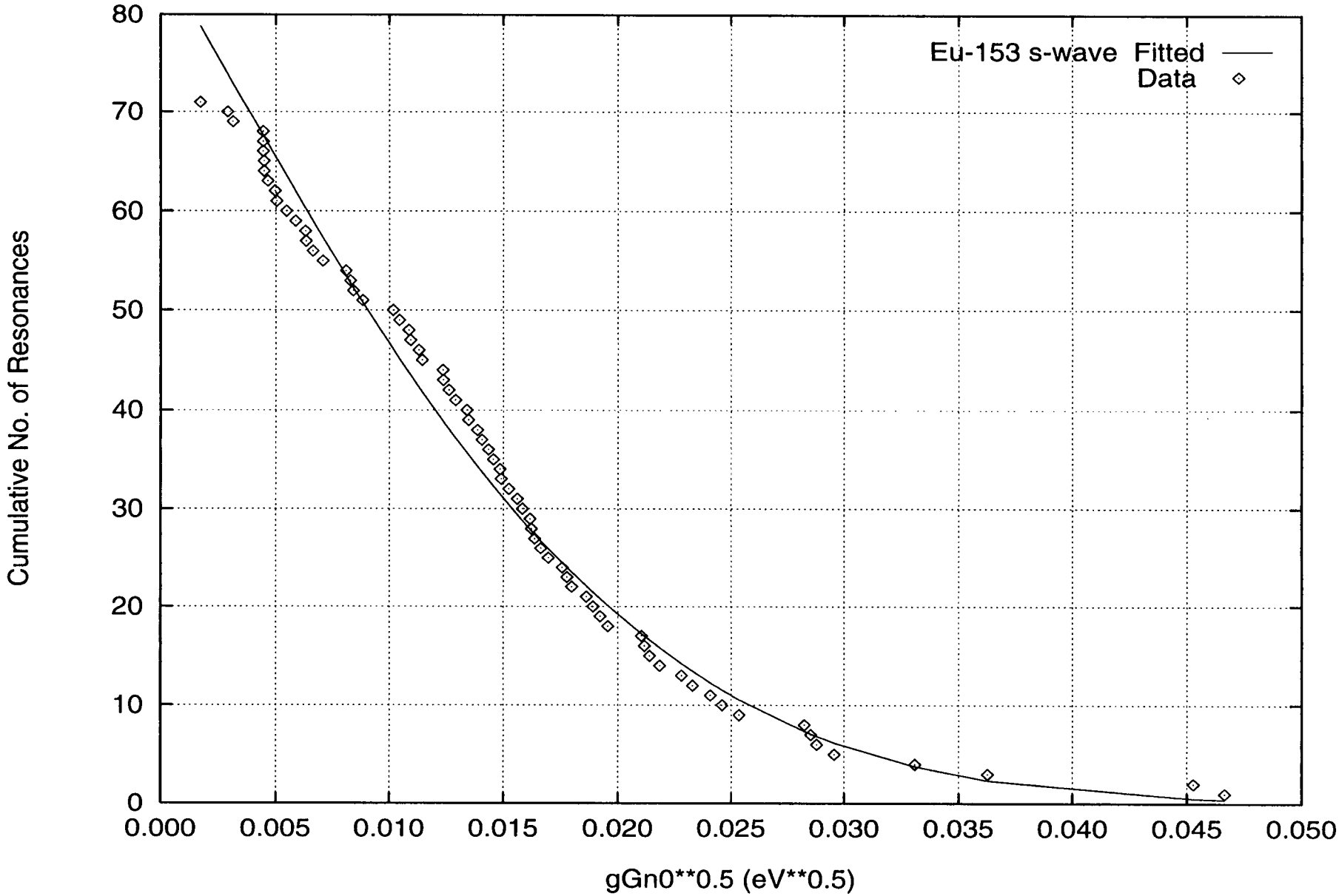

Fig. 50. Complement of the Cumulative Distribution of Neutron Reduced Widths (^{153}Eu, s-wave)

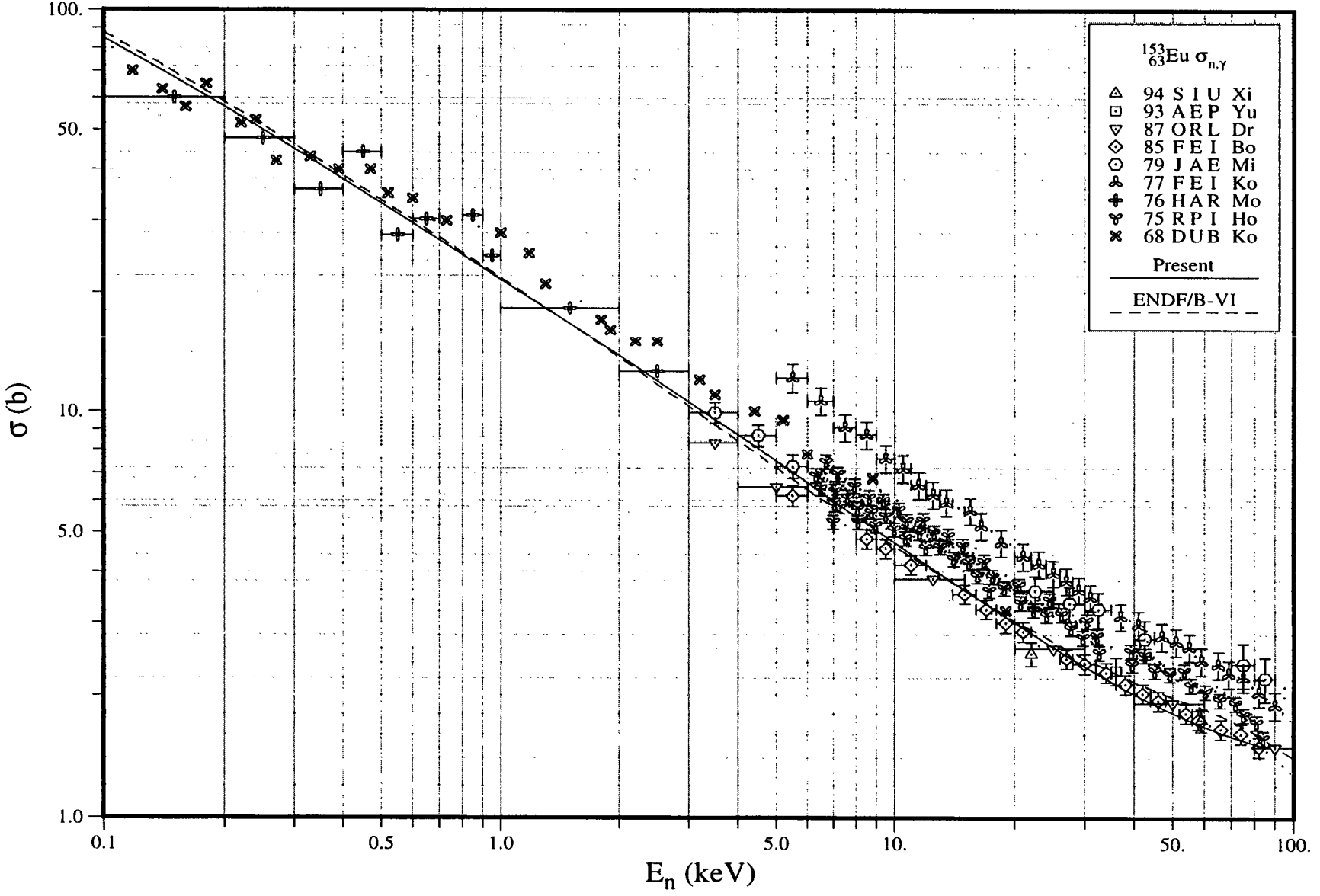

Fig. 51. Capture Cross Section in the Unresolved Resonance Region (^{153}Eu)

III.R. ^{155}Gd

1. Thermal Region

Within the reported uncertainty of the measured capture cross section, a negative energy resonance is not required to interpret the behavior of the cross section. The calculated thermal cross sections, coherent scattering amplitude, and the capture resonance integral are summarized in **Table 41**. In these calculations, a potential scattering radius of 8.0 fm, based on the systematics [Mu84], was assumed. The calculated Westcott factor for capture is 0.8440.

Since the first resonance at 0.0268 eV of ^{155}Gd is very close to thermal energy, the scattering, capture, and total cross sections vary significantly with energy. At low energies, the variation of the total cross section multiplied by the square root of the energy, as calculated in the present study, is displayed in **Fig. 52** and is compared with Moeller's data [Mo60].

Utilizing R-matrix least-squares fit of the data [Mo60], Lynn and Seeger [Ly90], derived the parameters of the first resonance, which are listed in the third column of **Table 42**. The calculated energy variation of the real part of the bound coherent scattering length, Re(b'), [Ly90], designated by open diamonds, is shown in **Fig. 53**. Applying the Breit-Wigner formalism, we carried out a similar calculation where all positive-energy resonances were included. Our result, represented by a solid line, is displayed in **Fig. 53**. In our analysis, the parameters of the first positive energy resonance are listed in the last column of **Table 42**. As indicated, a large discrepancy exists between our calculation and that of Lynn and Seeger [Ly90]. To understand this disagreement, we carried out several additional calculations. In one calculation, the resonance parameters of the first resonance were changed to those of Lynn and Seeger [Ly90]. Except for a small decrease in the coherent scattering length below 0.04 eV, this calculation, indicated by a dotted line, is the same as our former result. In a second calculation in which the effect of the first resonance was taken into account, we obtained the result represented by a dashed line. The calculations are larger than those of [Ly90] throughout the energy region under consideration. In a third calculation, designated by a dash-dotted line, the effect of the second and third resonances at 2.008 eV and 2.568 eV were excluded. For this case, reasonable agreement is achieved with Lynn and Seeger result [Ly90]. The contributions of the second and third resonances to the coherent scattering length are calculated as +0.12 fm and +0.63 fm, respectively.

2. Resolved Resonance Parameters

The resonance parameters of the BNL compilation [Mu84] were adopted in this evaluation. In addition, the resonance spin assignments of Belyaev *et al.* [Be90], which were made by the gamma multiplicity method in the energy range from 6.3 to 183.3 eV, were considered.

The weighted-average radiative width was determined as 114±3 meV from 61 resonances with reported radiative widths.

All of the reported resonances were determined as s-wave according to Bayesian analysis. As displayed in **Fig. 54**, the analysis of reduced neutron widths according to the Porter-Thomas distribution suggests that many weak s-wave resonances are missed. A least-squares fit to the Porter-Thomas distribution was carried out for values of $\left(g\Gamma_n^0\right)^{1/2} > 0.007$ eV. The average s-wave resonance parameters determined from this analysis are listed in **Table 43**.

The upper energy of the resolved resonance region was set to 183.4 eV.

3. Unresolved Resonance Parameters

Since inelastic neutron scattering to the first excited state of ^{155}Gd is at 60.009 keV in the center-of-mass system, the upper energy limit of the unresolved resonance region was set to 60.40 keV.

The capture data of Shorin *et al.* at IPPE [Sh74], Beer and Macklin at ORELA [Be88], Nakajima *et al.* at JAERI [Na89], and Wisshak *et al.* at Karlsruhe [Wi95] were considered. As shown in **Fig. 55**, Shorin's data is higher than the more recent results [Be88, Na89, Wi95].

In the present evaluation, the average s-wave resonance parameters obtained from resolved resonances were adopted without adjustments. The energy-dependent level spacing was assumed to vary with energy and spin according to Gilbert-Cameron level density formula with associated parameters of Mughabghab and Dunford [Mu98a] and a spin dispersion parameter of 3.5 [Mu98b]. Since d-wave contribution is negligible below 60 keV, its effect was not included in the calculations. The average p-wave parameters, $< \Gamma_{\gamma 1} >$ = 0.050 eV, S_1 =2.0, were adopted from the systematics and optical model calculations [Mu84]. As shown in **Fig. 55**, the calculated capture cross sections supports the measurement of Wisshak *et al.* [Wi95] and Beer and Macklin [Be88]. Note that the ENDF/B-VI evaluation significantly diverges from the present evaluation below 20 keV.

Maxwellian average capture cross section for a temperature of 30 keV was computed as 2564 mb. The computation was carried out up to 1 MeV. The capture cross section was constructed with the present parameters up to 60.4 keV and from this energy to 1MeV with that of the ENDF/B-VI evaluation. Our result is to be compared with 2648±30 mb [Wi95] and 2721±90 mb [Be92].

Table 41. Thermal Characteristics (^{155}Gd)

Quantity	Unit	BNL Compilation	98CRC [Ho98]	ENDF/ B-VI	JEF-2.2	JENDL-3.2	Present
R'	fm			6.70	6.70	6.70	8.0
Re(b')*	fm	13.8		12.74		12.74	14.02
σ_γ	barns	60900 ± 500	61000 ± 1000	61100	60790	60890	60730
σ_s	barns	60		58.9	59.0	59.0	60.7
σ_{coh}	barns	38.6					38.6
RI-capt.	barns	1447 ± 100	1540 ± 100	1555	1543	1540	1537

* at 0.08 eV.

Table 42. Parameters of the First Resonance and Scattering Lengths (Real Part) of ^{155}Gd

Parameter	Unit	Lynn	Present
Scattering Radius	fm	6.831*	8.00
Resonance Energy	eV	0.0281	0.0268
Neutron Width	meV	0.104	0.104
Radiative Width	meV	105	108
Scattering Length at 0.08 eV	fm	15.27	14.02

* Potential radius for R-matrix formulation.

Table 43. Average Resonance Parameters in the Unresolved Resonance Region (^{155}Gd)

Quantity	Unit	ENDF/B-VI	JEF-2.2	JENDL-3.2 [a]	BNL Compil.	Present	
						PT Analysis	Adopted
R'	fm	6.70	3.59	6.83	6.7±1.5		8.00
$<D_0>$	eV	1.27	2.20	0.857	1.8±0.2	1.45±0.09	1.45 [b]
S_0	$\times 10^{-4}$	3.08	3.00	2.00	2.0±0.2	2.13±0.35	2.13
$<\Gamma_{\gamma 0}>$	meV	112	120	110	110±3		114
$<D_1>$	eV	1.27	1.10	0.429			0.81 [b]
S_1	$\times 10^{-4}$	0.80	3.70	1.10			2.00
$<\Gamma_{\gamma 1}>$	meV	112	120	110			50.0
$<D_2>$	eV		0.705	0.274			
S_2	$\times 10^{-4}$		1.0	2.30			
$<\Gamma_{\gamma 2}>$	meV		120	110			

a: At the lowest energy (182 eV) of the unresolved resonance region.
b: At the neutron separation energy of ^{156}Gd.

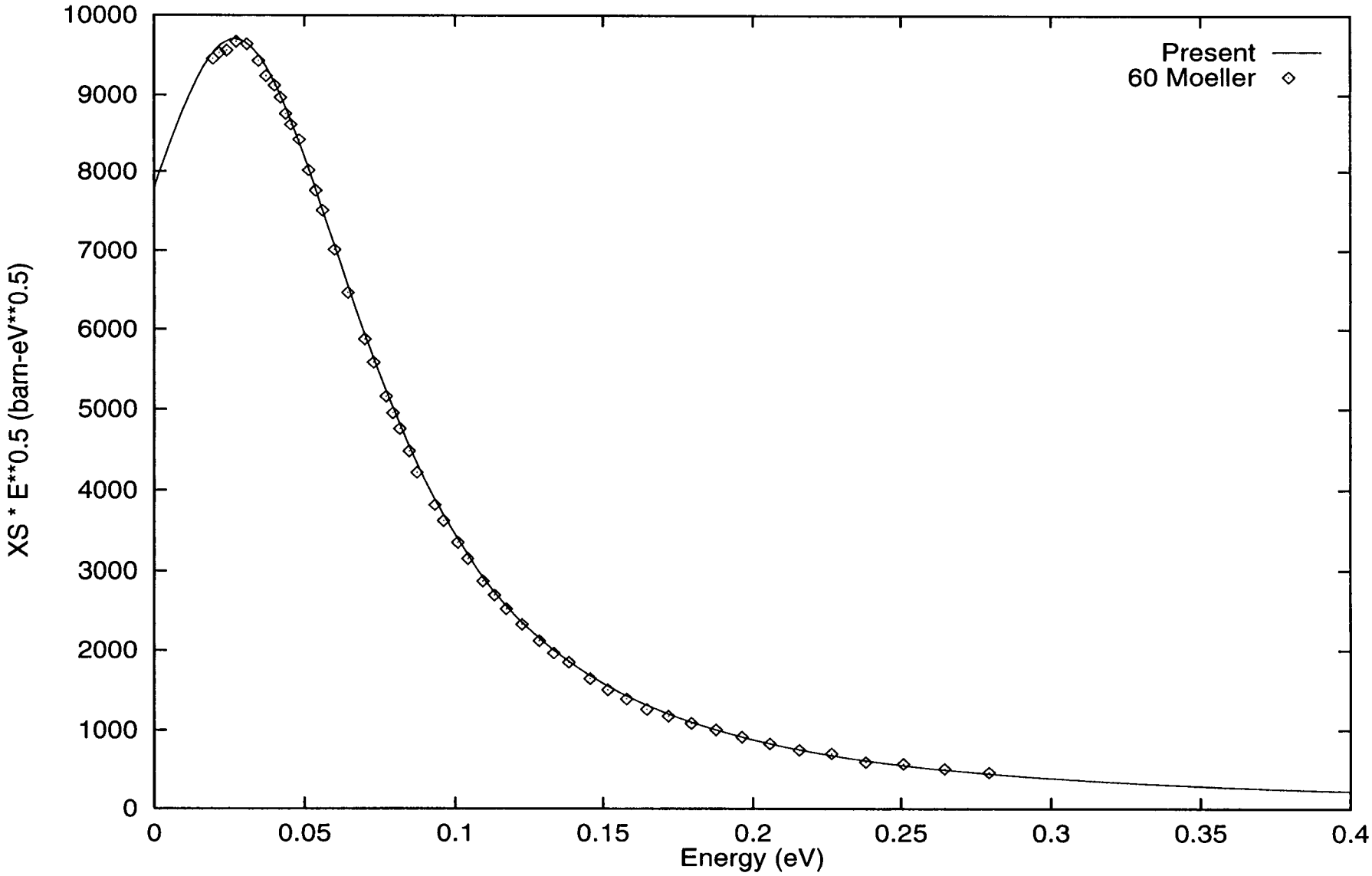

Fig. 52. The Total Cross Section Multiplied by the Square-root of Energy (^{155}Gd)

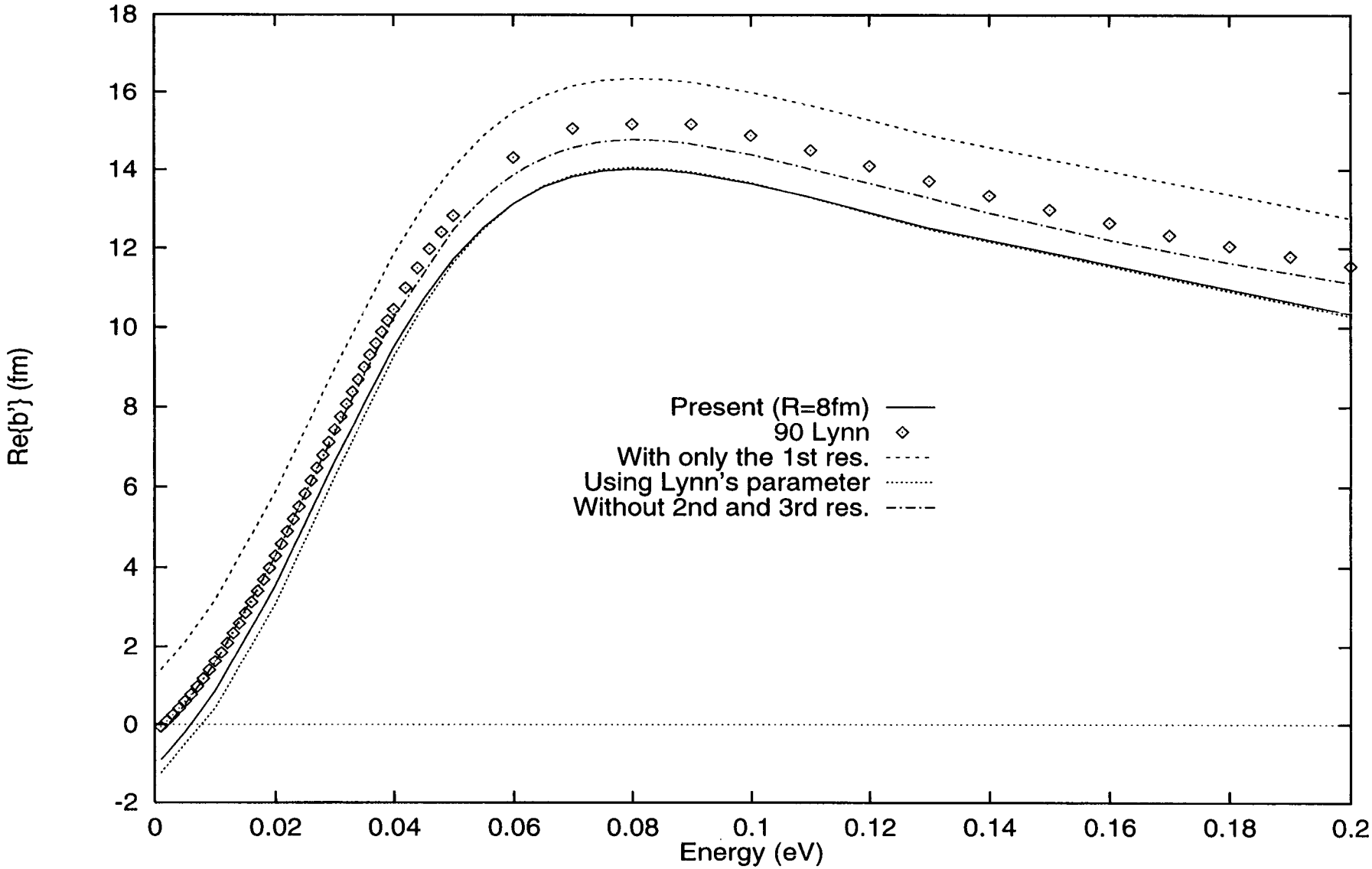

Fig. 53. Real Part of the Bound Coherent Scattering Length of ^{155}Gd

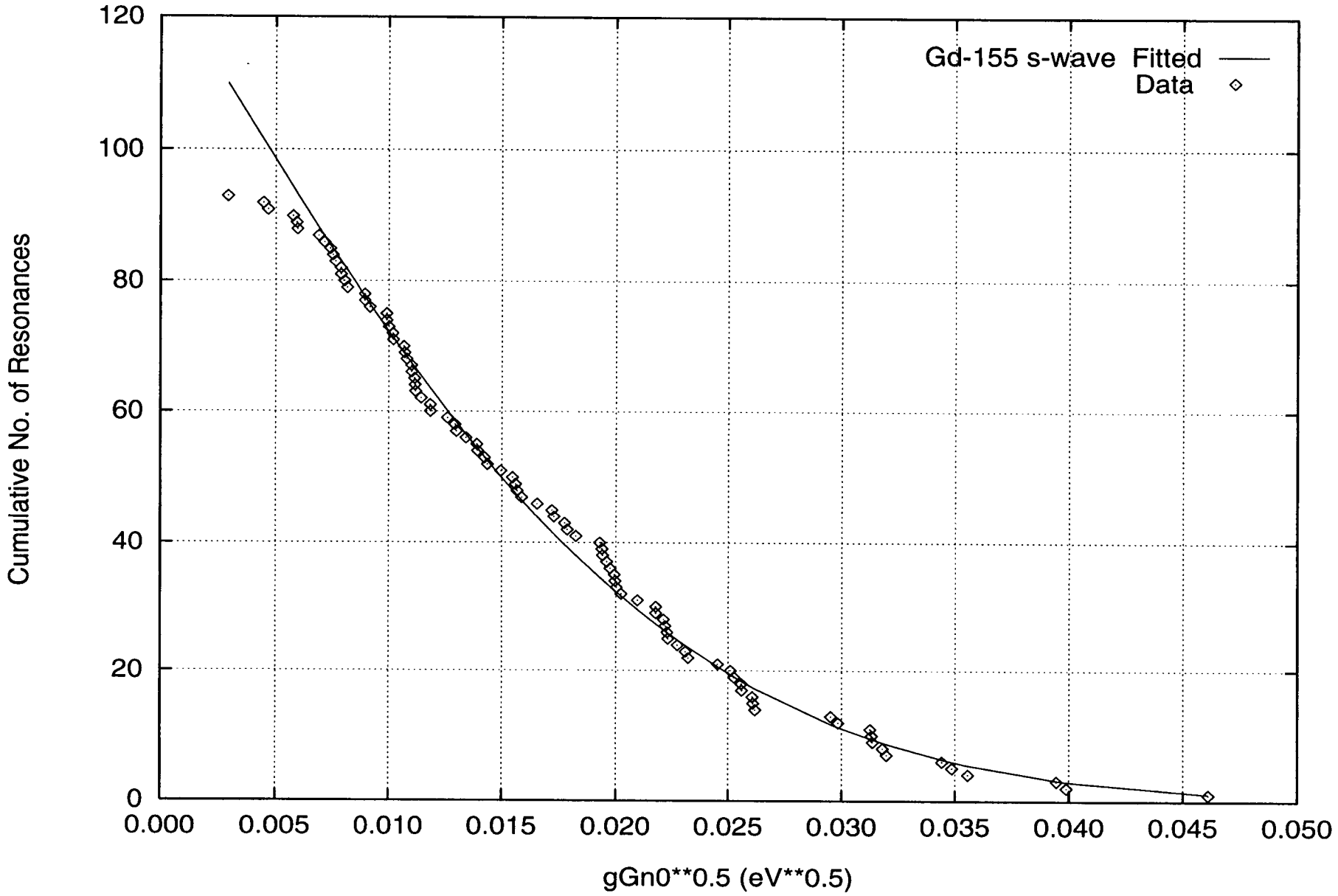

Fig. 54. Complement of the Cumulative Distribution of Neutron Reduced Widths (^{155}Gd, s-wave)

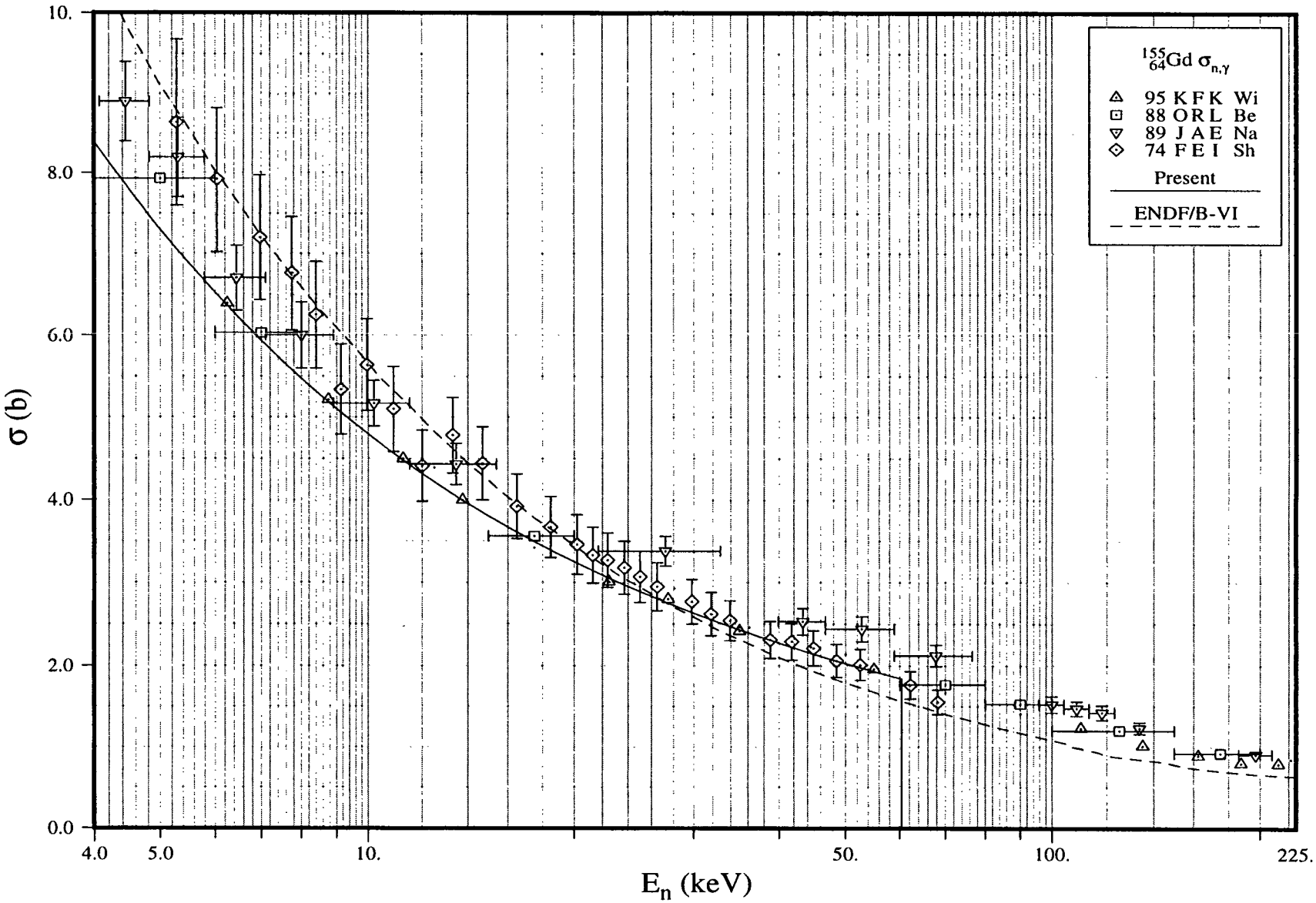

Fig. 55. Capture Cross Section in the Unresolved Resonance Region (^{155}Gd)

III.S. ^{157}Gd

1. Thermal Region

The resolved resonance parameters were adopted from Mughabghab's compilation [Mu84]; an effective scattering radius R' of 7.8 fm, which was read off from a deformed optical model calculation [Mu84], was assumed. For this nuclide, the total contribution of positive-energy resonances to the thermal capture cross section at 0.0253 eV is calculated as 253.7 kb, which is consistent with the value in the BNL compilation (254.0±0.815 kb). Therefore, a bound level is not required. The thermal characteristics are summarized in **Table 44**.

Because of the strong resonance at 0.0314 eV, the energy dependence of the real and imaginary parts of the coherent scattering lengths was investigated. **Figure 56** shows our calculated coherent scattering length, which is based on the present resonance parameters, and is compared with the calculations of Lynn and Seeger [Ly90].

2. Resolved Resonance Parameters

The resolved resonance parameters were adopted from the BNL compilation [Mu84]. Spin assignments made by Belyaev *et al.* [Be90] by the γ ray multiplicity method were incorporated into the present evaluation. On the basis of Bayesian analysis, all of the 60 resonances up to an energy of 306.6 eV were assigned as s-wave. Spins of 53 resonances are reported in the BNL compilation. For the remaining resonances, spins were assigned randomly on the basis of the (2J+1) dependence of the level density. Weighted averaging of 27 measured gamma widths resulted in a value of 100±8 meV; this value was assumed for the remaining resonances. The average radiative width is consistent with those reported in the BNL compilation (97±8 meV) [Mu84], and determined by Nakajima *et al.* [Na89], 115±28 meV.

The distribution of reduced neutron widths was analyzed in terms of a Porter-Thomas distribution. None of the weak resonances was excluded from the fitting. **Figure 57** shows a fit to the data, which resulted in $\langle D_0 \rangle = 4.48 \pm 0.33$ eV, $\langle g\Gamma_n^0 \rangle = 1.01 \pm 0.19$ meV, and s-wave strength function of $S_0 = 2.25 \pm 0.44$. The present $\langle D_0 \rangle$ is consistent with reported values, (4.9±0.4) [Mu84] and (4.9±0.5) [Re98], within the associated uncertainty. The S_0 value is consistent with those quoted in the BNL compilation (1.9±0.2), RIPL (2.2±0.4), and Nakajima *et al.* [Na89] (2.23±0.57).

3. Unresolved Resonance Parameters

The present unresolved region covers the energy range from 306.6 eV to 54.88 keV. The latter energy corresponds to the threshold energy for inelastic neutron scattering to the first excited level of ^{157}Gd at 54.53 keV. For this isotope, s- and p-wave average resonance parameters were provided. Since the upper energy is relatively low, d-wave contribution is negligible. The level spacing varies with energy according to Gilbert-Cameron level density formula with associated parameters adopted from Mughabghab and Dunford [Mu98]. Based on a (2J+1) dependence of the level density, the p-wave level spacing is assumed to be 1/2 of the s-wave spacing.

In the unresolved resonance region, the average capture cross sections measured by Wisshak *et al.* [Wi95], Nakajima *et al.* [Na89], and Beer and Macklin [Be88] were taken into consideration. These sets show good agreement with each other. The final unresolved resonance parameters, listed in the last column of **Table 45**, resulted in a calculated capture cross section in agreement with the experimental data (**Fig. 58**).

Table 44. Thermal Characteristics (^{157}Gd)

Quantity	Unit	BNL compil.	98CRC [Ho98]	ENDF/ B-VI	JEF-2.2	JENDL-3.2	LIPAR [Ab97]	Present
R'	fm			4.90	4.90	4.90		7.80
σ_γ^0	kbarn	254±0.815	254±3	255.8	253.4	254.1	253.5	253.7
σ_s^0	barn	1000		1015	1756	1007	1005	1009
σ_{coh}^0	barn	622						627
σ_{incoh}^0	barn	378						382
gw*				0.8500	0.8514	0.8522	0.8527	0.8515
RI-capt.**	barn	700±20	800±100	759	762	763	711+	754
RI-total**	barn			960	946	936		989

* Westcott factor for capture cross section.
** Integrated from 0.5 eV to 100 keV with 1/E spectrum.
\+ Integrated from 0.5 to 215 eV.

Table 45. Average Resonance Parameters for the Unresolved Resonance Region (^{157}Gd)

Quantity	Unit	BNL compil.	ENDF/ B-VI	JEF-2.2	JENDL-3.2*	Present	
						PT Analysis	Adopted
R'	fm		4.90		6.88		7.80
$\langle D_0 \rangle$	eV	4.9±0.4	3.53		3.94	4.48±0.33	4.48**
S_0	$\times 10^{-4}$	1.9±0.2	2.92		1.90	2.25±0.44	2.25
$\langle \Gamma_{\gamma 0} \rangle$	meV	97±8	98.0		97.0		100.0
$\langle D_1 \rangle$	eV		3.53		1.97		2.24**
S_1	$\times 10^{-4}$		0.76		1.10		1.60
$\langle \Gamma_{\gamma 1} \rangle$	meV		98.0		97.0		100.0
$\langle D_2 \rangle$	eV				1.26		
S_2	$\times 10^{-4}$				2.30		
$\langle \Gamma_{\gamma 2} \rangle$	meV				97.0		

* Average parameters at the low energy of the unresolved region (304 eV).
** At the neutron separation energy of ^{158}Gd.

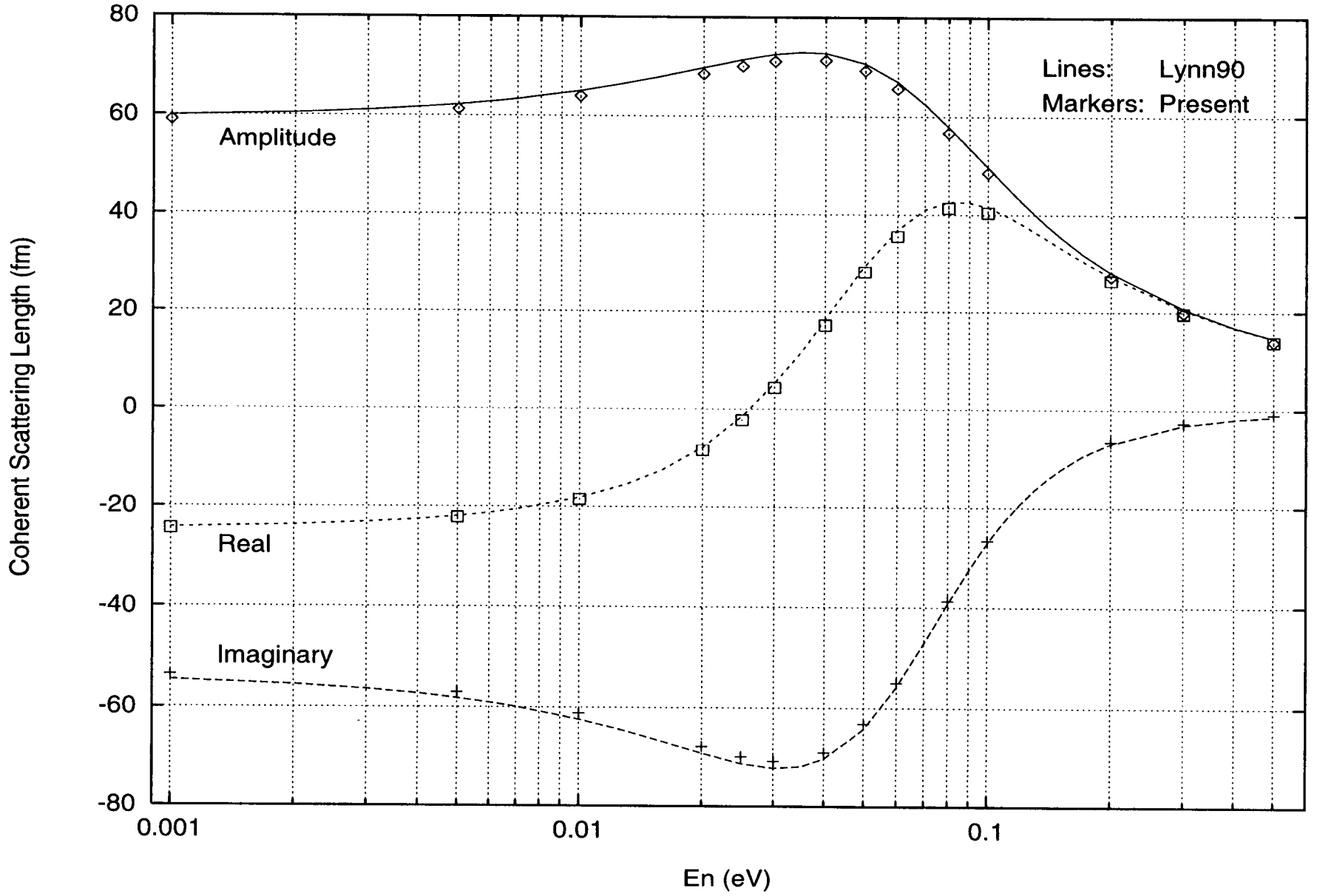

Fig. 56. Bound Coherent Scattering Lengths of ^{157}Gd

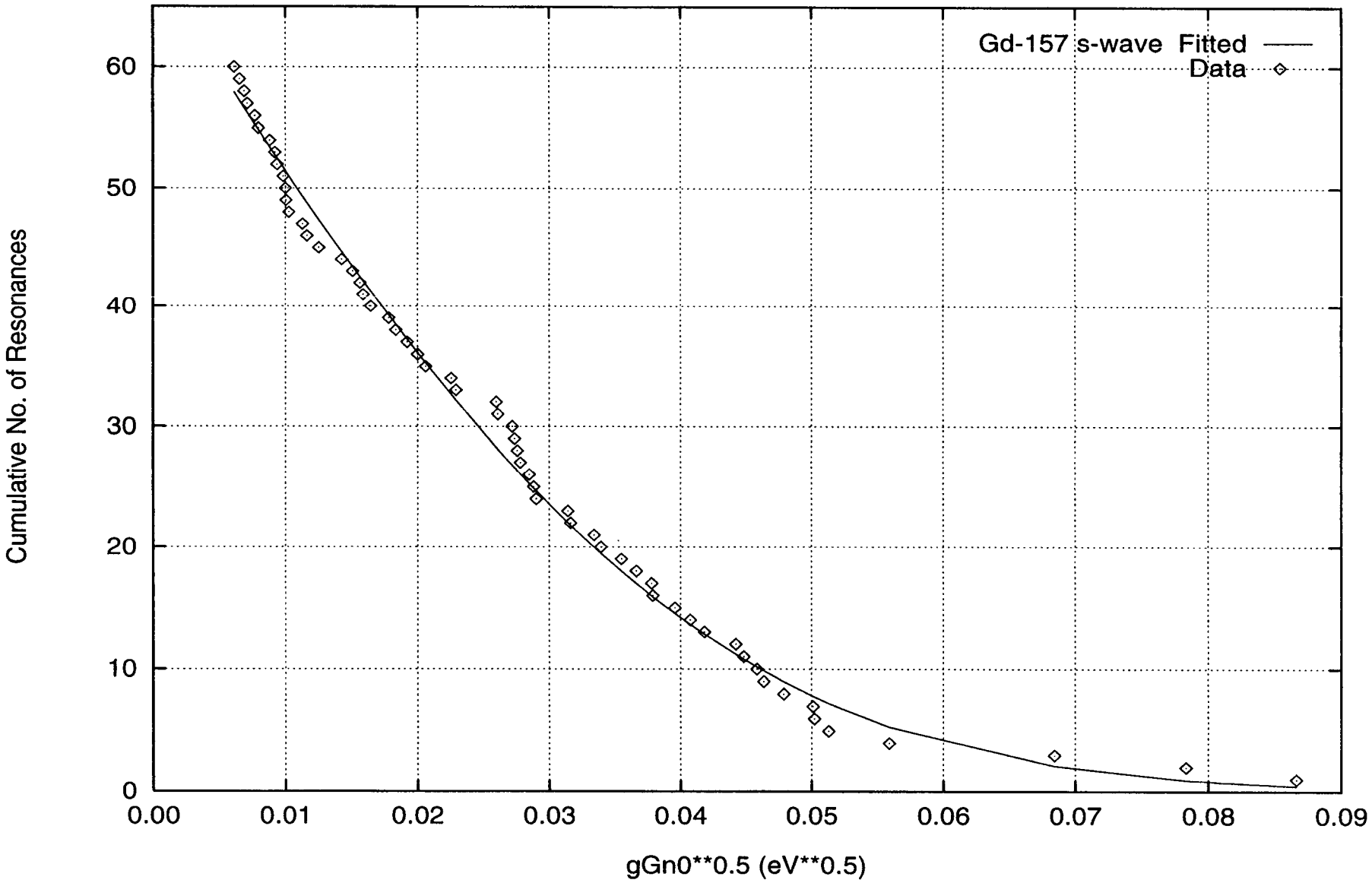

Fig. 57. Complement of the Cumulative Distribution of Neutron Reduced Widths (^{157}Gd, s-wave)

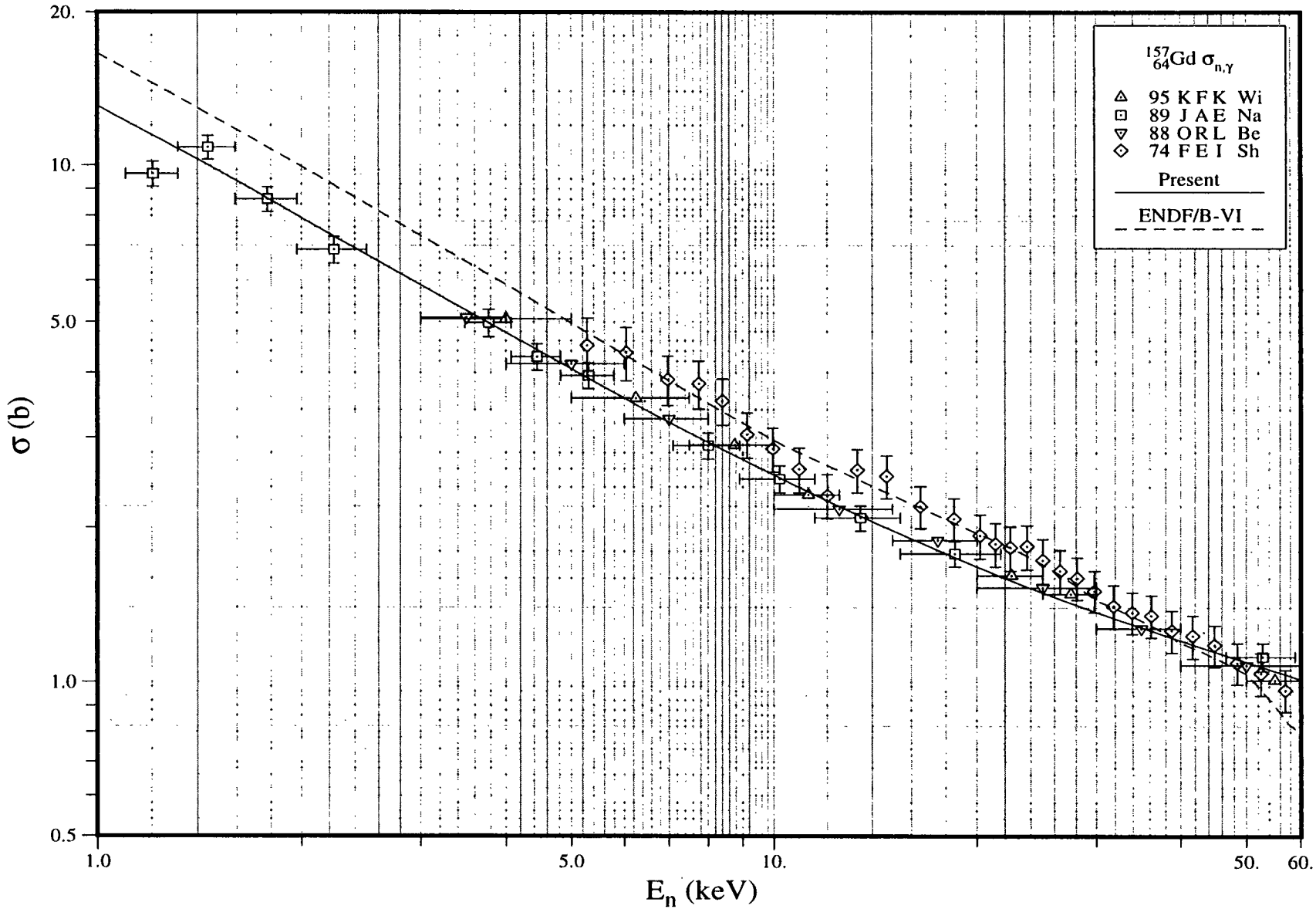

Fig. 58. Capture Cross Section in the Unresolved Resonance Region (^{157}Gd)

IV. COMPARISONS WITH OTHER EVALUATIONS

In this section, we present a brief over-all summary of the evaluations of the 19 fission-product nuclei and compare our results with previous evaluations, high-lighting the major differences and disagreements with other evaluations.

IV.A Resolved and Unresolved Resonance Data Files

Table 46 gives a summary of the resolved and unresolved energy regions of the present and ENDF/B-VI evaluations. As shown for ^{99}Tc, ^{103}Rh, ^{105}Pd, ^{109}Ag, ^{131}Xe, ^{133}Cs ^{141}Pr, ^{147}Sm, and ^{149}Sm, the resonance regions of the present evaluations are represented by more additional resonances than those of the ENDF/B-6 evaluations.

IV.B Thermal Cross Sections

In **Table 47**, the thermal capture cross sections of the nuclei ^{95}Mo, ^{105}Pd, ^{145}Nd, ^{147}Sm, and ^{150}Sm display absolute differences greater than 3% between the present evaluations and those of ENDF/B-6. However, good agreement is achieved with other evaluations for these isotopes.

IV.C Capture Resonance Integrals

As demonstrated in **Table 48**, disagreements larger than ±5% between the present results and those of ENDF/B-6 exist in the calculated capture resonance integrals for ^{99}Tc, ^{105}Pd, ^{131}Xe, ^{131}Cs, and ^{141}Pr.

IV.D Thermal Elastic Cross Sections

Table 49 shows that the calculated thermal scattering cross sections of the present study are larger than any of the evaluations for ^{95}Mo, ^{105}Pd , and ^{151}Sm while for ^{131}Xe it is smaller than the other evaluations.

IV.E Effective Scattering Radii

The potential scattering radii implemented in the resolved and unresolved energy regions of the various evaluations are summarized in **Table 50**. With the exception of ^{155}Gd and ^{157}Gd, general agreement exits among the various evaluations. However, our values for these two isotopes, which are consistent with the systematic study [Mu84], are much larger than those of the other evaluations.

IV.F Wescott Factors for Capture Cross Sections

As shown in **Table 51**, there is good agreement between the present calculations of the Wescott factors for capture and those of other evaluations.

IV.G Wescott Factors for Scattering and Total Cross Sections

Table 52 gives a summary of the calculated scattering and total resonance integrals of the various evaluations. Major disagreements, larger than 15%, exist among the various evaluations of the scattering resonance integrals for ^{101}Ru, ^{105}Pd, ^{150}Sm, ^{151}Sm, ^{155}Gd, and ^{157}Gd.

IV.H S-Wave Strength Functions

In **Table 53**, the s-wave neutron strength functions, implemented in the unresolved-energy regions of the various evaluations, as well as those reported in [Mu81, Mu84, Re98], are compared. Within the uncertainty limits generated by the Porter-Thomas analysis in the resolved energy region, general agreement exists among the different evaluations

IV.I S-Wave Radiative Widths

In **Table 54**, the s-wave average level spacings, implemented in the unresolved energy region of the various evaluations, as well as those of [Mu81], [Mu84] and [Re98] are compared. With the exception of ^{95}Mo, ^{143}Nd and ^{152}Sm, the level spacings of the present study, derived from the resolved energy region, are applied in the unresolved energy region without any adjustments.

IV.J S-Wave Radiative Widths

In **Table 55**, the s-wave average radiative widths, implemented in the unresolved energy regions of the various evaluations, as well as those reported in [Mu81], [Mu84] and [Re98], are compared. In the present study, the average values obtained from the resolved energy region were generally applied in the unresolved region. Varying adjustments in the radiative widths were carried out in order to fit the unresolved capture cross section. Adjustments larger than 20% were made on the radiative widths of ^{99}Tc, ^{145}Nd, and ^{149}Sm, none on ^{101}Ru, ^{105}Pd, ^{131}Xe, ^{133}Cs, ^{147}Sm, ^{150}Sm, ^{153}Eu, ^{155}Gd, and ^{157}Gd, and minor ones on the remainder.

IV.K Maxwellian Capture Cross Sections at 30 KeV

Because of interest in astrophysical calculations, we computed the Maxwellian capture cross sections at a temperature of 30 keV on the basis of the present evaluated capture cross sections, as well as those of ENDF/B-6. The results are included in **Table 56** and are compared with Beer's [Be92] and Bao's [Ba87] compilations. When compared with the results derived on the basis of the ENDF/B-6 evaluations, differences larger than 10% exist for ^{103}Rh, ^{143}Nd, ^{149}Sm. However, our results for these nuclei are in good agreement with those of [Be92] and [Ba87].

Table 46. Status of Resonance Data in MF=2

Isotope	1st Inelastic Excited Level (keV) [a]	Upper Energy of RRR (keV)		No. of Resolved Resonances [b]		Upper Energy of URR (keV)	
		ENDF/B-VI	Present	ENDF/B-VI	Present	ENDF/B-VI	Present
42-Mo-95	204.12	2.188	2.141	25+ 30 (0)	20+ 35 (1)	–	206.3
43-Tc-99	140.51	0.800	0.983	42+ 25 (1)	41+ 54 (1)	141.4	141.9
44-Ru-101	127.23	1.000	1.035	40+ 0 (0)	41+ 7 (0)	100.0	128.5
45-Rh-103	39.756	1.500	4.116	59+ 60 (0)	101+178 (1)	40.4	40.2
46-Pd-105	280.51	1.000	2.054	80+ 0 (1)	141+ 57 (2)	–	283.2
47-Ag-109	88.034	2.509	4.996	83+ 0 (0)	236+ 71 (0)	–	88.8
54-Xe-131	80.185	4.000	3.945	39+ 0 (1)	45+ 2 (1)	–	80.8
55-Cs-133	80.997	2.500	3.989	123+ 0 (0)	148+ 39 (2)	–	81.6
59-Pr-141	145.44	0.991	10.049	15+ 0 (0)	79+ 47 (2)	–	146.5
60-Nd-143	742.05	5.285	5.503	121+ 27 (1)	122+ 27 (1)	100.0	225.0
60-Nd-145	67.220	4.140	3.979	212+ 0 (1)	194+ 0 (1)	50.0	67.7
62-Sm-147	121.22	1.000	1.998	140+ 0 (1)	211+ 0 (1)	30.0	122.1
62-Sm-149	22.507	0.100 [c]	0.520	29+ 0 (1)	158+ 0 (1)	10.0	100.0 [d]
62-Sm-150	333.86	1.600	1.563	22+ 0 (1)	22+ 0 (1)	100.0	336.1
62-Sm-151	4.821	0.300	0.296	120+ 0 (1)	120+ 0 (1)	–	66.2 [e]
62-Sm-152	121.78	5.025	5.102	91+ 0 (1)	91+ 0 (1)	100.0	122.6
63-Eu-153	83.367	0.097	0.098	71+ 0 (1)	71+ 0 (1)	1.0	83.9
64-Gd-155	60.009	0.183	0.183	92+ 0 (0)	92+ 0 (0)	10.4	60.4
64-Gd-157	54.533	0.307	0.307	56+ 0 (0)	60+ 0 (0)	10.4	54.9

a: In the center-of-mass system

b: Number of s-wave positive-energy resonances + Number of p-wave resonances; Number of bound level resonances in parentheses

c: Lower limit of the resolved resonance region(RRR) is 2.361 eV.

d: The second inelastic level is 277.075 keV in the center-of-mass system.

e: This corresponds to the second inelastic level.

Table 47. Capture Cross Sections at 0.0253 eV (barn)

Isotope	BNL Compilation	98CRC	ENDF/B-VI [a]	JEF-2.2 [a]	JENDL-3.2 [b]	LIPAR-5	Present [c]	Relative Diff. (%) [d]
42-Mo-95	14.0±0.5	13.4±0.3	14.6	14.0	14.0	–	13.6	−7.4
43-Tc-99	20±1	23±2	19.6	19.1	19.6	–	20.0	2.0
44-Ru-101	3.4±0.9	5±1	3.43	3.42	3.36	–	3.45	0.6
45-Rh-103	145±2	145	147	146	147	–	145	−1.4
46-Pd-105	20.0±3.0	22±2	20.1	21.8	20.3	–	20.9	3.8
47-Ag-109	91.0±1.0	91.2	91.0	90.8	90.5	90.7	90.8	−0.2
54-Xe-131	85±10	90±10	90.6	85.1	85.0	–	90.0	−0.7
55-Cs-133	29.0±1.5	30.4	29.7	29.1	29.0	–	29.0	−2.4
59-Pr-141	11.5±0.3	11.5	11.5	11.5	11.5	–	11.5	0.0
60-Nd-143	325±10	330±10	325	323	330	319	325	0.0
60-Nd-145	42±2	47±6	42.1	41.9	43.8	41.9	49.8	15.5
62-Sm-147	57±3	56±4	57.5	57.2	58.0	56.7	50.0	−15.0
62-Sm-149	40140±600	40100±600	39730	40480	40150	39420	40530	2.0
62-Sm-150	104±4	102±5	104	103	109	108.2	100	−3.9
62-Sm-151	15200±300	15200±300	15250	15190	15160	15160	15170	−0.5
62-Sm-152	206±6	206±15	207	206	206	202	206	−0.5
63-Eu-153	312±7	300±20	313	300	313	312	312	0.0
64-Gd-155	60900±500	61000±1000	61100	60790	60890	60710	60730	−0.6
64-Gd-157	254000±815	254000±3000	255800	253400	254100	253500	253700	−0.8

a: From JEF Report 14, OECD/NEA, Paris (1994)

b: From General Description (MF=1) of JENDL-3.2

c: Calculated using LINEAR–RECENT–SIGMA1–INTER codes

d: Relative Difference = $(1 - \sigma_\gamma^{\text{ENDF/B-VI}} / \sigma_\gamma^{\text{Present}}) \times 100$

Table 48. Capture Resonance Integrals (barn)

Isotope	BNL Compilation	98CRC	ENDF/B-VI [a]	JEF-2.2 [a]	JENDL-3.2 [b]	LIPAR-5 [c]	Present [d]	Relative Diff. (%) [e]
42-Mo-95	109±5	109±5	113	110	119	–	111	−2.2
43-Tc-99	340±20	–	350	304	312	–	312	−12.2
44-Ru-101	100±20	110±30	111	111	100	–	111	0.1
45-Rh-103	1100±50	1180	1035	1035	1040	–	1036	0.1
46-Pd-105	62.2	60±20	111	93.1	96.8	–	95.2	−16.6
47-Ag-109	1400±48	1480	1471	1473	1470	1467	1476	0.4
54-Xe-131	900±100	900±100	1016	890	900	–	882	−15.2
55-Cs-133	437±26	422	383	439	396	–	421	9.0
59-Pr-141	17.4±2.0	14±3	19.0	17.9	18.4	–	17.6	−7.7
60-Nd-143	128±30	128±30	130	130	130	127	130	0.7
60-Nd-145	240±35	260±40	231	231	204	228	245	5.7
62-Sm-147	–	710±50	789	794	781	721	777	−1.4
62-Sm-149	3390	3100±500	3258	3484	3490	3355	3482	6.4
62-Sm-150	358±50	290±30	338	339	325	334	334	−1.2
62-Sm-151	3520±160	3520±60	3449	3465	3410	3397	3430	−0.6
62-Sm-152	2970±100	3000±300	2981	2977	2770	2958	2976	−0.2
63-Eu-153	1420±100	1800±400	1499	1448	1410	1305	1408	−6.5
64-Gd-155	1447±100	1540±100	1555	1543	1540	1437	1537	−1.2
64-Gd-157	700±20	800±100	759	762	763	711	754	−0.7

a: From JEF Report 14, OECD/NEA, Paris (1994)

b: From General Description (MF=1) of JENDL-3.2

c: Integrated from 0.5 eV to the upper energy of resolved resonance region

d: Calculated using LINEAR–RECENT–SIGMA1–INTER codes; Integrated from 0.5 eV to 100 keV with 1/E spectrum

e: Relative Difference = $(1 - I_\gamma^{\text{ENDF/B-VI}} / I_\gamma^{\text{Present}}) \times 100$

Table 49. Elastic Scattering Cross Sections at 0.0253 eV (barn)

Isotope	BNL Compilation	ENDF/B-VI [a]	JEF-2.2 [a]	JENDL-3.2 [b]	LIPAR-5	Present [c]
42-Mo-95	–	2.48	5.21	5.57	–	6.41
43-Tc-99	–	6.88	3.54	3.44	–	5.81
44-Ru-101	–	3.23	5.05	3.74	–	4.50
45-Rh-103	–	4.69	3.43	3.28	–	4.37
46-Pd-105	5.0±0.6	5.01	5.22	5.13	–	7.36
47-Ag-109	2.55±0.06	2.25	2.30	2.48	2.42	2.12
54-Xe-131	–	4.32	24.3	24.0	–	1.19
55-Cs-133	–	4.98	3.88	4.29	–	3.97
59-Pr-141	2.54±0.06	2.18	2.59	2.54	–	2.71
60-Nd-143	80±2	80.6	80.8	80.3	80.0	80.4
60-Nd-145	–	17.4	18.3	20.3	17.9	18.7
62-Sm-147	–	39.1	39.9	1.06	3.8	1.06
62-Sm-149	197	139	176	173	163	194
62-Sm-150	–	19.0	21.2	8.34	10.3	27.7
62-Sm-151	–	43.5	39.3	50.4	34.4	62.0
62-Sm-152	3.0±0.2	3.12	2.93	0.95	7.49	3.11
63-Eu-153	9.7±0.7	9.04	6.75	10.3	7.68	9.00
64-Gd-155	60	58.9	59.0	59.0	58.6	60.7
64-Gd-157	1000	1015	1756	1007	1005	1009

a: From JEF Report 14, OECD/NEA, Paris (1994)

b: From General Description (MF=1) of JENDL-3.2

c: Calculated using LINEAR–RECENT–SIGMA1–INTER codes

Table 50. Effective Scattering Radii (fm)

Isotope	BNL Compilation	ENDF/B-VI		JEF-2.2		JENDL-3.2		Present *
		In RRR	In URR	In RRR	In URR	In RRR	In URR	
42-Mo-95	7.0±0.2	5.50		7.00		7.00	6.68	7.00
43-Tc-99	6.0±0.5	7.91	←	6.00	6.80	6.00	6.22	7.00
44-Ru-101		5.62	←	6.90	←	6.10	5.06	6.53
45-Rh-103	6.2±0.3	7.09	←	6.20	6.56	6.20	6.52	6.56
46-Pd-105	6.6±0.3	6.60		6.70	←	6.50	4.60	6.60
47-Ag-109	6.6±0.2	6.60		6.60	6.30	7.05	6.62	6.60
54-Xe-131		5.85		5.40		5.31	5.63	5.40
55-Cs-133	5.3±0.5	7.52		5.30	5.50	5.35	5.84	5.30
59-Pr-141	4.9±0.5	6.28		4.40	←	4.90	5.18	4.93
60-Nd-143		5.54	←	5.60	7.34	5.60	4.13	5.60
60-Nd-145		6.80	←	6.00	5.00	6.00	7.68	6.00
62-Sm-147	8.3±0.2	8.30	←	8.30	6.37	8.30	6.64	8.30
62-Sm-149	8.3±0.2	5.09	←	8.30	5.09	7.52	7.90	8.30
62-Sm-150		6.41	←	6.40		8.08	5.92	8.00
62-Sm-151		8.30		7.20	7.46	7.95	5.72	8.30
62-Sm-152	8.3±0.2	8.30	7.67	8.30	6.44	8.20	7.56	8.30
63-Eu-153	8.2±0.2	8.80	←	8.80	←	8.63	6.42	8.20
64-Gd-155		6.70	←	6.70	3.59	6.70	6.83	8.00
64-Gd-157		4.90	←	4.90		4.90	6.88	7.80

* The same value is adopted for both resolved and unresolved resonance regions.

Table 51. Westcott Factors for Capture

Isotope	ENDF/B-VI [a]	JEF-2.2 [a]	JENDL-3.2 [a]	LIPAR-5	Present [b]
42-Mo-95	0.9990	0.9987	0.9994	–	1.0000
43-Tc-99	1.004	1.004	1.004	–	1.0036
44-Ru-101	1.003	1.001	1.001	–	1.0016
45-Rh-103	1.022	1.023	1.022	–	1.0229
46-Pd-105	0.9973	0.9951	0.9986	–	0.9995
47-Ag-109	1.006	1.005	1.005	1.0050	1.0053
54-Xe-131	0.9996	1.001	1.001	–	1.0014
55-Cs-133	1.004	1.002	1.002	–	1.0029
59-Pr-141	1.002	0.9997	0.9990	–	0.9995
60-Nd-143	0.9981	0.9961	0.9961	0.9961	0.9966
60-Nd-145	1.002	0.9996	1.000	0.9998	1.0000
62-Sm-147	0.9990	1.001	0.9946	0.9942	0.9965
62-Sm-149	1.704	1.717	1.685	1.7088	1.7171
62-Sm-150	1.000	0.9979	0.9938	0.9936	0.9985
62-Sm-151	0.9308	0.9271	0.9278	0.9256	0.9274
62-Sm-152	1.004	1.003	1.003	1.0032	1.0035
63-Eu-153	0.9738	0.9662	0.9869	0.9801	0.9871
64-Gd-155	0.8419	0.8435	0.8437	0.8446	0.8440
64-Gd-157	0.8500	0.8514	0.8522	0.8527	0.8515

a: Calculated with values of σ_γ^0 and $\sigma_{\gamma,Maxw.}$ in JEF Report 14, OECD/NEA, Paris (1994)

b: Calculated using LINEAR–RECENT–SIGMA1–INTER codes

Table 52. Elastic Scattering and Total Resonance Integrals*

Isotope	Elastic Scattering Resonance Integral (barn)				Total Resonance Integral (barn)			
	ENDF/B-VI	JEF-2.2	JENDL-3.2	Present	ENDF/B-VI	JEF-2.2	JENDL-3.2	Present
42-Mo-95	178	196	216	205	291	306	334	315
43-Tc-99	113	84.7	74.8	97.1	463	389	386	409
44-Ru-101	72.9	89.6	73.9	89.3	184	200	173	200
45-Rh-103	94.1	79.8	78.5	89.5	1129	1115	1121	1126
46-Pd-105	88.7	82.2	72.1	90.8	200	175	168	186
47-Ag-109	219	216	218	214	1691	1690	1689	1691
54-Xe-131	1862	2068	2039	1883	2877	2958	2938	2765
55-Cs-133	135	117	113	114	518	556	508	535
59-Pr-141	284	216	221	220	303	234	239	237
60-Nd-143	597	597	567	598	726	726	696	728
60-Nd-145	567	566	573	562	797	798	776	807
62-Sm-147	871	845	745	728	1660	1639	1524	1505
62-Sm-149	560	485	578	538	3819	3969	4071	4021
62-Sm-150	492	501	475	556	830	840	799	890
62-Sm-151	267	297	343	325	3726	3765	3752	3765
62-Sm-152	6074	6070	5977	6068	9055	9048	8740	9045
63-Eu-153	199	196	196	181	1699	1644	1605	1590
64-Gd-155	171	162	134	168	1726	1705	1667	1705
64-Gd-157	200	182	175	234	960	946	936	989

* Integrated from 0.5 eV to 100 keV with 1/E spectrum: Present values are calculated using LINEAR–RECENT–SIGMA1–INTER codes. Others are from JEF Report 14, OECD/NEA, Paris (1994).

Table 53. s-wave Neutron Strength Functions in the Unresolved Resonance Region ($\times 10^4$)

Isotope	BNL Compilation	ENDF/B-VI	JEF-2.2	JENDL-3.2 *	RIPL	Present	
						PT Analysis	Adopted
42-Mo-95	0.35±0.07	–	–	0.37	0.60±0.10	0.45±0.16	0.45
43-Tc-99	0.45±0.05	0.43	0.55	0.54	0.48±0.07	0.43±0.10	0.43
44-Ru-101	0.54±0.04	0.59	0.59	0.59	0.56±0.05	0.62±0.15	0.62
45-Rh-103	0.6±0.1	0.43	0.49	0.45	0.47±0.06	0.57±0.09	0.57
46-Pd-105	0.60±0.05	–	0.58	0.60	0.60±0.05	0.66±0.08	0.50
47-Ag-109	0.46±0.15	–	0.64	0.54	0.75±0.08	0.52±0.05	0.57
54-Xe-131	1.2±0.4	–	–	0.70	1.20±0.30	0.79±0.20	0.79
55-Cs-133	0.7±0.07	–	0.80	0.70	0.76±0.10	0.73±0.09	0.73
59-Pr-141	1.5±0.2	–	1.00	1.50	1.70±0.30	1.77±0.30	1.77
60-Nd-143	3.2±0.3	3.50	3.40	2.62	3.80±0.40	3.62±0.51	3.62
60-Nd-145	4.4±0.4	4.00	5.20	2.93	3.20±0.40	4.75±0.52	4.75
62-Sm-147	4.8±0.5	4.80	4.26	4.80	4.80±0.50	4.86±0.50	4.86
62-Sm-149	4.6±0.6	3.20	4.13	4.60	6.30±1.20	4.53±0.54	4.53
62-Sm-150	3.6±1.1	3.60	–	3.60	3.40±0.60	4.31±1.42	4.31
62-Sm-151	4.2±0.4	–	4.50	4.20	3.40±0.50	4.06±0.56	4.06
62-Sm-152	2.2±0.3	2.50	2.30	2.20	3.00±0.40	2.23±0.35	2.23
63-Eu-153	2.5±0.2	2.50	2.50	2.80	2.20±0.30	2.37±0.43	2.37
64-Gd-155	2.0±0.2	3.08	3.00	2.00	2.00±0.30	2.13±0.35	2.13
64-Gd-157	1.9±0.2	2.92	–	1.90	2.20±0.40	2.25±0.44	2.25

* At the lowest energy of the unresolved resonance region

Table 54. s-wave Average Level Spacings in the Unresolved Resonance Region (eV)

Isotope	BNL Compilation	ENDF/B-VI	JEF-2.2	JENDL-3.2 [a]	RIPL	Present	
						PT Analysis	Adopted [b]
42-Mo-95	55±8	–	–	78.9	105 ± 10	80.7 ±13.1	69.4
43-Tc-99	10.7±1.8	12.1	18.3	20.6	12.8 ± 1.8	15.4 ± 2.0	15.4
44-Ru-101	16±2 [c]	20.4	18.3	25.6	18.0 ± 3.0	19.3 ± 1.8	19.3
45-Rh-103	16±1	10.1	25.8	32.1	32.0 ± 4.0	28.6 ± 1.6	28.6
46-Pd-105	10.0±0.5 [c]	–	10.3	5.31	10.3 ± 0.5	10.3 ± 0.5	10.3
47-Ag-109	14±2	–	16.1	19.4	15.1 ± 1.4	20.0 ± 0.8	20.0
54-Xe-131	70±20 [c]	–	–	35.5	49.0 ± 15.0	42.8 ± 5.0	42.8
55-Cs-133	20.65±2.3	–	21.8	16.5	21.0 ± 2.0	19.8 ± 0.9	19.8
59-Pr-141	88±9	–	120.0	134.2	110 ± 20	118.0 ± 7.2	118.0
60-Nd-143	45±4	32.5	36.0	36.4	35.0 ± 5.0	38.0 ± 2.0	36.0
60-Nd-145	22±2	17.3	18.2	17.2	17.0 ± 3.0	18.0 ± 0.8	18.0
62-Sm-147	5.7±0.5	5.70	6.32	5.70	5.10 ± 0.50	6.05 ± 0.23	6.05
62-Sm-149	2.2±0.2	3.43	1.97	1.54	2.10 ± 0.30	2.45 ± 0.11	2.45
62-Sm-150	55±9	48.0	–	59.8	46.0 ± 8.0	46.5 ± 8.6	46.5
62-Sm-151	1.2±0.2	–	1.20	4.85	1.04 ± 0.15	1.48 ± 0.09	1.48
62-Sm-152	51.8±3.3	28.0	52.5	33.5	48.0 ± 5.0	47.5 ± 2.7	34.6
63-Eu-153	1.3±0.2	1.30	1.30	1.66	1.10 ± 0.20	1.14 ± 0.08	1.14
64-Gd-155	1.8±0.2	1.27	2.20	0.857	1.70 ± 0.20	1.45 ± 0.09	1.45
64-Gd-157	4.9±0.4	3.53	–	3.95	4.90 ± 0.50	4.48 ± 0.33	4.48

a: At the lowest energy of unresolved resonance region
b: At the neutron separation energy of target+n
c: Observed level spacing

Table 55. s-wave Average Radiative Widths in the Unresolved Resonance Region (meV)

Isotope	BNL Compilation	ENDF/B-VI	JEF-2.2	JENDL-3.2	RIPL	Present	
						Average [a]	Adopted
42-Mo-95	160±20	–	–	232	150 ±20	158 ±14	150
43-Tc-99	160	122	131.4	187	160 ±50	173 ±16	130
44-Ru-101	180±15	180	180	173	180 ±15	184 ±10	184
45-Rh-103	160±15	153	161.3	230	160 ±15	162 ±28	170
46-Pd-105	145±8	–	155	145	150 ± 8	148 ± 4	148
47-Ag-109	130	–	132.3	130	130 ±20	130 ± 3	133
54-Xe-131	–	–	–	114	114 ±37	112 ±11	112
55-Cs-133	120	–	125.3	120	120 ±10	123 ± 4	123
59-Pr-141	–	–	85.0	86	88 ± 9	86.0± 2.0	86.0
60-Nd-143	80±9	80	68.0, 78.0	79.1	86 ± 9	79.9± 2.0	79.9
60-Nd-145	54±5	75	89.1	97.5	87 ± 9	63.8± 3.8	76.5 [b]
62-Sm-147	69±2	69	87.6	69	69 ± 2	73.8± 1.5	73.8
62-Sm-149	62±2	62	75.1	62	62 ± 2	56.7± 8.9	78.5 [b]
62-Sm-150	60±5	60	–	60	87 ±16	60.0± 0.02	60.0
62-Sm-151	92±7	–	96	92	95 ± 4	92.9± 3.7	92.9
62-Sm-152	61±7	61	71.8	61	67 ± 5	60.0± 5.4	72.7
63-Eu-153	93±3	95.8	95.8	94	95 ±12	93 ± 2	93.0
64-Gd-155	110±3	112	120	110	108 ±10	114 ± 3	114
64-Gd-157	97±8	98	–	97	97 ±22	100 ± 8	100

a: Uncertainty-weighted average of known radiative widths of resolved resonances

b: Unweighted average radiative width

Table 56. Average Capture Cross Sections Weighted with Maxwellian Spectrum at 30 keV (mb)

Isotope	Measured			Calculated [a]		
	Beer's Compilation [b]	Bao's Compilation [c]	Recent Data	ENDF/B-VI	Present	Relative Diff. (%)
Mo-95	292 ± 12	374 ± 50		375	377	0.4
Tc-99	782 ± 39	779 ± 40		855	795	-7.5
Ru-101	996 ± 40	996 ± 40		952	970	1.8
Rh-103	810 ± 14	875 ± 35		943	836	-12.7
Pd-105	1199 ± 60	1199 ± 60		1150	1190	3.3
Ag-109	779 ± 23	779 ± 23		807	787	-2.6
Xe-131	453 ± 81	348		291	306	5.1
Cs-133	509 ± 21	509 ± 21		552	513	-7.5
Pr-141	119 ± 15	119 ± 15		115	117	1.7
Nd-143	242 ± 10	253 ± 10 [d]	244.6 ± 3.1 [e]	287	239	-19.9
Nd-145	485 ± 100	485 ± 100	424.8 ± 4.5 [e]	444	423	-5.0
Sm-147	1005 ± 100	1005 ± 100	973.1 ± 10.0 [f]	931	929	-0.2
Sm-149	1409 ± 65	1454 ± 66	1819.9 ± 17.2 [f]	2384	1866	-27.8
Sm-150	434 ± 26	447 ± 26	421.9 ± 3.8 [f]	378	409	7.5
Sm-151	1932 ± 206	1932	1825 ± 450 [g]	2466	2569	4.0
Sm-152	401 ± 24	396 ± 22 [d]	473.2 ± 4.4 [f]	494	460	-7.4
Eu-153	3170 ± 317	3170 ± 317		2575	2486	-3.5
Gd-155	2721 ± 90	2800 ± 280	2648 ± 30 [h]	2592	2564	-1.1
Gd-157	1355 ± 39	1538 ± 154	1369 ± 15 [h]	1387	1361	-2.0

a: Using INTER; integrated from 10^{-5} eV to 1 MeV. b: Beer, H., Voss, F. and Winters, R.R., Astrophys. J. Suppl. Ser. **80**, 403 (1992) c: Bao, Z.Y. and Kaeppeler, F., Atomic Data and Nucl. Data Tables **36**, 411 (1987) d: Renormalized value in Ratynski, W. and Kaeppeler F., Phys. Rev. C**37**, 595 (1988) e: Wisshak, K. et al., Phys. Rev. C**57**, 391 (1998) f: Wisshak, K. et al., Phys. Rev. C**48**, 1401 (1993)
g: Calculated value in Toukan, K.A. et al., Phys. Rev. C**51**, 1540 (1995) h: Wisshak, K. et al., Phys. Rev. C**52**, 2762 (1995)

This page has been intentionally left blank.

REFERENCES

[Ab97] Abagyan, L.P., "The LIPAR Resonance Parameter Library," INDC(CCP)-406, IAEA (1997).

[Ai61] Aitken, K.L. and Cornish, F.W., "The Neutron Capture Cross Sections of Sm-149 and Sm-150," J. Inorg. Nucl. Chem. **17**, 6 (1961).

[Ak76] Akopian, G.G. *et al.*, "Neutron Spin States Amplitudes and Scattering Cross-Sections for Rare-Earth Nuclei," *Proc. Int'l Conf. on Interactions of Neutrons with Nuclei*, Vol. 2, p.1243, Lowell, July 6-9 (1976).

[Al82] Allen, B.J. *et al.*, "Stable Isotope Capture Cross Sections from the Oak Ridge Electron Linear Accelerator – Part II," Nucl. Sci. Eng., **82**, 230 (1982).

[Al82b] Alfimenkov, V.P. *et al.*, "Investigation of Spin Dependence of Neutron Cross Sections and of Strenghth Functions for Rare Earth Nuclei in Experiments with Polarized Neutrons and Nuclei," Nucl. Phys. **A376**, 229 (1982).

[An78] Anufriev, V.A. *et al.*, "Resonance Parameters of ^{133}Cs and ^{134}Cs Isotopes at Energies up to 400 eV," Sov. Atomic Enegy **43**, 828 (1978).

[An79] Anufriev, V.A. et al, Atom. Energiya **47**, 269 (1979).

[An80] Antonov, A.V. *et al.*, *Proc. 5th All-Union Conf. on Nucl. Phys.*, p.125, Sept. 15-19, Kiev (1980).

[An85] Anufriev, V.A. *et al.*, "Total Neutron Cross Section of ^{101}Ru and ^{102}Ru in the Neutron Energy Range 0.01– 1750 eV," Sov. Atomic Energy **58**, 326 (1985).

[Ba87] Bao, Z.Y. and Kaeppeler, F., "Neutron Capture Cross Sections for s-Process Studies," Atomic Data and Nucl. Data Tables **36**, 411 (1987).

[Be88] Beer, H. and Macklin, R.L., "The ^{151}Sm Branching; A Probe for the Irradiation Time Scale of the s-Process," Astrophys. J. **331**, 1047 (1988).

[Be90] Belyaev, F.N. *et al.*, "Study of ^{155,157}Gd Resonances by γ ray Multiplicity," Sov. J. Nucl. Phys. **52**, 401 (1990).

[Be92] Beer, H. *et al.*, "On the Calculation of Maxwellian-Averaged Capture Cross Sections," Astrophys. J. Suppl. Ser., **80**, 403 (1992).

[Bo68] Bollinger, L.M. and Thomas, G.E., "p-Wave Resonances of U^{238}," Phys. Rev. **171**, 1293 (1968).

[Bo85] Bokhovko, M.V. *et al.*, Yad. Konst. 1985(3), 12 (1985).

[Bo85b] Bokhovko, M.V. *et al.*, "Neutron Radiation Cross-Section, Neutron Transmission and Average Resonance Parameters for Some Fission Product Nuclei," Yad. Konst. 1985(2), 44 (1985).

[Bo87] Bokhovko, M.V. *et al.*, "Measurement of the Neutron Capture Cross-Sections for Silver in the Energy Region 4 – 400 keV," INDC(CCP)-280/L, p.15 (Translation of Yad. Konst., 1987(2), 21 (1987)).

[Bo91] Bokhovko, M.V. *et al.*, "Average Fast Neutron Radiative Capture Cross-Sections for Fission Products and for Isotopes of Rare Earth Elements," *Proc. Int'l Conf. Nucl. Data for Sci. Technol.*, p.62, Juelich, May 13-17 (1991).

[Bu82] Buyl, R. and Corvi, F., "Thermal Capture Measurements of ^{105}Pd and ^{108}Pd," NEANDC(E) 232U, Vol. III, p.18 (1982).

[Ca71] Cauvin, B. et al, *Proc. of 3rd Conf. Neutron Cross Sections and Technology*, p.785, March 15-17, Knoxville (1971).

[Ca71b] Carlson, A.D. and Fricke, M.P., UC-34, Gulf Radiation Tech. (1971).
[Ch73] Chou, J.C. and Werle, H., J. Nucl. Energy **27**, 811 (1973).
[Co82] Cornelis, E. *et al.*, "Average Capture Cross Section of the Fission Product Nuclei ^{104,105,106,108}Pd," *Proc. Int. Conf. on Nucl. Data for Sci. and Technol.*, p.222, Antwerp, Sept. 6-10 (1982).
[Co97] Corvi, F., private communication. Also see: Corvi, F., *et al.*, "Parity Dependence of Low Level Populations in the ^{107}Ag(n,γ) and ^{109}Ag(n,γ) Resonance Reactions," *Proc. Int'l Conf. Nucl. Data for Sci. Technol.*, p.731, Trieste, May 19-24 (1997).
[Da67] Dakowski, M. *et al.*, Nucl. Phys. **A97**, 187 (1967).
[De95] M.D. DeHart, 1995. "Sensitivity and Parametric Evaluations of Significant Aspects of Burnup Credit for PWR Spent Nuclear Fuel Packages," ORNL/TM-12973, Oak Ridge National Laboratory, Martin Marietta Energy Systems, Inc. (to be published).
[Dy63] Dyson, F.J. and Mehta, M.L., "Statistical Theory of the Energy Levels of Complex Systems. IV," J. Mathematical Phys., **4**, 701 (1963).
[Ei74] Eiland, H.M. *et al.*, "Neutron Cross Sections of Samarium-147 and Samarium-150," Nucl. Sci. Eng. **54**, 286 (1974).
[EX] http://www.nea.fr/html/dbdata/x4 or http://www.nndc.bnl.gov/nndc/exfor
[Fe67] Fenner, N.C. and Large, R.S., "Measurement of the Neutron Capture Cross Sections of ^{147}Pm, ^{148}Pm, ^{148m}Pm and ^{147}Sm," J. Inorg. Nucl. Chem. **29**, 2147 (1967).
[Fi78] Fischer, P. *et al.*, Neutron Physics and Nuclear Data, p.718, Harwell (Sept. 1978).
[Fr70] Fiesenhan, S.J. *et al.*, Nucl. Phys. **A146**, 337.
[Ga81] Garg, J.B., Tikku, V.K., and Harvey, J.A., Phys. Rev. **C23**, 671 (1981).
[Ge92] Georgiev, G.P. *et al.*, JINR-P3-92-346, Joint Institute of Nuclear Research (1992).
[Ge93] Georgiev, G. at al., "Determination of ^{147}Sm and ^{148}Sm Resonance Parameters," Nucl. Phys. **A565**, 643 (1993).
[Gi61] Gibbons, J.H. *et al.*, "Average Radiative Capture Cross Sections for 7- to 170-keV Neutrons," Phys. Rev., **122**, 182 (1961).
[Gl79] Glaettli, H. *et al.*, "Experimental Values of Spin Dependent Nuclear Scattering Lengths of Slow Neutrons," J. de Physique **40**, 629 (1979).
[Gl87] Glaettli, H. *et al.*, "Spin-Dependent Scattering Lengths Slow Neutron-Nucleous by Pseudo-Magnetic Measurements," Z. Phys. A- Atomic Nuclei, **327**, 149 (1987).
[Gu97] Gunsing, F. *et al.*, *Proc. Int. Conf. On Nucl. Data for Sci. Technol.*, p.1293, 19-24 May 1997, Trieste. (1997).
[Ha62] Halperin, J. *et al.*, "Thermal Neutron Cross Section and Resonance Integral of Sm-150," Trans. Amer. Nucl. Soc. **5**, 376 (1962).
[Ha65] Halperin, J. *et al.*, "Neutron Capture Cross Sections of ^{99,100,101}Ru," ORNL-3832, p.4 (1965).
[Ha75] Haste, T.J. and Thomas, B.W., J. Phys. G: Nucl. Phys. **1**, 981 (1975).
[Ha95] Harada, H. *et al.*, J. Nucl. Sci. Tech. **32**, 395 (1995).
[Ho75] Hockenbury, R.W. *et al.*, COO-2479-4, Rensselaer Polytechnic Institute (1975).
[Ho75b] Hockenbury, R.W. *et al.*, "Fission Product Capture Cross Sections in the keV Region," *Proc. Conf. Nucl. Cross Section and Technol.*, March 3-7, Washington, p.905 (1975).
[Ho98] Holden, N.E., "Neutron Scattering and Absorption Properties," CRC Handbook of Chemistry and Physics, 78th Ed., CRC Press (1998).

[Ka64] Kapchigashev, S.P. and Popov, Yu.P., "Neutron Capture Cross Section Measurements for Several Molybdenum Isotopes," *Proc. Conf. on Neutron Interactions*, p.104, Dubna (1964).

[Ka69] Karzhavina, E.N. *et al.*, Sov. J. of Nucl. Phys. **8**, 371 (1969).

[Ko64] Konks, V.A. *et al.*, "Cross Sections for Radiative Capture of Neutrons with Energies up to 50 keV by La-139, Pr-141, Ta-181, and Au-197," Soviet Phys., **19**, 56 (1964).

[Ko68] Konks, V.A. *et al.*, "Radiative Capture of Neutrons by Nuclei with A=140-200," Sov. J. Nucl. Phys., 7, 310 (1968) (EXFOR 40362).

[Ko77] Kononov, V.N. *et al.*, "Fast-Neutron Capture Cross Sections for Indium, Tantalum, Gold, Samarium, and Europium," Sov. J. Nucl. Phys., **26**, 500 (1977).

[Ko78] Kononov, V.N. *et al.*, "Fast-Neutron Capture Cross Sections for Even-Even Isotopes of Neodymium, Samarium, Gadolinium, and Erbium," Sov. J. Nucl. Phys. **27**, 5 (1978).

[Ko81] Kononov, V.N. *et al.*, "Fast-Neutron Radiative Capture Cross Sections and d-wave Strength Functions," *Proc. 4th Int'l Sympo. Neutron Capture Gamma-Ray Spectroscopy and Related Topics*, p.518, Grenoble, Sept. 7-11 (1981).

[Ko87a] Koester, L. *et al.*, "Interaction of Slow Neutrons with the Isotopes of Molybdenum," Z. Phys. A-Atomic Nuclei, **326**, 227 (1987).

[Ko87b] Koester, L. *et al.*, "Experimental Study on the 3p Size Resonance in the p-wave Neutron Strength Function," Z. Phys. A- Atomic Nuclei, **326**, 185 (1987).

[Ko91] Koester, L. *et al.*, "Neutron Scattering Lengths: A Survey of Experimental Data and Method," Atom. Data and Nucl. Data Tables, **49**, 65 (1991).

[Li77] Little, R.C. and Block, R.C., Trans. Amer. Nucl. Soc. **26**, 574 (1977).

[Lo97] Lowie, L.Y. *et al.*, "Neutron Resonance Spectroscopy of ^{107}Ag and ^{109}Ag," Phys.Rev. C, 56, 90 (1997).

[Lu77] Lucas, M. *et al.*, *Proc. Mtg. of the Technical Committee on Natural Fission Reactors*, Vol. 1, p.431, Dec.19-21, Paris (1977).

[Lu94] Luo Xiao-bing *et al.*, "Measurement of Neutron Capture Cross Section for ^{152}Sm," Chinese J. Nucl. Phys., **16**, 275 (1994).

[Ly90] Lynn, J.E. and Seeger, P.A., "Resonance Effects in Neutron Scattering Lengths of Rare-Earth Nuclides," At. Data Nucl. Data Tables **44**, 191 (1990).

[Ma63] Macklin, R.L. *et al.*, "Neutron Capture in the Samarium Isotopes and the Formation of the Element of the Solar System," Nature **197**, 369 (1963).

[Ma79] Macklin, R.L. *et al.*, "^{104,105,106,108,109}Pd(n,γ) Cross Sections Above 2.6 keV," Nucl. Sci. Eng., **71**, 182 (1979).

[Ma80] Macklin, R.L. and Halperin, J., "^{100,101,102,104}Ru(n,γ) and ^{103}Rh(n,γ) Cross Sections above 2.6 keV," Nucl. Sci. Eng. **73**, 174 (1980).

[Ma81] Macklin, R.L. and Winters, R.R., "Stable Isotope Capture Cross Sections from the Oak Ridge Electron Linear Accelerator," Nucl. Sci. Eng. **78**, 110 (1981).

[Ma82] Macklin, R.L., Nucl. Sci. Eng. **81**, 520 (1982).

[Ma82b] Macklin, R.L., "Neutron Capture Cross Sections of the Silver Isotopes ^{107}Ag and ^{109}Ag from 2.6 to 2000 keV," Nucl. Sci. Eng., **82**, 400 (1982).

[Ma82c] Macklin, R.L., "Cesium-133 Neutron Capture Cross Section," Nucl. Sci. Eng. **81**, 418 (1982).

[Ma86] Macklin, R.L., EXFOR 12966 (1986).

[Ma87] Macklin, R.L. and Young, P.G., "Neutron Capture Cross Sections of ^{151}Eu and ^{153}Eu from 3 to 2200 keV," Nucl. Sci. Eng., **95**, 189 (1987) (EXFOR 12873).

[Mc88] McLane, V. *et al.*, Neutron Cross Sections, Vol. 2: Neutron Cross Section Curves, Academic Press (1988).

[Mi79a] Mizumoto, M. *et al.*, "Low-Energy Neutron Resonances in ^{206}Pb," Phys. Rev. C**19**, 335 (1979).

[Mi79] Mizumoto, M. *et al.*, "Average Neutron Capture Cross Sections of ^{151}Eu and ^{153}Eu from 3 to 100 keV," J. Nucl. Sci. Technol., **16**, 711 (1979).

[Mi81] Mizumoto, M., "Neutron Resonance Parameters and Radiative Capture Cross Sections of ^{147}Sm and ^{149}Sm," Nucl. Phys. **A357**, 90 (1981).

[Mi83] Mizumoto, M. *et al.*, "Neutron Resonance Parameters of Silver-107 and Silver-109," J. Nucl. Sci. Technol., **20**, 883 (1983).

[Mo60] Moeller, H.J. *et al.*, Nucl. Sci. Eng. **8**, 183 (1960).

[Mo69] Morgenstern, J. *et al.*, "Parametres des Resonances et Fonctions Densites S_0 et S_1 pour Cl, ^{51}V, ^{89}Y, Zr, La, ^{141}Pr et ^{209}Bi," Nucl. Phys. **A123**, 561 (1969).

[Mo76] Moxon, M.C. *et al.*, "The Neutron Capture Cross-Section of Eu-151 and Eu-153 in the Energy Range 0.1 to 100 keV," Ann. Nucl. Energy, **3**, 399 (1976).

[Mu71] Mughabghab, S.F. *et al.*, "Reaction Mechanism for p-Wave Neutron Capture in Mo^{92} and Mo^{98}," Phys. Rev. Letters, **26**, 1118 (1971).

[Mu76] Musgrove, A.R. de L. *et al.*, "Average Neutron Resonance Parameters and Radiative Capture Cross Sections for the Isotopes of Molybdenum," Nucl. Phys. **A270**, 108 (1976).

[Mu77] Musgrove, A.R. *et al.*, AAEC/E401 (1977).

[Mu81] Mughabghab, S.F. *et al.*, Neutron Cross Sections, Vol.1, Part A, Academic Press (1981).

[Mu84] Mughabghab, S.F., Neutron Cross Sections, Vol.1, Part B, Academic Press (1984).

[Mu98a] Mughabghab, S.F. and Dunford, C.L., *Proc. Int. Conf. on Phys. of Nucl. Sci. and Technol.*, p.784, Long Island, Oct. 5-8 (1998).

[Mu98b] Mughabghab, S.F. and Dunford, C.L., Phys. Rev. Lett. **81**, 4083 (1998).

[Mu99] Mughabghab, S.F. and Dunford, C.L., "A Unified Model for E1 Photon Strength Functions and the Landau Migdal Constants," BNL-NCS-66524 (1999). Also see "On the Questions of the Nuclear Level Density and the E1 Photon Strength Functions," *Int. School on Nucl. Phys., Neutron Phys., and Nucl. Energy*, Sept. 27 – Oct. 3, 1999, Varna, Bulgaria.

[Na78] Nakajima, Y. *et al.*, *Proc. Int. Conf. on Neutron Phys. and Nucl. Data for Reactors and Other Applied Purposes*, p.438, Sept. 25-29, Harwell (1978).

[Na89] Nakajima, Y. *et al.*, "Neutron Capture Cross Section Measurements of ^{155}Gd and ^{157}Gd from 1.1 to 235 keV," Ann. Nucl. Energy **16**, 589 (1989).

[Na90] Nakajima, Y. *et al.*, "Neutron Resonances in ^{133}Cs," Ann. Nucl. Energy **17**, 569 (1990).

[Oh99] Oh, S.Y., "The Probability Density Function of Neutron Reduced Width," Nuclear Data Evaluation Lab. Calculation Note, NDL-32/99, KAERI (Nov. 1999).

[Or70] Orphan, V.J. *et al.*, "Line and Continuum Gamma-Ray Yields from Thermal-Neutron Capture in 75 Elements," GA-10248, Gulf General Atomic (1970).

[Pa58] Pattenden, N.J., *Proc. Second UN Int. Conf. Peaceful Uses of Atomic Energy*, v.16, p.44, Sept. 1-13, Geneva (1958).

[Pa92] Pandita, A. and Agrawal, H.M., "Statistical Analysis of s-Wave Neutron Reduced Widths," J. Phys. Soc. Japan, **61**, 3524 (1992).

[Po56] Porter, C.E. and Thomas, R.G., "Fluctuations of Nuclear Reaction Widths," Phys. Rev. **104**, 483 (1956).

[Po79] Popov, A.B. *et al.*, "Parameters of Ru neutron resonances," Sov. J. Nucl. Phys. **29**, 285 (1979).

[Po81] Popov, A.B. and Tzeciak, K., "Parameters of Iodine and Cesium Neutron Resonances in 20-250 eV range," P3-81-721, JINR (1981).

[Pr86] Press, W.H. *et al.*, Numerical Recipes, Section 14.4, Cambridge Univ. Press, Cambridge (1986).

[Ra97] Raepsaet, C. *et al.*, *Proc. Int. Conf. On Nucl. Data for Sci. Technol.*, p.1289, 19-24 May 1997, Trieste. (1997).

[Re98] Reffo, G., "Average Neutron Resonance Parameters," in Reference Input Parameter Library, IAEA-TECDOC-1034, p.25 (1998).

[Ri69] Ribon, P., "Etudes des Quelques Proprietes des Niveaus Excites des Noyaux Composes Formes par 103-Rh, Xe, 155-Gd, 157-Gd, 232-Th," CEA-N-1149 (1969) –Doctoral Thesis.

[Ri70] Ribon, P. *et al.*, Nucl. Phys. **A143**, 130 (1970).

[Ro71] Rohr, G. *et al.*, *Proc. of 3rd Conf. Neutron Cross Sections and Technology*, p.743, March 15-17, Knoxville (1971).

[Sh74] Shorin, V.S. *et al.*, "Neutron Radiative-Capture Cross Sections in the Energy Region 5-70 keV for Gd and Er Isotopes," Sov. J. Nucl. Phys. **19**, 2 (1974).

[Sk96] Skoy, V.R. *et al.*, "Isotopic Identification of the Parity-Violating Neutron p-wave Resonance at Energy E_0=3.2 eV in Xe," Phys. Rev. **C53**, 2573 (1996).

[Sm91] Smith, D.L., Probability, Statistics, and Data Uncertainties in Nuclear Science and Technology, American Nuclear Society (1991).

[St72] Stolovy, A. *et al.*, Phys. Rev. C **5**, 2030 (1972).

[St79] Staveloz, P. *et al.*, "Neutron Resonance Parameters for Palladium Isotopes," *Proc. Specialists' Mtg. on Neutron Cross Sections of Fission Product Nuclei,*" p.53, Bologna, Dec. 12-14 (1979); NEANDC(E) 209 L.

[Ta60] Tattersall, R.B. *et al.*, J. Nucl. Energy/A **12**, 32 (1960).

[Ta79] Taylor, R.B. *et al.*, "keV Neutron Capture in ^{141}Pr," Aust. J. Phys., **32**, 551 (1979).

[Te71] Tellier, H., CEA-N-1459 (1971).

[To95] Toukan, K.A. *et al.*, "Stellar Neutron Capture Cross Sections of Nd, Pm, and Sm Isotopes," Phys. Rev. **C51**, 1540 (1995).

[Ve74] Vertebnyi, V.P. *et al.*, YFI-17, p.37, Fiziko-Energ. Institute, Obninsk (1974).

[Wa70] Watanabe, T. and Reeder, S.D., Nucl. Sci. Eng. **41**, 188 (1970).

[Wi57] Wigner, E.P., *Conf. on Neutron Physics by Time of Flight*, Gatlinburg, 1956, p. 59, ORNL-2309 (1957).

[Wi86] Winters, R.R. *et al.*, " ^{148,150}Sm: A Test for s-process Nucleosynthesis," Astrophys. J. **300**, 41 (1986).

[Wi87] Winters, R.R. and Macklin, R.L., "Maxwellian-Averaged Neutron Capture Cross Sections for ^{99}Tc and $^{95-98}$Mo," Astrophys. J., **313**, 808 (1987).

[Wi90] Wisshak, K. *et al.*, Phys. Rev. **C42**, 1731 (1990).

[Wi93] Wisshak, K. *et al.*, "Neutron Capture in $^{148, 150}$Sm: A Sensitive Probe of the s-process Neutron Density," Phys.Rev. C48, 1401 (1993).

[Wi95] Wisshak, K. *et al.*, "Stellar Neutron Capture Cross Sections of the Gd Isotopes," Phys. Rev. **C52**, 2762 (1995).

[Wi98] Wisshak, K. *et al.*, Phys. Rev. C **57**, 391 (1998).
[Wo82] Word, R.E. and Werner, S.A., Phys. Rev. B **26**, 4190 (1982).
[Wy68] Wynchank, S. *et al.*, "Neutron Resonance Spectroscopy. VI. Mo, Sb, Te, and Pr," Phys. Rev., **166**, 1234 (1968).
[Xi94] Xia Yijin *et al.*, "Activation Cross Section Measurement for the Eu(n,γ) Reactions," *Proc. Int. Conf. Nucl. Data for Sci. Technol.*, May 9-13, Gatlinburg, Tennessee, p.251 (1994).
[Ya79] Yamamuro, N. and Asami, A. *Proc. of Specialist's Mtg. in Neutron Cross Sections of Fission Product Nuclei*, p.19, Dec. 12-14, Bologna, Italy (1979).
[Ya83] Yamamuro, N. *et al.*, "KeV-Neutron Capture in Cesium-133, Gold-197 and Tantalum-181," J. Nucl. Sci. Technol. **20**, 797 (1983).
[Yu93] Yu Weixiang *et al.*, "Activation Cross Section Measurement for the Eu(n,γ) Reactions," Chinese J. Nucl. Phys., **15**, 71 (1993).
[Za71] Zaikin, G.G. *et al.*, "Fast-Neutron Radiative Capture Cross-Sections for the Isotopes ^{69}Ga, ^{71}Ga, ^{139}La and ^{141}Pr," INDC(CCP)-15/U, p.52 (1971).
[Zh92] Zhao, Z. and Huang, Z., "Bayesian Approach to Evaluate Average Level Spacing," *Proc. Int. Sympo. on Nucl. Data Eval. Methodology*, p.327, Upton, Oct. 12-16 (1992).

APPENDICES

Appendix A: Evaluation Procedure

Figure A1 describes the steps of the evaluation procedure and **Fig. A2** presents a flow chart of the computer codes, which were used in accomplishing the various evaluation tasks. As a first step in the evaluation of each nuclide, the bibliographic information is retrieved from CINDA, the Computerized Index to Nuclear Data [CI], and Nuclear Science References [NS]. In addition, recent measured resonance parameters, as well as other data such as thermal cross sections and capture cross sections in the keV energy region, are obtained from CSISRS [CS], which is the NNDC version of EXFOR database [EX]. After reviewing the available measurements and updating the data reported in the BNL compilations, a computerized data file of resolved resonance parameters, *BNL325.TXT*, is prepared.

In the next step, as described in the main text, the *l* and J values for resonances, which have not been determined from the measurements, are assigned by applying the Bayesian method and a random assignment method, respectively. In addition, the measured radiative widths are averaged and this averaged value is assigned to resonances with unknown radiative widths. The parameters for each resolved resonance are compiled into a File 2 in the ENDF-6 format. The resulting file is named *ENDFA.TXT*. In addition, the fitting of reduced neutron widths to the Porter-Thomas distribution is performed. The computer code PTANAL (Fig. A2) performs all the tasks in this step. The resulting average parameters are then adopted in preparing the input file for WRIURR.

In the next step, a check is made as to whether the present resolved resonances reproduce reference thermal cross sections, scattering lengths, and resonance integrals. The thermal cross sections and scattering lengths are calculated by the PSY325 computer code. If necessary, one or two bound levels are invoked. The bound levels are included in the file *ENDFR.TXT*. The thermal characteristics are checked again with PSY325, and, if necessary, the bound level parameters are adjusted to achieve agreement with the measurements.

The energy-dependent average resonance parameters are then appended to the *ENDFR.TXT* by the WRIURR computer code. A set of parameters consists of energy dependent level spacing, reduced neutron width, and gamma width. The competition and fission widths are set as zero. Multiple sets of parameters, which show the energy dependence, are provided for each *l* and J. The energy points are defined in the input file for WRIURR code. The file *ENDFU.TXT* is generated by WRIURR.

ENDFU.TXT is converted to the point-wise cross sections by the RECENT computer code. After extracting capture cross sections in the unresolved region from the *endfu.pw* file with the aid of PWC code, the calculated capture cross sections, together with measured data retrieved from EXFOR database, are plotted by the BNL325 plotting code. If the calculated cross sections do not show acceptable agreement with measured data, the resonance parameters for the unresolved region are then adjusted and a revised *ENDFU.TXT* file is then generated again. Note that the effect of Doppler broadening at a temperature of 300 K is negligible in the keV energy region.

To compare the present evaluation with other evaluated libraries or data sources, the thermal cross sections, resonance integrals, Maxwellian-averaged cross sections, and so on are calculated with the finalized *ENDFU.TXT* file. For this calculation, the point-wise cross sections are broadened to 300 K by using SIGMA1 code. Subsequently, the INTER code calculates the above quantities using the *broadened.pw* file resulting from SIGMA1.

Descriptions of the computer codes PSY325, LINEAR, RECENT, SIGMA1, and INTER can be found in [Le96].

References

[CI] http://www.nndc.bnl.gov/nndc/cinda or http://www-nds.iaea.or.at/cinda

[CS] http://www.nndc.bnl.gov/nndc/exfor

[EX] http://www-nds.iaea.or.at/exfor

[Le96] Lemmel, H.D., "Index of Nuclear Data Libraries," IAEA-NDS-7, Rev. 96/11, IAEA (1996).

[NS] http://www.nndc.bnl.gov/nndc/nsr

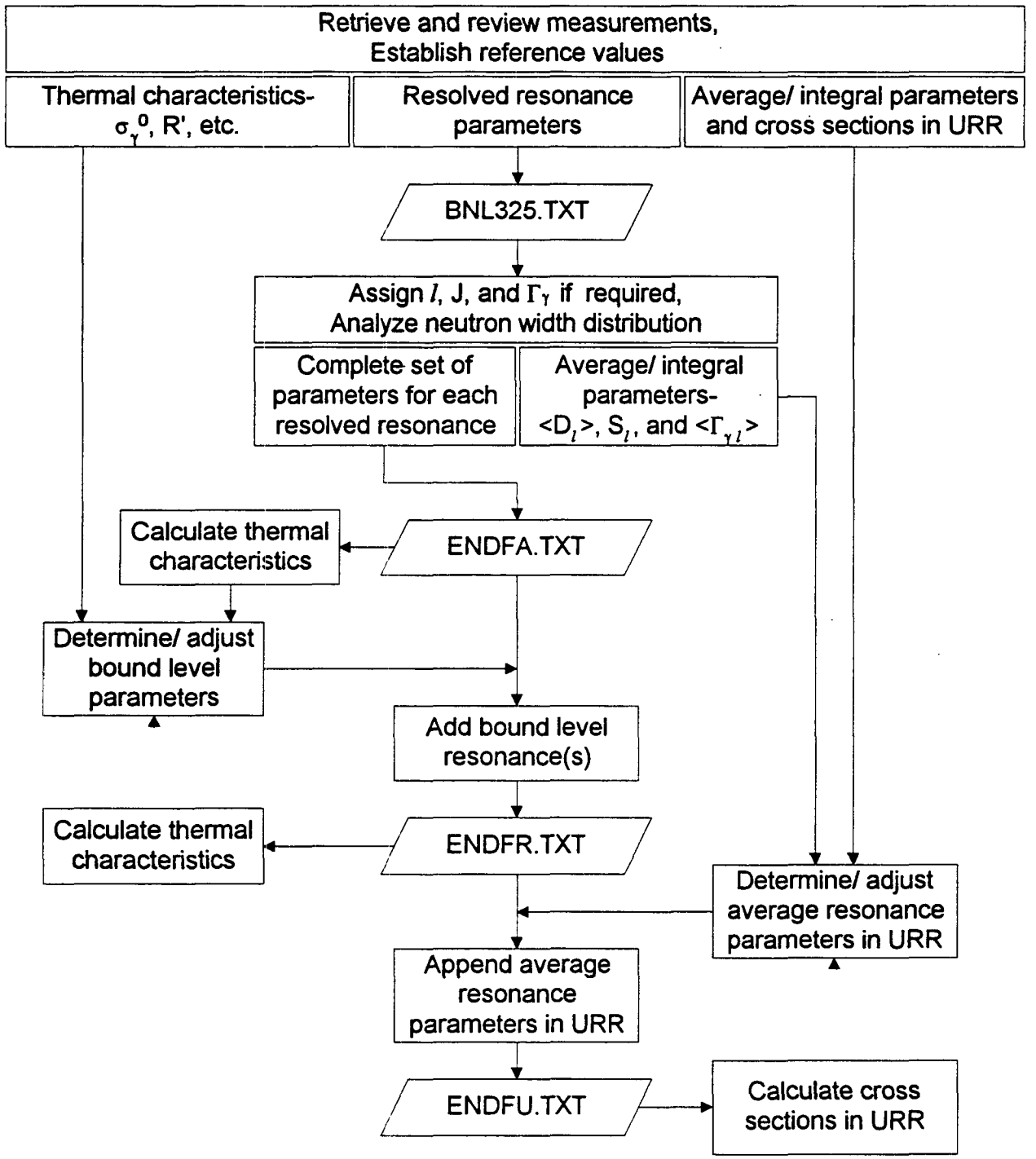

Figure A1. Evaluation Procedure

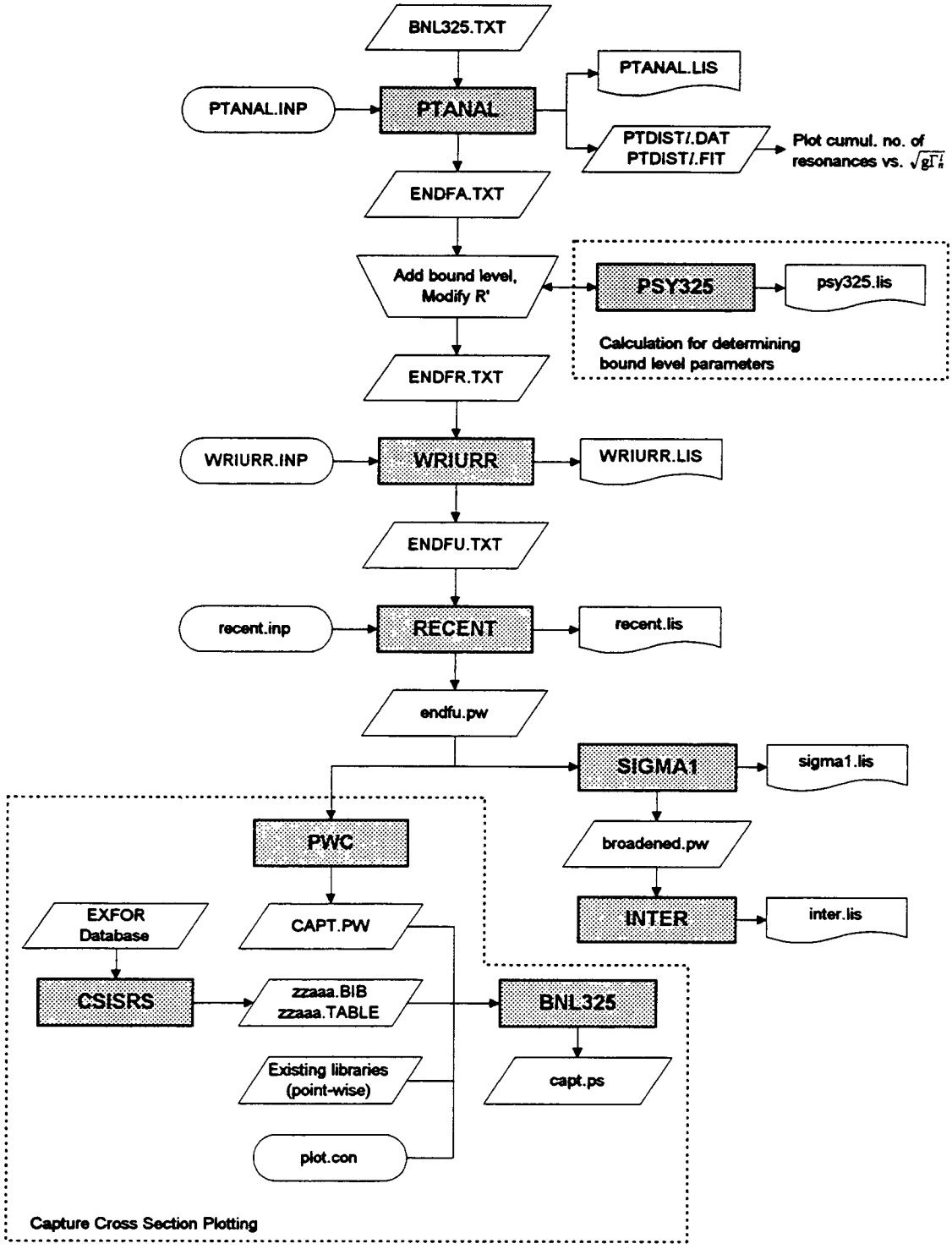

Figure A2. Flow of Computer Codes

Appendix B: PTANAL User's Guide

The PTANAL program is used for obtaining the average resonance parameters from the analysis of the Porter-Thomas distribution for the reduced neutron widths in the resolved resonance energy region. It also assigns the *l* and J values, which have not been determined from the measurements, by applying the Bayesian method and random assignment method, respectively. In addition, the known radiative widths are averaged in two ways: one is an arithmetic average and the other is the weighted-average with the inverse variance of the experimental value. Another purpose of PTANAL is to convert the resonance parameters from the CFMTA format into an ENDF-6 format for file 2.

The program requires two input files PTANAL.INP and BNL325.TXT. The PTANAL.INP file is the standard input in the name-list input format. This file consists of :

First card (in other words, record or line): "&data" from column 2 to 6;
In the second to (last-1) cards: data section with the name-list keywords; and
Last card: "&end" from column 2 to 5.

The data section includes variables shown in Table B1. In the name list input, a user does not need to keep the order of variables. A sample input is shown at the end of **Table B1**.

The BNL325.TXT file contains recommended resonance parameters in CFMTA format. Two records are provided for each resonance as shown in **Table B2**. Flags indicating the status of given parameter are 'R' for recommended, 'F' for preferred, 'A' for assumed, ' '(blank) for undetermined. The PTANAL program deals only with the flags for the resonance spin and angular momentum. Unless the flag was set as 'A' or ' ', the program does not alter the *l* value in the BNL325.TXT file regardless of the results of the Bayesian analysis. In the same context, the random assignment of J is applied only to resonances with the flag 'A' or ' '.

The program generates output files PTANAL.LIS, ENDFA.TXT, PTDISTx.DAT, and PTDISTx.FIT files. The PTANAL.LIS is the standard output summarizing the results and ENDFA.TXT is the File 1 and 2 of the ENDF-6 format containing resolved resonance parameters. The PTDISTx.DAT (x = null for all resonances, 0 for s-wave, or 1 for p-wave) files include the number of cumulative "measured" resonances vs. the neutron reduced widths multiplied by the spin statistical factor, g, in the unit of meV in ascending order. The PTDISTx.FIT is same to .DAT file except "fitted" number of resonances.

Table B1. Variables appearing in the PTANAL.INP file

Name	Unit	Description	Default Value
awt	none	Atomic weight of the target nuclide. The program calculates AWRI as AWRI = awt/1.008665.	none
zam	none	ZZAAA of the target nuclide	none
spin	none	Spin of the target nuclide	none
mat	none	Material number of the target	none
inflag	none	1 or 2. The program will read inflag*$g\Gamma_n$ from the BNL325.TXT. Of usual, inflag=2 for odd and =1 for even nuclide.	none
sf0	1E-04	s-wave neutron strength function for the Bayesian analysis. The s-wave strength function is obtained from the fitting of reduced neutron widths. Since the fitted value may be different from this input value, it is recommended to re-run PTANAL with fitted strength function. Note, however, that the s-wave probability is not so sensitive to the strength function.	0.
sf1(1), sf1(2), sf1(3)	1E-04	A set of three trial p-wave neutron strength functions. The p-wave probability is calculated with each sf1.	0.
sf2	1E-04	d-wave neutron strength function for the Bayesian analysis.	0.
iset	none	Index number selected among sf1 values. (1, 2, or 3) The 'sf1(iset)' value is used for final decision making from the Bayesian p-wave probability.	1
D0	eV	Average spacing of s-wave resonances for the Bayesian analysis	0.
ecut	eV	Upper energy limit for the analysis. Recommended: Energy of the last resonance + 2*Γ	100000
ggavg(1) ggavg(2)	meV	Average gamma width for s- and p-wave, respectively. These values are assigned to resonances with unknown gamma widths.	0.
gncut(1) gncut(2)	meV	Weak resonance cutoff reduced width for s- and p-wave, respectively. Resonances having widths smaller than the values are excluded from the fitting process.	0.
gncuth	meV	Strong resonance cutoff reduced width for s- wave. Resonances having widths larger than this value are excluded from the fitting process. Large doublet or triplet resonances may be excluded from the analysis by using this feature.	10000
uncert	%	Default uncertainty of $g\Gamma_n$ of which uncertainty is not given in BNL325.TXT file. If 'uncert' is less than zero, its absolute value overrides all the uncertainties given in the BNL325.TXT.	10
disp	none	Spin dispersion parameter, σ, for the Bethe formula Note: with a large 'disp', the level density follows (2J+1) law.	100

Sample input (for Dy-160)

```
&data
awt=159.925, zam=66160, spin=0, mat=6637, inflag=1, ecut=1994.5
sf0=2.0, sf1=0.7, 1.4, 2.0, sf2=2.2, D0=27.3
gncut=0.0, 0.0, gncuth=100., ggavg=2*105.8, uncert=20., disp=3.
&end
```

Table B2. CFMTA Format (for each resonance)

Column No.	Format	Description	Note
Record 1			
1~7	I7	ZZAAA	
8~9	A2	'RP'	
10~18 19~24 25	E9.4 E6.2 A1	Resonance energy [eV] Uncertainty [eV], and Flag indicating the status of the energy	 'R'
26	A1	Parity	
27~29 30	F3.1 A1	Resonance spin, J, and Flag indicating the status of given J	 Of usual 'F' or ' '(blank)
31 32	I1 A1	Angular momentum, *l*, and Flag indicating the status of given *l*	 Of usual 'F' or ' '
33~40 41~47 48	E8.4 E7.4 A1	Total width Γ [eV], Uncertainty [eV], and Flag indicating the status of given value	Of usual, not provided
49~56 57~63 64	E8.4 E7.4 A1	$g\Gamma_n$ or 2 $g\Gamma_n$ [eV], Uncertainty [eV], and Flag indicating the status of given value	See 'inflag' in PTANAL.INP
65~72 73~79 80	E8.4 E7.4 A1	Radiative width Γ_γ [eV], Uncertainty [eV], and Flag indicating the status of given value	PTANAL accepts this value even if the flag is 'A'.
81~88 89~95 96	E8.4 E7.4 A1	s-wave reduced width $g\Gamma_n^0$ or 2 $g\Gamma_n^0$ [eV], Uncertainty [eV], and Flag indicating the status of given value	Not used in PTANAL
97~104 105~111 112	E8.4 E7.4 A1	Miscellaneous quantity, Uncertainty, and Flag indicating the status of given value	Of usual, capture area $g\Gamma_n\Gamma_\gamma / \Gamma$ [eV] is provided. In this case, if $g\Gamma_n$ is not provided, PTANAL calculates $g\Gamma_n$ from this quantity with assumed g and Γ_γ.,
113~115	A3	'BNL'	
116~119	A4	Date in 'YYMM'	
120~124	I5	'10000'	
125~132		Parameter codes	
Record 2			
1~7		Same as Record 1	
8~9	A2	'R2'	
10~25		Same as Record 1	
26~32		Blanks	
33~112		Reserved for 5 additional quantities	
113~124		Same as Record 1	

Appendix C: WRIURR User's Guide

The WRIURR program appends the average resonance parameters for the unresolved resonance region to the end of the resolved region data in File 2 of ENDF-6 format.

The program requires two input files, WRIURR.INP and ENDFR.TXT. The ENDFR.TXT file contains resolved resonance parameters in ENDF-6 format. The ENDFR.TXT file is the same as the ENDFA.TXT file, except that it contains bound level resonance parameters, if any.

The WRIURR.INP file is the standard input file in a name-list format. This file consists of:

First card: "&urr" from column 2 to 6 (Not '&data' as in PTANAL);
In the second to (last-1) cards: a data section with the name-list keywords; and
Last card: "&end" from column 2 to 5.

The data section includes variables shown in Table C1.

WRIURR.LIS and ENDFU.TXT are the output files. The former one is the standard output summarizing the input information and calculated results of level spacing. ENDFU.TXT contains Files 1 and 2: the File 2 contains complete resonance parameter information in both the resolved and unresolved energy regions. One may edit the File 1 (general description) manually.

Table C1. Variables appearing in the WRIURR.INP file

Name	Unit	Description
sf(1) sf(2) sf(3)	1E-04	Neutron strength functions of s-, p-, and d-wave, respectively
gg(1) gg(2) gg(3)	meV	Average gamma widths of s-, p-, and d-wave, respectively
ds0(1) ds0(2) ds0(3)	eV	Average level spacing of s-, p-, and d-wave, respectively Normally only ds0(1) is required then ds0(2) and ds0(3) are calculated in the program using the Bethe formula. If ds0(2) and ds0(3) are provided, energy-independent level spacing and Γ_n^l are written in ENDFU.TXT.
e0	eV	Low energy boundary of the unresolved resonance region
de(i), i = 1 to up to 300	eV	Energy intervals The energy points that will be written in File 2 are calculated as e0 (first energy point), e0+de(1), e0+de(1)+de(2), and so on.
bn	MeV	Neutron binding energy of the target nuclide
pair	MeV	Pairing energy of the target nuclide
dena	MeV^{-1}	Level density parameter of the target nuclide
disp	none	Spin dispersion parameter, σ, of the target nuclide
icon(1) icon(2) icon(3)	none	Flags indicating the energy dependence of level spacing and Γ_n^l for s-, p-, and d-wave, respectively. If it is 1, the program writes energy-dependent level spacing and reduced width using the Bethe formula. Otherwise, the program writes energy-independent values. Note that the strength functions are energy-independent in any case. Parameters such as 'bn', 'pair', 'dena', and 'disp' are used in the calculation of energy-dependent level spacings.
Sample input (for Eu-153)		
&urr bn=6.435, pair=0., dena=20.00, icon=3*1, sf=2.37,0.6,5.4, gg=3*93., ds0=1.14 e0=97.8, de=402.2, 500., 1000., 4*2000., 7*10000., 3910. &end		